ADAPTATION OF DRYLAND PLANTS TO A CHANGING ENVIRONMENT

EDITED BY: Zhiyou Yuan, Yinglong Chen, Jairo A. Palta and P. V. Vara Prasad

PUBLISHED IN: Frontiers in Plant Science

frontiers Research Topics

frontiers

ISSN 1664-8714
ISBN 978-2-88963-315-9
DOI 10.3389/978-2-88963-315-9

About Frontiers

Frontiers is more than just an open-access publisher of scholarly articles: it is a pioneering approach to the world of academia, radically improving the way scholarly research is managed. The grand vision of Frontiers is a world where all people have an equal opportunity to seek, share and generate knowledge. Frontiers provides immediate and permanent online open access to all its publications, but this alone is not enough to realize our grand goals.

Frontiers Journal Series

The Frontiers Journal Series is a multi-tier and interdisciplinary set of open-access, online journals, promising a paradigm shift from the current review, selection and dissemination processes in academic publishing. All Frontiers journals are driven by researchers for researchers; therefore, they constitute a service to the scholarly community. At the same time, the Frontiers Journal Series operates on a revolutionary invention, the tiered publishing system, initially addressing specific communities of scholars, and gradually climbing up to broader public understanding, thus serving the interests of the lay society, too.

Dedication to Quality

Each Frontiers article is a landmark of the highest quality, thanks to genuinely collaborative interactions between authors and review editors, who include some of the world's best academicians. Research must be certified by peers before entering a stream of knowledge that may eventually reach the public - and shape society; therefore, Frontiers only applies the most rigorous and unbiased reviews.
Frontiers revolutionizes research publishing by freely delivering the most outstanding research, evaluated with no bias from both the academic and social point of view. By applying the most advanced information technologies, Frontiers is catapulting scholarly publishing into a new generation.

What are Frontiers Research Topics?

Frontiers Research Topics are very popular trademarks of the Frontiers Journals Series: they are collections of at least ten articles, all centered on a particular subject. With their unique mix of varied contributions from Original Research to Review Articles, Frontiers Research Topics unify the most influential researchers, the latest key findings and historical advances in a hot research area! Find out more on how to host your own Frontiers Research Topic or contribute to one as an author by contacting the Frontiers Editorial Office: researchtopics@frontiersin.org

ADAPTATION OF DRYLAND PLANTS TO A CHANGING ENVIRONMENT

Topic Editors:
Zhiyou Yuan, Northwest A&F University, China
Yinglong Chen, University of Western Australia, Australia
Jairo A. Palta, Commonwealth Scientific and Industrial Research Organisation (CSIRO), Australia
P. V. Vara Prasad, Kansas State University, United States

Citation: Yuan, Z., Chen, Y., Palta, J. A., Prasad, P. V. V., eds. (2020). Adaptation of Dryland Plants to a Changing Environment. Lausanne: Frontiers Media SA.
doi: 10.3389/978-2-88963-315-9

Table of Contents

frontiers in Plant Science

EDITORIAL
published: 08 October 2019
doi: 10.3389/fpls.2019.01228

Editorial: Adaptation of Dryland Plants to a Changing Environment

Zhiyou Yuan[1,2], Yinglong Chen[1,2,3], Jairo A. Palta[3,4] and P. V. Vara Prasad[5]*

[1] State Key Laboratory of Soil Erosion and Dryland Farming on the Loess Plateau, Northwest A&F University, Yangling, China, [2] State Key Laboratory of Soil Erosion and Dryland Farming on the Loess Plateau, Institute of Soil and Water Conservation, Chinese Academy of Sciences and Ministry of Water Resources, Yangling, China, [3] The UWA Institute of Agriculture and School of Agriculture and Environment, The University of Western Australia, Perth, WA, Australia, [4] CSIRO Agriculture & Food, Wembley, WA, Australia, [5] Department of Agronomy, Kansas State University, Manhattan, KS, United States

Keywords: future climates, drylands, ecosystem functioning, global change, plant adaptation, vegetation dynamics

Editorial on the Research Topic

Adaptation of Dryland Plants to A Changing Environment

Currently, the earth is undergoing rapid and major environmental changes mostly because of anthropogenic activities (IPCC, 2014). The biogeochemical cycles and the structure and function of ecosystems in several regions of the world are being substantially changed due to water scarcity and climate change (Koutroulis, 2019). The dryland ecosystem, which covers 40–50% of earth's terrestrial surface and is home to more than a third of the world's human population (Mortimore et al., 2009; Schimel, 2010), is being dramatically affected the most. The changes in the environment are not only amplifying the pressure exerted on the drylands but also placing new challenges (Gonzalez-Megias and Menendez, 2012; Reed et al., 2012; Koutroulis, 2019). The effect of such human-caused environmental changes is already recognizable in the responses and dynamics of dryland ecosystems (e.g., Maestre et al., 2015; Butterfield and Munson, 2016; Schlaepfer et al., 2017). The adaptation of dryland plants and their development, fitness, and competitiveness in a changing environment, however, are currently poorly understood. There is no doubt that scientists need to improve their understanding of the mechanisms of plant adaptation and the processes that are triggered by human-driven changes to the environment and provide that information to policy makers and dryland managers to develop strategies for sustainable management of dryland ecosystems. The studies included in this research topic examined how dryland plants respond and evolve in a changing environment. Addressing questions on the impact of environmental change on drylands, with a particular focus on drought (limited water) and heat (high temperature), not only offers new perspectives but also provides ideas and outlines critical challenges that need to be researched.

Typically, the ecological understanding of the response to environmental conditions and changes rely on three approaches: (i) manipulative experiments, (ii) long-term observational records by monitoring the response to ambient environmental fluctuations using repeat sampling of plots, and (iii) space-for-time substitutions derived from sampling along environmental gradients and across time scales. The three approaches are valuable but sometimes produce inconsistent estimates of the magnitude of plant community response to environmental changes (Yuan et al., 2017; Barner et al., 2018; Knapp et al., 2018). There is therefore a need for using a combination of experimental, monitoring, and gradient approaches to provide different insights on the response to environmental changes. This research topic brings together the results from a number of studies exploring plant adaptation to a changing environment in drylands using such different methods.

Six of the 12 articles in the issue deal with manipulative experiments, an ongoing commonly used approach in ecology research. They address a variety of topics, notably the responses of a vast range

OPEN ACCESS

Edited and reviewed by:
William Walter Adams III, University of Colorado Boulder, United States

****Correspondence:***
Zhiyou Yuan
zyyuan@ms.iswc.ac.cn

Specialty section:
This article was submitted to Plant Abiotic Stress, a section of the journal Frontiers in Plant Science

Received: *22 August 2019*
Accepted: *04 September 2019*
Published: *08 October 2019*

Citation:
Yuan Z, Chen Y, Palta JA and Prasad PVV (2019) Editorial: Adaptation of Dryland Plants to a Changing Environment. Front. Plant Sci. 10:1228. doi: 10.3389/fpls.2019.01228

of dryland plant species to experimental drought (Mahajan et al.; Wang et al; Li et al.) and nutrient addition (Cui et al.). Mahajan et al. quantified the impact of moisture stress on the physiological changes and reproductive capacity of emerging problematic weed species (*Sisymbrium thellungii*) to understand reasons for its spread and develop appropriate management strategies. Wang et al. measured the performance of root systems of two contrasting plant species (*Bothriochloa ischaemum*, C_4 herbaceous species, and *Lespedeza davurica*, C_3 leguminous species) under different soil moisture regimes to understand interactions between the shrub–grass species. Cui et al. measured the N response of two temperate desert plant species (*Malcolmia africana*, an ephemeral, and *Salsola affinis*, an annual) to understand their aboveground and belowground growth performance and N retention, thus helping understand the relative competitiveness and species composition under different environmental conditions. Li et al. conducted experiments to understand the interaction between endophytes isolated from desert plants on the performance of *Hedysarum scoparium* under different soil water conditions. They observed that endophytes established a positive symbiosis and further enhanced the biomass and antioxidant activities of the host plant particularly under water-deficit conditions.

The study of Zhou et al. reviewed leaf gas exchange in response to experimental drought in drylands and provides new information on the responses of plant function to drought, highlighting the importance of linking plant traits and particularly the correlation between hydraulic conductivity and photosynthesis. In their study in northern China, Liu et al. describe the effects of defoliation caused by animal grazing and hay production on plant regrowth and conclude that resource reallocation is specific to species. In drylands, particularly in deserts, plants and their seeds often experience various degrees of sand burial and exposure to wind erosion. Plant adaptation to these environmental stresses is thus critical for successful seed germination, seedling emergence, and initial establishment (Pimentel and Kounang, 1998). The study of Fan et al. showed that desert shrubs take a bet-hedging strategy to adapt to such arid environments. All of these studies report significant changes in the processes of dryland plants responding to various experimental treatments, highlighting the importance of even a tiny alteration of environments in drylands for their functioning. Therefore, the studies on this research topic could provide a powerful tool to establish cause–effect relationships and to test specific hypotheses regarding the impacts of environmental change.

In the study of Haberstroh et al. terpenoid emissions from two woody species that have developed photoprotective mechanisms to adapt to environmental pressures associated with Mediterranean climate were monitored. Gang et al. monitored drought conditions in China's drylands over 12 years and found that the carbon assimilated and the water used by dryland forests were more affected by drought than in dryland grasslands. Yan et al. investigated the possible drought-related patterns of plant functional traits across a macroecological gradient, that is, a precipitation transect where they sampled 39 dominant species in 22 sites in the Inner Mongolian grassland, finding that dryland plants have adapted to drought in four different ways. Fang et al. focused on the variation in plant/soil carbon, nitrogen, and phosphorus stoichiometry along a latitudinal gradient of ~500 km in northern China's drylands. Both studies demonstrate that environmental changes are likely to affect plant cover, community composition, and functional traits. The studies also highlight that environmental change can cause significant impacts on drylands. By analyzing 720 soil samples from 72 paired sites in northeastern China, Wu et al. discuss the role of deep soils on dryland plants at a large geographic scale.

The research described in this research topic highlights the various mechanisms underlying the potential response of dryland plants to a changing environment, dependent on the component considered and the amount and duration of the abiotic or biotic stress. The plant-soil-environment feedback, together with other disturbances, might lead to functional alterations of ecosystem resilience in drylands. Short- and long-term adaptations may differ, which is why experiments, monitoring, and gradient observations are needed (Elmendorf et al., 2015; Yuan and Chen, 2015; Blume-Werry et al., 2016; Yuan et al., 2017). In particular, long-term environmental changes could result in a new stable state of the dryland ecosystem, and its structural persistence might strongly depend on the adaptive capacity/plasticity of individuals and populations to environmental impacts. As shown in this special issue, drylands are inhabited by many species that respond in different ways to a changing environment. Undoubtedly, the broad range of articles in this research topic could deepen our current understanding of ecological mechanisms by which plants respond and adapt to environmental changes in dryland ecosystems. This topic still remains as a frontier in plant science with an urgent need to be understood to predict the impacts of environmental changes on drylands.

AUTHOR CONTRIBUTIONS

ZY organized the research topic together with YC, JP, and PP. ZY wrote the first draft of the editorial, with all coauthors jointly editing the final version.

FUNDING

This work was supported by the National Key Research and Development Program of China (2016YFA0600801) and the National Natural Sciences Foundation of China (31570438) toZY, Chinese Academy of Sciences' "100 Talent" Program to ZY and YC.

ACKNOWLEDGMENTS

We thank the authors, reviewers, and the Frontiers Editorial Office for their support in creating this research topic.

REFERENCES

Barner, A. K., Coblentz, K. E., Hacker, S. D., and Menge, B. A. (2018). Fundamental contradictions among observational and experimental estimates of non-trophic species interactions. *Ecology* 99, 557–566. doi: 10.1002/ecy.2133

Blume-Werry, G., Kreyling, J., Laudon, H., and Milbau, A. (2016). Short-term climate change manipulation effects do not scale up to long-term legacies: effects of an absent snow cover on boreal forest plants. *J. Ecol.* 104, 1638–1648. doi: 10.1111/1365-2745.12636

Butterfield, B. J., and Munson, S. M. (2016). Temperature is better than precipitation as a predictor of plant community assembly across a dryland region. *J. Veg. Sci.* 27, 938–947. doi: 10.1111/jvs.12440

Elmendorf, S. C., Henry, G. H. R., Hollister, R. D., Fosaa, A. M., Gould, W. A., Hermanutz, L., et al. (2015). Experiment, monitoring, and gradient methods used to infer climate change effects on plant communities yield consistent patterns. *Proc. Natl. Acad. Sci. U. S. A.* 112, 448–452. doi: 10.1073/pnas.1410088112

Gonzalez-Megias, A., and Menendez, R. (2012). Climate change effects on above- and below-ground interactions in a dryland ecosystem. *Philos. Trans. R. Soc. B-Biol. Sci.* 367, 3115–3124. doi: 10.1098/rstb.2011.0346

IPCC. (2014). Climate Change 2014: Synthesis Report. Contribution of working groups I, II and III to the fifth assessment report of the intergovernmental panel on climate change. 151 pp. [Core Writing Team, R.K. Pachauri and L.A. Meyer (eds.)]. IPCC, Geneva, Switzerland.

Knapp, A. K., Carroll, C. J. W., Griffin-Nolan, R. J., Slette, I. J., Chaves, F. A., Baur, L. E., et al. (2018). A reality check for climate change experiments: do they reflect the real world? *Ecology* 99, 2145–2151. doi: 10.1002/ecy.2474

Koutroulis, A. G. (2019). Dryland changes under different levels of global warming. *Sci. Total Environ.* 655, 482–511. doi: 10.1016/j.scitotenv.2018.11.215

Maestre, F. T., Delgado-Baquerizo, M., Jeffries, T. C., Eldridge, D. J., Ochoa, V., Gozalo, B., et al. (2015). Increasing aridity reduces soil microbial diversity and abundance in global drylands. *Proc. Natl. Acad. Sci. U. S. A.* 112, 15684–15689. doi: 10.1073/pnas.1516684112

Mortimore, M., S. Anderson., L. Cotula., J. Davies., K. Faccer., C. Hesse., J. Morton., W. Nyangena., J. Skinner., and C. Wolfangel. (2009). Dryland Opportunities: A new paradigm for people, ecosystems and development. IUCN, Gland, Switzerland.

Pimentel, D., and Kounang, N. (1998). Ecology of soil erosion in ecosystems. *Ecosystems* 1, 416–426. doi: 10.1007/s100219900035

Reed, S. C., Coe, K. K., Sparks, J. P., Housman, D. C., Zelikova, T. J., and Belnap, J. (2012). Changes to dryland rainfall result in rapid moss mortality and altered soil fertility. *Nat. Clim. Chang.* 2, 752–755. doi: 10.1038/nclimate1596

Schimel, D. S. (2010). Drylands in the Earth system. *Science* 327, 418–419. doi: 10.1126/science.1184946

Schlaepfer, D. R., Bradford, J. B., Lauenroth, W. K., Munson, S. M., Tietjen, B., Hall, S. A., et al. (2017). Climate change reduces extent of temperate drylands and intensifies drought in deep soils. *Nat. Commun.* 8, e14196. doi: 10.1038/ncomms14196

Yuan, Z. Y., and Chen, H. Y. H. (2015). Decoupling of nitrogen and phosphorus in terrestrial plants associated with global changes. *Nat. Clim. Chang.* 5, 465–469. doi: 10.1038/nclimate2549

Yuan, Z. Y., Jiao, F., Shi, X. R., Sardans, J., Maestre, F. T., Delgado-Baquerizo, M., et al. (2017). Experimental and observational studies find contrasting responses of soil nutrients to climate change. *eLife* 6, e23255. doi: 10.7554/eLife.23255

Conflict of Interest: The authors declare that the research was conducted in the absence of any commercial or financial relationships that could be construed as a potential conflict of interest.

frontiers in Plant Science

ORIGINAL RESEARCH
published: 23 July 2018
doi: 10.3389/fpls.2018.01071

Terpenoid Emissions of Two Mediterranean Woody Species in Response to Drought Stress

Simon Haberstroh[1,2], Jürgen Kreuzwieser[1], Raquel Lobo-do-Vale[2], Maria C. Caldeira[2], Maren Dubbert[1] and Christiane Werner[1]*

[1] Ecosystem Physiology, University of Freiburg, Freiburg, Germany, [2] Centro de Estudos Florestais, Instituto Superior de Agronomia, Universidade de Lisboa, Lisbon, Portugal

Drought is a major environmental constrain affecting plant performance and survival, particularly in Mediterranean ecosystems. Terpenoids may play a protective role under these conditions, however, observations of drought effects on plant terpenoid emissions are controversial ranging from decreased emissions to unaffected or increased release of terpenoids. In the present study we investigated terpenoid emissions of cork oak (*Quercus suber*) and gum rockrose (*Cistus ladanifer*) in response to summer drought stress in 2017. Pre-dawn leaf water potential (Ψ_{PD}) decreased from −0.64 to −1.72 MPa in *Q. suber* and from −1.69 to −4.05 MPa in *C. ladanifer*, indicating a transition from mild to severe drought along summer. Total terpenoid emissions decreased with drought, but differed significantly between species ($p < 0.001$) and in response to Ψ_{PD}, air temperature and assimilation rates. *C. ladanifer* emitted a large variety of >75 compounds comprising monoterpenes, sesquiterpenes and even diterpenes, which strongly decreased from 1.37 ± 0.23 μg g^{-1} h^{-1} to 0.40 ± 0.08 μg g^{-1} h^{-1} ($p < 0.001$) in response to drought. Total emission rates were positively correlated to air temperature ($p < 0.001$). *C. ladanifer* behavior points toward terpenoid leaf storage depletion and reduced substrate availability for terpenoid synthesis with increasing drought, most likely accelerated by high air temperatures. *Q. suber* emitted mainly monoterpenes and emissions declined significantly from June (0.50 ± 0.08 μg g^{-1} h^{-1}) to August (0.29 ± 0.02 μg g^{-1} h^{-1}) ($p < 0.01$). Emission rates were weakly correlated with net assimilation rates ($R^2 = 0.19$, $p < 0.001$), but did not respond strongly to Ψ_{PD} and air temperature. Early onset of drought in 2017 most likely reduced plant metabolism in *Q. suber*, resulting in diminished, but stable terpenoid fluxes. Calculation of standard emission factors (at 30°C) revealed contrasting emission patterns of decreasing, unaffected, or increasing fluxes of single terpenoid compounds. Unaffected or drought-enhanced emissions of compounds such as α-pinene, camphene or manoyl oxide may point toward a specific role of these terpenoids in abiotic stress adaptation. In conclusion, these results suggest a strong negative, but species- and compound-specific effect of severe drought on terpenoid fluxes in Mediterranean ecosystems.

Keywords: BVOC, drought stress, adaptation, Mediterranean ecosystems, *Quercus suber*, *Cistus ladanifer*

OPEN ACCESS

Edited by:
Jairo A. Palta, Commonwealth Scientific and Industrial Research Organisation (CSIRO), Australia

Reviewed by:
Carsten Kulheim, Australian National University, Australia
Celia Faiola, University of California, Irvine, United States

****Correspondence:***
Simon Haberstroh
simon.haberstroh@cep.uni-freiburg.de

Specialty section:
This article was submitted to Plant Abiotic Stress, a section of the journal Frontiers in Plant Science

Received: *30 April 2018*
Accepted: *02 July 2018*
Published: *23 July 2018*

Citation:
Haberstroh S, Kreuzwieser J, Lobo-do-Vale R, Caldeira MC, Dubbert M and Werner C (2018) Terpenoid Emissions of Two Mediterranean Woody Species in Response to Drought Stress. Front. Plant Sci. 9:1071. doi: 10.3389/fpls.2018.01071

INTRODUCTION

Vegetation exerts a strong impact on atmospheric trace gasses, e.g., by buffering the effect of elevated CO_2 through enhanced carbon sequestration, but inversely by emitting a diverse array of reactive hydrocarbons to the atmosphere. These biogenic volatile organic compounds (BVOC) are involved in a variety of functions in plants such as defense, reproduction or adaptation to stressful conditions (Kesselmeier and Staudt, 1999; Possell and Loreto, 2013). Terrestrial vegetation is estimated to emit around 1000 Tg carbon per year as BVOC (Guenther et al., 2012). Once released into the atmosphere BVOCs are highly reactive and exert a strong influence on atmospheric chemistry and air quality (Atkinson and Arey, 2003; Loreto et al., 2014), as they are involved in tropospheric ozone production, aerosol formation and ultimately influence climate (Holopainen and Gershenzon, 2010). BVOCs include a variety of chemical compounds such as terpenoids, alkanes, alkenes, alcohols, esters, carbonyls, or organic acids (Kesselmeier and Staudt, 1999; Dudareva et al., 2013), with terpenoids being the largest and most diverse cluster (Tholl, 2015). Terpenoids are organic substances all sharing a common C5 building block synthesized via the plastidic 2-C-methyl-D-erythritol 4-phosphate (MEP) pathway or the cytosolic mevalonic acid (MVA) pathway (Vickers et al., 2009; Tholl, 2015). Further transformation of C5 building blocks results in a large variety of compounds such as hemiterpenes (C5), monoterpenes (C10), sesquiterpenes (C15), diterpenes (C20), and terpenoids with even higher molecular mass (Vickers et al., 2009). Hemiterpenes, monoterpenes, and sesquiterpenes are considered to be volatile compounds as they have a high vapor pressure (Dudareva et al., 2006; Loreto et al., 2014). Diterpenes on the other hand, are either considered semi- or non-volatile (Niinemets, 2010; Loreto et al., 2014), but have recently been reported in terpenoid emissions of Mediterranean shrub species (Yáñez-Serrano et al., 2018). Especially emissions of the hemiterpene isoprene are thought to have a large influence on various protective mechanisms against abiotic and biotic stresses (Kesselmeier and Staudt, 1999; Loreto et al., 2014). In non-isoprene emitting plants, monoterpenes and sesquiterpenes are assumed to fulfill similar functions (Vickers et al., 2009; Loreto et al., 2014). These compounds act, for example, as membrane stabilizers, antioxidants or signal substances (Peñuelas et al., 2005; Vickers et al., 2009; Possell and Loreto, 2013).

While the response of BVOC emissions to abiotic factors such as temperature or light is well described (e.g., Kesselmeier and Staudt, 1999), results regarding their response to drought stress are more controversial (Staudt et al., 2002; Ormeno et al., 2007; Lluisà et al., 2016). Several studies suggest, that the intensity of stress appears to be the key predictor for emissions, as mild stress increases emissions, while they strongly decrease under severe drought (Ormeno et al., 2007; Lluisà et al., 2016). These emission patterns are often related to a decline in photosynthetic activity induced by prolonged drought (Lavoir et al., 2009). However, it is of high importance to comprehend the BVOC emission pattern of plants and ecosystems to drought stress, as the uncertainty of stress response strongly limits the reliability of models predicting BVOC emissions and, thus, projections of future emissions and impact on atmospheric chemistry (Niinemets, 2010; Guenther et al., 2012).

A region which is considered to contribute substantially to those uncertainties is the Mediterranean basin, where climate change impacts are already visible, such as prolonged drought periods and heat waves (Costa et al., 2010; Caldeira et al., 2015). Mediterranean ecosystems are characterized by pronounced summer drought and are, due to co-occurring high light intensities and air temperatures, strong BVOC emitters (Seco et al., 2011). Recent studies and models regarding climate change report an increasing risk of prolonged drought periods due to changed precipitation patterns and rising temperatures (Páscoa et al., 2017). Consequently, climate change will most likely influence BVOC emissions of Mediterranean ecosystems significantly. An excellent model system to study BVOC emission patterns in this regard are savannah type, man-made cork oak (*Quercus suber*) ecosystems, also called "montados" or "dehesas". Given their large distribution, especially in the Iberian Peninsula (David et al., 2007), montado BVOC emissions may potentially affect regional atmospheric chemistry. In some areas, these socio-economically and ecologically important ecosystems are threatened by the invasion of shrubs such as gum rockrose (*Cistus ladanifer*), often as a result of land abandonment (Bugalho et al., 2011). While this native shrub itself has a high potential for BVOC emissions (Alías et al., 2012), it competes with *Q. suber* and *Q. ilex*, thereby reducing water and carbon fluxes, as well as resilience and resistance of trees (Rolo and Moreno, 2011; Caldeira et al., 2015). However, while we are only at the beginning of understanding the interaction between invasive species and native trees under drought (Rascher et al., 2011; Caldeira et al., 2015), even less is known, on how BVOC emissions of these different plant types respond to severe drought. To this end, we aim to shed new light onto the emission patterns of *Q. suber* and *C. ladanifer* under natural conditions in response to drought stress. We focus on terpenoids, since this BVOC class has been shown to play a vital role in plant stress responses (e.g., Dudareva et al., 2006). *Q. suber* is regarded as monoterpene emitter (Staudt et al., 2004, 2008; Pio et al., 2005; Bracho-Nunez et al., 2013) with a large intraspecific variability in emissions (Loreto et al., 2009). The lack of specialized storage organs for terpenoids indicates a high dependency of emissions on photosynthetic activity and light intensity (Loreto et al., 1996; Kesselmeier and Staudt, 1999). *C. ladanifer*, on the other hand, also emits monoterpenes (Pio et al., 1993), but possesses secretarial trichomes on its leaf surfaces, where terpenoids are accumulated (Gülz et al., 1996). This species has the potential to emit substantial amounts of monoterpenes, sesquiterpenes, and diterpenes (Yáñez-Serrano et al., 2018), which is in line with reported high terpenoid contents in essential oils of this species (Gomes et al., 2005; Verdeguer et al., 2012). Significant isoprene emissions have neither been detected from *Q. suber,* nor from *C. ladanifer* (Pio et al., 1993, 2005; Staudt et al., 2004). However, little is known on the influence of environmental drivers on terpenoid emissions of these species, particularly in response to prolonged summer drought. In this regard, we hypothesize that (i) the terpenoid emissions of *Q. suber* and *C. ladanifer* may rise with mild drought stress, but significantly

decrease with severe plant water deficit, and that (ii) the emission patterns and emitted terpenoid compounds differ between the two investigated species.

MATERIALS AND METHODS

Experimental Set-Up and Study Site

The effects of drought stress on terpenoid emissions were studied in a cork oak ecosystem partially invaded by the native shrub *C. ladanifer* in Vila Viçosa (Alentejo, 38° 47′ N, 7° 22′ W, 430 m a.s.l.), Portugal. The climate is characterized as typical Mediterranean with mild winters and a mean annual temperature of 15.9°C[1] (Instituto Português do Mar e da Atmosfera [IPMA], 1981–2010). The bulk of the mean annual precipitation of 585 mm falls in winter, which leads to a distinct period of drought in summer (Caldeira et al., 2015). *Q. suber* is an evergreen tree belonging to the Eurasian subgenus *Cerris* and expressing a high intraspecific variability in plant traits (Manos et al., 1999; Loreto et al., 2009). Trees are adapted to the Mediterranean climate and withstand summer drought mainly by accessing deep water resources, hydraulic lift and stomatal control of transpiration (David et al., 2007; Grant et al., 2010). *C. ladanifer* is a woody semi-deciduous shrub belonging to the family Cistaceae which is well distributed in the Mediterranean Basin (Núñez-Olivera et al., 1996; Frazao et al., 2018). High growth rates and water-use-efficiency characterize this species (Correia et al., 1987; Werner et al., 1999; Correia and Ascensao, 2016). The density of *Q. suber* in this ecosystem is 160 ± 18.6 trees per ha. Shrubs form a dense understorey in monoculture (21,667 ± 2602 shrubs per ha), suppressing any other vegetation. Trees are approximately 6.6 ± 0.5 m high and on average 50 years old. The even aged *C. ladanifer* shrub layer reaches 2–3 m in height at an average age of 15 years. The soils are about 0.4 m deep with a high proportion of gravel, derived from schist and classified as haplic Leptosol (FAO, 2006). Terpenoid sampling and gas exchange measurements were conducted during three field campaigns in 2017 from 14 – 16 June, 11 – 13 July, and 2 – 4 August. Those dates usually represent three divergent phases of plant water status in the Mediterranean climate: (1) pre-drought period (2) onset of drought stress and (3) severe drought period (e.g., Otieno et al., 2006). All sampling days were characterized by stable weather conditions and clear skies. Measurements of meteorological conditions, water availability, sap flux density and leaf water potential were already started in May to characterize the meteorological and ecophysiological conditions prior to the terpenoid sampling.

Meteorological Conditions and Water Availability

Meteorological parameters such as air temperature, relative humidity, precipitation and photosynthetically active photon flux density (PPFD) were retrieved continuously from a meteorological station installed on a scaffold tower and stored half-hourly on a data logger (DL2e, Delta-T Devices Ltd., Cambridge, United Kingdom). Vapour pressure deficit (VPD) was calculated from half-hourly values of air temperature and relative humidity. Further meteorological data was retrieved from a meteorological station nearby[1] (Instituto Português do Mar e da Atmosfera [IPMA], 1981–2010). Volumetric soil water content from four different depths (0.1, 0.2, 0.3, and 0.4 m) was measured continuously with EC-10 probes (Decagon Devices, Pullman, WA, United States) in four profiles and stored half-hourly on a data logger (CR10X and AM16/32 multiplexer, Campbell Scientific, Logan, UT, United States).

Ecophysiological Parameters

To determine the water status and overall physiological performance of the sampled plants, several ecophysiological parameters were measured during the field campaigns. Seven shrubs and nine trees were included to allow for a more robust identification of differences between species. Pre-dawn (Ψ_{PD}) and midday (Ψ_{MD}) leaf water potential measurements of *Q. suber* and *C. ladanifer* were conducted with a Scholander-type pressure chamber (PMS 1000, PMS Instruments, Corvalis, Oregon, OR, United States) between 3 and 6 am and 1 and 3 pm, respectively. Ψ_{50} for *Q. suber* and *C. ladanifer* was retrieved from literature (Quero et al., 2011; Pinto et al., 2012) and safety margins calculated as in Choat et al. (2012) as the difference of Ψ_{MD} and Ψ_{50}. Ψ_{50} corresponds to the value where plants have already lost 50% of their hydraulic conductivity, and is considered to be a critical value, as surpassing this margin will likely result in persistent xylem damage and negative long-term effects (Choat et al., 2012). Sap flux density was measured continuously on site with Granier-type thermal dissipation probes (TDP30 sensors, Dynamax, Texas, United States) for seven trees as described in Caldeira et al. (2015). Thermal dissipation probes were installed radially at breast height with a north-west orientation to minimize the influence of external environmental factors on measurements. Due to the small diameter of the stems of *C. ladanifer*, sap flow of shrubs ($n = 4$) was measured via sap flow gauges (SGA13, Dynamax, Texas, United States) using the stem heat balance method of Sakuratani (1984). Measurements of terpenoids were not conducted on individuals with sap flow gauges, but on neighboring plants which were growing under the same conditions. Values for sap flow gauges and thermal dissipation probes were recorded every minute and stored as 30-min average on a data logger (CR1000 and AM16/32 multiplexer, Campbell Scientific, Logan, UT, United States). For determination of functional sap wood area of trees and shrubs, installation and protection of sensors see Caldeira et al. (2015). Gas exchange parameters such as net CO_2 assimilation rate and stomatal conductance were recorded with a LI-6400XT portable photosynthesis system (LI-COR Inc., Nebraska, United States) with a light source and CO_2 mixer. Measurements were conducted on sun exposed leaves of both species in the morning between 8 and 9 am and during midday between 1 and 2 pm. PPFD was set to 1200 μmol $m^{-2}s^{-1}$ for sun leaves, which is known to be saturating for photosynthesis (Tenhunen et al., 1985). CO_2-concentration in the chamber was set to 400 ppm; relative humidity and leaf temperature followed ambient values. The

[1] www.ipma.pt

flow through the system was set to 500 ml min^{-1}. Due to the inaccessibility of leaves at the height of the sunlit tree canopy, large branches were cut and leaves immediately measured. Tests were previously performed, indicating stable gas exchange readings for about 2 min after cutting (Lobo-do-Vale et al., 2017, unpublished data). In rare cases of stomatal closure new branches were sampled. *C. ladanifer* and *Q. suber* leaves not filling the cuvette (6 cm^2) completely were taken and measured for actual leaf area with a customary scanner (EPSON EXPRESSION 1680) and analyzed with the software WinSEEDLE (Regent Instruments Inc., Canada) in the laboratory. Afterwards, gas exchange was corrected for the obtained leaf area.

Terpenoid Sampling

On each BVOC sampling day, terpenoids were measured on up to four different twigs of the same individual. In total, eight *Q. suber* and four *C. ladanifer* individuals were selected for measurements. Care was taken that always the same individuals were chosen. Selected twigs included visually healthy current or last year leaves 2 – 3 m above ground for *Q. suber* and 0.3 – 1 m above ground for *C. ladanifer*. Twigs from the lower part of the open tree canopies had to be selected for terpenoid sampling, due to constrains regarding the accessibility of the tree crown and to avoid condensation problems arising in fully sunlit enclosures in both species. Where necessary, twigs were shielded with neutral density meshes to avoid direct sunlight causing condensation due to enhanced transpiration and to assure a comparable sampling treatment. Terpenoids were collected using a dynamic enclosure system. Selected twigs were placed in custom-made enclosures (∼460 ml volume), which were made of chemically inert Nalophan foil (Bratschlauch, Toppits®, Minden, Germany) (Kessler et al., 2015) and perfluoroalkoxy (PFA) tubing (Swagelok, Karlsruhe, Germany). The outlets were connected via PFA tubing to air sampling pumps (210-1003MTX, SKC, Germany), to minimize terpenoid losses due to reactions and/or adsorption to enclosure walls and tubing. For emission measurement, twigs with 4–26 leaves were carefully placed into the enclosures, which were slightly, but not completely closed to allow non-treated, ambient air to enter the system. Prior to terpenoid sampling, enclosured twigs were flushed thoroughly for approximately 5 min to allow the leaves to acclimate to the new conditions. Subsequently, adsorbent tubes filled with polydimethylsiloxane (PDMS) foam (GERSTEL GmbH & Co. KG, Müllheim a.d. Ruhr, Germany) were installed between the outlet of the enclosure and the air sampling pumps for terpenoid trapping. During sampling, adsorbent tubes were covered with aluminum foil. The sampling time was set to 60 – 90 min at a flow rate of 200 ml min^{-1}. In addition, controls with empty enclosures were installed approximately 2 m above ground and sampled concurrently to correct for ambient terpenoid concentrations. Immediately after sampling, twigs were cut and gas exchange was measured at a PPFD of 300 μmol m^{-2} s^{-1} to match the light conditions of terpenoid measurements under shaded conditions. Leaves were stored in a cooler bag for the determination of leaf area (see above) and dry leaf weight; adsorbent tubes were also stored cool before taking them to the laboratory, where they were kept at 4°C in Labco Exetainers (Labco Limited, Lampeter Ceredigion, United Kingdom) to avoid external influences until the analysis. For the determination of dry leaf weight, leaves were dried at 65°C for 48 h and weighed. The whole terpenoid sampling procedure was conducted between 8 am and 3 pm on each sampling day.

Terpenoid Analysis

Terpenoids were analyzed on a gas chromatograph (GC, model 6890A, Agilent Technologies Böblingen, Germany) connected to a mass-selective detector (MSD, 5975C, Agilent Technologies Böblingen, Germany) and equipped with a thermodesorption/cold injection system (TDU-CIS, Gerstel, Germany). Sampling tubes were heated to 220°C, and, thermodesorbed volatiles channeled into the cold injection system where they were cryotrapped at −50°C; subsequently the cold injection system was heated to 240°C, releasing the volatiles onto the separation column (DB-5UI, Agilent Technologies Böblingen, Germany). Helium was used as a carrier gas at a flow of 1 ml min^{-1}. The GC oven and MSD conditions as well as identification and quantification procedures are given in Kleiber et al. (2017). Briefly, the oven temperature began at 40°C, increasing at a rate of 6°C min^{-1} until 100°C were reached, thereafter the temperature ramp speeded up to 16°C min^{-1} until the oven was heated up to 230°C. The MSD was run at 70 eV at an ion source temperature of 230°C and a quadrupole temperature of 150°C. Retention index (RI) values were calculated using the tool of Lucero et al. (2009). As standards, the monoterpenes α-pinene, β-pinene, limonene and 1,8-cineole, the sesquiterpene caryophyllene and the diterpene ent-16-kaurene were chosen to quantify the final concentration of measured terpenoids. The mass spectra were analysed with the MassHunter Software (Agilent Technologies Böblingen, Germany). Measured terpenoid flux rates (E_m) in μg g^{-1} h^{-1} were calculated with equation 1:

$$E_m = \frac{(c_o - c_i)}{d_w * t} \quad (1)$$

where c_o (μg) is the terpenoid concentration in plant enclosures, c_i (μg) is the terpenoid background concentration in control samples, d_w (g) is the dry weight of leaves and t (h) is the sampling time. Terpenoids were grouped into monoterpenes (MT), oxygenated monoterpenes (MTO), sesquiterpenes (SQT), and diterpenes (DT). To account for the temperature dependence of emissions, standard emissions factors (E_s) were calculated using equation 2 (Guenther et al., 1993) to standardize measured emission rates (E_m) to a standard temperature (T_s) of 30°C, by:

$$E_m = E_s \ exp\ [\beta\,(T - T_s)] \quad (2)$$

where T (°C) is the ambient temperature during the terpenoid sampling, T_s is the standard temperature (30°C) and β (°C^{-1}) is an empirical temperature coefficient varying for different terpenoids. E_s (μg C g^{-1} h^{-1}) were calculated for all terpenoid compound groups and single compounds the same way for both species.

Statistical Analysis

To identify significant differences in terpenoid emission rates, standard emission factors and ecophysiological parameters between species and over time, two-way repeated measure analysis of variance (RMANOVA) were performed and *post hoc* Tukey's test applied when statistical differences were found. If the assumptions for ANOVA were not met (normal distribution, equality of variances), the data was transformed. Data was tested for normal distribution with the Shapiro–Wilks test. Terpenoid emission rates, standard emission factors, leaf water potential, sap flux density and gas exchange data were either log- or square root transformed. Sap flux density was fitted with a non-parametric smoothing kernel regression for plotting purposes. To test for correlations of environmental factors with terpenoid emissions, linear and exponential regressions were performed. Heat maps were created using the packages 'MetaboAnalystR' and 'pheatmap' in R. 'MetaboAnalystR' was used to log-transform and cluster emission data (method: 'complete') to identify similar emission patterns over time for single terpenoid compounds. The package 'pheatmap' allowed to produce publication ready heat maps. For statistical analysis and plots of terpenoid emissions only parameters of the measured plant individuals were used. Graphical plots except heat maps were created with SigmaPlot (version 14, Systat, United States). Statistical analysis and heat maps were conducted with the statistical software R (version 3.3.1 for Windows 10).

RESULTS

Meteorological Conditions and Plant Water Status

Meteorological conditions in spring and summer 2017 were characterized by an early onset of drought due to rapidly rising air temperatures and only minor precipitation events (**Figure 1**). In general, all three sampling dates fell into heat waves with air temperatures and VPD reaching maximum values of 40.9°C and 6.2 kPa in June, 43.7°C and 7.9 kPa in July and 39.0°C and 5.3 kPa in August, respectively (**Figure 1A**). The last significant rainfall event occurred in May, thereafter soil water content declined, succeeded by only minor (<5 mm) precipitation, one occurring shortly before the second campaign in July as a short, intense convective event (**Figure 1B**). Therefore, cumulative precipitation from June to August was only 5.2 mm. The bulk of precipitation in the hydrological year fell in winter from October to February (325 mm), followed by 141 mm of rainfall from March to May prior to the terpenoid measurements. Overall precipitation of the hydrological year was 481 mm which is below the long-term average[2] of 585 mm (Instituto Português do Mar e da Atmosfera [IPMA], 1981–2010).

The decline in soil water content from mid-May onwards was visible in all soil depths (**Figure 1B**), and clearly reflected onto the plant water status of both species (**Figure 2**): a significant decrease ($p < 0.001$) in pre-dawn water potentials (Ψ_{PD}) and sap flux density ($p < 0.01$) was evident for both species from the beginning to the end of the experiment. However, clear interspecific differences were detected in response to plant water deficit. *C. ladanifer* was able to endure lower Ψ_{PD} and Ψ_{MD}, which strongly declined from June to August (from −1.69 MPa to −4.05 MPa and from −2.99 MPa to −4.67 MPa, respectively). Subsequently, safety margins at Ψ_{50}, i.e., the margin to Ψ when 50% xylem cavitation occurs, diminished by more than half. Still *C. ladanifer* maintained a significantly higher safety margin in August, compared to *Q. suber* ($p < 0.01$). The deep-rooted oak on the other hand, maintained much higher water potentials through the entire drought period. While Ψ_{PD} responded to declining water resources and approached values of Ψ_{MD} (**Figures 2A,B**), midday water potentials never declined below −2 MPa and both, Ψ_{MD} and safety margins (0.95 ± 0.04 MPa) maintained stable over time. Such isohydric behavior came at the expense of lower sap flux density, which was markedly reduced in *Q. suber* over time (**Figure 2C**). In contrast, sap flux density was significantly higher in *C. ladanifer* throughout the measurement period ($p < 0.001$). Noticeably, sap flux density rapidly declined in both species from June onwards after a peak corresponding to the last strong rainfall in the middle of May. This indicates an

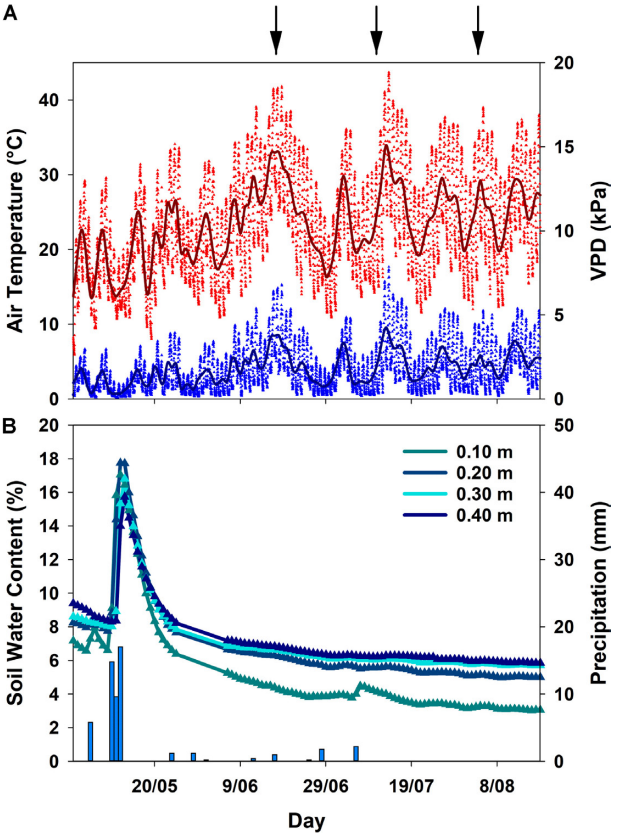

FIGURE 1 | Smoothing mean for air temperature and vapor pressure deficit (VPD) **(A)**, mean daily soil water content ($n = 4$ per depth) and total precipitation **(B)** in Vila Viçosa during the sampling period. Symbols indicate values measured half-hourly. Due to sensor failure, the period between 25 May and 6 June represents an overall trend in soil water content, but not actually measured values. Arrows indicate the sampling campaigns.

[2]www.ipma.pt

early onset of drought in June with progressive development until August.

Gas Exchange and Total Terpenoid Emissions

Carbon assimilation rates of *Q. suber* and *C. ladanifer* sun leaves illustrated two different patterns (**Figures 3A,B**). Net assimilation rates of *C. ladanifer* decreased from 9.16 ± 1.28 to 3.69 ± 1.45 μmol m^{-2} s^{-1} from June to August in the morning period (**Figure 3B**), as VPD increased and water availability declined. Stomatal conductance declined concomitantly, though not being as strongly reduced as net assimilation rates in August compared to June (**Figure 3D**). In June, *Q. suber* sun leaves showed already reduced assimilation of 6.12 ± 0.42 μmol m^{-2} s^{-1} compared to *C. ladanifer* (**Figure 3A**). However, *Q. suber* was able to maintain stable net assimilation rates over time, resulting in higher rates in August (6.71 ± 0.78 μmol m^{-2} s^{-1}) at lower stomatal conductance, compared to *C. ladanifer* (**Figures 3C,D**). Especially for *Q. suber*, a midday depression of carbon assimilation was evident, responding to rising VPD and stomatal closure. Hence, highest net assimilation rates were measured in the morning period.

Similarly, to assimilation rates and stomatal conductance, total measured terpenoid emissions differed between species. Emissions of *Q. suber* were in the range of 0.24 – 0.50 μg g^{-1} h^{-1} and decreased significantly from June to July ($p < 0.01$). Thereafter, a slight, but not significant increase in emissions occurred (**Figure 3E**). In total, 14 monoterpenes (MT), 10 oxygenated monoterpenes (MTO), and 8 sesquiterpenes (SQT) could be identified in *Q. suber*. SQT emissions decreased from 1.50 × 10^{-3} ± 5.50 × 10^{-4} μg g^{-1} h^{-1} in June to 8.84 × 10^{-5} ± 2.30 × 10^{-5} μg g^{-1} h^{-1} in August (data not shown). Overall emissions of *C. ladanifer* were in the range of 0.40 – 1.37 μg g^{-1} h^{-1} and were not only significantly higher than those of *Q. suber* ($p < 0.001$) but also more variable and diverse. Emissions decreased consistently from June to August, which was most pronounced for SQT (**Figure 3F**). In August, terpenoid emissions reached a significantly lower level ($p < 0.01$) than in previous months, comparable to the emissions of *Q. suber*. Overall, emissions comprised 14 MTs, 19 MTOs, 37 SQTs, and even 4 diterpenes (DT). Measured emissions of the DTs cembrene, manoyl oxide, verticillol and ent-16-kaurene were low at rates of 7.92 × 10^{-5} – 13.97 × 10^{-5} μg g^{-1} h^{-1}, but the exclusive presence of these species in terpenoid emissions is noticeable.

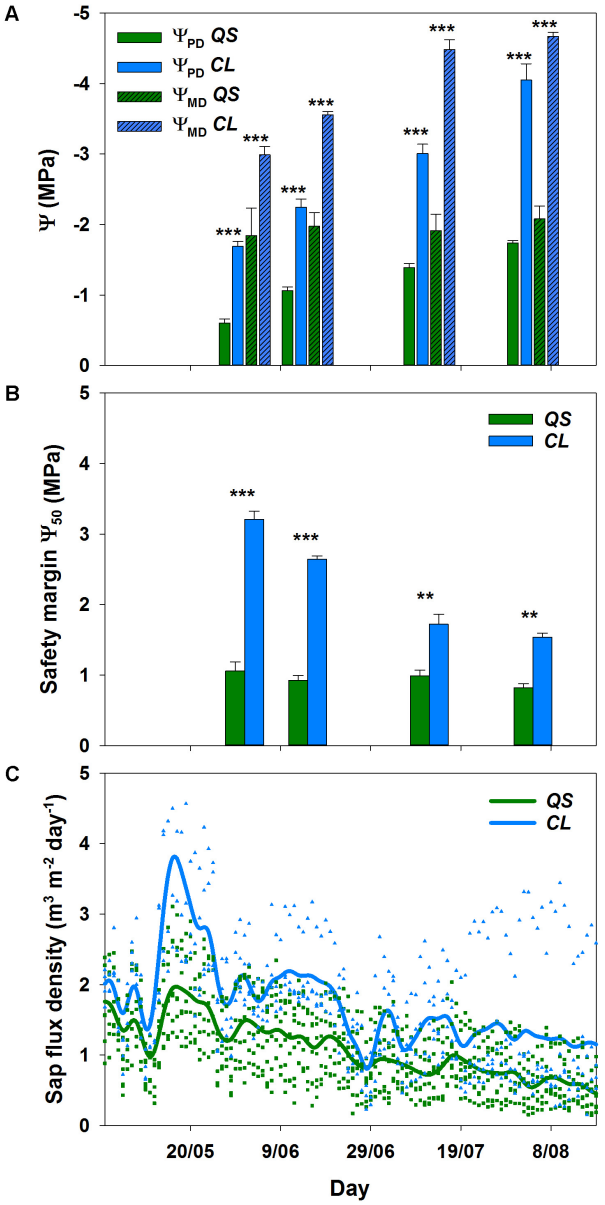

FIGURE 2 | Pre-dawn (Ψ_{PD}) and midday leaf water potential (Ψ_{MD}) for *Quercus suber* (*QS*, $n = 9$) and *Cistus ladanifer* (*CL*, $n = 7$) with standard error **(A)**. Safety margins **(B)** were calculated according to Choat et al. (2012). Sap flux density for *Q. suber* (*QS*, $n = 7$) and *C. ladanifer* (*CL*, $n = 4$) was fitted as non-parametric kernel-regression **(C)**. Symbols are the values measured for each individual. Statistical differences (RMANOVA) between species are indicated by asterisks over bars at a significance level of $^{*}p < 0.05$, $^{**}p < 0.01$, $^{***}p < 0.001$.

Correlations of Terpenoid Emission With Environmental Factors

The correlation between terpenoid emissions and environmental factors during drought differed clearly between species. *Q. suber* revealed only a slight, non-significant decrease in emissions with declining Ψ_{PD} (**Figure 4A**). Terpenoid emissions of *C. ladanifer*, on the other hand, were significantly ($p < 0.001$) negatively correlated with decreasing Ψ_{PD} (**Figure 4B**). Similarly, increasing air temperatures also exerted a significant positive influence on terpenoid emissions (**Figure 4D**). Especially in July, when the highest air temperatures occurred, the pronounced exponential increase of emissions at higher air temperatures was highly significant ($R^2 = 0.68$, $p < 0.001$). Hence, terpenoid emissions of *C. ladanifer* were temperature-standardized for further analysis to account for the variability caused by diurnal air temperature variations. Similar to Ψ_{PD}, the relationship of emissions and air temperature was weak in *Q. suber* (**Figure 4C**). At most,

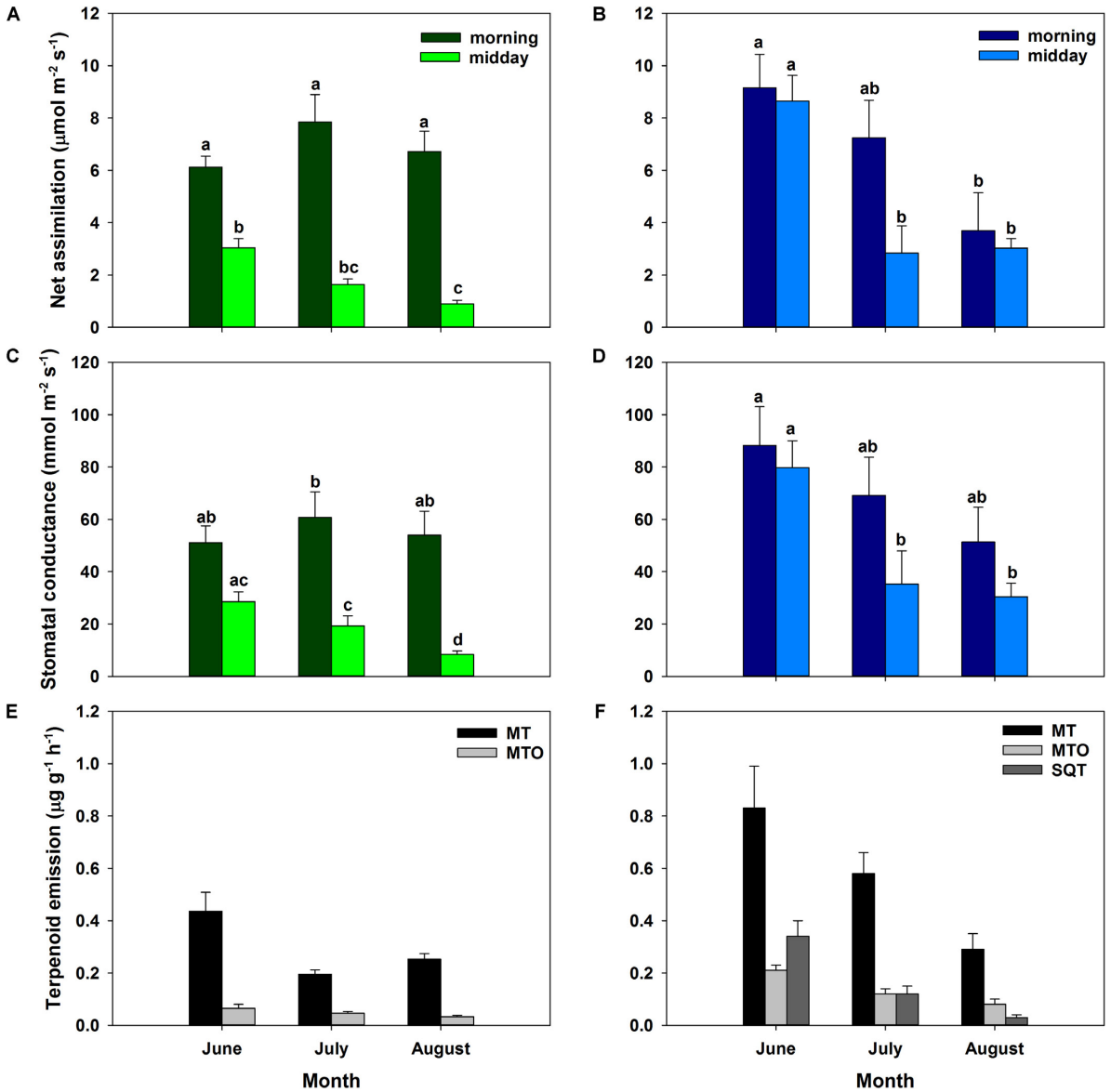

FIGURE 3 | Assimilation rates and stomatal conductance for sun leaves for *Q. suber* (left, $n = 9$, **A,C**) and *C. ladanifer* (right, $n = 7$, **B,D**) with standard error for June, July, and August field campaigns. Letters indicate statistical differences (RMANOVA) of assimilation rates and stomatal conductance between sampling periods at a significance level of $p < 0.05$ for each species separately. Average measured terpenoid emissions of *Q. suber* (left, $n = 6$ for June, $n = 8$ for July and August, **E**) and *C. ladanifer* (right, $n = 3$ for June, $n = 4$ for July and August, **F**) with standard error. Emissions are grouped into monoterpenes (MT), oxygenated monoterpenes (MTO), and sesquiterpenes (SQT).

a slight, non-significant tendency of decreasing emissions with increasing air temperature was evident in June; whereas in July and August no correlation was found. However, there was a weak, yet significant correlation of assimilation rates and stomatal conductance with terpenoid emissions of *Q. suber* (**Figures 5A,C**). Hence, more terpenoids were released at higher carbon assimilation and stomatal conductance. Due to the high degree of correlation of stomatal conductance and assimilation rates ($R^2 = 0.76$), the influence of each individual factor on terpenoid emissions is difficult to evaluate. In addition, results have to be interpreted with care as the R^2 of regressions were low (**Figures 5A,C**). *C. ladanifer* showed decreasing carbon assimilation and stomatal conductance in the sampling period, yet no correlation with standardized or measured terpenoid emissions was found (**Figures 5B,D** and Supplementary Figures 1A,B).

Standard Emission Factors of Single Terpenoid Compounds

To allow for a better comparability of emission rates with progressing drought, standard emission factors at an air

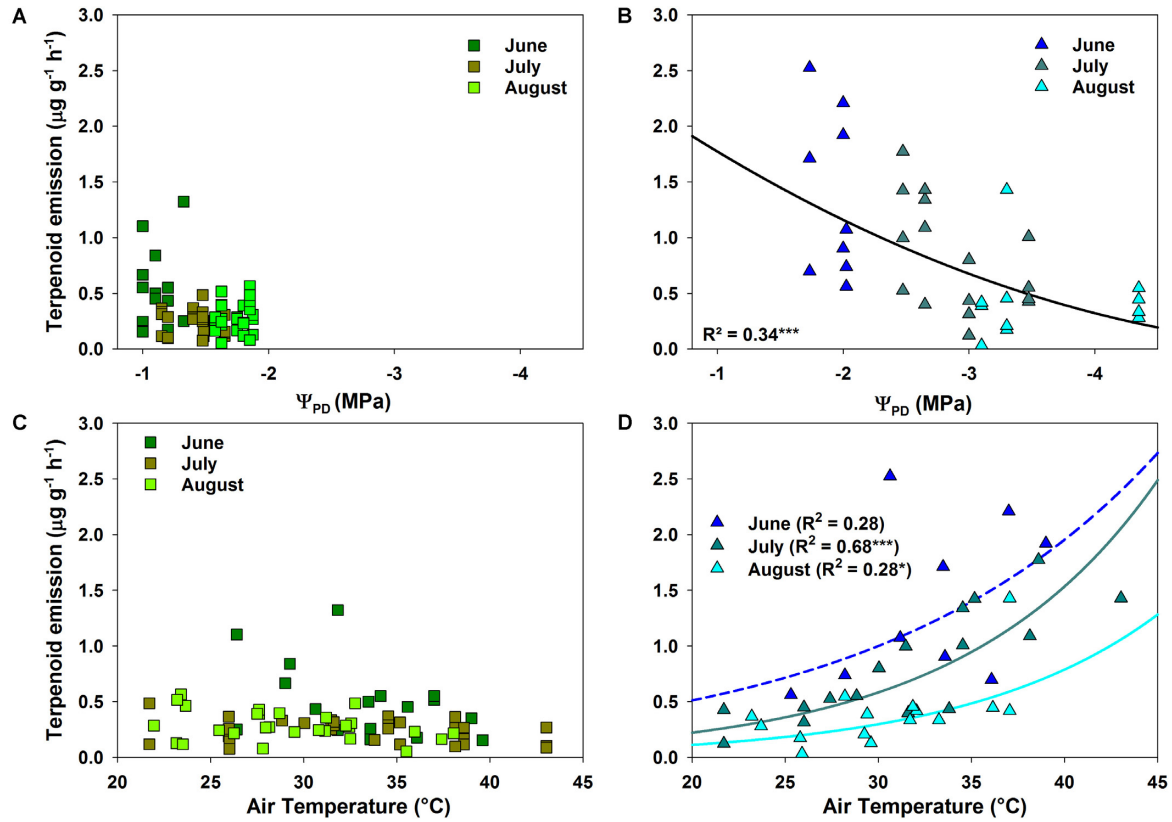

FIGURE 4 | Response of measured terpenoid emission rates to pre-dawn leaf water potential (Ψ_{PD}) and air temperature for *Q. suber* **(A,C)** and *C. ladanifer* **(B,D)**. Significant trends (linear and exponential regressions) are illustrated by solid lines at a significance levels of $^{*}p < 0.05$, $^{**}p < 0.01$, $^{***}p < 0.001$.

temperature of 30°C were calculated. It must be denoted that no significant correlation of air temperature and terpenoid emission rates was found for total terpenoid emissions of *Q. suber*. Nevertheless, emissions were standardized to 30°C to allow for a comparison of standard emission factors of both species and literature. Due to the low temperature dependence, the standardization procedure did not alter the pattern of emission rates for MT and MTO emissions, as only SQT emissions of *Q. suber* did express a temperature dependence. For a comparison, calculations with non-standardized emissions of *Q. suber* are also shown in the appendix (Supplementary Figure 2). To identify common temporal patterns within the diversity of emitted terpenoids, heat maps clustering compounds with similar emission patterns, were created, showing the relative change in standard emission factors over time (**Figures 6**, **7**). Overall, increasing (red, 0 – 1), unaffected (white, 0), and decreasing (blue, 0 – −1) emission patterns of single terpenoid compounds were found, which could be assigned to two main clusters for *Q. suber* (**Figure 6**) and three main cluster for *C. ladanifer* (**Figure 7**). The biggest cluster (I) in both species was characterized by different terpenoids whose emissions decreased with progressive drought (**Figures 6**, **7**), and dominated the total terpenoid emissions, as already evident from **Figures 3**, **4**. Most of the emitted SQTs, such as δ-cadinene (**Figure 8D**) could be allocated to this cluster, but also MT such as β-pinene or sabinene (see also **Tables 1A,B**). Nevertheless, there were also a few compounds in this cluster with emission peaks in July, such as limonene or the DT ent-16-kaurene for *C. ladanifer* or the SQTs alloaromadendrene and ledene for *Q. suber*. However, those changes were non-significant ($p > 0.05$), as evident from **Figures 8A,E** for limonene and ent-16-kaurene emissions of *C. ladanifer*. The second cluster II was characterized by more irregular patterns of standard emissions factors (**Figures 6**, **7**). For *Q. suber*, cluster II contained compounds with lowest standard emission factors in July and increases somewhat thereafter, best illustrated by the MTs α-pinene, camphene and γ-terpinene (**Figures 6**, **8B,C** and **Table 1A**). While the changes of α-pinene were minor and non-significant ($p > 0.05$), the increase of camphene in August was highly significant ($p < 0.001$). Although, α-pinene and camphene did not show the same pattern in *C. ladanifer*, cluster II also contained compounds with lowest standard emission factor in July, such as myrcene or 1,8-cineole (**Figure 7**). However, there was a small, third cluster containing larger compounds, such as the DTs manoyl oxide and verticillol, whose standard emission factors increased progressively over time (**Figure 8E** and **Table 1B**). While this increase was not significant for manoyl oxide ($p > 0.05$), it was highly significant ($p < 0.001$) for verticillol from June to July. The standard emission factor of cembrene on the other hand decreased non-significantly from June to July (**Figure 8E**). Because heat maps only illustrate relative changes in

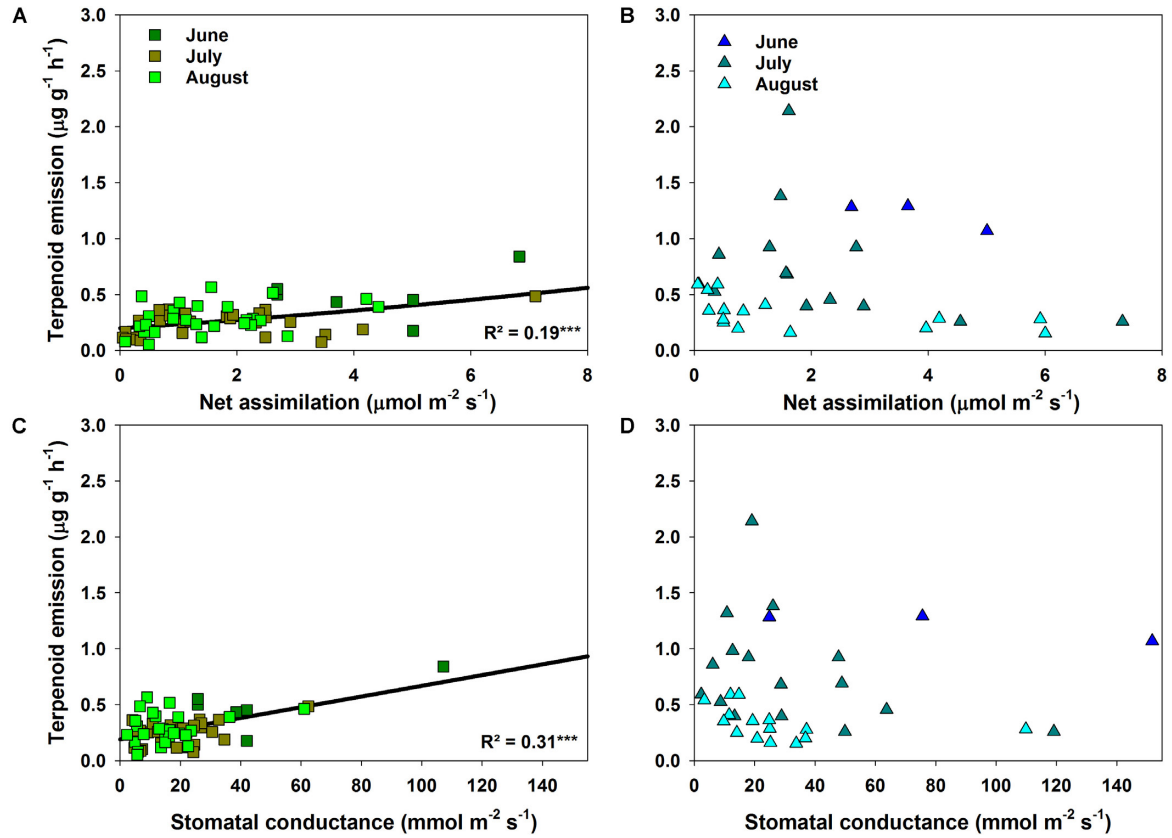

FIGURE 5 | Relationship of measured terpenoid emission rates for *Q. suber* **(A,C)** and standardized terpenoid emission rates for *C. ladanifer* **(B,D)** to net assimilation rate and stomatal conductance. Significant trends (linear and exponential regressions) are illustrated by solid lines at a significance levels of $*p < 0.05$, $**p < 0.01$, $***p < 0.001$.

emissions, the standard emission factors as well as the empirical temperature coefficients (β) of the most important terpenoid compounds are compiled in **Tables 1A,B** for each species. The only compound group which revealed a positive correlation with air temperature for *Q. suber* were SQT emissions, as evident from positive β-values. β-values of MT and MTO emissions were mostly negative and should be interpreted with care. On the other hand, β values of all terpenoid compound groups of *C. ladanifer* were positive and increased in the following order: MTs < MTOs < DTs < SQTs (**Table 1B**). Interestingly, β values of SQTs increased strongly over time from 0.111 ± 0.029 in June to 0.201 ± 0.037 in August. Manoyl oxide and cembrene had the highest β value amongst the four emitted diterpenes. A table of all emitted compounds including standard emission factor, empirical temperature coefficient (β), RI values and match factors of compound identification is given in Supplementary Tables 1, 2 of the Supplementary Material.

DISCUSSION

Our results show that the decline in terpenoid emissions from co-occurring *Q. suber* and *C. ladanifer* during summer was significantly correlated with increasing drought stress. This correlation was clearly species-specific, which showed differences in terpenoid emission rates, emitted compounds and reaction to environmental conditions (water stress and diurnal temperature changes). Standard emission factors revealed interesting patterns of decreasing, unaffected and increasing emission rates of individual terpenoid compounds with increasing summer drought.

Terpenoid Emissions in Relation to Drought Adaptation Strategies

Cistus ladanifer was not only characterized by higher terpenoid emission rates than *Q. suber,* but, in particular, by a high diversity of over 75 different compounds. Overall, the emission rates observed in our study were in the lower range of emissions reported earlier for *Cistus* spp. (3 – 21 $\mu g\, g^{-1}\, h^{-1}$, Pio et al., 1993; Ormeno et al., 2007; Lluisà et al., 2010). Compared to *Q. suber*, *C. ladanifer* showed a stronger responsiveness to changing environmental conditions. This pattern is in agreement with the characteristic adaptation strategy of this species to withstand summer drought. Low thresholds for xylem cavitation and hydraulic failure (Quero et al., 2011) allow a high physiological activity, even when water resources start to decline (Núñez-Olivera et al., 1996; Ramírez et al., 2012). As terpenoid production

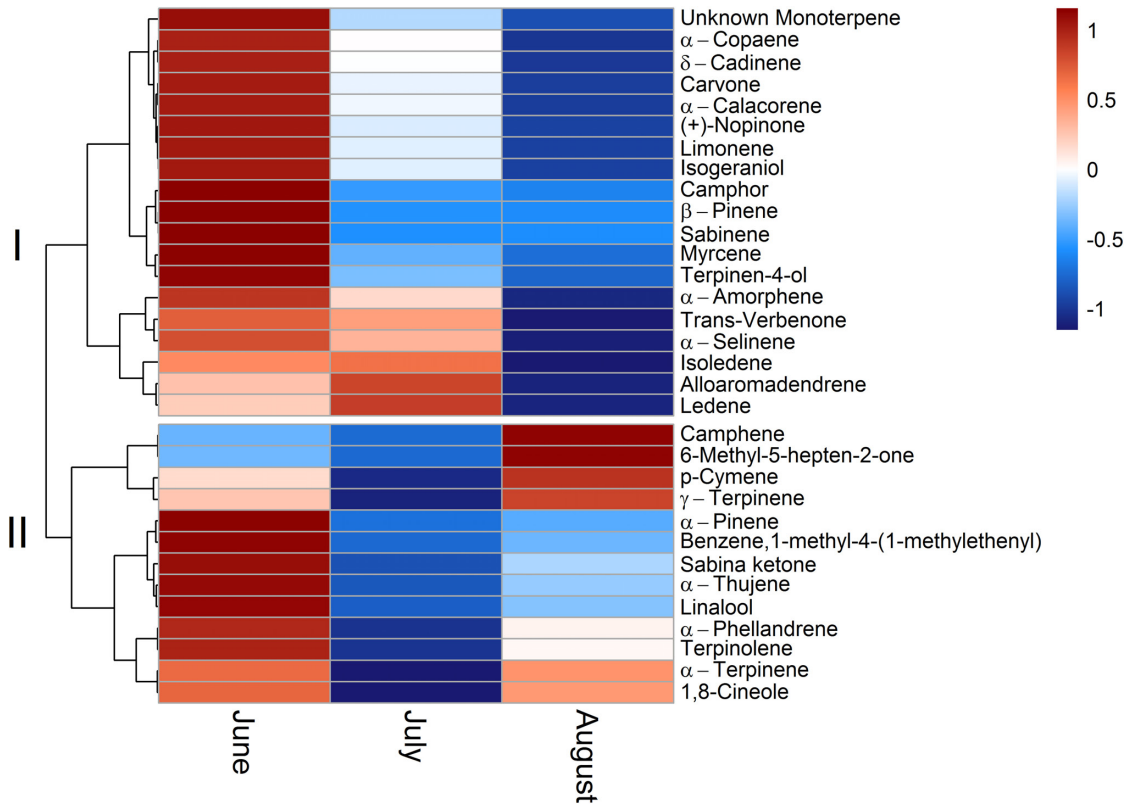

FIGURE 6 | Relative change of single terpenoid compound emissions over time for *Q. suber* illustrated as clustered heat maps. Emissions are standardized to a temperature of 30°C (Guenther et al., 1993). The color code indicates the relative changes of emissions over time. Red colors indicate increasing emission rates on a scale from 0 to 1; where a color code of 0 corresponds to unaffected emission rates and a color code of 1 corresponds to strongly increased emission rates. Blue colors indicate decreasing emission rates on a scale from 0 to –1, where a color code of 0 corresponds to unaffected emission rates and a color code of –1 corresponds to strongly decreased emission rates.

is dependent on plant metabolism (e.g., Kesselmeier and Staudt, 1999), it is likely that *C. ladanifer* was able to synthesize a substantial amount of terpenoids in June, when assimilation rates were still quite high (Ramírez et al., 2012). Most probably, these compounds were either emitted directly or maintained in the storage pools of terpenoids present in the leaves of this species (Alías et al., 2012), as also demonstrated for *C. albidus* and *C. monspeliensis* under drought conditions (Lluisà and Peñuelas, 1998; Lluisà et al., 2010). Lluisà and Peñuelas (1998) suggested that plants under mild to moderate drought stress accumulate carbon which is then often allocated to defense compounds such as terpenoids, when growth is restricted by water limitation. The emission of stored terpenoids is mostly temperature dependent (Lluisà and Peñuelas, 1998; Staudt et al., 2017), because the volatility of these compounds increases at higher air temperatures (Lerdau et al., 1997; Peñuelas and Lluisà, 2001), which is supported here by the significant correlation with diurnal temperature variations (**Figure 4D**). Nevertheless, with prolonged drought conditions terpenoid fluxes declined, which was clearly visible in the seasonal patterns of standard emission factors and in line with declining Ψ_{PD} and carbon assimilation, indicating an increase of shrub and tree drought stress over time (Grassi and Magnani, 2005). In the absence of severe drought stress seasonal terpenoid emissions have been shown to increase from spring to summer for *Cistus* spp. (Lluisà and Peñuelas, 2000; Rivoal et al., 2010) and *Q. suber* (Staudt et al., 2004; Pio et al., 2005), only declining in autumn, probably caused by lower air temperatures and leaf senescence. Hence, it is likely that severe drought stress was the determining factor for the observed reduction in terpenoid emissions. Although no direct link between carbon assimilation and terpenoid emissions was found in *C. ladanifer*, diminished substrate availability for terpenoid biosynthesis probably contributed to the overall decline of emissions. With increasing drought stress, assimilation rates were stronger reduced compared to those of *Q. suber* as a result of the opportunistic, water-spending strategy of *C. ladanifer*. Compound concentrations in storage pools possibly got depleted by high air temperatures and cumulative drought stress over time and were not refilled to the same level (Lluisà et al., 2006; Staudt et al., 2017), as evident from SQT emissions which are known to be stored in leaves of *Cistus* spp. (Lluisà and Peñuelas, 2000; Ormeno et al., 2007). There is also substantial evidence, that terpenoid storing species may release terpenoids from *de novo* biosynthesis dependent on substrate availability from photosynthesis (Lluisà et al., 2010; Staudt et al., 2017), which decreased strongly in *C. ladanifer*

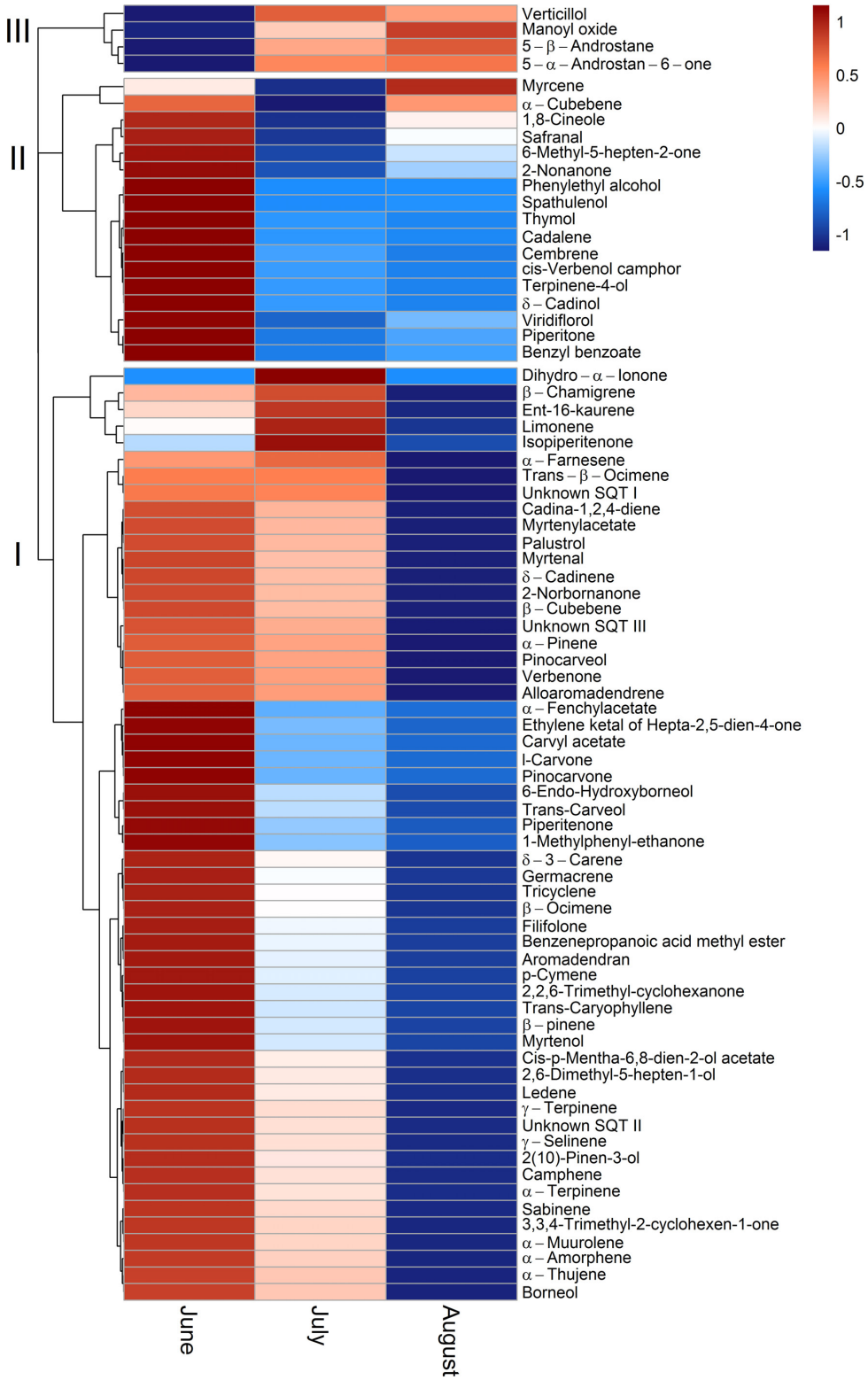

FIGURE 7 | Relative change of single terpenoid compound emissions over time for *C. ladanifer* illustrated as clustered heat maps. Emissions are standardized to a temperature of 30°C (Guenther et al., 1993). The color code indicates the relative changes of emissions over time. Red colors indicate increasing emission rates on a scale from 0 to 1; where a color code of 0 corresponds to unaffected emission rates and a color code of 1 corresponds to strongly increased emission rates. Blue colors indicate decreasing emission rates on a scale from 0 to –1, where a color code of 0 corresponds to unaffected emission rates and a color code of –1 corresponds to strongly decreased emission rates.

TABLE 1 | Standard emission factor E_S (μg C g^{-1} h^{-1}) with 95% confidence interval and empirical temperature coefficient β ($°C^{-1}$) with 95% confidence interval for *Quercus suber* **(A)** and *Cistus ladanifer* **(B)**.

(A)

Compound	E_S	β	E_S	β	E_S	β
Quercus suber	**June (*n* = 18)**		**July (*n* = 32)**		**August (*n* = 32)**	
Total terpenoids	0.543 ± 0.208	−0.062 ± 0.038	0.224 ± 0.043	−0.021 ± 0.015	0.245 ± 0.047	−0.033 ± 0.023
Monoterpenes	0.456 ± 0.202	−0.068 ± 0.043	0.186 ± 0.039	−0.038 ± 0.016	0.216 ± 0.042	−0.036 ± 0.023
Oxy. Monoterpenes	0.053 ± 0.032	−0.047 ± 0.058	0.026 ± 0.009	0.035 ± 0.027	0.025 ± 0.007	−0.007 ± 0.031
Sesquiterpenes	$5.32 \times 10^{-4} \pm 4.29 \times 10^{-4}$	0.139 ± 0.077	$2.56 \times 10^{-4} \pm 1.17 \times 10^{-4}$	0.168 ± 0.036	$3.53 \times 10^{-5} \pm 2.76 \times 10^{-5}$	0.164 ± 0.091
Limonene	0.159 ± 0.109	−0.005 ± 0.067	0.077 ± 0.038	−0.059 ± 0.038	0.043 ± 0.026	−0.092 ± 0.071
α-Pinene	0.039 ± 0.043	−0.149 ± 0.107	0.022 ± 0.008	−0.084 ± 0.027	0.024 ± 0.008	−0.001 ± 0.040
β-Pinene	0.036 ± 0.033	−0.131 ± 0.091	0.012 ± 0.005	−0.068 ± 0.032	0.012 ± 0.004	−0.048 ± 0.043
γ-Terpinene	0.017 ± 0.014	−0.121 ± 0.077	0.007 ± 0.003	−0.030 ± 0.030	0.025 ± 0.008	−0.043 ± 0.038
Sabinene	0.031 ± 0.033	−0.151 ± 0.103	0.005 ± 0.003	−0.053 ± 0.041	0.005 ± 0.002	0.003 ± 0.053

(B)

Cistus ladanifer	**June (*n* = 9)**		**July (*n* = 16)**		**August (*n* = 16)**	
Total terpenoids	1.027 ± 0.345	0.064 ± 0.033	0.590 ± 0.119	0.099 ± 0.017	0.298 ± 0.109	0.097 ± 0.043
Monoterpenes	0.630 ± 0.270	0.053 ± 0.042	0.428 ± 0.098	0.089 ± 0.019	0.223 ± 0.084	0.087 ± 0.044
Oxy. Monoterpenes	0.181 ± 0.051	0.038 ± 0.027	0.092 ± 0.015	0.092 ± 0.014	0.057 ± 0.021	0.111 ± 0.042
Sesquiterpenes	0.200 ± 0.060	0.111 ± 0.029	0.063 ± 0.015	0.149 ± 0.020	0.014 ± 0.005	0.201 ± 0.037
Diterpenes	$4.98 \times 10^{-5} \pm 3.34 \times 10^{-5}$	0.116 ± 0.066	$6.04 \times 10^{-5} \pm 1.09 \times 10^{-5}$	0.084 ± 0.015	$5.98 \times 10^{-5} \pm 2.29 \times 10^{-5}$	0.135 ± 0.045
γ-Terpinene	0.208 ± 0.129	0.053 ± 0.060	0.135 ± 0.032	0.096 ± 0.020	0.068 ± 0.028	0.121 ± 0.047
α-Pinene	0.150 ± 0.041	0.043 ± 0.027	0.125 ± 0.032	0.074 ± 0.022	0.051 ± 0.017	0.057 ± 0.040
Limonene	0.033 ± 0.021	0.082 ± 0.061	0.046 ± 0.010	0.086 ± 0.019	0.024 ± 0.008	0.074 ± 0.041
2,6-dimethyl-5-hepten-1-ol	0.049 ± 0.022	0.032 ± 0.043	0.032 ± 0.009	0.059 ± 0.024	0.018 ± 0.007	0.125 ± 0.048
α-Terpinene	0.047 ± 0.044	0.039 ± 0.090	0.029 ± 0.008	0.093 ± 0.022	0.015 ± 0.004	0.140 ± 0.034
Manoyl oxide	$1.32 \times 10^{-5} \pm 7.64 \times 10^{-6}$	0.122 ± 0.056	$1.83 \times 10^{-5} \pm 4.25 \times 10^{-6}$	0.108 ± 0.020	$2.14 \times 10^{-5} \pm 8.25 \times 10^{-6}$	0.139 ± 0.045
Cembrene	$2.28 \times 10^{-5} \pm 1.80 \times 10^{-5}$	0.124 ± 0.076	$1.21 \times 10^{-5} \pm 4.40 \times 10^{-6}$	0.103 ± 0.031	$1.13 \times 10^{-5} \pm 7.17 \times 10^{-6}$	0.131 ± 0.075
Verticillol	$3.23 \times 10^{-6} \pm 3.03 \times 10^{-6}$	0.079 ± 0.093	$2.20 \times 10^{-5} \pm 5.49 \times 10^{-6}$	0.063 ± 0.021	$1.64 \times 10^{-5} \pm 7.69 \times 10^{-6}$	0.130 ± 0.055
Ent-16-kaurene	$3.13 \times 10^{-6} \pm 4.60 \times 10^{-6}$	0.089 ± 0.142	$3.31 \times 10^{-6} \pm 8.33 \times 10^{-7}$	0.066 ± 0.021	$2.84 \times 10^{-6} \pm 1.16 \times 10^{-6}$	0.119 ± 0.048

E_S and β were calculated according to Guenther et al. (1993) (see equation 2), where E_S is the y-intercept and β the slope of the regression. For Q. suber the different terpenoid compound groups and the five terpenoid compounds with the highest emission rates are displayed, for C. ladanifer single diterpene compounds are additionally displayed.

over time. Since the diurnal temperature dependence, as well as the decrease of MT emissions with drought was lower compared to SQT, it seems likely that a substantial amount of MTs originated from *de novo* biosynthesis, as recently suggested by Yáñez-Serrano et al. (2018). However, these effects cannot be disentangled from our field measurements, where emissions might have been influenced by other co-varying factors, such as PPFD or biotic interactions. Nevertheless, studies of terpenoid emissions in a natural environment are rare and illustrate actual emission patterns more closely than controlled environment experiments.

Quercus suber pursues a different strategy to cope with water scarcity compared to *C. ladanifer*. The access to deep water resources with a tap root system and stomatal control over transpiration (David et al., 2007) allow this species to maintain relatively high water potentials and to minimize transpiration losses, probably to avoid hydraulic failure. However, this strategy leads to reduced carbon assimilation rates and the typical midday depression of gas exchange (e.g., Chaves, 1991) and affects the metabolism of plants. As *Q. suber,* in contrast to *C. ladanifer*, does not possess specialized storage organs for terpenoids in the leaves, emissions are assumed to be almost completely dependent on *de novo* biosynthesis (Loreto et al., 1996). Hence, lower emission rates in periods of water scarcity are most likely a direct consequence of this drought avoiding strategy and the lack of specialized terpenoid storage pools. However, in contrast to our assumptions, terpenoid emissions of *Q. suber* were not strongly dependent on Ψ_{PD} and air temperatures within the sampling period, as observed in closely related species such as *Q. ilex* (e.g., Lavoir et al., 2009). Thus, most likely, *Q. suber* did respond to the early onset of drought in June, as Ψ_{PD}, Ψ_{MD} and sap flux density indicate that trees were already trying to avoid substantial water losses, possibly to prevent hydraulic failure (Pinto et al., 2012; Kurz-Besson et al., 2014). In agreement with this assumption, net assimilation rates of *Q. suber* of 6.12 ± 0.42 μmol m^{-2} s^{-1} were already reduced in

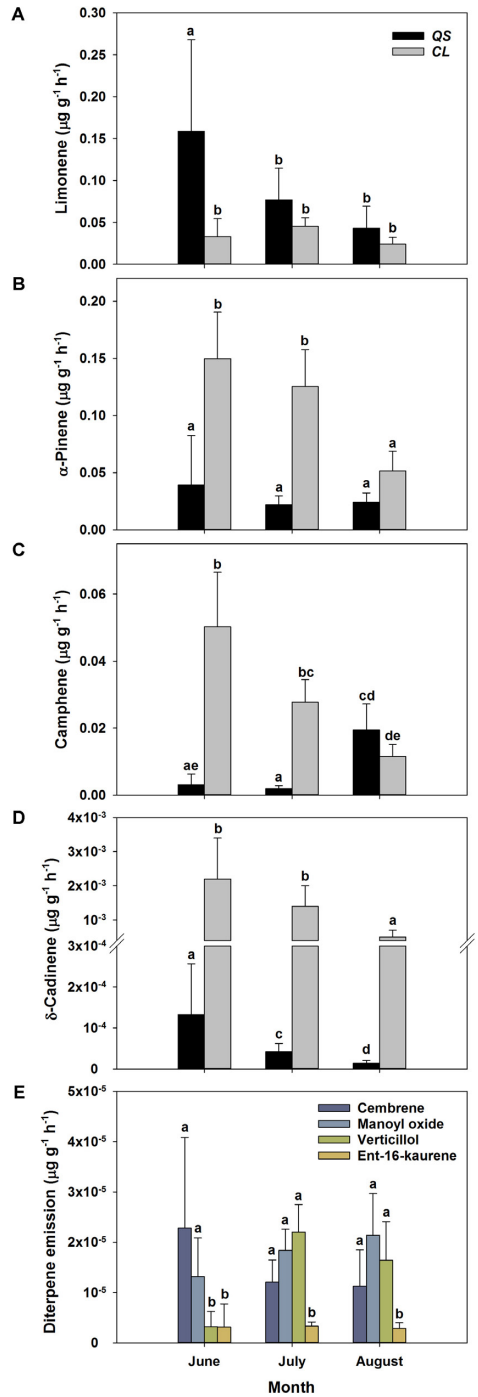

FIGURE 8 | Absolute change of standard emissions factors (30°C, Guenther et al., 1993) of selected terpenoid compounds over time for *Q. suber* **(A–D)** (n = 18 for June, n = 32 for July and August) and *C. ladanifer* **(A–E)** (n = 9 for June, n = 16 for July and August) with a confidence interval of 95%. Selected compounds are the monoterpenes limonene **(A)**, α-pinene **(B)**, camphene **(C)**, the sesquiterpene alloaromadendrene **(D)** and the diterpenes cembrene, manoyl oxide, verticillol and ent-16-kaurene **(E)**. Compounds were selected according to their quantitative importance and development of emissions over time. Letters indicate statistical differences (RMANOVA) of selected terpenoid emissions between sampling periods and species at a significance level of $p < 0.05$.

June, compared to typical spring values of 13 – 14 µmol m^{-2} s^{-1} (Tenhunen et al., 1985; Kurz-Besson et al., 2014), but more stable than assimilation rates of the water spending shrub *C. ladanifer*. The tendency of declining emissions at higher air temperatures in June, especially for MTs and MTOs, can be regarded as an interaction of drought and heat stress, which can lead to an inhibition of enzymes involved in *de novo* emissions of terpenoids (Loreto and Schnitzler, 2010). Hence, at higher air temperatures, primary substrate availability and terpenoid synthesis are reduced in non-storing species (Lavoir et al., 2009; Grote et al., 2010). Under severe drought, this response to air temperature is offset in non-storing plants (Brilli et al., 2007; Fortunati et al., 2008), which explains the pattern observed in July and August. A further indication that drought conditions were nevertheless an important determinant of emissions is given by the weak relationship of terpenoid emissions and carbon assimilation, which are usually highly correlated in non-storing species (Kesselmeier and Staudt, 1999; Niinemets et al., 2014). This finding further points toward a limitation in the terpenoid synthesis pathway. Although SQT emissions were low and declined strongly in *Q. suber*, they expressed a high temperature dependence, comparable to the SQTs emitted by *C. ladanifer*. Hence, it seems possible that SQTs were not only emitted from *de novo* biosynthesis, but also from small, probably temporary, storage pools in leaves of *Q. suber* (Pio et al., 2005). Noteworthy, the terpenoid emissions of *Q. suber* in our study were low compared to previously published results (10 – 43 µg g^{-1} h^{-1}, Staudt et al., 2004; Pio et al., 2005; Staudt et al., 2008; Bracho-Nunez et al., 2013). As stated above, such low emission rates were most likely a consequence of the predominant environmental conditions during spring and summer 2017, which were characterized by very low precipitation compared to the long-term average, in combination with high air temperatures during the terpenoid sampling dates. Hence, to further unravel the effect of severe drought on terpenoid emissions of *Q. suber* and *C. ladanifer,* more studies characterizing emission patterns in pre-drought and recovery periods are required. Next to the different environmental conditions present in our experiments compared to other studies on terpenoid emissions of *Q. suber* (Staudt et al., 2004, 2008; Pio et al., 2005; Bracho-Nunez et al., 2013) and *Cistus* spp. (Pio et al., 1993; Ormeno et al., 2007; Lluisà et al., 2010), it must be denoted that emission rates may be underestimated for those terpenoids which show fast reaction with ozone (Vickers et al., 2009), because we did not use ozone scrubbers during terpenoid sampling in the field. Apart from varying environmental conditions, other differences in methodology, such as sampling flow rate, enclosure volume, terpenoid storage and analysis were minor and thus, should have had a negligible effect on terpenoid emission rates.

Significance of Emitted Compounds for Stress Adaptation

In contrast to the decline in total terpenoid emission rates with enhanced drought stress over the season, emission of some individual terpenoid species was unaffected or even increased

in both species, as evident from standard emission factors. Among these compounds were the MTs α-pinene, camphene and γ-terpinene (**Figure 6**). Standard emissions of α-pinene, a main compound emitted by both investigated species, were essentially unaffected in *Q. suber* and partly also in C. *ladanifer*. Camphene and γ-terpinene were emitted even at higher rates in *Q. suber* in August (**Figure 8C** and **Table 1A**). As emission of terpenoids represents a carbon loss (e.g., Vickers et al., 2009), this investment is likely to have a beneficial effect for the plants (Possell and Loreto, 2013). In contrast, emissions of other terpenoids such as limonene, the dominant MT of *Q. suber* in Portugal (Loreto et al., 2009), were decreasing continuously, indicating their minor role in stress adaptation, as also suggested by Lluisà et al. (2005) for limonene. It is well understood that prolonged drought stress in combination with high air temperatures and light intensities can increase the abundance of reactive oxygen species in leaves (e.g., Miller et al., 2008), which potentially damages the photosynthetic apparatus of plants (Peñuelas et al., 2005; Velikova and Loreto, 2005). Particularly for the long-lived leaves of *Q. suber*, any damage would be costly for trees (Loreto et al., 2014); thus these evergreen Mediterranean trees have developed multiple strategies to protect these organs (Werner et al., 2002). Hence, when preventing hydraulic failure by stomatal closure, those terpenoids showing increased emission rates might play a particular role to avoid permanent damage to the photosynthetic apparatus under stressful conditions (Vickers et al., 2009; Loreto et al., 2014), e.g., by maintaining the stability of thylakoid membranes (Velikova et al., 2011, 2012). Specific terpenoids therefore might provide effective protection during summer drought (Delfine et al., 2000; Loreto et al., 2004; Copolovici et al., 2005; Possell and Loreto, 2013). MT emission seems to be a general feature of Mediterranean plants, which supports the assumption that they provide a strategy to withstand drought, heat and light stress.

Leaves of *C. ladanifer* on the other hand, are reported to remain photo-protected and potentially active during the early onset of summer drought, to take immediate advantage of favorable conditions such as short summer rains (Núñez-Olivera et al., 1996; Ramírez et al., 2012). To this end, higher carotenoid content in leaves, exudation of flavonoids and DTs and the incorporation of phenolic substances into the xylem have been reported as effective protection measures against oxidative stress (Núñez-Olivera et al., 1996; De Micco and Aronne, 2007; Valares Masa et al., 2016). Hence, the diverse blend of terpenoids detected in the emissions of this species likely also contributes to the high drought tolerance of *C. ladanifer*. Whereas the role of MTs in stress response is quite well established, the role of SQTs is less well understood (Vickers et al., 2009). Decreasing release of SQTs, such as δ-cadinene with progressing drought, suggests that the main function of SQT is not solely abiotic stress adaptation. Several SQT compounds have been identified in the allelopathic oil of *C. ladanifer* (Gomes et al., 2005) indicating an important role in biotic interactions (Verdeguer et al., 2012). Even more intriguing is the role of DTs in terpenoid emissions of *C. ladanifer*. Although only small emission rates occurred, DTs were so far rather considered as semi-volatile or non-volatile (Dudareva et al., 2006; Niinemets, 2010; Loreto et al., 2014) and indeed there are very few studies which report volatile diterpenoid emissions (Otsuka et al., 2004; Von Schwartzenberg et al., 2004; Matsunga et al., 2012). However, recently Yáñez-Serrano et al. (2018) detected significant emissions of the DT ent-16-kaurene not only from *C. ladanifer*, but also from *Halimium halimifolium*, a related Mediterranean shrub species. Moreover, the DTs manoyl oxide and ent-16-kaurene are known as major components in essential oils of other related species such as *C. monspeliensis* and *C. creticus* (Demetzos et al., 1997; Angelopoulou et al., 2002), which could indicate that DT emissions may occur from more Mediterranean species than previously thought. The ecological role of DT emissions is yet to be determined, but there is evidence that they are involved in photoprotective mechanisms during stressful periods (Munné-Bosch and Alegre, 2000; Munné-Bosch et al., 2001) and possess allelopathic and antimicrobial properties (Demetzos et al., 1997; Alías et al., 2012). Increasing and unaffected emissions of verticillol, manoyl oxide and ent-16-kaurene under progressing drought might indeed indicate an important role of DTs in abiotic stress adaptation. Hence, the compound-rich blend of biochemicals identified in *C. ladanifer* might provides a competitive advantage for this species to withstand stressful periods (De Micco and Aronne, 2007; Valares Masa et al., 2016). Next to the scarce knowledge about DT emissions, the influence of these long-chained terpenoids on atmospheric chemistry is yet to be determined (Otsuka et al., 2004; Yáñez-Serrano et al., 2018). While the reaction rate constant toward ozone and hydroxyl radicals is low for ent-16-kaurene (1.2×10^{-17} cmł molec^{-1} s^{-1} and 72.5×10^{-12} cmł molec^{-1} s^{-1}) and manoyl oxide (1.8×10^{-18} cmł molec^{-1} s^{-1} and 56.7×10^{-12} cmł molec^{-1} s^{-1}) (EPI Suite, Environmental Protection Agency, United States), verticillol and cembrene are assumed to react faster. The reaction rate constant toward ozone is approximately twofold higher for verticillol (86.0×10^{-17} cmł molec^{-1} s^{-1}) and fourfold higher for cembrene (186.0×10^{-17} cmł molec^{-1} s^{-1}) compared to β-caryophyllene (44.2×10^{-17} cmł molec^{-1} s^{-1}) or α-pinene (43.0×10^{-17} cmł molec^{-1} s^{-1}). In comparison to isoprene (105.1×10^{-12} cmł molec^{-1} s^{-1}), verticillol (201.6×10^{-12} cmł molec^{-1} s^{-1}) and cembrene 375.7×10^{-12} cmł molec^{-1} s^{-1}) are assumed to react approximately two and four times faster toward hydroxyl radicals (EPI Suite, Environmental Protection Agency, United States). Thus, given the large impact of other terpenoids in ozone production and aerosol formation (Holopainen and Gershenzon, 2010), DT emissions might amplify the impact of terpenoids on atmospheric chemistry.

CONCLUSION

Our results suggest a species- and terpenoid-specific behavior of severe drought and terpenoid emissions. *Q. suber* and *C. ladanifer* differed strongly in relation to the diversity of emissions and reactions to assimilation rates, water potentials and diurnal air temperature variations. While overall terpenoid emissions strongly decreased over time, unaffected or increasing emissions of some terpenoid compounds illustrate the importance of terpenoids in drought adaptation.

AUTHOR CONTRIBUTIONS

SH conducted the field work, statistical analysis, and wrote the manuscript. JK planned the experiment, performed the TD-GC-MS analysis, and processed the data. RL-d-V and MC helped in planning the experiment, conducted the field work, and assisted the interpretation of the data. MD helped in planning the experiment and interpretation of the data. CW planned the experiment, assisted the field work and the interpretation of the data. All authors critically discussed and reviewed the manuscript.

FUNDING

We would like to acknowledge funding from the ERC project VOCO$_2$ (647008), DFG (WE 2681/10-1; DU 1688/1-1) and IF/740/2014 (from FCT, the Portuguese Fundação para a Ciência e a Tecnologia I.P.). SH would like to acknowledge funding from the Studienstiftung des deutschen Volkes. RL-d-V was funded by a postdoctoral fellowship from the FCT (SFRH/BPD/86938/2012). Centro de Estudos Florestais (CEF) is a research unit funded by FCT, Portugal (UID/AGR/00239/2013). We thank the Fundação da Casa de Bragança for permission to undertake research at the field site. The article processing charge was funded by the German Research Foundation (DFG) and the University of Freiburg in the funding program Open Access Publishing.

ACKNOWLEDGMENTS

We would like to thank Joaquim Mendes for field assistance and Anna Beck for her help with the TD-GC-MS analysis.

SUPPLEMENTARY MATERIAL

The Supplementary Material for this article can be found online at: https://www.frontiersin.org/articles/10.3389/fpls.2018.01071/full#supplementary-material

REFERENCES

Alías, J. C., Sosa, T., Valares, C., Escudero, J. C., and Chaves, N. (2012). Seasonal variation of *Cistus ladanifer* L. diterpenes. *Plants* 1, 6–15. doi: 10.3390/plants1010006

Angelopoulou, D., Demetzos, C., and Perdetzoglou, D. (2002). Diurnal and seasonal variation of the essential oil labdanes and clerodanes from *Cistus monspeliensis* L. leaves. *Biochem. Syst. Ecol.* 30, 189–203. doi: 10.1016/S0305-1978(01)00074-6

Atkinson, J., and Arey, J. (2003). Gas-phase tropospheric chemistry of biogenic volatile organic compounds: a review. *Atmos. Environ.* 37, 197–219. doi: 10.1016/S1352-2310(03)00391-1

Bracho-Nunez, A., Knothe, N. M., Staudt, M., Costa, W. R., Liberato, M. A. R., Piedade, M. T. F., et al. (2013). Leaf level emissions of volatile organic compounds (VOC) from some Amazonian and Mediterranean plants. *Biogeosciences* 10, 5855–5873. doi: 10.5194/bg-10-5855-2013

Brilli, F., Barta, C., Fortunati, A., Lerdau, M., Loreto, F., and Centritto, M. (2007). Response of isoprene emission and carbon metabolism to drought in white poplar (*Populus alba*) saplings. *New Phytol.* 175, 244–254. doi: 10.1111/j.1469-8137.2007.02094.x

Bugalho, M. N., Caldeira, M. C., Pereira, J. S., Aronson, J., and Pausas, J. G. (2011). Mediterranean cork oak savannas require human use to sustain biodiversity and ecosystem services. *Front. Ecol. Environ.* 9:278. doi: 10.1890/100084

Caldeira, M. C., Lecomte, X., David, T. S., Pinto, J. G., Bugalho, M. N., and Werner, C. (2015). Synergy of extreme drought and shrub invasion reduce ecosystem functioning and resilience in water-limited climates. *Sci. Rep.* 5:15110. doi: 10.1038/srep15110

Chaves, M. M. (1991). Effects of water deficits on carbon assimilation. *J. Exp. Bot.* 42, 1–16. doi: 10.1093/jxb/42.1.1

Choat, B., Jansen, S., Brodribb, T. J., Cochard, H., Delzon, S., Bhaskar, R., et al. (2012). Global convergence in the vulnerability of forests to drought. *Nature* 491, 752–755. doi: 10.1038/nature11688

Copolovici, L., Filella, I., Lluisà, J., Niinemets, Ü, and Peñuelas, J. (2005). The capacity for thermal protection of photosynthetic electron transport varies for different monoterpenes in *Quercus ilex*. *Plant Physiol.* 139, 485–496. doi: 10.1104/pp.105.065995

Correia, O., and Ascensao, L. (2016). "Summer semi-deciduous species of the Mediterranean landscape: a winning strategy of cistus species to face the predicted changes of the Mediterranean climate," in *Plant Biodiversity. Monitoring, Assessment and Conservation*, eds A. A. Ansari, S. S. Gill, Z. K. Abbas, and M. Naeem (Wallingford: CAB International), 195–217.

Correia, O., Catarino, F. M., Tenhunen, J. D., and Lange, O. L. (1987). "Regulation of water use by four species of Cistus in the scrub vegetation of the Serra da Arrábida, Portugal," in *Plant Responses to Stress. Functional Analysis in Mediterranean Ecosystems*, eds J. D. Tenhunen, F. M. Catarino, O. L. Lange, and W. C. Oechel (Berlin: Springer-Verlag), 247–258.

Costa, A., Pereira, H., and Madeira, M. (2010). Analysis of spatial patterns of oak decline in cork oak woodlands in Mediterranean conditions. *Ann. For. Sci.* 67:204. doi: 10.1051/forest/2009097

David, T. S., Henriques, M. O., Kurz-Besson, C., Nunes, J., Valente, F., Vaz, M., et al. (2007). Water-use strategies in two co-occurring Mediterranean evergreen oaks: surviving the summer drought. *Tree Physiol.* 27, 793–803. doi: 10.1093/treephys/27.6.793

De Micco, V., and Aronne, G. (2007). Anatomical features, monomer lignin composition and accumulation of phenolics in 1-year-old branches of the Mediterranean *Cistus ladanifer* L. *Bot. J. Linn. Soc.* 155, 361–371. doi: 10.1111/j.1095-8339.2007.00705.x

Delfine, S., Csiky, O., Seufert, G., and Loreto, F. (2000). Fumigation with exogenous monoterpenes of a non-isoprenoid-emitting oak (*Quercus suber*): monoterpene acquisition, translocation, and effect on the photosynthetic properties at high temperatures. *New Phytol.* 146, 27–36. doi: 10.1046/j.1469-8137.2000.00612.x

Demetzos, C., Katerinopoulos, H., Kouvarakis, A., Stratigakis, N., Loukis, A., Ekonomakis, C., et al. (1997). Composition and antimicrobial activity of the essential oil of *Cistus creticus* subsp. *eriocephalus*. *Planta Med.* 63, 477–479. doi: 10.1055/s-2006-957742

Dudareva, N., Klempien, A., Muhlemann, J. K., and Kaplan, I. (2013). Biosynthesis, function and metabolic engineering of plant volatile organic compounds. *New Phytol.* 198, 16–32. doi: 10.1111/nph.12145

Dudareva, N., Negre, F., Nagegowda, D. A., and Orlova, I. (2006). Plant volatiles: recent advances and future perspectives. *Crit. Rev. Plant Sci.* 25, 417–440. doi: 10.1080/07352680600899973

FAO (2006). *World Reference Base for Soil Resources 2006. A Framework for International Classification, Correlation and Communication*. Rome: Food and Agriculture Organization of the United Nations.

Fortunati, A., Barta, C., Brilli, F., Centritto, M., Zimmer, I., Schnitzler, J.-P., et al. (2008). Isoprene emission is not temperature-dependent during and after severe-drought stress: a physiological and biochemical analysis. *Plant J.* 55, 687–697. doi: 10.1111/j.1365-313X.2008.03538.x

Frazao, D. F., Raimundo, J. R., Domingues, J. L., Quintela-Sabarís, C., Goncalves, J. C., and Delgado, F. (2018). *Cistus ladanifer* (Cistaceae): a natural resource in Mediterranean-type ecosystems. *Planta* 247, 289–300. doi: 10.1007/s00425-017-2825-2

Gomes, P. B., Mata, V. G., and Rodrigues, A. E. (2005). Characterization of the portuguese-grown *Cistus ladanifer* essential oil. *J. Essent. Oil Res.* 17, 160–165. doi: 10.1080/10412905.2005.9698864

Grant, O. M., Tronina, Ł, Ramalho, J. C., Besson, C. K., Lobo-do-Vale, R., Pereira, J. S., et al. (2010). The impact of drought on leaf physiology of *Quercus suber* L. trees: comparison of an extreme drought event with chronic rainfall reduction. *J. Exp. Bot.* 61, 4361–4371. doi: 10.1093/jxb/erq239

Grassi, G., and Magnani, F. (2005). Stomatal, mesophyll conductance and biochemical limitations to photosynthesis as affected by drought and leaf ontogeny in ash and oak trees. *Plant Cell Environ.* 28, 834–849. doi: 10.1111/j.1365-3040.2005.01333.x

Grote, R., Lavoir, A.-V., Rambal, S., Staudt, M., Zimmer, I., and Schnitzler, J.-P. (2010). Modelling the drought impact on monoterpene fluxes from an evergreen Mediterranean forest canopy. *Oecologia* 160, 213–223. doi: 10.1007/s00442-009-1298-9

Guenther, A. B., Jiang, X., Heald, C. L., Sakulyanontvittaya, T., Duhl, T., Emmons, K., et al. (2012). The model of emissions of gases and aerosols from nature version 2.1 (MEGAN2.1): an extended and updated framework for modeling biogenic emissions. *Geosci. Model Dev.* 5, 1471–1492. doi: 10.5194/gmd-5-1471-2012

Guenther, A. B., Zimmerman, P. R., Harley, P. C., Monson, R. K., and Fall, R. (1993). Isoprene and monoterpene emission rate variability- model evaluation and sensitivity analyses. *J. Geophys. Res.* 98, 12609–12617. doi: 10.1029/93JD00527

Gülz, P. G., Herrmann, T., and Hangst, K. (1996). Leaf trichomes in the genus Cistus. *Flora* 191, 85–104. doi: 10.1016/S0367-2530(17)30692-8

Holopainen, J. K., and Gershenzon, J. (2010). Multiple stress factors and the emission of plant VOCs. *Trends Plant Sci.* 15, 176–184. doi: 10.1016/j.tplants.2010.01.006

Instituto Português do Mar e da Atmosfera [IPMA] (1981–2010). *Normais Climatológicas - (provisórias) – Évora*. Available at: https://www.ipma.pt/pt/oclima/normais.clima/1981-2010/007/ [accessed November 12, 2017].

Kesselmeier, J., and Staudt, M. (1999). Biogenic volatile organic compounds (VOC): an overview on emission, physiology and ecology. *J. Atmos. Chem.* 33, 23–88. doi: 10.1023/A:1006127516791

Kessler, M., Connor, E., and Lehnert, M. (2015). Volatile organic compounds in the strongly fragrant fern genus *Melpomene* (Polypodiaceae). *Plant Biol.* 17, 430–436. doi: 10.1111/plb.12252

Kleiber, A., Duan, Q., Jansen, K., Junker, L. V., Kammerer, B., Rennenberg, H., et al. (2017). Drought effects on root and needle terpenoid content of a coastal and interior Douglas fir provenance. *Tree Physiol.* 37, 1648–1658. doi: 10.1093/treephys/tpx113

Kurz-Besson, C. K., Lobo-do-Vale, R., Rodrigues, M. L., Almeida, P., Herd, A., Grant, O. M., et al. (2014). Cork oak physiological responses to manipulated water availability in a Mediterranean woodland. *Agric. For. Meteorol.* 184, 230–242. doi: 10.1016/j.agrformet.2013.10.004

Lavoir, A.-V., Staudt, M., Schnitzler, J. P., Landais, D., Massol, F., Rocheteau, A., et al. (2009). Drought reduced monoterpene emissions from the evergreen Mediterranean oak *Quercus ilex*: results from a throughfall displacement experiment. *Biogeosciences* 6, 1167–1180. doi: 10.5194/bg-6-1167-2009

Lerdau, M., Guenther, A., and Monson, R. (1997). Plant production and emissions of volatile organic compounds. *BioScience* 47, 373–383. doi: 10.2307/1313152

Lluisà, J., and Peñuelas, J. (1998). Changes in terpene content and emission in potted Mediterranean woody plants under severe drought. *Can. J. Bot.* 76, 1366–1373. doi: 10.1139/b98-141

Lluisà, J., and Peñuelas, J. (2000). Seasonal patterns of terpene content and emission from seven Mediterranean woody species in field conditions. *Am. J. Bot.* 87, 133–140. doi: 10.2307/2656691

Lluisà, J., Peñuelas, J., Alessio, G. A., and Estiarte, M. (2006). Seasonal contrasting changes of foliar concentrations of terpenes and other volatile organic compounds in four dominant species of a Mediterranean shrubland submitted to field experimental drought and warming. *Physiol. Plant.* 127, 632–649. doi: 10.1111/j.1399-3054.2006.00693.x

Lluisà, J., Peñuelas, J., Asensio, D., and Munné-Bosch, S. (2005). Airborne limonene confers limited thermotolerance to *Quercus ilex*. *Physiol. Plant.* 123, 40–48. doi: 10.1111/j.1399-3054.2004.00426.x

Lluisà, J., Peñuelas, J., Ogaya, R., and Alessio, G. (2010). Annual and seasonal changes in foliar terpene content and emission rates in *Cistus albidus* L. submitted to soil drought in Prades forest (Catalonia, NE Spain). *Acta Physiol. Plant.* 32, 387–394. doi: 10.1007/s11738-009-0416-y

Lluisà, J., Roahtyn, S., Yakir, D., Rotenberg, E., Seco, R., Guenther, A., et al. (2016). Photosynthesis, stomatal conductance and terpene emission response to water availability in dry and mesic Mediterranean forests. *Trees* 30, 749–759. doi: 10.1007/s00468-015-1317-x

Loreto, F., Bagnoli, F., and Fineschi, S. (2009). One species, many terpenes: matching chemical and biological activity. *Trends Plant Sci.* 14, 416–420. doi: 10.1016/j.tplants.2009.06.003

Loreto, F., Ciccioli, P., Cecinato, A., Brancaleoni, E., Frattoni, M., Fabozzi, C., et al. (1996). Evidence of the photosynthetic origin of monoterpenes emitted by *Quercus ilex* L. leaves by 13C labeling. *Plant Physiol.* 110, 1317–1322. doi: 10.1104/pp.110.4.1317

Loreto, F., Pinelli, P., Manes, F., and Kollist, H. (2004). Impact of ozone on monoterpene emissions and evidence for an isoprene-like antioxidant action of monoterpenes emitted by *Quercus ilex* leaves. *Tree Physiol.* 24, 361–367. doi: 10.1093/treephys/24.4.361

Loreto, F., Pollastri, S., Fineschi, S., and Velikova, V. (2014). Volatile isoprenoids and their importance for protection against environmental constraints in the Mediterranean area. *Environ. Exp. Bot.* 103, 99–106. doi: 10.1016/j.envexpbot.2013.09.005

Loreto, F., and Schnitzler, J.-P. (2010). Abiotic stresses and induced BVOCs. *Trends Plant Sci.* 15, 154–166. doi: 10.1016/j.tplants.2009.12.006

Lucero, M., Estell, R., Tellez, M., and Fredrickson, D. (2009). A retention index calculator simplifies identification of plant volatile organic compounds. *Phytochem. Anal.* 20, 378–384. doi: 10.1002/pca.1137

Manos, P. S., Doyle, J. J., and Nixon, K. C. (1999). Phylogeny, biogeography, and processes of molecular differentiation in *Quercus* subgenus *Quercus* (Fagaceae). *Mol. Phylogenet. Evol.* 12, 333–349. doi: 10.1006/mpev.1999.0614

Matsunga, S. N., Chatani, S., Nakatsuka, S., Kusumoto, D., Kubota, K., Utsumi, Y., et al. (2012). Determination and potential importance of diterpene (kaur-16-ene) emitted from dominant coniferous trees in Japan. *Chemosphere* 87, 886–893. doi: 10.1016/j.chemosphere.2012.01.040

Miller, G., Shulaev, V., and Mittler, R. (2008). Reactive oxygen signaling and abiotic stress. *Physiol. Plant.* 133, 481–489. doi: 10.1111/j.1399-3054.2008.01090.x

Munné-Bosch, S., and Alegre, L. (2000). Changes in carotenoids, tocopherols and diterpenes during drought and recovery, and the biological significance of chlorophyll loss in *Rosmarinus officinalis* plants. *Planta* 210, 925–931. doi: 10.1007/s004250050699

Munné-Bosch, S., Mueller, M., Schwarz, K., and Alegre, L. (2001). Diterpenes and antioxidative protection in drought-stressed Salvia officinalis plants. *J. Plant Physiol.* 158, 1431–1437. doi: 10.1078/0176-1617-00578

Niinemets, Ü. (2010). Mild versus severe stress and BVOCs: thresholds, priming and consequences. *Trends Plant Sci.* 15, 145–153. doi: 10.1016/j.tplants.2009.11.008

Niinemets, Ü., Fares, S., Harley, P., and Jardine, K. J. (2014). Bidirectional exchange of biogenic volatiles with vegetation: emission sources, reactions, breakdown and deposition. *Plant Cell Environ.* 37, 1790–1809. doi: 10.1111/pce.12322

Núñez-Olivera, E., Martínez-Abaigar, J., and Escudero, J. C. (1996). Adaptability of leaves of *Cistus ladanifer* to widely varying environmental conditions. *Funct. Ecol.* 10, 636–646. doi: 10.2307/2390174

Ormeno, E., Mévy, J. P., Vila, B., Bousquet-Mélou, A., Greff, S., Bonin, G., et al. (2007). Water deficit stress induces different monoterpene and sesquiterpene emission changes in Mediterranean species. Relationship between terpene emissions and plant water potential. *Chemosphere* 67, 276–284. doi: 10.1016/j.chemosphere.2006.10.029

Otieno, D. O., Kurz-Besson, C., Liu, J., Schmidt, M. W. T., Lobo-do-Vale, R., David, T. S., et al. (2006). Seasonal variations in soil and plant water status in a *Quercus suber* L. stand: roots as determinants of tree productivity and survival in the Mediterranean-type ecosystem. *Plant Soil* 283, 119–135. doi: 10.1007/s11104-004-7539-0

Otsuka, M., Kenmoku, H., Ogawa, M., Okada, K., Mitsuhashi, W., Sassa, T., et al. (2004). Emission of ent-kaurene, a diterpenoid hydrocarbon precursor for gibberellins, into the headspace from plants. *Plant Cell Physiol.* 45, 1129–1138. doi: 10.1093/pcp/pch149

Páscoa, P., Gouveia, C. M., Russo, A., and Trigo, R. M. (2017). Drought trends in the Iberian Peninsula over the last 112 years. *Adv. Meteorol.* 2017:4653126. doi: 10.1155/2017/4653126

Peñuelas, J., and Lluisà, J. (2001). The complexity of factors driving volatile organic compound emissions by plants. *Biol. Plant.* 44, 481–487. doi: 10.1023/A:1013797129428

Peñuelas, J., Lluisà, J., Asensio, D., and Munné-Bosch, S. (2005). Linking isoprene with plant thermotolerance, antioxidants and monoterpene emissions. *Plant Cell Environ.* 28, 278–286. doi: 10.1111/j.1365-3040.2004.01250.x

Pinto, C. A., David, J. S., Cochard, H., Caldeira, M. C., Henriques, M. O., Quilhó, T., et al. (2012). Drought-induced embolism in current-year shoots of two Mediterranean evergreen oaks. *For. Ecol. Manage.* 285, 1–10. doi: 10.1016/j.foreco.2012.08.005

Pio, C. A., Nunes, T. V., and Brito, S. (1993). "Volatile hydrocarbon emissions from common and native species of vegetation in Portugal," in *General Assessment of Biogenic Emissions and Deposition of Nitrogen Compounds, Sulphur Compounds and Oxidants in Europe*, eds J. Slanina, G. Angeletti, and S. Beilke (Anjou,: CEC), 291–298.

Pio, C. A., Silva, P. A., Cerqueira, M. A., and Nunes, T. V. (2005). Diurnal and seasonal emissions of volatile organic compounds from cork oak (*Quercus suber*) trees. *Atmos. Environ.* 39, 1817–1827. doi: 10.1016/j.atmosenv.2004.11.018

Possell, M., and Loreto, F. (2013). "The role of volatile organic compounds in plant resistance to abiotic stress: responses and mechanisms," in *Biology, Controls and Models of Tree Volatile Organic Compounds Emissions*, ed. Ü. Niinemets (Berlin: Springer), 209–235. doi: 10.1007/978-94-007-6606-8_8

Quero, J. L., Sterck, F. J., Martínez-Vilalta, J., and Villar, R. (2011). Water-use strategies of six co-existing Mediterranean woody species during a summer drought. *Oecologia* 166, 45–57. doi: 10.1007/s00442-011-1922-3

Ramírez, D. A., Parra, A., Resco de Dios, V., and Moreno, J. M. (2012). Differences in morpho-physiological leaf traits reflect the response of growth to drought in a seeder but not in a resprouter Mediterranean species. *Funct. Plant Biol.* 39, 332–341. doi: 10.1071/FP11232

Rascher, K. G., Große-Stoltenberg, A., Máguas, C., and Werner, C. (2011). Understorey invasion by *Acacia longifolia* alters the water balance and carbon gain of a Mediterranean pine forest. *Ecosystems* 14:904. doi: 10.1007/s10021-011-9453-7

Rivoal, A., Fernandez, C., Lavoir, A. V., Olivier, R., Lecareux, C., Greff, S., et al. (2010). Environmental control of terpene emissions from *Cistus monospeliensis* L. in natural Mediterranean shrubland. *Chemosphere* 78, 942–949. doi: 10.1016/j.chemosphere.2009.12.047

Rolo, V., and Moreno, G. (2011). Shrub species affect distinctively the functioning of scattered *Quercus ilex* trees in Mediterranean open woodlands. *For. Ecol. Manage.* 261, 1750–1759. doi: 10.1016/j.foreco.2011.01.028

Sakuratani, T. (1984). Improvement of the probe for measuring water flow rate in intact plants with the stem heat balance method. *J. Agric. Meteorol.* 40, 273–277. doi: 10.2480/agrmet.40.273

Seco, R., Peñuelas, J., Filella, I., Lluisà, J., Molowny-Horas, R., Schallhart, S., et al. (2011). Contrasting winter and summer VOC mixing ratios at a forest site in the Western Mediterranean Basin: the effect of local biogenic emissions. *Atmos. Chem. Phys.* 11, 13161–13179. doi: 10.5194/acp-11-13161-2011

Staudt, M., Bourgeois, I., Al Halabi, R., Song, W., and Williams, J. (2017). New insights into the parametrization of temperature and light responses of mono - and sesquiterpene emissions from Aleppo pine and rosemary. *Atmos. Environ.* 152, 212–221. doi: 10.1016/j.atmosenv.2016.12.033

Staudt, M., Ennajah, A., Mouillot, F., and Joffre, R. (2008). Do volatile organic compound emissions of Tunisian cork oak populations originating from contrasting climate conditions differ in their responses to summer drought? *Can. J. For. Res.* 38, 2965–2975. doi: 10.1139/X08-134

Staudt, M., Mir, C., Joffre, R., Rambal, S., Bonin, A., Landais, D., et al. (2004). Isoprenoid emissions of *Quercus* spp. (*Q. suber* and *Q. ilex*) in mixed stands contrasting in interspecific genetic introgression. *New Phytol.* 163, 573–584. doi: 10.1111/j.1469-8137.2004.01140.x

Staudt, M., Rambal, S., and Joffre, R. (2002). Impact of drought on seasonal monoterpene emissions from *Quercus ilex* in southern France. *J. Geophys. Res.* 107:4602. doi: 10.1029/2001JD002043

Tenhunen, J. D., Lange, O. L., Harley, P. C., Beyschlag, W., and Mayer, A. (1985). Limitations due to water stress on leaf net photosynthesis of *Quercus coccifera* in the Portuguese evergreen scrub. *Oecologia* 67, 23–30. doi: 10.1007/BF00378446

Tholl, D. (2015). Biosynthesis and biological functions of terpenoids in plants. *Adv. Biochem. Eng. Biotechnol.* 148, 63–106. doi: 10.1007/10_2014_295

Valares Masa, C. V., Alías Gallego, J. C., Chaves Lobón, N., and Díaz, T. S. (2016). Intra-population variation of secondary metabolites in *Cistus ladanifer* L. *Molecules* 21:E945. doi: 10.3390/molecules21070945

Velikova, V., and Loreto, F. (2005). On the relationship between isoprene emission and thermotolerance in Phragmites australis leaves exposed to high temperatures and during the recovery from a heat stress. *Plant Cell Environ.* 28, 318–327. doi: 10.1111/j.1365-3040.2004.01314.x

Velikova, V., Sharkey, T. D., and Loreto, F. (2012). Stabilization of thylakoid membranes in isoprene-emitting plants reduces formation of reactive oxygen species. *Plant Signal. Behav.* 7, 139–141. doi: 10.4161/psb.7.1.18521

Velikova, V., Varkonyi, Z., Szabo, M., Maslenkova, L., Nogues, I., Kovacs, L., et al. (2011). Increased thermostability of thylakoid membranes in isoprene-emitting leaves probed with three biophysical techniques. *Plant Physiol.* 157, 905–916. doi: 10.1104/pp.111.182519

Verdeguer, M., Blázquez, M. A., and Boira, H. (2012). Chemical composition and herbicidal activity of the essential oil from a *Cistus ladanifer* L. population from Spain. *Nat. Prod. Res.* 26, 1602–1609. doi: 10.1080/14786419.2011.592835

Vickers, C. E., Gershenzon, J., Lerdau, M. T., and Loreto, F. (2009). A unified mechanism of action for volatile isoprenoids in plant abiotic stress. *Nat. Chem. Biol.* 5, 283–291. doi: 10.1038/nchembio.158

Von Schwartzenberg, K., Schultze, W., and Kassner, H. (2004). The moss Physcomitrella patens releases a tetracyclic diterpene. *Plant Cell Rep.* 22, 780–786. doi: 10.1007/s00299-004-0754-6

Werner, C., Correia, O., and Beyschlag, W. (1999). Two different strategies of Mediterranean macchia plants to avoid photoinhibitory damage by excessive radiation levels during summer drought. *Acta Oecol.* 20, 15–23. doi: 10.1016/S1146-609X(99)80011-3

Werner, C., Correia, O., and Beyschlag, W. (2002). Characteristic patterns of chronic and dynamic photoinhibition of different functional groups in a Mediterranean ecosystem. *Funct. Plant Biol.* 29, 999–1011. doi: 10.1071/PP01143

Yáñez-Serrano, A. M., Fasbender, L., Kreuzwieser, J., Dubbert, D., Haberstroh, S., Lobo-do-Vale, R., et al. (2018). Volatile diterpene emission by two Mediterranean *Cistaceae* shrubs. *Sci. Rep.* 8:6855. doi: 10.1038/s41598-018-25056-w

Conflict of Interest Statement: The authors declare that the research was conducted in the absence of any commercial or financial relationships that could be construed as a potential conflict of interest.

frontiers in Plant Science

ORIGINAL RESEARCH
published: 06 August 2018
doi: 10.3389/fpls.2018.01050

Soil Moisture Availability at Early Growth Stages Strongly Affected Root Growth of *Bothriochloa ischaemum* When Mixed With *Lespedeza davurica*

Zhi Wang[1,2†], Weizhou Xu[3†], Zhifei Chen[1], Zhao Jia[1], Jin Huang[1,2], Zhongming Wen[1,2], Yinglong Chen[1,2] and Bingcheng Xu[1,2]*

[1] State Key Laboratory of Soil Erosion and Dryland Farming on the Loess Plateau, Northwest A&F University, Yangling, China, [2] Institute of Soil and Water Conservation, Chinese Academy of Sciences and Ministry of Water Resources, Yangling, China, [3] College of Life Science, Yulin University, Yulin, China

OPEN ACCESS

Edited by:
Randy D. Allen,
Oklahoma State University,
United States

Reviewed by:
Peng Yu,
Universität Bonn, Germany
Iván Prieto,
Centro de Edafología y Biología Aplicada del Segura (CEBAS), Spain

***Correspondence:**
Bingcheng Xu
bcxu@ms.iswc.ac.cn

[†] These authors have contributed equally to this work.

Specialty section:
This article was submitted to Plant Abiotic Stress, a section of the journal Frontiers in Plant Science

Received: 03 March 2018
Accepted: 28 June 2018
Published: 06 August 2018

Citation:
Wang Z, Xu W, Chen Z, Jia Z, Huang J, Wen Z, Chen Y and Xu B (2018) Soil Moisture Availability at Early Growth Stages Strongly Affected Root Growth of Bothriochloa ischaemum When Mixed With Lespedeza davurica. Front. Plant Sci. 9:1050. doi: 10.3389/fpls.2018.01050

Rainfall is the main resource of soil moisture in the semiarid areas, and the altered rainfall pattern would greatly affect plant growth and development. Root morphological traits are critical for plant adaptation to changeable soil moisture. This study aimed to clarify how root morphological traits of *Bothriochloa ischaemum* (a C_4 herbaceous species) and *Lespedeza davurica* (a C_3 leguminous species) in response to variable soil moisture in their mixtures. The two species were co-cultivated in pots at seven mixture ratios under three soil water regimes [80% (HW), 60% (MW), and 40% (LW) of soil moisture field capacity (FC)]. At the jointing, flowering, and filling stages of *B. ischaemum*, the LW and MW treatments were rewatered to MW or HW, respectively. At the end of growth season, root morphological traits of two species were evaluated. Results showed that the root morphological response of *B. ischaemum* was more sensitive than that of *L. davurica* under rewatering. The total root length (TRL) and root surface area (RSA) of both species increased as their mixture ratio decreased, which suggested that mixed plantation of the two species would be beneficial for their own root growth. Among all treatments, the increase of root biomass (RB), TRL, and RSA reached the highest levels when soil water content increased from 40 to 80% FC at the jointing stage. Our results implied that species-specific response in root morphological traits to alternated rainfall pattern would greatly affect community structure, and large rainfall occurring at early growth stages would greatly increase their root growth in the semiarid environments.

Keywords: rewatering, root morphology, growth stage, total root length, root surface area, mixture ratio

INTRODUCTION

Grasslands play a key role in improving ecological environment in the semiarid and arid regions (Niu et al., 2016; Xiong et al., 2017). Rainfall, as the main resource of soil moisture, greatly affects the development of natural grasslands in such areas (Zhu et al., 2014; Gao et al., 2015). It is forecasted that climate change will alter the seasonal distribution, frequency, and intensity of rainfall events in the semiarid and arid areas, which may result in more serious drought with

fewer and heavier rainfall events (Li et al., 2012; IPCC, 2014). Amount and seasonal changes of precipitation would strongly affect not only plant growth and distribution, but also community structure (Miranda et al., 2011; Niu et al., 2016). The root system is the central part of plant or community, evaluating root response characteristics to variable soil moisture environment that will provide insights into how variable rainfall affects plant growth and ecosystem process (Bardgett et al., 2014; Nie et al., 2014; Han et al., 2015; de Vries et al., 2016; Ramamoorthy et al., 2017).

Root morphological characters, such as total root length (TRL), root average diameter (RAD), and root surface area (RSA), are the key components of the root response mechanism under variable soil moisture environments (Li et al., 2011; Zeppel et al., 2014; Xu et al., 2015). In general, mild drought would stimulate plants to increase TRL and produce finer roots (Subere et al., 2009; Bengough et al., 2011; Li et al., 2011), whereas severe drought greatly limits root growth (Xu et al., 2012; Zhao et al., 2017). Root morphological response to drought differs at different growth stages (Kano et al., 2011; Han et al., 2015). Plant root systems usually have higher morphological plasticity when suffering drought stress at the early growth stages, and higher root morphological plasticity is strongly related to the carbohydrate allocation strategy, physiological activity, growth rate, and water requirement (Dhief et al., 2011; Xu et al., 2015; Niu et al., 2016). Under highly pulsed and irregular rainfall conditions, plants' survival not only depends on their drought resistance but also on their ability to recover after rainfall in which root morphological characters play a critical role (Li et al., 2011; Chen et al., 2016). The excellent performance of cassava yield is attributed to the quick recovery of its adventitious root elongation under dramatic fluctuation in soil moisture conditions (Subere et al., 2009). Moreover, root morphological response to soil water improvement is also affected by antecedent soil water contents (Ogle and Reynolds, 2004; Xiong et al., 2017; Zhao et al., 2017). Tap roots of shrubs distributed in the semiarid Patagonia steppe did not always respond to large precipitation events, only when the 30–60 cm soil layer was relatively dry where their roots distributed (Golluscio et al., 1998). The effects of the timing and intensity of drought on root growth have been widely evaluated, but how root morphology in response to variable rewatering at different growth stages under rainfall alternation in semiarid and arid regions was largely ignored (Li et al., 2011; Padilla et al., 2013; Han et al., 2015).

Root growth and morphological response to soil moisture fluctuation are also affected by interspecific or intraspecific competition as well as root types (Ogle and Reynolds, 2004; Xiong et al., 2017; Zhao et al., 2017). Intercropping or mixture of plants with contrasting root traits, such as legume shrub (taproot system)–grass (fibrous root system) mixture, could alleviate intraspecific competition and promote root growth, RSA, and TRL in dry environments, compared with pure stand of the same species (Xu et al., 2012, 2015; Qiu and Li, 2016). Rational mixed sowing of legume shrubs plus gramineous grass is beneficial for improving plant biomass accumulation, water use efficiency, and ecosystem service, because there exist complementary and mutually reinforcing roles, which are closely related to their root characters (Qiu and Li, 2016; Zhao et al., 2017; Xu et al., 2018). Generally, fibrous root systems develop thinner lateral roots to obtain water from the shallow soil layer, whereas taproot systems mainly absorb water from the deep soil layer, and the latter exhibit lower responsive plasticity than fibrous root systems under drought conditions (Zeppel et al., 2014; Barkaoui et al., 2016; Zhao et al., 2017). Morphological responses including RSA and TRL of fibrous roots tend to be more sensitive to variable drought stress than taproots as well as the physiological and growth response, which have been confirmed in *Bothriochloa ischaemum* (a C_4 gramineae species, fibrous root system) and *Lespedeza davurica* (a perennial C_3 leguminous sub-shrub, tap root system) in our previous studies (Xu et al., 2012, 2015; Zhao et al., 2017).

In the semiarid Loess Plateau region, *B. ischaemum* and *L. davurica* are codominant species and occupy great positions in natural grasslands (Xu et al., 2015, 2016; Liu et al., 2017). Water is the most crucial environmental factor affecting their growth and distribution. In the area, the mean annual rainfall is about 540.4 mm with 60–80% distribution in July to September (Niu et al., 2016; Xiong et al., 2017). The unevenly distributed and unpredictable rainfall is the main resource of soil moisture (Niu et al., 2016; Xiong et al., 2017). Plants distributed in this region are continuously exposed to drought followed by rewatering under field conditions (Xu et al., 2016; de Vries et al., 2016; Liu et al., 2017). However, knowledge about the response characters of the contrasting root systems under rewatering in *B. ischaemum* and *L. davurica* is scarce, especially when grown in mixtures. Here, we conducted a soil moisture-controlled pot experiment to investigate the response of their root growth and morphological traits including RAD, TRL, and RSA to rewatering in the community at three main growth stages. Under different water supplies, three rewatering regimes were applied at each growth stage to test the performance of these root traits. Meanwhile, the differences of root response between *B. ischaemum* and *L. davurica* in both mixture and monoculture were evaluated. We hypothesized that: (1) response degrees of root morphological traits are strongly influenced by the intensity and timing of rewatering; (2) root morphological response of *B. ischaemum* under rewatering is more sensitive than that of *L. davurica*; (3) mixture plantation is beneficial for improving root density, RSA, and root growth of the two species under rewatering after phase drought.

MATERIALS AND METHODS

Plant Material and Growth Condition

The seeds of *B. ischaemum* (L.) Keng and *L. davurica* (L.) Schindl were harvested in the autumn of 2011 from the natural grassland at the Ansai Research Station (ARS) of the Chinese Academy of Sciences (36°51′30″N, 109°19′23″E, 1068 to 1309 m a.s.l.). The station is located in the central part of the semiarid hilly gully Loess Plateau region. Seed germination rates of two species were both above 90% at 25°C in the culture chamber.

Seeds were sown in the cylindrical plastic pots (20 cm in diameter and 30 cm in depth) with a plastic pipe adjacent to the inner wall for watering. The loess soil obtained from the upper 20 cm of an arable field in ARS was utilized. The soil was sandy loam with the properties as described in **Supplementary Table S1**. As basal fertilizers, 0.481 g CON_2H_4 and 3.949 g KH_2PO_4 were mixed with 9.0 kg air-dried soil for each pot. The pot experiments were conducted under a rainout shelter in the Institute of Soil and Water Conservation located in Yangling, Shaanxi Province, China (34°12′N, 108°7′E, 530 m a.s.l.). The mean monthly temperature ranged from −1°C (January) to 26.7°C (July), while the mean annual temperature is 13.0°C.

Species Combination and Water Treatment

According to the replacement series design described in the previous study (Xu et al., 2015), two species were grown at seven mixture planting ratios (12:0, 10:2, 8:4, 6:6, 4:8, 2:10, and 0:12) with a density of 12 plants per pot on April 1, 2012. All pots were well watered [80 ± 5% FC (field capacity)] to ensure seedling establishment till the tillering stage (June 10) of *B. ischaemum* when drought stress was imposed.

The water treatments were implemented according to the growth stage of *B. ischaemum* with three water regimes [80 ± 5% FC (HW), 60 ± 5% FC (MW), and 40 ± 5% FC (LW)] commenced at the tillering stage of *B. ischaemum* (June 10, 2012). Then, three rewatering regimes were carried out at three rewatering periods as follows: at the jointing stage (July 10), flowering stage (August 10), and filling stage (September 10) of *B. ischaemum*, soil water contents were raised from MW to HW (referred to as M-HW), LW to HW (L-MW), and LW to MW (L-HW) through rewatering, respectively (**Supplementary Figure S1**). For the nursing of desired water regimes, the water losses caused by daily evapo-transpiration were replaced at 18:00 after weighing the pots. A layer of perlite (20 g, approximately 2.0 cm deep) was put on the soil surface of each pot to reduce evaporation. And the levels of soil water contents after rewatering were maintained until withering stage (October 10). Each treatment of constant water regimes or rewatering was replicated five times. A total of 420 pots were used in this study.

Shoot and Root Samplings

Shoot and root samples of each species were separately collected from three randomly selected pots for each treatment at the end of the growth stage (October 10). Particularly, the whole root system of each pot was carefully washed using a gentle water jet and collected all roots through a sieve (aperture size 0.25 mm, 60 meshes). In each pot, the roots were carefully separated for each species in water. Due to the difficulty of separating each species into individual and large root biomass, approximately 30% of total roots of each species were selected to assess root morphological traits. The selected root subsamples were dyed using 0.5% methylene blue solution for 5 min and gently dried with absorbent paper, and then fixed through two transparent plastic sheets. The dyed root systems were scanned (BENQ color scanner 5560) and analyzed (DT-Scan, Delta T-Devices) to determine TRL (m), RSA (cm^2), and RAD (mm). Then, the selected subsamples and the rest of roots and shoots samples were oven-dried for 48 h at 80°C. Specific root length (SRL, m g^{-1}) and specific root area (SRA, cm^{-2} g^{-1}) were determined by the root length and root area of subsamples divided the corresponding root dry biomass. TRL and RSA were calculated through SRL and SRA by individual root dry weight of each individual plant, respectively. The root/shoot ratio (RSR) was calculated through dividing the root dry biomass by the shoot dry biomass of each individual plant (Xu et al., 2015).

Statistical Analysis

Differences in the mean values of root biomass and each morphological trait were compared among treatments (rewatering period and regime, mixture ratio, species or mixture vs. monoculture) by one-way analysis of variance (ANOVA) followed by the Tukey least significant difference (LSD) multiple range tests in SPSS 19 (IBM, United States). Statistical significance was set at $P \leq 0.05$. To evaluate the interactive effects of rewatering period and regime on root morphological traits and root biomass of each species, the mixed linear model was used, in which rewatering period and regime were fixed factors and mixture ratio and antecedent soil water contents as random effects. To clarify the effect of mixture ratio on root morphological traits and root biomass of each species, the mixed linear model was used and in which mixture ratio was the fixed factor and rewatering period and regime were the random effects. To investigate the effect of species on the response of these root traits to rewatering, the mixed linear model with species as fixed factor including the mixture ratio, rewatering period and regime as random effects was performed. To assess the relationship among root biomass (RB), TRL and RSA and reveal the effects of water treatments on these root traits, the linear regression analysis was carried out for each species under each water treatment.

RESULTS

Root Biomass and Root/Shoot Ratio

Under each rewatering treatment, the RB of *B. ischaemum* was significantly higher than that of *L. davurica* at the same mixture ratio. The RB of *B. ischaemum* per plant evidently decreased as its ratio increased in the mixture, while such a trend was not detected in *L. davurica* (**Figure 1**).

The regime and period of rewatering and their interaction generated significant effects on RB of *B. ischaemum* and *L. davurica* (**Table 1**). When soil water contents (SWC) increased from 40 to 80% FC at the jointing stage, RB of *B. ischaemum* and *L. davurica* increased about 190.0 and 45.0% compared with those under 40% FC, respectively. The RB increment of each species was higher than those under the other rewatering treatments. Under each rewatering regime, RB response degrees of both species reached the lowest levels at the filling stage. The RB of *B. ischaemum* per plant evidently decreased as its ratio increased in the mixture, whereas such a trend was not detected in *L. davurica* (**Figure 1**). Meanwhile, the shoot biomass

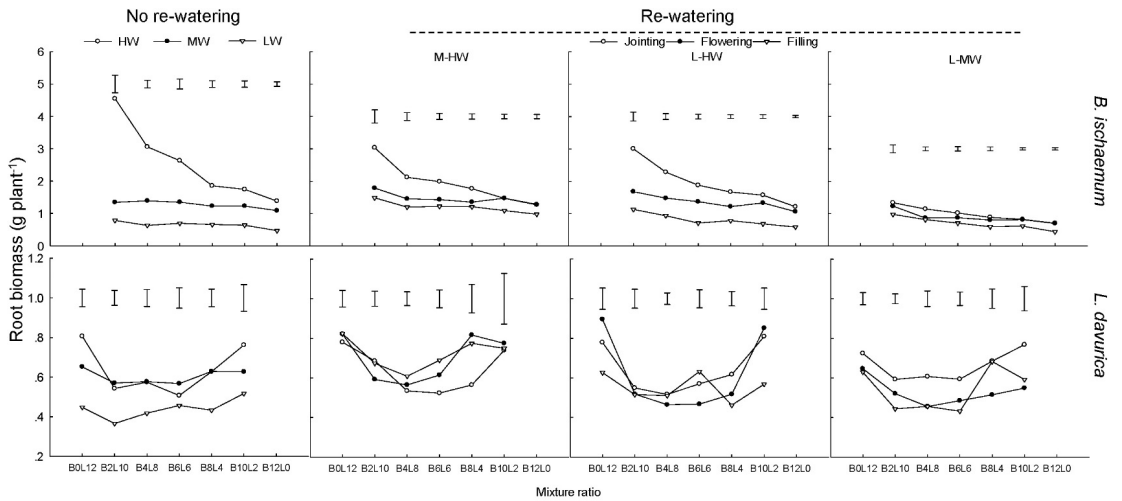

FIGURE 1 | Root biomass (RB) per plant of *B. ischaemum* (B) and *L. davurica* (L) at different mixture ratios under each water treatment. HW: 80 ± 5% FC; MW: 60 ± 5% FC; LW: 40 ± 5% FC; M-HW: soil water content increased from MW to HW; L-MW: soil water content increased from LW to MW; L-HW: soil water content increased from LW to HW. The vertical bars indicate the LSD values ($P \leq 0.05$) for the RB difference of each species among rewatering periods at each mixture ratio.

of each species showed similar trends with RB in response to rewatering across mixture ratios (**Supplementary Figure S2**). The RSR response degree of both species also got the highest levels when SWC increased from 40 to 80% FC at the jointing stage. The corresponding RSR of *B. ischaemum* and *L. davurica* significantly decreased about 27.0 and 39.0% compared with those under 40% FC, respectively (**Supplementary Figure S3**). Rewatering regime and period and their interaction significantly affected the RSR of the two species (**Table 1**).

Root Average Diameter

For *B. ischaemum*, the averaged RAD value in mixtures was significantly higher than that of monoculture under L-HW (40–80% FC) at the jointing and flowering stages as well as M-HW (60–80% FC) at the jointing stage. No significant difference between mixture and monoculture was detected in the RAD of *L. davurica* under rewatering treatments (**Figure 2**). For each rewatering period, there was no notable changing trend of RAD for *B. ischaemum* or *L. davurica* among three rewatering regimes (**Figure 2**). Rewatering regime generated significant effects on the RAD of both species. The effects of rewatering period on *L. davurica* and the interaction of rewatering period and regime on *B. ischaemum* were significant (**Table 1**).

Total Root Length

For each rewatering treatment, the TRL level of *B. ischaemum* was significantly greater than that of *L. davurica*. The TRL of both species tended to decrease as their ratios increased in the mixtures (**Figure 3**).

Rewatering period and regime and their interaction produced significant effects on the TRL of *B. ischaemum* and *L. davurica* except rewatering regime on *L. davurica* (**Table 1**). When SWC increased from 40 to 80% FC at the jointing stage, the TRL of *B. ischaemum* increased about 1.6 times compared with those under 40% FC, and the increased degree was higher than under other rewatering treatments. When SWC increased from 60 to 80% FC, the TRL of *B. ischaemum* increased about 48.0% at the jointing stage and 34.0% at the flowering stage. When SWC increased from 40 to 60% FC, remarkable improvement of TRL of about 47.0% at the jointing stage and 52.0% at the flowering stage were detected in *B. ischaemum*. However, there was no obvious change detected in the TRL of *B. ischaemum* at the filling stage under three rewatering regimes. For *L. davurica*, TRL ranged from 1.6 m to 20.8 m per plant, and there was no remarkable change trend detected among rewatering periods or regimes (**Figure 3**). Under each rewatering treatment, only *B. ischaemum* had linear relationships between TRL and RB, and the slopes of regressed lines of TRL on RB at the flowering and filling stages were greater than that at the jointing stage (**Supplementary Table S2**).

Root Surface Area

The RSA of *B. ischaemum* and *L. davurica* decreased as their ratios increased in the mixtures under each rewatering regime. The averaged RSA values of *B. ischaemum* were approximately 20.1 times higher than those of *L. davurica* in the mixture, and 21.5 times higher in the monoculture (**Figure 4**).

Rewatering period and regime and their interaction significantly affected the RSA of *B. ischaemum* and *L. davurica* with the exception of rewatering regime on *L. davurica* (**Table 1**). Both *B. ischaemum* and *L. davurica* exhibited the highest increase in RSA of about 240 and 67.7% when SWC increased from 40 to 80% FC at the jointing stage, respectively. For *B. ischaemum*, RSA increased about 62.0 and 34.9% when SWC improved from 60 to 80% FC at the jointing stage and flowering stage. At the same rewatering periods, 62.2 and 82.0% improvement of RSA were achieved in *B. ischaemum* when SWC increased from 40 to 60% FC, respectively. For *L. davurica*, RSA increased about 41.25 and 56.94% when SWC improved from 40 to 60% FC at

TABLE 1 | Analysis of variance for the effects of rewatering period and regime on root biomass (RB), root/shoot ratio (RSR), root average diameter (RAD), total root length (TRL), root surface area (RSA), specific root length (SRL), and specific root area (SRA) of *B. ischaemum* (B) and *L. davurica* (L).

Effect	RB (g plant^{-1}) *P*-value		RSR *P*-value		RAD (mm) *P*-value		TRL (m plant^{-1}) *P*-value		RSA (cm^2 plant^{-1}) *P*-value		SRL (m g^{-1}) *P*-value		SRA (cm^2 g^{-1}) *P*-value	
	B	L	B	L	B	L	B	L	B	L	B	L	B	L
Re-watering period (RP)	**<0.001**	**0.012**	**<0.001**	**<0.001**	**0.033**	**0.026**	**<0.001**	**<0.001**	**<0.001**	**<0.001**	**<0.001**	**0.01**	**0.003**	0.090
Re-watering regime (RR)	**<0.001**	0.126	**<0.001**	**<0.001**	**<0.001**	0.133	**<0.001**	0.719	**<0.001**	0.754	**<0.001**	0.897	0.431	0.324
RP × RR	**<0.001**	0.051	**<0.001**	**0.001**	0.186	0.453	**<0.001**	**0.014**	**<0.001**	**0.007**	**0.048**	0.154	**0.002**	0.179

Probabilities considered statistically significant ($P \leq 0.05$) are indicated in bold.

the jointing and flowering stages. However, there was no obvious change of RSA detected in *L. davurica* when SWC increased from 60 to 80% FC (**Figure 4**). Under rewatering, *B. ischaemum* had significant ($P \leq 0.05$) linear correlativity between RSA and RB, whereas no such trend was identified in *L. davurica*; when rewatering was applied at the flowering and filling stages, the slope of linear regression of RSA on root biomass was greater than that at the jointing stage in *B. ischaemum* (**Supplementary Table S3**). Significant linear correlations between RSA and TRL were also detected in both species (**Supplementary Table S4**).

Specific Root Length and Specific Root Area

For each rewatering treatment, the SRL and SRA of *L. davurica* remarkably decreased as its ratio increased in the mixture, which was not detected in *B. ischaemum*. The mean values of SRL and SRA in *B. ischaemum* were about 8.7 times and 8.6 times larger than those of *L. davurica* in the mixtures, and about 18.75 times and 17.69 times larger in the monoculture, respectively (**Figures 5**, **6**). Except the SRA of *L. davurica*, rewatering period produced significant effects on the SRL and SRA of two species, whereas rewatering regime just generated significant effects on the SRL of *B. ischaemum*. The interaction of rewatering period and regime significantly affected the SRA of two species and the SRL of *L. davurica* (**Table 1**).

DISCUSSION

Rewatering stimulated the root growth of *B. ischaemum* and increased TRL and RSA to enlarge soil exploration and root–soil contact interface (**Table 1** and **Figures 1**, **3**, **4**), but the response degree of roots was associated with the rewatering regime as well as antecedent soil water content (Han et al., 2015; Sandhu et al., 2016). When soil water contents increased from 40 to 80% FC, the response degrees in root biomass, TRL, and RSA of *B. ischaemum* were greater than those under the other two rewatering treatments, respectively (**Figures 1**, **3**, **4**). The decreased intensities in TRL and RSA production per unit of root biomass were positively correlated ($P \leq 0.05$) with the rewatering degree at the jointing stage (**Supplementary Tables S2, S3**), revealing that the energetic costs of TRL and RSA were negatively related to the increment of soil water contents (Xu et al., 2012). Moreover, the response degrees of TRL and RSA of *L. davurica* to the same increase of soil water content under 40% FC were greater than those under 60% FC (**Figures 1**, **3**, **4**). These confirmed our hypothesis that root morphological response of the two species enhanced with the increment of soil water contents and closely related to antecedent soil water contents (Elazab et al., 2012, 2016).

The root morphological response is closely associated with rewatering timing (Subere et al., 2009; Han et al., 2015). Greater water and nutrient availability at early growth stages would improve the root proliferation in the shallow soil layer (Elazab et al., 2016). Rainfall change occurring early in the growing season had larger effects on plant productivity, which was closely related to root morphological response (Zeppel et al., 2014;

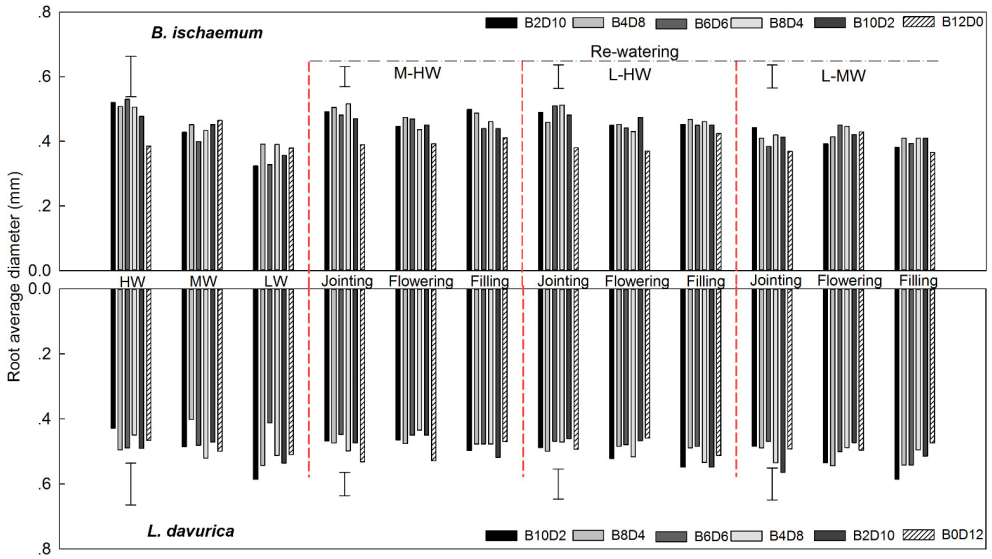

FIGURE 2 | Root average diameter (RAD) of *B. ischaemum* (B) and *L. davurica* (L) at various mixture ratios under each water treatment. HW: 80 ± 5% FC; MW: 60 ± 5% FC; LW: 40 ± 5% FC; M-HW: soil water content increased from MW to HW; L-MW: soil water content increased from LW to MW; L-HW: soil water content increased from LW to HW. The vertical bars indicate the LSD values ($P \leq 0.05$) for the RAD difference of each species among water treatments and mixture ratios under each rewatering period or constant water supply.

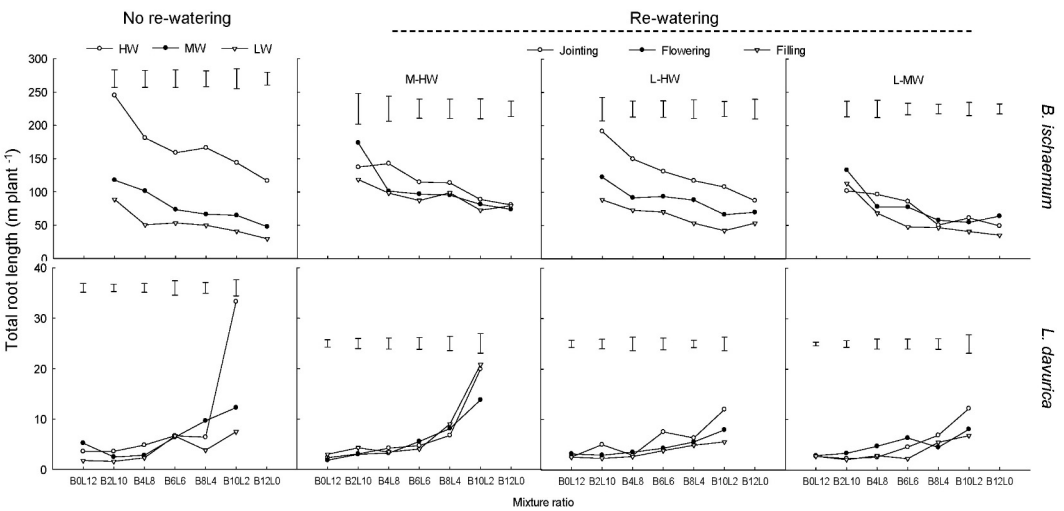

FIGURE 3 | Total root length (TRL) per plant of *B. ischaemum* (B) and *L. davurica* (L) at various mixture ratios under each water treatment. HW: 80 ± 5% FC; MW: 60 ± 5% FC; LW: 40 ± 5% FC; M-HW: soil water content increased from MW to HW; L-MW: soil water content increased from LW to MW; L-HW: soil water content increased from LW to HW. The vertical bars indicate the LSD values ($P \leq 0.05$) for the TRL difference of each species among water treatments at each mixture ratio.

Ramamoorthy et al., 2017). Here, rewatering periods generated significant effects on root growth and morphological traits in both species except the RAD of *B. ischaemum* (**Table 1**). *B. ischaemum* exhibited considerable increases in root biomass, TRL, and RSA under rewatering at the jointing and flowering stages, whereas no obvious change was detected at the filling stage (**Figures 1**, **3**, **4**). The higher sensitivities at early growth stages might be due to the changes of the biomass allocation strategy along with growth stages or the difference of water amount received among rewatering treatments. The biomass invested to roots would be decreased from the vegetative growth stage to the reproductive stage (Xie et al., 2006; Vandoorne et al., 2012; Han et al., 2015). Higher physiological activities including IAA, photosynthesis, and sucrose metabolism of plants at early growth stages could also contribute to high root morphological plasticity (Han et al., 2015; Backer et al., 2017). Our previous studies showed that leaf photosynthesis in June was greater than that in August in their mixtures (Niu et al., 2016; Xiong et al., 2017), which could be an explanation for their higher root morphological plasticity under rewatering at early growth stages.

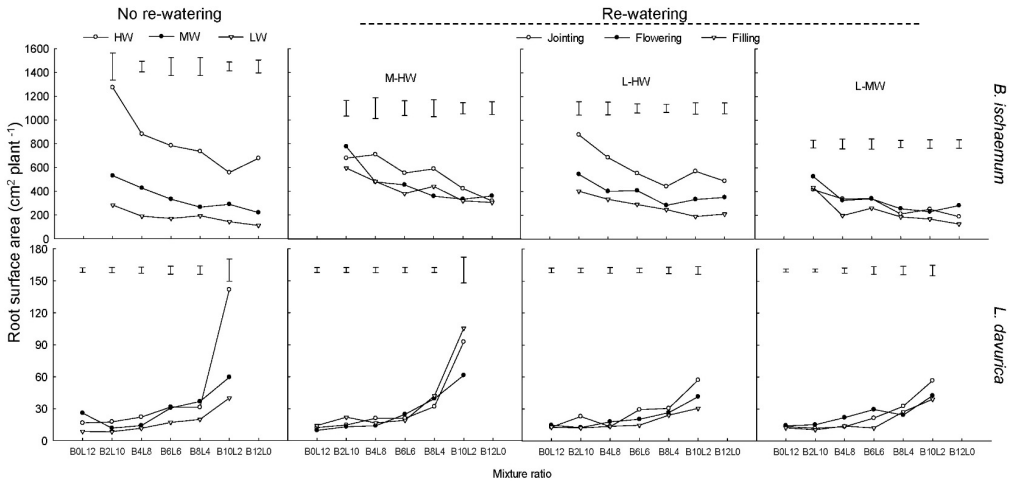

FIGURE 4 | Root surface area (RSA) per plant of *B. ischaemum* (B) and *L. davurica* (L) at various mixture ratios under each water treatment. HW: 80 ± 5% FC; MW: 60 ± 5% FC; LW: 40 ± 5% FC; M-HW: soil water content increased from MW to HW; L-MW: soil water content increased from LW to MW; L-HW: soil water content increased from LW to HW. The vertical bars indicate the LSD values ($P \leq 0.05$) for the RSA difference of each species among water treatments at each mixture ratio.

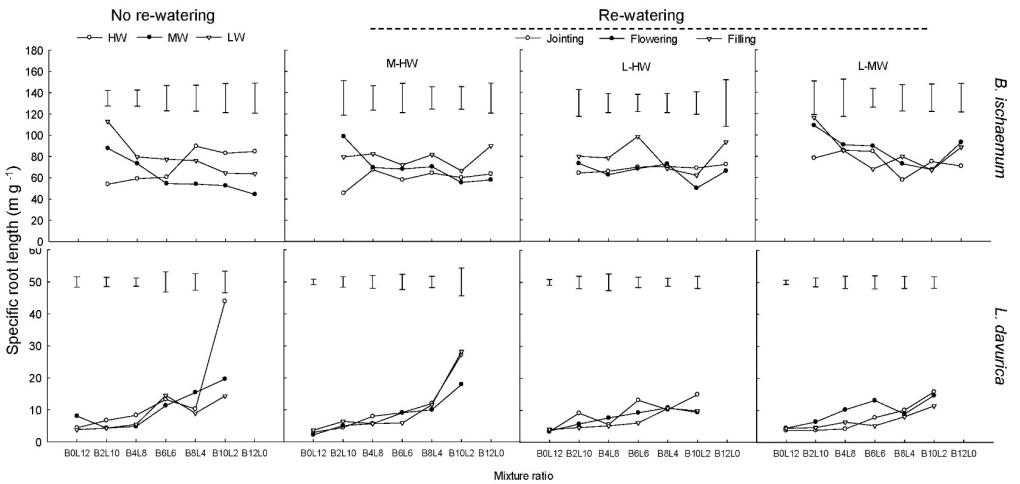

FIGURE 5 | Specific root length (SRL) of *B. ischaemum* (B) and *L. davurica* (L) at various mixture ratios under each water treatment. HW: 80 ± 5% FC; MW: 60 ± 5% FC; LW: 40 ± 5% FC; M-HW: soil water content increased from MW to HW; L-MW: soil water content increased from LW to MW; L-HW: soil water content increased from LW to HW. The vertical bars indicate the LSD values ($P \leq 0.05$) for the SRL difference of each species among water treatments at each mixture ratio.

On the basis of the performance of root morphological response to rewatering periods, we considered that rewatering applied at early growth stages would be better for the root growth (Niu et al., 2016).

As we hypothesized, the sensitivity of root morphological responses of *B. ischaemum* was much higher than *L. davurica* among different rewatering periods. It reported that root morphological response differed in plant functional types (Subere et al., 2009; Li et al., 2014; Elazab et al., 2016; Xiong et al., 2017). Fine roots are more sensitive to nutrient and moisture than taproots (Zhao et al., 2017). Consistent with the previous study, root biomass, TRL, and RSA of both species significantly ($P \leq 0.05$) declined under 60% FC and 40% FC, and the C_4 gramineous *B. ischaemum* (fibrous root system) had a larger reduction in root growth than the C_3 leguminous *L. davurica* (taproot system) (Jangpromma et al., 2012; Xu et al., 2012, 2015; Zhao et al., 2017). Even so, the recovery magnitude of root biomass, TRL, and RSA in *B. ischaemum* under rewatering was higher than that in *L. davurica* (**Figures 1**, **3**, **4**). The greater plasticity of root biomass could enable *B. ischaemum* root to display more notable morphological plasticity (de Vries et al., 2016). Higher plasticity of these root traits (root biomass, TRL, and RSA) might contribute to improved competitiveness of *B. ischaemum* in the mixtures under rewatering (Kano et al., 2011; Xu et al., 2011; de Vries et al., 2016; Zhao et al., 2017). Besides, the relative insensitive performance of *L. davurica*'s taproots might be caused by the stronger competitiveness of *B. ischaemum*'s fibrous roots (Xu et al., 2011, 2013).

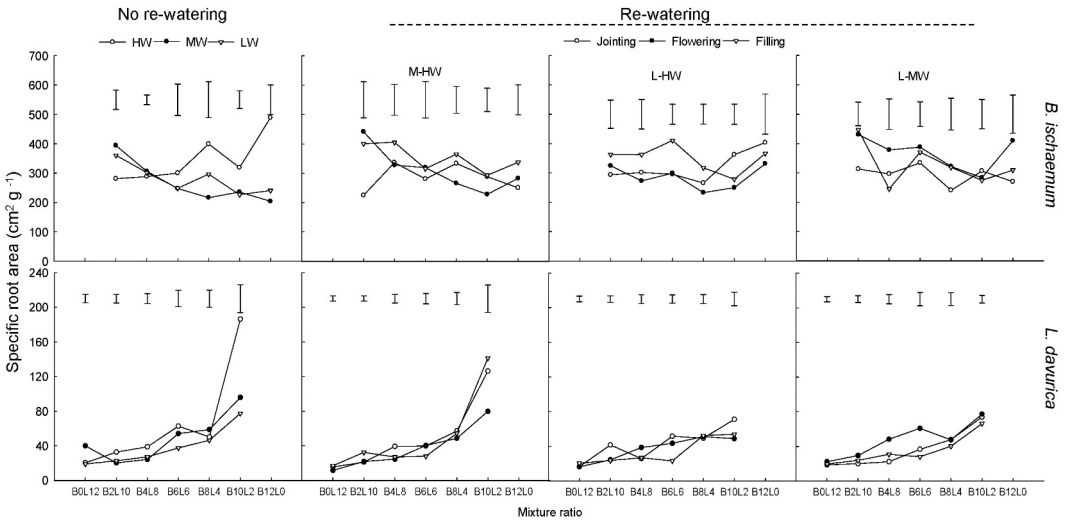

FIGURE 6 | Specific root area (SRA) of *B. ischaemum* (B) and *L. davurica* (L) at various mixture ratios under each water treatment. HW: 80 ± 5% FC; MW: 60 ± 5% FC; LW: 40 ± 5% FC; M-HW: soil water content increased from MW to HW; L-MW: soil water content increased from LW to MW; L-HW: soil water content increased from LW to HW. The vertical bars indicate the LSD values ($P \leq 0.05$) for the SRA difference of each species among water treatments at each mixture ratio.

SRL and SRA are considered as efficient indicators for root resource uptake ability (Hajek et al., 2013; Elazab et al., 2016; Olmo et al., 2016; Page et al., 2016). Compared with *L. davurica*, the significantly higher values of SRL and SRA indicate that *B. ischaemum* could invest less biomass to construct a root system with larger root density and root–soil interface area in a given soil volume (Xie et al., 2006; Bonifas and Lindquist, 2009; Lynch et al., 2014). Furthermore, a significantly linear relationship between TRL or RSA and root biomass was detected in *B. ischaemum*, but not in *L. davurica* among rewatering treatments (**Supplementary Tables S2, S3**). Both SRL and SRA are negatively correlated with RAD (Ostonen et al., 2007; Song et al., 2010; Elazab et al., 2016). Although the rewatering regime generated a significant difference on RAD of *B. ischaemum* and *L. davurica* (**Table 1**), the response of their RAD was relatively insensitive compared with those of TRL or RSA (**Figure 2**) (Xu et al., 2015). The synergic changes in TRL, RSA, and root biomass, and the relatively stable RAD alleviated the effects on the SRL and SRA of both species caused by the different rewatering intensities. The RSR reveals the allocation strategy of carbohydrates between roots and shoots (Elazab et al., 2016). Similar to other reports (Elazab et al., 2012; Carvalho et al., 2014), the RSR of the two species showed a negative relationship to soil water content, especially *L. davurica*. Among the rewatering regimes, the declined degree of RSR in *L. davurica* positively correlated with the increment of soil water content. Compared with *L. davurica*, the RSR of *B. ischaemum* was relatively stable among all the rewatering regimes, which might be attributed to the simultaneous growth regulation in shoot and root of *B. ischaemum*, and the lower plasticity of root growth and morphological traits in *L. davurica* in their mixtures (**Supplementary Figures S2, S3**) (Xu et al., 2011; Zhao et al., 2017).

Our previous studies found that the mixed plantation of *B. ischaemum* and *L. davurica* could improve their root growth and increase the TRL and RSA under water deficit. In the current study, the average values of TRL and RSA in the mixture were significantly higher than those in the monoculture regardless of the species under each rewatering regime (**Figures 3**, **4**), indicating that the capacity in uptaking soil water was enhanced in their mixture, which accorded with our last hypothesis. It is reported that root growth and extension would be greater as the non-self-neighborhood increased in the mixture, especially in the initial growth stage (de Kroon, 2007). The intraspecific competition in roots was more intense than the interspecific competition when plants with the fibrous roots intercropped with plants with taproots (Zhao et al., 2017). The root biomass, TRL, and RSA of *B. ischaemum* declined as its ratio increased in the mixtures with *L. davurica* under each rewatering treatment (**Figures 1**, **3**, **4**). The TRL and RSA of *L. davurica* had similar performance with *B. ischaemum* among mixture ratios under rewatering as well as its SRL and SRA (**Figures 3–6**). All these suggested that the mixed plantations of species with different root types (such as taproot system and fibrous root system) would favor them to coexist and adapt to the altered rainfall in the semiarid and arid grassland community (Zhao et al., 2017).

CONCLUSION

Our results showed that root morphological traits of the two codominant native species were significantly affected by the magnitude and timing of rewatering and mixture ratio. The response of root biomass, TRL, and RSA showed positive relationships with rewatering degree, particularly in *B. ischaemum*. Higher sensitivity of their root morphological response to rewatering at the jointing stage revealed that sufficient water at early growth stages would be beneficial for their

root growth. This implied that an increase of rainfall amount during early growth stages would stimulate plant growth and community dynamics. Greater plasticity of TRL and RSA under rewatering indicated that *B. ischaemum* would be superior to *L. davurica* in their communities. Meanwhile, mixed plantations enhanced root density and root–soil contact interface of each species under rewatering. These observations implied that the coexistence of legume shrub–grass would be helpful for their growth and grassland stability under variable rainfall in the semiarid and arid areas. In this study, we focused only on the effects of rewatering time and regime on root morphological traits, whereas the potential effect of rewatering amount on root morphology at different growth stages should also be considered, which needs further investigation.

AUTHOR CONTRIBUTIONS

WX and BX conceived and designed the experiment. WX performed the experiments. ZW, ZC, ZJ, and YC analyzed the data. ZMW, JH, and BX contributed reagents, materials, and analysis tools. ZW and BX wrote the paper.

FUNDING

This work was financially supported by National Key Research and Development Program of China (2016YFC0501703), National Natural Science Foundation of China (41701602), and Key cultivation project of Chinese Academy of Sciences "The promotion and management of ecosystem functions of restored vegetation on the Loess Plateau".

SUPPLEMENTARY MATERIAL

The Supplementary Material for this article can be found online at: https://www.frontiersin.org/articles/10.3389/fpls.2018.01050/full#supplementary-material

REFERENCES

Backer, R. G. M., Saeed, W., Seguin, P., and Smith, D. L. (2017). Root traits and nitrogen fertilizer recovery efficiency of corn grown in biochar-amended soil under greenhouse conditions. *Plant Soil* 415, 465–477. doi: 10.1007/s11104-017-3180-6

Bardgett, R. D., Mommer, L., and De Vries, F. T. (2014). Going underground: root traits as drivers of ecosystem processes. *Trends Ecol. Evol.* 29, 692–699. doi: 10.1016/j.tree.2014.10.006

Barkaoui, K., Roumet, C., and Volaire, F. (2016). Mean root trait more than root trait diversity determines drought resilience in native and cultivated Mediterranean grass mixtures. *Agric. Ecosyst. Environ.* 231, 122–132. doi: 10.1016/j.agee.2016.06.035

Bengough, A. G., McKenzie, B. M., Hallett, P. D., and Valentine, T. A. (2011). Root elongation, water stress, and mechanical impedance: a review of limiting stresses and beneficial root tip traits. *J. Exp. Bot.* 62, 59–68. doi: 10.1093/jxb/erq350

Bonifas, K. D., and Lindquist, J. L. (2009). Effects of nitrogen supply on the root morphology of corn and velvetleaf. *J. Plant Nutr.* 32, 1371–1382. doi: 10.1080/01904160903007893

Carvalho, P., Azam-Ali, S., and Foulkes, M. J. (2014). Quantifying relationships between rooting traits and water uptake under drought in Mediterranean barley and durum wheat. *J. Integr. Plant Biol.* 56, 455–469. doi: 10.1111/jipb.12109

Chen, D., Wang, S., Cao, B., Cao, D., Leng, G., Li, H., et al. (2016). Genotypic variation in growth and physiological response to drought stress and re-watering reveals the critical role of recovery in drought adaptation in maize seedlings. *Front. Plant Sci.* 6:1241. doi: 10.3389/fpls.2015.01241

de Kroon, H. (2007). How do roots interact? *Science* 318, 1562–1563. doi: 10.1126/science.1150726

de Vries, F. T., Brown, C., and Stevens, C. J. (2016). Grassland species root response to drought: consequences for soil carbon and nitrogen availability. *Plant Soil* 409, 297–312. doi: 10.1007/s11104-016-2964-4

Dhief, A., Abdellaoui, R., Tarhouni, M., Belgacem, A. O., Smiti, S. A., and Neffati, M. (2011). Root and aboveground growth of rhizotron-grown seedlings of three Tunisian desert *Calligonum* species under water deficit. *Can. J. Soil Sci.* 91, 15–27. doi: 10.1139/CJSS09059

Elazab, A., Molero, G., Serret, M. D., and Araus, J. L. (2012). Root traits and δ13C and δ18O of durum wheat under different water regimes. *Funct. Plant Biol.* 39, 379–393. doi: 10.1071/fp11237

Elazab, A., Serret, M. D., and Araus, J. L. (2016). Interactive effect of water and nitrogen regimes on plant growth, root traits and water status of old and modern durum wheat genotypes. *Planta* 244, 125–144. doi: 10.1007/s00425-016-2500-z

Gao, R., Yang, X., Liu, G., Huang, Z., and Walck, J. L. (2015). Effects of rainfall pattern on the growth and fecundity of a dominant dune annual in a semi-arid ecosystem. *Plant Soil* 389, 335–347. doi: 10.1007/s11104-014-2366-4

Golluscio, R. A., Sala, O. E., and Lauenroth, W. K. (1998). Differential use of large summer rainfall events by shrubs and grasses: a manipulative experiment in the Patagonian steppe. *Oecologia* 115, 17–25. doi: 10.1007/s004420050486

Hajek, P., Hertel, D., and Leuschner, C. (2013). Intraspecific variation in root and leaf traits and leaf-root trait linkages in eight aspen demes (*Populus tremula* and *P. tremuloides*). *Front. Plant Sci.* 4:415. doi: 10.3389/fpls.2013.00415

Han, H., Tian, Z., Fan, Y., Cui, Y., Cai, J., Jiang, D., et al. (2015). Water-deficit treatment followed by re-watering stimulates seminal root growth associated with hormone balance and photosynthesis in wheat (*Triticum aestivum* L.) seedlings. *Plant Growth Regul.* 77, 201–210. doi: 10.1007/s10725-015-0053-y

IPCC (2014). "Climate change 2014: synthesis report," in *Contribution of Working Groups I, II and III to the Fifth Assessment Reportofthe Intergovernmental Panelon Climate Change*, eds R. K. Pachauri and R. L. Meyer (Geneva: IPCC).

Jangpromma, N., Thammasirirak, S., Jaisil, P., and Songsri, P. (2012). Effects of drought and recovery from drought stress on above ground and root growth, and water use efficiency in sugarcane (*Saccharum officinarum* L.). *Aust. J. Crop Sci.* 6, 1298–1304.

Kano, M., Inukai, Y., Kitano, H., and Yamauchi, A. (2011). Root plasticity as the key root trait for adaptation to various intensities of drought stress in rice. *Plant Soil* 342, 117–128. doi: 10.1007/s11104-010-0675-9

Li, C., Sun, J., Li, F., Zhou, X., Li, Z., Qiang, X., et al. (2011). Response of root morphology and distribution in maize to alternate furrow irrigation. *Agric. Water Manag.* 98, 1789–1798. doi: 10.1016/j.agwat.2011.07.005

Li, H., Ma, Q., Li, H., Zhang, F., Rengel, Z., and Shen, J. (2014). Root morphological responses to localized nutrient supply differ among crop species with contrasting root traits. *Plant Soil* 376, 151–163. doi: 10.1007/s11104-013-1965-9

Li, Z., Zheng, F. L., Liu, W. Z., and Jiang, D. J. (2012). Spatially down scaling GCMs outputs to project changes in extreme precipitation and temperature events on the Loess Plateau of China during the 21st Century. *Glob. Planet. Change* 82, 65–73. doi: 10.1016/j.gloplacha.2011.11.008

Liu, Y., Li, P., Xu, G. C., Xiao, L., Ren, Z. P., and Li, Z. B. (2017). Growth, morphological, and physiological responses to drought stress in *Bothriochloa ischaemum*. *Front. Plant Sci.* 8:230. doi: 10.3389/fpls.2017.00230

Lynch, J. P., Chimungu, J. G., and Brown, K. M. (2014). Root anatomical phenes associated with water acquisition from drying soil: targets for crop improvement. *J. Exp. Bot.* 65, 6155–6166. doi: 10.1093/jxb/eru162

Miranda, J. D., Armas, C., Padilla, F. M., and Pugnaire, F. I. (2011). Climatic change and rainfall patterns: effects on semi-arid plant communities of the Iberian Southeast. *J. Arid Environ.* 75, 1302–1309. doi: 10.1016/j.jaridenv.2011.04.022

Nie, Y., Chen, H., Wang, K., and Ding, Y. (2014). Rooting characteristics of two widely distributed woody plant species growing in different karst habitats of southwest China. *Plant Ecol.* 215, 1099–1109. doi: 10.1007/s11258-014-0369-0

Niu, F., Duan, D., Chen, J., Xiong, P., Zhang, H., Wang, Z., et al. (2016). Eco-physiological responses of dominant species to watering in a natural grassland community on the semi-arid Loess Plateau of China. *Front. Plant Sci.* 7:66. doi: 10.3389/fpls.2016.00663

Ogle, K., and Reynolds, J. F. (2004). Plant responses to precipitation in desert ecosystems: integrating functional types, pulses, thresholds, and delays. *Oecologia* 141, 282–294. doi: 10.1007/s00442-004-1507-5

Olmo, M., Villar, R., Salazar, P., and Alburquerque, J. A. (2016). Changes in soil nutrient availability explain biochar's impact on wheat root development. *Plant Soil* 399, 333–343. doi: 10.1007/s11104-015-2700-5

Ostonen, I., Püttsepp, Ü., Biel, C., Alberton, O., Bakker, M. R., Lõhmus, K., et al. (2007). Specific root length as an indicator of environmental change. *Plant Biosyst.* 141, 426–442. doi: 10.1080/11263500701626069

Padilla, F. M., Aarts, B. H. J., Roijendijk, Y. O. A., Caluwe, H., Mommer, L., and Visser, E. J. W. (2013). Root plasticity maintains growth of temperate grassland species under pulsed water supply. *Plant Soil* 369, 377–386. doi: 10.1007/s11104-012-1584-x

Page, G. F. M., Merchant, A., and Grierson, P. F. (2016). Inter-specific differences in the dynamics of water use and pulse-response of co-dominant canopy species in a dryland woodland. *J. Arid Environ.* 124, 332–340. doi: 10.1016/j.jaridenv.2015.09.004

Qiu, M. J., and Li, L. (2016). Perspectives for intercropping in modern agriculture. *EC Agric. ECO* 01, 01–02.

Ramamoorthy, P., Lakshmanan, K., Upadhyaya, H. D., Vadez, V., and Varshney, R. K. (2017). Root traits confer grain yield advantages under terminal drought in chickpea (*Cicer arietinum* L.). *Field Crops Res.* 201, 146–161. doi: 10.1016/j.fcr.2016.11.004

Sandhu, N., Raman, K. A., Torres, R. O., Audebert, A., Dardou, A., Kumar, A., et al. (2016). Rice root architectural plasticity traits and genetic regions for adaptability to variable cultivation and stress conditions. *Plant Physiol.* 171, 2562–2576. doi: 10.1104/pp.16.00705

Song, L., Zhang, D. W., Li, F. M., Fan, X. W., Ma, Q., and Turner, N. C. (2010). Drought stress: soil water availability alters the inter- and intracultivar competition of three spring wheat cultivars bred in different eras. *J. Agron. Crop Sci.* 196, 323–335. doi: 10.1111/j.1439-037X.2010.00419.x

Subere, J. O. Q., Bolatete, D., Bergantin, R., Pardales, A., Belmonte, J. J., Mariscal, A., et al. (2009). Genotypic variation in responses of cassava (Crantz) to drought and rewatering: root system development. *Plant Prod. Sci.* 12, 462–474. doi: 10.1626/pps.12.462

Vandoorne, B., Mathieu, A. S., Van den Ende, W., Vergauwen, R., Périlleux, C., Javaux, M., et al. (2012). Water stress drastically reduces root growth and inulin yield in *Cichorium intybus* (var. *sativum*) independently of photosynthesis. *J. Exp. Bot.* 63, 4359–4373. doi: 10.1093/jxb/ers095

Xie, Y., An, S., Wu, B., and Wang, W. (2006). Density-dependent root morphology and root distribution in the submerged plant *Vallisneria natans*. *Environ. Exp. Bot.* 57, 195–200. doi: 10.1016/j.envexpbot.2005.06.001

Xiong, P., Shu, J., Zhang, H., Jia, Z., Song, J., Palta, J. A., et al. (2017). Small rainfall pulses affected leaf photosynthesis rather than biomass production of dominant species in semi-arid grassland community on Loess Plateau of China. *Funct. Plant Biol.* 44, 1229–1242. doi: 10.1071/FP17040

Xu, B., Gao, Z., Wang, J., Xu, W., and Huang, J. (2015). Morphological changes in roots of *Bothriochloa ischaemum* intercropped with *Lespedeza davurica* following phosphorus application and water stress. *Plant Biosyst.* 149, 298–306. doi: 10.1080/11263504.2013.823132

Xu, B., Gao, Z., Wang, J., Xu, W., Palta, J. A., and Chen, Y. (2016). N: P ratio of the grass *Bothriochloa ischaemum* mixed with the legume *Lespedeza davurica* under varying water and fertilizer supplies. *Plant Soil* 400, 67–79. doi: 10.1007/s11104-015-2714-z

Xu, B., Niu, F., Duan, D., Xu, W., and Huang, J. (2012). Root morphological characteristics of *Lespedeza davurica* (L.) intercropped with *Bothriochloa ischaemum* (L.) Keng under water stress and P application conditions. *Pak. J. Bot.* 44, 1857–1864.

Xu, B.-C., Xu, W.-Z., Gao, Z.-J., Wang, J., and Huang, J. (2013). Biomass production, relative competitive ability and water use efficiency of two dominant species in semiarid Loess Plateau under different water supply and fertilization treatments. *Ecol. Res.* 28, 781–792. doi: 10.1007/s11284-013-1061-x

Xu, B., Xu, W., Huang, J., Shan, L., and Li, F. M. (2011). Biomass production and relative competitiveness of a C3 legume and a C4 grass co-dominant in the semi-arid Loess Plateau of China. *Plant Soil* 347, 7–23. doi: 10.1007/s11104-012-1213-8

Xu, B., Xu, W., Wang, Z., Chen, Z., Palta, J. A., and Chen, Y. (2018). Accumulation of N and P in the legume *Lespedeza davurica* in controlled mixtures with the grass *Bothriochloa ischaemum* under varying water and fertilization conditions. *Front. Plant Sci.* 9:165. doi: 10.3389/fpls.2018.00165

Zeppel, M. J. B., Wilks, J. V., and Lewis, J. D. (2014). Impacts of extreme precipitation and seasonal changes in precipitation on plants. *Biogeosciences* 11, 3083–3093. doi: 10.5194/bg-11-3083-2014

Zhao, Y., Li, Z., Zhang, J., Song, H., Liang, Q., Tao, J., et al. (2017). Do shallow soil, low water availability, or their combination increase the competition between grasses with different root systems in karst soil? *Environ. Sci. Pollut. Res.* 24, 10640–10651. doi: 10.1007/s11356-017-8675-4

Zhu, Y., Yang, X., Baskin, C. C., Baskin, J. M., Dong, M., and Huang, Z. (2014). Effects of amount and frequency of precipitation and sand burial on seed germination, seedling emergence and survival of the dune grass *Leymus secalinus* in semi-arid China. *Plant Soil* 374, 399–409. doi: 10.1007/s11104-013-1892-9

Conflict of Interest Statement: The authors declare that the research was conducted in the absence of any commercial or financial relationships that could be construed as a potential conflict of interest.

frontiers in Plant Science

ORIGINAL RESEARCH
published: 08 August 2018
doi: 10.3389/fpls.2018.01167

The Bet-Hedging Strategies for Seedling Emergence of *Calligonum mongolicum* to Adapt to the Extreme Desert Environments in Northwestern China

Baoli Fan[1,2], Yongfeng Zhou[3,4], Quanlin Ma[2], Qiushi Yu[2], Changming Zhao[3] and Kun Sun[1]**

[1] College of Life Science, Northwest Normal University, Lanzhou, China, [2] State Key Laboratory of Desertification and Aeolian Sand Disaster Combating, Gansu Desert Control Research Institute, Lanzhou, China, [3] State Key Laboratory of Grassland Agro-Ecosystems, School of Life Sciences, Lanzhou University, Lanzhou, China, [4] Department of Ecology and Evolutionary Biology, University of California, Irvine, Irvine, CA, United States

OPEN ACCESS

Edited by:
Zhiyou Yuan,
Northwest A&F University, China

Reviewed by:
Chunhui Zhang,
Qinghai University, China
Gehan Jayasuriya,
University of Peradeniya, Sri Lanka
Xinping Wang,
Cold and Arid Regions Environmental and Engineering Research Institute (CAS), China
Xiaoan Zuo,
Cold and Arid Regions Environmental and Engineering Research Institute (CAS), China

***Correspondence:**
Changming Zhao
zhaochm@lzu.edu.cn;
zhaochangming2016@163.com
Kun Sun
kunsun@163.com

Specialty section:
This article was submitted to Plant Abiotic Stress, a section of the journal Frontiers in Plant Science

Received: 03 March 2018
Accepted: 23 July 2018
Published: 08 August 2018

Citation:
Fan B, Zhou Y, Ma Q, Yu Q, Zhao C and Sun K (2018) The Bet-Hedging Strategies for Seedling Emergence of Calligonum mongolicum to Adapt to the Extreme Desert Environments in Northwestern China. Front. Plant Sci. 9:1167. doi: 10.3389/fpls.2018.01167

Calligonum mongolicum is a dominant native perennial shrub on sand dunes in arid deserts of northwestern China, and is therefore widely used in sand dune stabilization in these regions. However, it remains largely unknown how seedling emergence of *C. mongolicum* has adapted to unpredictable sand movement and extreme drought. Here we examined effects of seed burial depth, light intensity, and seed age on seedling emergence, and considered seed germination and seedling emergence strategies for the shrub's adaption to the desert environment. In our pot experiment, the optimum seeding depth for emergence of *C. mongolicum* was 2 cm, indicating that for germination and seedling emergence only moderate sand burial is required. Light intensity at the surface soil (0 cm) was important for seedling emergence, while there was no significant difference between 50 and 20% light flux density, at burial depths of 1 and 2 cm, indicating that *C. mongolicum* seeds had adapted to sand burial, while not exposure from sand erosion. We also found *C. mongolicum* seedlings emerged in spring and in late summer to early autumn. Meanwhile, seedling emergence percentage for 3-year-old seeds was similar to that of 1-year-old seeds, which meant that *C. mongolicum* seeds were well preserved under normal sand dune conditions, thus were capable of developing a persistent, but shallow soil seed-bank. These results indicated that germination and seedling emergence take a bet-hedging strategies to adapt to variable desert environments. Our study confirmed that *C. mongolicum* desert shrubs combine strategies in its adaption to arid and variable sand environments.

Keywords: desert pioneer shrub, seed burial depth, light intensity, seed age, seedling emergence strategy

INTRODUCTION

Understanding how organisms cope with and adapt to changes in their environments is a central theme to evolutionary ecology (Botero et al., 2015). Germination and seedling emergence are critical transition periods during which a plant leaves the relative safety of the seed stage and enters the highly vulnerable seedling stage (Gremer et al., 2016). The ecology of seeds and their

germination patterns determine a species' adaptation to various environments and allows us to explain and predict ecological dynamics (Huang et al., 2016). In deserts, seeds and plants often face varying degrees of sand burial and exposure by wind erosion, thus their ability to respond to these environmental cues is of great importance for successful seed germination, seedling emergence, and initial establishment, which may ultimately affect population viability. It is well known that seed germination and seedling emergence depend on many factors, such as soil light intensity (Tobe et al., 2006; Zhang et al., 2014), moisture (Tobe et al., 2005), temperature (Liu et al., 2013) and others. Sand burial and exposure from wind erosion can easily affect these factors in the microenvironment of dune plants (Poulson, 1999; Qu et al., 2014), which may influence seed germination and seedling emergence of the plants. Although tolerance to burial was found to differ considerably among species, burial was considered an important selective force (Maun, 2004; Dech and Maun, 2005; Liu et al., 2007; Xu et al., 2013).

For some species, the timing of emergence plays a critical role in seedling establishment (Bush and Van Auken, 1991) and as expected, also a strong selective force (Gremer et al., 2016). Delaying germination for a year or within season time scales, which is described as biological bet-hedging, has been demonstrated to significantly benefit plants by escaping unfavorable conditions and spreading risk of seedling failure (Simons, 2009; Gremer and Venable, 2014; Gremer et al., 2016). Meanwhile, the volume of seeds persisting in the soil reflects the relative risks around a seed remaining viable in the soil and to germinate under conditions that are more favorable. Plants that can reduce the effect of environmental uncertainty in this way are considered to exhibit a bet-hedging strategy (Arroyo et al., 2006; Yu et al., 2007). Many studies have reported on seed germination and seedling emergence of annual plants growing in different deserts of the world (Went, 1949; Tevis, 1958; Venable and Brown, 1988; Venable, 2007; Gremer et al., 2016; Huang et al., 2016). However, very few studies of this type have been applied to desert perennial shrubs (Baskin et al., 1993; Gutterman, 2000). The reproductive strategies employed by plants are very important for adaption to extreme desert environments. Accordingly, it is either phenotypic plasticity (Angert et al., 2010; Botero et al., 2015) or a bet-hedging strategy (Simons, 2011) or both (Simons, 2014; Gremer et al., 2016) that are essential for plants to adapt to desert environments. Thus, it remains unknown which strategy was adopted by pioneer shrubs to inhabit mobile sand dunes and to adapt to unpredictable sand movement and extreme drought. *Calligonum mongolicum* (Polygonaceae) is a dominant native perennial shrub in active sand dunes in arid deserts of northern China, and is widely used for vegetation restoration in desert region (Fan et al., 2018). In these sandy habitats, each mature shrub produces numerous quantities of fruit and seeds are dispersed considerable distances by prevailing winds. In recent years, *C. mongolicum* exhibited a population expansion in mobile sand dunes in the arid Minqin Desert. Previous greenhouse experiments on the species have shown the impact of hydration–dehydration cycles as well as different pre-sowing seed treatments on seed germination of several *Calligonum* sp. (Ren and Tao, 2003, 2004), despite all of the above, it remains unclear how *C. mongolicum* seedling emergence has adapted to the sand environment. In this study, we investigated *C. mongolicum* seedling emergence by examining the effects of seed burial depth, light intensity and seed age. The objective was to investigate seed germination and seedling emergence strategies in the shrub's adaption to arid desert environments, and to evaluate its usage in conservation strategies of mobile sand dunes.

MATERIALS AND METHODS

Seed Collection and Selection

Over the previous three growing seasons in the Minqin County, fresh seeds from *C. mongolicum* were collected from the surface of desert sand dunes under the shrubs. These seeds were air dried in paper bags and stored in year-collected batches for use in germination and emergence pot trials. Meanwhile, we randomly selected 3 subsamples of 100 seeds from these fresh seeds and measured, seed length, seed width, seed bristle length and weight. All seeds were air-dried at room temperature by spreading on tables. Prior to the pot experiment, 50 seeds from each seed age group (one- and three-year-old), were subjected to the tetrazolium chloride viability test, which indicated that in each seed age group >90% of the embryos appeared light colored and thus were regarded as viable.

Field Seedling Emergence Experiments

Based on *C. mongolicum*'s ability to endure considerable sand movement, the potted seedling emergence experiment included three treatments: sand burial, burial depth with light intensity, and burial depth with seed age.

Sand Burial Experiments

All sand burial treatments consisted of five replicates of 20 seeds. Each replicate of 20 seeds were planted at 0, 1, 2, 4, 6, and 8 cm depths in plastic pots (14 cm in diameter) filled with sand from mobile dunes. The potted sand dune soil dried quickly in the hot, dry conditions of our study site, however, previous unpublished work indicated that flooding with excess irrigation water limited *C. mongolicum*'s emergence. Therefore, the pots were moistened daily with a garden watering-can, fitted with a fine rosette to mimic light rainfall in very small quantities, as would be the case in the desert, i.e., moist soil with maximized air filled porosity, the volume of which was based on our previous unpublished work. Meanwhile, seedling appearance at the sand surface was recorded daily for 5 months, and on completion of the study.

Light Intensity, Seed Age, and Sand Burial Experiments

Seed burial depth preliminary experiment on seed burial depth indicated an optimal seeding depth of 2 cm, followed by 1 cm and with no germination from seeds placed on the soil surface (0 cm). Therefore, these three depths (0, 1, and 2 cm) were chosen to assess emergence

response to light density and burial depth. Shade netting was used to obtain three levels of light intensity, 100% natural light (CK), 50% light flux density (LFD) and 20% LFD.

To assess the impact of seed age on germination percentage, seeds that were dry stored for 1 and 3 years were sown in pots containing sandy soil from mobile sand dunes at five seed burial depths (0, 1, 2, 4, and 6 cm). Since seedlings failed to emerge from 3-year-old seeds at burial depths of 0 and 6 cm from previous work, time to emergence was only recorded at 1, 2, and 4 cm seeding depths for both seed ages.

Statistical Analyses

Seedling emergence was measured using two indices: the final emergence percentage and the initial emergence time. The percentage of seedling emergence was the number of seedlings at the end of the experiment divided by the number sown. The initial emergence time was defined as the time from sowing to the first seedling emergence day, i.e., days after sowing (DAS).

The statistical package SPSS 16.0 software (SPSS, Chicago, IL, United States) was used for the analyses. One-way ANOVA was used to test the differences in initial emergence time and the final percentage emergence among different seed burial depths. A two-way ANOVA was used to analyze the effect of light intensity, seed burial depth and their interaction, seed age, seed burial depth, and their interaction on the seedling emergence percentage. Where there was a significant difference, a multiple comparison LSD determined the level of difference among treatments at $P < 0.05$. Before analysis, data were arcsine transformed for homogeneity of variance. Data means ± SE and figures were created with Origin 8.0.

RESULTS

Mean seed weight of the collected *C. mongolicum* seeds was 0.11 ± 0.00 g (mean ± SE) with a length of 1.64 ± 0.16 cm. Mean bristle length was 4.15 ± 0.91 mm and was about 25 percent of the length of the seed.

C. mongolicum Seedling Emergence Process at Different Seeding Depths

Under field conditions and within the same season, *C. mongolicum* seedlings largely emerge at two different times during June and August. In the pot trials, seedlings at seed burial depths of 1 and 2 cm began to emerge 15 DAS, while those at 4 cm depth began to emerge 16 DAS. The DAS did not differ significantly among seed burial depths of 1, 2, and 4 cm (**Figure 1**). However, at 0, 6, and 8 cm seeding depths, seedlings failed to emerge in July, but finally emerged in August. Emergence percentage at 1 and 2 cm seeding depths was significantly higher than 0, 4, and 6 cm seeding depths. Seedling emergence percentage was only 1% at 0 cm and 3% at 6 cm seeding depths, in contrast to 7, 3, and 10% emergence for 1, 2, and 4 cm seeding depths in August, respectively (**Figure 2**). Seedling emergence in August at 1 and 2 cm depths was significantly lower than those at corresponding depths in July (**Figure 2**). Two-way ANOVA showed that the percentage of seedling emergence of *C. mongolicum* were significantly affected by soil depth, time and their interactions ($P < 0.001$) (**Table 1**).

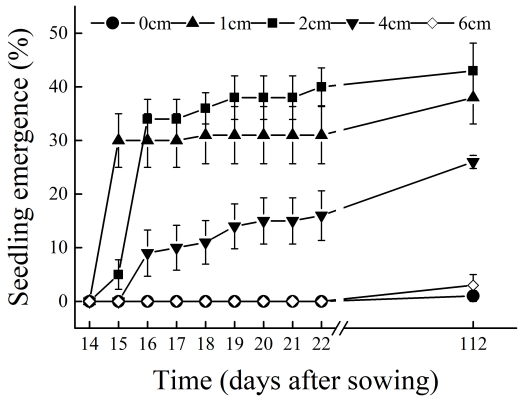

FIGURE 1 | Seedling emergence process of *C. mongolicum* at different seed burial depths [14–22 days after sowing (DAS) is in May; 112 DAS is in August].

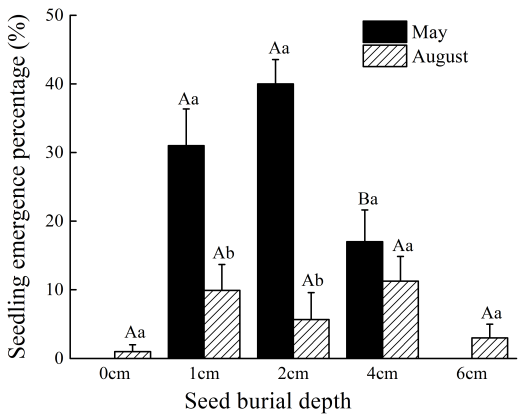

FIGURE 2 | Effects of seed burial depth on the seedling emergence percentage of *C. mongolicum* in June and August. Values with different uppercase letters within each seed burial depth in the same month are significantly different ($P < 0.05$); Values with different lowercase letters between months under same seed burial depth are significantly different ($P < 0.05$).

TABLE 1 | Effects of time and seed burial depth on the seedling emergence percentage.

Source	SS	*df*	MS	*F*
Time	1633.02	1	1633.01	29.72***
Burial depth	4358.78	4	1089.69	19.83***
Time × Burial depth	2532.52	4	633.13	11.52***

****P < 0.001.*

TABLE 2 | Two-way analysis of variance of the effect of light intensity, seed burial depth and their interactions on final seedling emergence in pot trials.

Source	SS	*df*	MS	*F*-value	*p*-value
Light intensity	103.333	2	51.667	0.216	0.807
Burial depth	6603.333	2	3301.667	13.789	0
Light intensity × Burial depth	1173.333	4	293.333	1.225	0.317

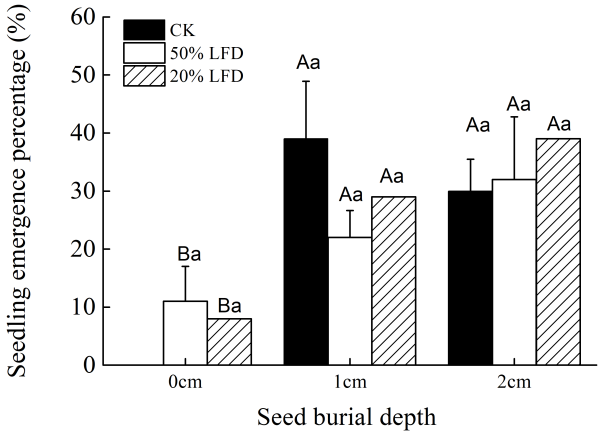

FIGURE 3 | Effects of light intensity and seed burial on the seedling emergence percentage of *C. mongolicum* (Mean ± SE). Values with different uppercase letters within each light treatment under same seed burial depth are significantly different ($P < 0.05$); Values with different lowercase letters among each seed burial depth under same light are significantly different ($P < 0.05$).

Effects of Light Intensity and Sand-Burial Depth on Seedling Emergence

Seeding depth had a significant effect on seedling emergence of *C. mongolicum*, while emergence was not affected by light intensity or the interaction of light intensity and seed burial depth (**Table 2**). Seedling emergence experiments under different light densities showed that seedlings failed to germinate placed on the sand surface (0 cm) in 100% LFD treatments, but emerged in 50 and 20% LFD with no significant difference between the two treatments, and both were not significantly different from that observed in 100% LFD (CK) (**Figure 3**). Meanwhile, there were no significant difference in seedling emergence percentages at 1 and 2 cm seeding depths among different light densities or different seed burial depths (**Figure 3**).

TABLE 3 | Two-way analysis of variance of the effect of seed age, seed burial depth and their interactions on final seedling emergence in pot trials.

Source	SS	*df*	MS	*F*-value	*p*-value
Seed age	46.944	1	46.944	0.204	0.657
Burial depth	2503.472	2	1251.736	5.438	0.014
Seed age × Burial depth	128.472	2	64.236	0.279	0.76

Effects of Seed Age and Sand-Burial Depth on Seedling Emergence

Calligonum mongolicum seedling emergence in pot trials was not affected by seed age or the interaction of seed age and seed burial depth. However, seed burial depth had a significant influence on seedling emergence (**Table 3**). Seedling emergence from the 2 cm seed burial depth was 39% for 1-year-old and 41% for 3-year-old seed. Seedling emergence significantly improved at 4 cm seeding depth. Seed buried at 1 cm was similar in emergence to 2 cm seeding depth, but as burial depth increased to 4 cm, seedling emergence significantly decreased by 51.3% for 1-year-old seeds and 76% for 3-year-old seeds (**Figure 4A**). The initial seedling emergence time (DAS) was not significantly different between 1- and 3-year-old seed, at either 1 or 4 cm seeding depths, except at 2 cm seeding depth (**Figure 4B**).

DISCUSSION

Calligonum mongolicum shrubs are simultaneously and quite often exposed to wind erosion and sand burial, but serve well as a pioneer species in the Minqin deserts (Fan et al., 2018). In this study, we investigated the effects of burial depth, seed age, and light intensity on the seedling emergence of *C. mongolicum*, and found that the species in seedling emergence stage are well adapted to sand, and have a procreation bet-hedging strategy to adapt to the extreme environment stresses in the desert.

Adaptation to Sand Burial Environments

Improved growth vigor of individual plants after sand burial is a characteristic feature of dune perennials, well-adapted to frequent sand burial conditions (Maun, 1998). In this study, *C. mongolicum* seeds showed characteristics typical for a species well adapted to sand burial environments. On one hand, seeds buried by sand ranging from 1 to 6 cm burial depths, showed a much better emergence, while our unpublished data on seed germination of *C. mongolicum* in laboratory, showed almost no seed germinated in Petri dishes (2.00 ± 1.22%) under light conditions or (1.00 ± 1.00%) under dark conditions, respectively. This is due to the high degree of seed dormancy of *C. mongolicum* seeds, which contain water-soluble germination inhibiting substances in peels and seeds (Yu and Wang, 1998). In the desert, these inhibition substances could decrease or even disappear with time, due to high gaseous exchange in sandy soil, which increases seedling emergence by up to 40%. Meanwhile, Baskin and Baskin (1989) noted that a "primary reason of non-dormant seeds not to germinate in the soil, is not having the light requirement for germination." Similarly, our study showed that light at surface soil (0 cm seed burial depth) was important for seedling emergence, while there was no significant difference between 50 and 20% LFD at burial depths of 1 and 2 cm, indicating that seeds of *C. mongolicum* may not require high-density light for their germination and emergence. Here we have extended this to sand burial, as the direct effect of burial on seed was a loss of illumination. A similar reaction to light

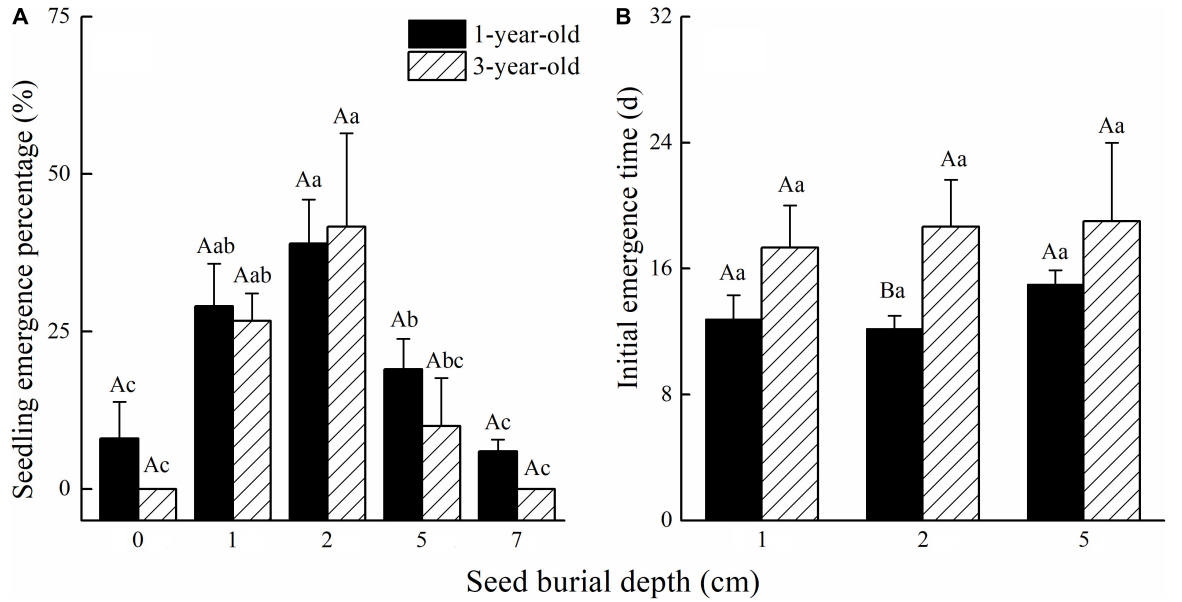

FIGURE 4 | Effects of seed age and seed burial depth on **(A)** seedling emergence and **(B)** days of first emergence of *C. mongolicum* ($P < 0.05$).

had been reported in other species distributed in deserts, e.g., *Agriophyllum squarrosum* (Tobe et al., 2005), *Larrea divaricata* (Barbour, 1969), and *Citrullus colocynthis* (Koller et al., 1963). However, unpublished data of seed germination in Petri dishes under light and dark conditions were not significantly different ($F = 0.4$, $p = 0.55$), which may be due to the very low seed germination percentages for these two light treatments. The data also indicated that light may not be the decisive factor for *C. mongolicum* germination, since sand burial could change many micro-environmental factors simultaneously. In general, there was substantial evidence from our research to conclude that *C. mongolicum* seeds are well adapted to sand burial, while not sand erosion.

Although seedling emergence of *C. mongolicum* possess adaptations for sand burial, in our pot experiment, seedlings of *C. mongolicum* emerged from 1, 2, 4, and 6 cm seeding depths, but not from depths greater than 6 cm. The results are essentially in agreement with other reports on seed germination of desert species, which is directly related to the depth at which the seeds are buried (Baskin and Baskin, 1989; Zhang and Maun, 1990; Gutterman, 1993; Benvenuti et al., 2001; Zheng et al., 2005; Liu et al., 2011; Zhu et al., 2014; Luo and Zhao, 2015). Both oxygen deficiency and higher mechanical resistance may inhibit germination and seedling elongation in deeper sand (Tobe et al., 2005). Additionally, the optimum depth for improved seedling emergence of a species is generally acknowledge to be related to seed size. *C. mongolicum* seeds at about 1.42–1.84 cm of fruit length, and 1.1–1.93 cm fruit width, indicated that the optimum seeding depth for seedling emergence was near 2 cm, which is in line with a previous investigation in the same species (Ren et al., 2002). Based on this result, seedling emergence of *C. mongolicum* in sand is regulated by seed burial depth, and the vertical distribution of seed bank is expected to determine the proportion of seeds able to germinate.

The Bet-Hedging Strategy

In a variable environment, organisms must have strategies to deal with unpredictable changes in conditions (Gremer et al., 2016). The bet-hedging strategy benefits plants by avoiding unfavorable conditions and to spread risks from extreme drought (Simons, 2009; Gremer and Venable, 2014; Gremer et al., 2016). Seed germination and seedling emergence timing influence the environmental conditions that seedlings will experience (Barga et al., 2017), thus they have important ecological implications (Huang et al., 2016). Under procreation bet-hedging, germinating and emerging at multiple times during the season can reduce the risk of emergence failure for seeds buried in deep sand (Simons, 2009). In Minqin desert, emerging and vulnerable seedlings are highly likely to suffer or die, due to erosion or sand burial from strong and unpredictable winds during early spring to summer. *C. mongolicum* seedling emergence generally occurs under suitable soil water and temperature conditions in spring. However, only about 40% of seedlings emerged under these conditions, while a further 7% emerged in the late summer or early autumn. Seeds that emerge in either July or August indicate that *C. mongolicum* emergence takes a "cautious" strategy to spread the risks, which is described as biological bet-hedging (Botero et al., 2015). The seedling emergence rate of *C. mongolicum* under pot trials in the field, was much higher at moderately seed burial depths in spring, than in early autumn, which could lower survival risk under more favorable conditions for growth and reproduction (Gremer et al., 2016), especially during annual summer rains in northwestern China.

Additionally, seeds that persist in the soil seed bank for more than 1 year are considered to exhibit a bet-hedging adaptation to environmental uncertainty (Yu et al., 2007). Plant communities in arid habitats persist in the face of high temperatures and low rainfall (Ooi et al., 2009). Thus only persistent long-lived seed banks will ensure that viable seeds are available to take advantage of sporadic rainfall events (Gutterman, 1993; Facelli et al., 2005) and play a significant role in the regeneration of plant communities (Bekker et al., 1997; Norbert and Annette, 2004). Our results indicated that final seedling emergence percentage for 3-year-old seeds was similar to that of 1-year-old seeds. As mentioned previously, mature *C. mongolicum* seeds contain significant germination inhibitors, resulting in deep dormancy (Yu and Wang, 1998). *C. mongolicum* seed viability appeared long-lived under natural conditions due to deep dormancy, which offers an effective mechanism for seeds to persist in the soil (Grime, 1981; Dalling et al., 2011). Thus, the results presented here suggest that *C. mongolicum* could be capable of developing a short-term shallow soil seed-bank in dunes, while waiting for suitable conditions to germinate, and it is thought to have evolved a bet-hedging adaptation in response to the unpredictable desert environment.

CONCLUSION

The present study indicated that faced with variable winds and scarce precipitation in Minqin desert environment, *C. mongolicum* has adopted bet-hedging strategies to adapt to desert conditions. On one hand, the species has evolved to spread the risk in an uncertain environment through an extended germination time. On the other hand, it has developed a persistent soil seed-bank strategy to adapt to wind erosion and sand burial. Although this represents an interesting perspective on the adaptation of *C. mongolicum* to sand dune environments, we stress that more investigations on natural-regeneration are required to understand the reproductive ecology of this important pioneer perennial shrub.

AUTHOR CONTRIBUTIONS

BF conceived, designed, analyzed the data, and wrote the manuscript. BF, QM, and QY performed the filed study. YZ, KS, and CZ reviewed and supervised the manuscript. All authors contributed critically to the drafts and provided final approval for publication.

FUNDING

This study was supported by the National Natural Science Foundation of China (Nos. 31360098, 31522013, and 31460224), the West Light Foundation of the Chinese Academy of Sciences, and Gansu Natural Science Foundation key project (18JR3RA020).

ACKNOWLEDGMENTS

We thank Shujiang Guo for his suggestion in choosing the journal, and we are grateful to the editor and the reviewers for their constructive comments, which contributed to improve the quality of this paper.

REFERENCES

Angert, A. L., Horst, J. L., Huxman, T. E., and Venable, D. L. (2010). Phenotypic plasticity and precipitation response in sonoran desert winter annuals. *Am. J. Bot.* 97, 405–411. doi: 10.3732/ajb.0900242

Arroyo, M. T. K., Chacón, P., and Cavieres, L. A. (2006). Relationship between seed bank expression, adult longevity and aridity in species of *Chaetanthera* (Asteraceae) in central Chile. *Ann. Bot.* 98, 591–600. doi: 10.1093/aob/mcl134

Barbour, M. G. (1969). Patterns of genetic similarity between *Larrea divaricata* of North 6 and South America. *Am. Midl. Nat.* 81, 54–67. doi: 10.2307/2423651

Barga, S., Dilts, T. E., and Leger, E. A. (2017). Climate variability affects the germination strategies exhibited by arid land plants. *Oecologia* 185, 437–452. doi: 10.1007/s00442-017-3958-5

Baskin, C. C., Chesson, P. L., and Baskin, J. M. (1993). Annual seed dormancy cycles in two desert winter annuals. *J. Ecol.* 81, 551–556. doi: 10.2307/2261533

Baskin, J. M., and Baskin, C. C. (1989). "Physiology of dormancy and germination in relation to seed bank ecology," in *Ecology of Soil Seed Banks*, eds M. Leck, V. Parker, and R. Simpson (San Diego, CA: Academic Press), 53–65.

Bekker, R. M., Verweij, G. L., Smith, R. E. N., Reine, R., Bakker, J. P., and Schneider, S. (1997). Soil seed banks in European grasslands: does land use affect regeneration perspectives. *J. Appl. Ecol.* 34, 1293–1310. doi: 10.2307/2405239

Benvenuti, S., Macchia, M., and Miele, S. (2001). Light, temperature and burial depth effects on *Rumex obtussifolius* seed germination and emergence. *Weed Res.* 41, 177–186. doi: 10.1046/j.1365-3180.2001.00230.x

Botero, C. A., Weissing, F. J., Wright, J., and Rubenstein, D. R. (2015). Evolutionary tipping points in the capacity to adapt to environmental change. *Proc. Natl. Acad. Sci. U.S.A.* 112, 184–189. doi: 10.1073/pnas.1408589111

Bush, J. K., and Van Auken, Q. W. (1991). Importance of time of germination and soil depth on growth of *Prosopis glandulosa* (Leguminosae) seedlings in the presence of a C4 grass. *Am. J. Bot.* 78, 1732–1739. doi: 10.1002/j.1537-2197.1991.tb14537.x

Dalling, J. W., Davis, A. S., Schutte, B. J., and Elizabeth Arnold, A. (2011). Seed survival in soil: interacting effects of predation, dormancy and the soil microbial community. *J. Ecol.* 99, 89–95. doi: 10.1111/j.1365-2745.2010.01739.x

Dech, J. P., and Maun, M. A. (2005). Zonation of vegetation along a burial gradient on the leeward slopes of Lake Huron sand dunes. *Can. J. Bot.* 83, 227–236. doi: 10.1139/b04-163

Facelli, J. M., Chesson, P., and Barnes, N. (2005). Differences in seed biology of annual plants in arid lands: a key ingredient of the storage effect. *Ecology* 86, 2998–3006. doi: 10.1890/05-0304

Fan, B. L., McHugh, A. D., Guo, S. J., Ma, Q., Zhang, J., Zhang, X., et al. (2018). Factors influencing the natural regeneration of the pioneering shrub Calligonum mongolicum in sand dune stabilization plantations in arid deserts of northwest China. *Ecol. Evol.* 8, 2975–2984. doi: 10.1002/ece3.3913

Gremer, J. R., Kimball, S., and Venable, D. L. (2016). Within-and among-year germination in Sonoran Desert winter annuals: bet hedging and predictive germination in a variable environment. *Ecol. Lett.* 19, 1209–1218. doi: 10.1111/ele.12655

Gremer, J. R., and Venable, D. L. (2014). Bet hedging in desert winter annual plants: optimal germination strategies in a variable environment. *Ecol. Lett.* 17, 380–387. doi: 10.1111/ele.12241

Grime, J. P. (1981). A comparative study of germination characteristics in a local flora. *J. Ecol.* 69, 1017–1059. doi: 10.2307/2259651

Gutterman, Y. (1993). *Seed Germination in Desert Plants*. Berlin: Springer. doi: 10.1007/978-3-642-75698-6

Gutterman, Y. (2000). Environmental factors and survival strategies of annual plant species in the Negev Desert, Israel. *Plant Species Biol.* 5, 113–125. doi: 10.1046/j.1442-1984.2000.00032.x

Huang, Z., Liu, S., Bradford, K. J., Huxman, T. E., and Venable, D. L. (2016). The contribution of germination functional traits to population dynamics of a desert plant community. *Ecology* 97, 250–261. doi: 10.1890/15-0744.1

Koller, D., Poljakoff-Mayber, A., Berg, A., and Diskin, T. (1963). Germination regulating mechanisms in *Citrullus colocynthis*. *Am. J. Bot.* 50, 597–603. doi: 10.1002/j.1537-2197.1963.tb07233.x

Liu, H. L., Xiang, S., Wang, J. C., Yin, L. K., Huang, Z. Y., and Zhang, D. Y. (2011). Effects of sand burial, soil water content and distribution pattern of seeds in sand on seed germination and seedling survival of Eremosparton songoricum (Fabaceae), a rare species inhabiting the moving sand dunes of the Gurbantunggut Desert of China. *Plant Soil* 345, 69–87. doi: 10.1007/s11104-011-0761-7

Liu, H. L., Zhang, L. W., Yin, L. K., and Zhang, D. Y. (2013). Effects of temperature, dry storage, and burial on dormancy and germination of seeds of 13 desert plant species from sand dunes in the Gurbantunggut Desert, Northwest China. *Arid Land Res. Manag.* 27, 65–78. doi: 10.1080/15324982.2012.719569

Liu, Z. M., Yan, Q. L., Liu, B., Ma, J. L., and Luo, Y. M. (2007). Persistent soil seed bank in *Agriophyllum squarrosum* (Chenopodiaceae) in a deep sand profile: variation along a transect of an active sand dune. *J. Arid Environ.* 71, 236–242. doi: 10.1016/j.jaridenv.2007.03.003

Luo, W. C., and Zhao, W. Z. (2015). Effects of wind erosion and sand burial on growth and reproduction of a clonal shrub. *Flora* 217, 164–169. doi: 10.1016/j.flora.2015.10.006

Maun, M. A. (1998). Adaptations of plants to burial in coastal sand dunes. *Can. J. Bot.* 76, 713–738. doi: 10.1139/b98-058

Maun, M. A. (2004). "Burial of plants as a selective force in sand dunes," in *Coastal Dunes: Ecology and Conservation*, eds M. L. Martinez and N. B. Psuty (Berlin: Springer-Verlag), 386.

Norbert, H., and Annette, O. (2004). Assessing soil seed bank persistence in flood-meadows: the search for reliable traits. *J. Veg. Sci.* 15, 93–100. doi: 10.1111/j.1654-1103.2004.tb02241.x

Ooi, M. K. J., Auld, T. D., and Denham, A. J. (2009). Climate change and bet-hedging: interactions between increased soil temperatures and seed bank persistence. *Glob. Change Biol.* 15, 2375–2386. doi: 10.1111/j.1365-2486.2009.01887.x

Poulson, T. L. (1999). Autogenic, allogenic and individualistic mechanisms of dune succession at Miller, Indiana. *Nat. Areas J.* 19, 172–176.

Qu, H., Zhao, H. L., and Zhou, R. L. (2014). Effects of sand burial on dune plants: a review. *Sci. Cold Arid Reg.* 6, 201–208.

Ren, J., and Tao, L. (2003). Effect of hydration–dehydration cycles on germination of seven *Calligonum* species. *J. Arid Environ.* 55, 111–122. doi: 10.1016/S0140-1963(02)00257-4

Ren, J., and Tao, L. (2004). Effects of different pre-sowing seed treatments on germination of 10 *Calligonum* species. *For. Ecol. Manage.* 195, 291–300. doi: 10.1016/j.foreco.2004.01.046

Ren, J., Tao, L., and Liu, X. M. (2002). Effect of sand burial depth on seed germination and seedling emergence of *Calligonum* L. species. *J. Arid Environ.* 51, 603–611. doi: 10.1016/S0140-1963(01)90979-6

Simons, A. M. (2009). Fluctuating natural selection accounts for the evolution of diversification bet hedging. *Proc. R. Soc. B Biol. Sci.* 276, 1987–1992. doi: 10.1098/rspb.2008.1920

Simons, A. M. (2011). Modes of response to environmental change and the elusive empirical evidence for bet hedging. *Proc. R. Soc. B Biol. Sci.* 278, 1601–1609. doi: 10.1098/rspb.2011.0176

Simons, A. M. (2014). Playing smart vs. playing safe: the joint expression of phenotypic plasticity and potential bet hedging across and within thermal environments. *J. Evol. Biol.* 27, 1047–1056. doi: 10.1111/jeb.12378

Tevis, L. (1958). A population of desert ephemerals germinated by less than one inch of rain. *Ecology* 39, 688–695. doi: 10.2307/1931609

Tobe, K., Zhang, L., and Omasa, K. (2005). Seed germination and seedling emergence of three annuals growing on desert sand dunes in China. *Ann. Bot.* 95, 649–659. doi: 10.1093/aob/mci060

Tobe, K., Zhang, L., and Omasa, K. (2006). Seed germination and seedling emergence of three Artemisia species (Asteraceae) inhabiting desert sand dunes in China. *Seed Sci. Res.* 16, 61–69. doi: 10.1079/SSR2005230

Venable, D. L. (2007). Bet hedging in a guild of desert annuals. *Ecology* 88, 1086–1090. doi: 10.1890/06-1495

Venable, D. L., and Brown, J. S. (1988). The selective interactions of dispersal, dormancy, and seed size as adaptations for reducing risk in variable environments. *Am. Nat.* 131, 360–384. doi: 10.1086/284795

Went, F. W. (1949). Ecology of desert plants. II. The effect of rain and temperature on germination and growth. *Ecology* 30, 1–13. doi: 10.2307/1932273

Xu, L., Huber, H., During, H. J., Dong, M., and Anten, N. P. (2013). Intraspecific variation of a desert shrub species in phenotypic plasticity in response to sand burial. *New Phytol.* 199, 991–1000. doi: 10.1111/nph.12315

Yu, S. L., Sternberg, M., Kutiel, P., and Chen, H. W. (2007). Seed mass, shape, and persistence in the soil seed bank of Israeli coastal sand dune flora. *Evol. Ecol. Res.* 9, 325–340.

Yu, Z., and Wang, L. H. (1998). Causes of seed dormancy of three species of Calligonum. *J. Northwest For. Coll.* 13, 9–13.

Zhang, C., Willis, C. G., Burghardt, L. T., Qi, W., Liu, K., Moura Souza-Filho, P. R., et al. (2014). The community-level effect of light on germination timing in relation to seed mass: a source of regeneration niche differentiation. *New Phytol.* 204, 496–506. doi: 10.1111/nph.12955

Zhang, J. H., and Maun, M. A. (1990). Effects of sand burial on seed germination, seedling emergence, survival, and growth of *Agropyron psammophilum*. *Can. J. Bot.* 68, 304–310. doi: 10.1139/b90-041

Zheng, Y. R., Xie, Z. X., Yu, Y., Jiang, L. H., Shimizu, H., and Rimmington, G. M. (2005). Effects of burial in sand and water supply regime on seedling emergence of six species. *Ann. Bot.* 95, 1237–1245. doi: 10.1093/aob/mci138

Zhu, Y. J., Yang, X. J., Baskin, C. C., Baskin, J. M., Dong, M., and Huang, Z. Y. (2014). Effects of amount and frequency of precipitation and sand burial on seed germination, seedling emergence and survival of the dune grass *Leymus secalinus* in semiarid China. *Plant Soil* 374, 399–409. doi: 10.1007/s11104-013-1892-9

Conflict of Interest Statement: The authors declare that the research was conducted in the absence of any commercial or financial relationships that could be construed as a potential conflict of interest.

frontiers in Plant Science

ORIGINAL RESEARCH
published: 28 August 2018
doi: 10.3389/fpls.2018.01241

Effect of Soil Moisture Regimes on Growth and Seed Production of Two Australian Biotypes of *Sisymbrium thellungii* O. E. Schulz

Gulshan Mahajan[1,2], Barbara George-Jaeggli[3,4], Michael Walsh[5] and Bhagirath S. Chauhan[1]*

[1] Queensland Alliance for Agriculture and Food Innovation, The University of Queensland, Gatton, QLD, Australia, [2] Department of Agronomy, Punjab Agricultural University, Ludhiana, India, [3] Queensland Alliance for Agriculture and Food Innovation, The University of Queensland, Warwick, QLD, Australia, [4] Agri-Science Queensland, Department of Agriculture and Fisheries, Warwick, QLD, Australia, [5] Sydney Institute of Agriculture, School of Life and Environmental Sciences, The University of Sydney, Narrabri, NSW, Australia

Sisymbrium thellungii O. E. Schulz is an emerging problematic weed in the northern grain region of Australia. Several different biotypes exist in this region but not all biotypes exhibit the same growth and reproduction behavior. This might be due to local adaptation to the different agro-ecosystems, however, information on this aspect is limited. To determine whether adaptation to water stress was a factor in biotype demographic growth and reproduction behavior, we evaluated the physiological and biochemical responses of two Australian *S. thellungii* biotypes, selected from high (Dalby) and medium (St. George) rainfall areas, to different pot soil moisture levels corresponding to 100, 75, 50, and 25% of soil water holding capacity (WHC). Averaged across moisture levels, the St. George biotype (medium rainfall area) had 89% greater biomass and produced 321% more seeds than the Dalby biotype. The St. George biotype was less affected by increased levels of water stress than the Dalby biotype. The Dalby biotype produced 4,787 seeds plant^{-1} at 100% WHC and only 28 seeds plant^{-1} at 25% WHC. On the other hand, the St. George biotype produced 4,061 seeds plant^{-1} at 25% WHC and its seed production at 100% WHC was 9,834 seeds plant^{-1}. On a per leaf area basis and averaged across all moisture levels, the St. George had significantly lower net carbon assimilation compared with the Dalby biotype, accompanied by a trend for lower stomatal conductance, which might indicate an adaptation to water stress. Across the moisture levels, the St. George biotype had higher phenolics and total soluble sugar, but free proline content was higher in the Dalby biotype compared with the St. George biotype. Like total soluble sugar, proline content increased with water stress in both biotypes, but it increased to a greater extent in the Dalby biotype, particularly at the 25% of WHC. Branching, flowering and maturity occurred earlier in the St. George biotype compared with the Dalby biotype, indicating relatively faster growth of the St. George biotype, which again seems to be an adaptation to water-limited environments. In conclusion, the St. George biotype of *S. thellungii* had higher reproductive capacity than the Dalby biotype across all the moisture regimes, which suggests greater invasiveness.

OPEN ACCESS

Edited by:
P. V. Vara Prasad, Kansas State University, United States

Reviewed by:
Ilias Travlos, Agricultural University of Athens, Greece
Djanaguiraman M, Kansas State University, United States

***Correspondence:**
Gulshan Mahajan
g.mahajan@uq.edu.au

Specialty section:
This article was submitted to Plant Abiotic Stress, a section of the journal Frontiers in Plant Science

Received: *12 February 2018*
Accepted: *06 August 2018*
Published: *28 August 2018*

Citation:
Mahajan G, George-Jaeggli B, Walsh M and Chauhan BS (2018) Effect of Soil Moisture Regimes on Growth and Seed Production of Two Australian Biotypes of Sisymbrium thellungii O. E. Schulz. Front. Plant Sci. 9:1241. doi: 10.3389/fpls.2018.01241

Overall, the large size and rapid growth of the *S. thellungii* population from the medium rainfall area, together with its physiological response to water stress and its ability to maintain seed production in dry conditions, may enable this biotype to become widespread in Australia.

Keywords: photosynthesis, ecology, proline, soluble sugar, water stress, drought adaptation, weed

INTRODUCTION

Sisymbrium thellungii O. E. Schulz is an emerging problematic C_3 weed of the northern grain region of Australia, where it has evolved resistance to acetolactate synthase (ALS) inhibiting herbicides (Heap, 2018); therefore, herbicidal control of this weed winter crops like canola (*Brassica napus* L.), chickpea (*Cicer arietinum* L.) and wheat (*Triticum aestivum* L.) is challenging. For this reason, a better understanding of the biology of *S. thellungii* has become a priority for its proper management.

Weeds compete with crops for resources like water, light, and nutrients. Among them, water is the most limiting factor for attaining optimum yield in any crop (Brown, 1995). Changes in cultural practices and rapid adaptability to climate change frequently favor the dominance of weeds in agro-ecosystems (Mahajan et al., 2012). Modeling studies on climate change have shown that rising temperatures in Australia would lead to an increase in the frequency of droughts and a reduction in rainfall events (DEE, 2017). It has been observed that crops in the northern grain region of Australia sometimes experience severe drought, resulting in weed abundance and yield loss (Parreira et al., 2015). Limited soil water availability influences crop-weed competition to a significant degree, and in general, weed growth is favored due to the greater plasticity of weeds as compared to crops (Crusciol et al., 2001; Chauhan and Mahajan, 2014; Mahajan et al., 2015). Drought plays an important role in weed invasion by affecting weed physiology and weed ecology (Bajwa et al., 2016). The availability of soil moisture determines whether weeds will establish and subsequently spread (Chauhan and Johnson, 2010). Weed species and even weed biotypes collected from different environmental conditions can vary in their response to soil moisture.

Higher atmospheric CO_2 levels as a result of global warming, may reduce stomatal conductance and transpiration in plants, thereby lowering latent heat loss and causing higher leaf temperature (Bernacchi et al., 2007). Besides stomatal control of photosynthesis, maintenance of a low level of photosynthesis and its early recovery related to conductance and water potential suggests that the non-stomatal control of photosynthesis is an important attribute of some drought-tolerant weeds (Hill and Germino, 2005).

Thus, in the future, plants including weeds are likely to experience increases in acute heat and drought stress, and if weeds are more robust to these conditions this can be expected to negatively influence crop productivity and promote weed invasiveness (Thomas et al., 2004). However, compared to crops, the literature related to the response of weeds to water stress is limited. Weeds or weed biotypes able to produce a high number of seeds at low soil moisture content exhibit drought tolerance and may pose tough competition to crops in a water-scarce environment. Such drought tolerance in weeds could be due to the maintenance of turgor by means of osmoregulation, increased elasticity of cells, decreased cell size, or desiccation tolerance through protoplasmic resistance (Sullivan and Ross, 1979). Osmoregulation in plants maintains turgor, which reduces the effect of water stress on physiological functions such as stomatal opening, photosynthesis and growth (Chimenti et al., 2002). Many weeds survive by having low osmotic potential before stress, prolonging the maintenance of turgor and delaying the leaf rolling mechanism (White et al., 1992; Mundree et al., 2002). Proline content in several desert weeds [e.g., *Haloxylon ammadendron* C. A. Mey., *Zygophyllum xanthoxylum* (Bunge) Engl., and *Artemisia sphenocephala* Krasch.] suggests that free proline accumulation may underpin their adaptation to arid environments. Many authors have found that the strong antioxidant system of weeds helps in alleviating the impact of radical oxygen species, generated by metabolic processes in response to water stress (Lu et al., 2008).

The effect of drought on plant phenology is variable and depends upon the plant species, as well as the timing, duration and extent of drought. Phenological responses to water stress are considered important drought avoidance mechanisms in plants (Stout and Simpson, 1978; Muchow and Carberry, 1989). Information is very limited on variations of phenological stages in weeds in response to water stress. Even under limited soil moisture conditions, it has been observed that some weeds and weed biotypes exhibited strong capacity to complete their life cycle, maintain growth and produce sizable amounts of seeds (Chauhan and Johnson, 2010; Kaur et al., 2016). Studies on summer annual weeds, such as *Amaranthus rudis* Sauer (Sarangi et al., 2016), *Rottboellia cochinchinensis* (Lour.) (Chauhan, 2013) and *Amaranthus palmeri* S. Wats. (Moran and Showler, 2005) showed that water stress negatively affected growth; however, the effects of soil moisture levels on growth and reproduction of winter annual weeds have not been tested. Therefore, an experiment was conducted to compare the effect of different soil moisture regimes on *S. thellungii* growth, physiological and biochemical changes, and its reproductive capacity. Such parameters could be helpful in evaluating and differentiating the invasive capacity of *S. thellungii* under future water-scarce climate scenarios.

MATERIALS AND METHODS

Experimental Design

The experiment was conducted in a completely randomized design with eight treatments (2 biotypes × 4 soil moisture

levels) in a factorial arrangement. Plants were grown in large pots in a naturally ventilated greenhouse at the Gatton Campus of the University of Queensland, Australia, during the winter season of 2017 (**Figure 1**). The weekly average temperature during the vegetative stage, flowering and maturity period of the plants varied from 13.8 to 18.1°C, 13.6 to 14.8°C, and 14.6 to 16.4°C, respectively (**Figure 2**). The optimum temperature for germination of African turnip weed is 20/10°C (day/night) but no information is available on the optimum temperature range for its growth. This experiment was conducted in the winter season, in which this weed grows in the field. The temperature in the naturally ventilated greenhouse was similar to the ambient temperature.

Two Australian biotypes of *S. thellungii* (St. George and Dalby) were grown at four different soil moisture levels, as determined by soil gravimetric water holding capacity (WHC): 100, 75, 50, and 25%. Each treatment had six replications. The St. George biotype was collected from a medium rainfall area with an average annual rainfall of around 515 mm. The Dalby biotype was sourced from a high rainfall area with an average annual rainfall of 680 mm[1]. Three seeds were sown per pot and after emergence, seedlings were thinned to a single plant per pot. The soil moisture levels

[1]http://www.bom.gov.au

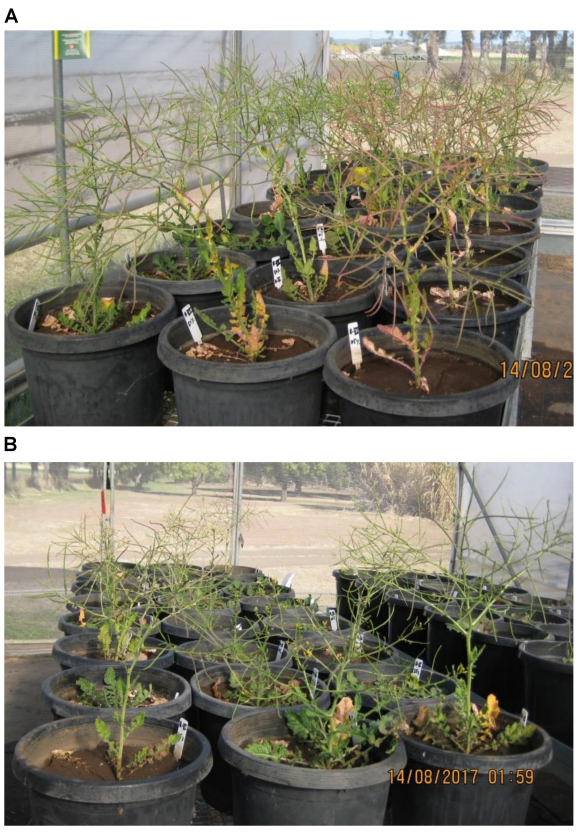

FIGURE 1 | St. George biotype **(A)** and Dalby biotype **(B)** of African turnip under different water regimes in naturally ventilated greenhouse.

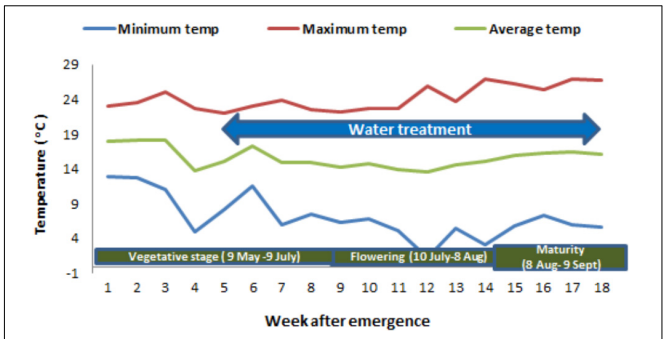

FIGURE 2 | Weekly mean maximum, minimum and average temperature (°C) during different stages of African turnip weed.

were maintained throughout the study period as per treatments. The soil, collected from the Gatton Research Farm, was a heavy clay loam with a pH of 6.7, an electrical conductivity of 0.14 dSm^{-1} and an organic matter content of 2.8%. The modified method of Chauhan and Johnson (2010) and Nguyen (2011) was used for calculating WHC. Three pots (30 cm diameter) containing approximately 13.5 kg of soil were saturated with tap water. The pot surface was then covered with a plastic container and the pots were allowed to drain for 48 h. Thereafter, from the middle of each pot, three soil samples (each *ca.* 300 g) were taken. These samples were weighed (wet weight of soil, A), oven-dried (90°C for 72 h) and re-weighed (dry weight of soil, B). The WHC was then calculated using the formula: $[(A - B) \times 100]/B$. The 75, 50%, and 25% WHC were estimated based on that fraction of the WHC. The water treatments were started 40 days after sowing (DAS) as the initial growth of the weeds was slow. A measured quantity of water as per treatment was applied every other week after the start of the treatments. The 1-week interval for water application at 100% WHC (field capacity) was standardized based on soil moisture meter reading.

For the initial 1 month of establishment, water was applied every alternative day to keep the pots moist. The experiment ran for 124 days until the plants were fully matured and seed production had ceased.

Growth, Phenology, Photosynthetic Parameters, and Seed Production

At peak vegetative growth (75 DAS), plant height in each pot was measured from the soil surface to the uppermost tip of the plant and all leaves on each plant were counted. The number of days after sowing to the appearance of the first branch and initiation of the first flower was recorded for each plant. Photosynthetic parameters were measured on healthy, fully expanded and undamaged leaves at 99 DAS to coincide with the biochemical analysis. Plants of all six replicates were measured; however, several plants could not be measured as their leaves were too small which resulted in incomplete replicates. Gas exchange measurements were taken between 1000 and 1300 h using a LI-6400 portable photosynthesis system (LI-COR Inc., Lincoln, NE, United States) with a 6400-40 leaf chamber fluorometer which measures 2 cm^2 of leaf. Measurements were taken on a random

rosette leaves at steady state controlling the following parameters: 300 μ mol^{-1} s^{-1} air flow to the sample, 1500 μmol quanta m^{-2} s^{-1} irradiance (PAR), 400 μmol mol^{-1} reference CO_2 and 27°C leaf temperature. The vapour pressure deficit (VPD) based on leaf temperature at the time of measurement ranged from 0.9 to 2.0 kPa.

At harvest, aboveground-biomass and root biomass (70°C for 72 h) were determined separately. Total seed number was estimated by multiplying the silique number with the average seed number of five randomly chosen siliques per plant.

Biochemical Analysis

Undamaged, healthy, fresh, and penultimate leaves (*ca.* 3 g) were taken from three replicates of each treatment at 100 days after sowing. The samples were stored at 4°C in zip lock polyethene bags until used for analysis *ca.* 7 days later. From these samples, the soluble phenolics were determined by following the Folin–Ciocalteu reagent method (Julkenen-Titto, 1985). The total soluble sugar content of each sample was determined by following the procedure of Dubios et al. (1956) modified according to Lee and Kim (2000). Free leaf proline content in each sample was measured by following the procedure of Bates et al. (1973).

Statistical Analyses

Growth, phenology and biochemical data were analyzed using analysis of variance (ANOVA) to evaluate differences between treatments (GENSTAT 16th edition; VSN International, Hemel Hempstead, United Kingdom). Means were separated using Fisher's protected least significant difference (l.s.d.) test at $P = 0.05$.

Due to missing data causing an unbalanced design, the photosynthetic parameter data were analyzed using the lme4 package in R (Bates et al., 2015) fitting a linear mixed model of the form $y = X\beta + Z\mu + e$ with Biotype and Water Regime fitted as fixed (vector β) and Replicate as random (vector μ) effects and e denoting an error term. The initial model included interactions between biotype and water regime, but this term was dropped as it was not significant for either variable presented here.

Figures were prepared using SigmaPlot software (SigmaPlot 13; Systat Software, San Jose, CA, United States) and R (R Core Team, 2016).

RESULTS

Growth Parameters and Phenology

By 75 DAS, the St. George and Dalby biotypes attained similar plant height at 100% WHC, however, plant height of the Dalby biotype was reduced with decreasing soil moisture levels ($P < 0.05$). Plant height of the St. George biotype was only reduced at the most severe treatment of 25% WHC (**Table 1**). By 75 DAS both biotypes had similar numbers of leaves at 100% WHC and leaf number was reduced at 25% WHC for both populations (**Table 1**). Water stress delayed branching and flowering initiation in both biotypes, but flowering was particularly affected in the Dalby biotype ($P < 0.05$) (**Table 1**). In the St. George biotype, plants started branching and flowering 34 and 28 days later, respectively, at 25% WHC compared with plants grown at 100% WHC. At this low WHC, branching and flowering of the Dalby biotype was delayed by 33 and 53 days, respectively, compared to plants at 100% WHC.

TABLE 1 | Effect of different soil moisture levels (factor 2) on final plant height, leaf number at 75 days after sowing and days taken to branching and flowering initiation of two Australian biotypes (St. George and Dalby; factor 1) of *Sisymbrium thellungii*.

Moisture level	St. George	Dalby	*Mean*
Plant height (cm)			
100% WHC	56.7a	51.7a	54.2a*
75% WHC	53.7a	34.0d	43.8b
50% WHC	65.4b	31.4d	48.4b
25% WHC	44.2c	24.2e	34.2c
Mean	55.0a	35.3b	
LSD ($P \leq 0.05$)	Biotype = 4.8; Water regime = 6.8; B × WR = 9.6		
Leaf number (75 DAS)			
100% WHC	27a	28a	28a
75% WHC	26a	24a	25a
50% WHC	28a	20a	24b
25% WHC	20a	16a	28a
Mean	25a	22b	
LSD ($P \leq 0.05$)	Biotype = 2.6; Water regime = 3.7; B × WR = NS		
Days taken to branching			
100% WHC	63a	68bc	65.5a
75% WHC	66ab	71cd	68.5ab
50% WHC	70bcd	73d	71.5b
25% WHC	97e	96e	96.5c
Mean	74a	77b	
LSD ($P \leq 0.05$)	Biotype = 2.3; Water regime = 3.2; B × WR = 4.5		
Days to flower initiation			
100% WHC	68a	67a	67.5a
75% WHC	71a	94b	82.5b
50% WHC	73a	105b	89.0b
25% WHC	96b	120c	108c
Mean	77a	96.5b	
LSD ($P \leq 0.05$)	Biotype = 6.6; Water regime = 9.4; B × WR = 13.3		

*WHC, Water holding capacity; LSD, Least significant difference; B, Biotype; NS, Not significant; WR, Water regime. Within terms Biotype (B), Water Regime (WR), B × WR, means followed by identical letters are not significantly different at α = 0.05. * indicates means value were compared with LSD of respective factor and thus, letters for each factor are separate.*

Biomass and Seed Production

Averaged across moisture levels, the St. George biotype (medium rainfall area) had 89% greater biomass and produced 321% more seeds than the Dalby biotype (**Table 2**). Increasing soil moisture stress affected biomass and seed production negatively in both biotypes. Averaged over biotypes, 25% WHC reduced *S. thellungii* biomass by 41% and seed production by 72% compared to 100% WHC. While there was no significant interaction between biotype and water regime for either trait, biomass of the St. George biotype, remained similar at 100, 75, and 50% WHC. Seed production of this biotype was also less affected by water

TABLE 2 | Effect of different soil moisture levels (factor 2) on different parameters of two Australian biotypes (St. George and Dalby; factor 1) of *Sisymbrium thellungii*.Moisture level

	St. George	Dalby	Mean
Biomass (g plant^{-1})			
100% WHC	9.64a	5.59a	7.61a
75% WHC	9.21a	4.45a	6.83a
50% WHC	9.01a	4.14a	6.58a
25% WHC	5.30a	3.62a	4.46b
Mean	8.29a	4.45b	
LSD ($P \leq 0.05$)	Biotype = 1.22; Water regime = 1.72; B × WR = NS		
Seeds plant^{-1} (number)			
100% WHC	9834a	4787a	7310a
75% WHC	9175a	1781a	5478b
50% WHC	7797a	730a	4264b
25% WHC	4061a	28a	2044c
Mean	7717a	1831b	
LSD ($P \leq 0.05$)	Biotype = 1357; Water regime = 1919; B × WR = NS		
Root: Shoot ratio (dry weight)			
100% WHC	0.08a	0.15a	0.11a
75% WHC	0.13a	0.12a	0.12a
50% WHC	0.12a	0.23a	0.17a
25% WHC	0.15a	0.19a	0.17a
Mean	0.12a	0.17b	
LSD ($P \leq 0.05$)	Biotype = 0.05; Water regimes = NS; B × WR = NS		

WHC, Water holding capacity; LSD, Least significant difference; B, Biotype; NS, Not significant; WR, Water regimes. Within terms Biotype (B), Water Regime (WR), B × WR, means followed by identical letters are not significantly different at α = 0.05.

TABLE 3 | Effect of different soil moisture levels (factor 2) on different parameters of two Australian Biotypes (St. George and Dalby; factor 1) of *Sisymbrium thellungii*.Moisture level

	St. George	Dalby	Mean
Free proline (μ moles g^{-1} dry weight)			
100% WHC	0.61a	1.26a	0.91a
75% WHC	2.29a	2.33a	2.31a
50% WHC	1.86a	2.42a	2.14a
25% WHC	0.38a	7.58b	3.90a
Mean	1.29c	3.39d*	
LSD ($P \leq 0.05$)	Biotype = 1.58; Water regime = NS; B × WR = 3.17		
Water soluble carbohydrate % (dry weight)			
100% WHC	17.4a	14.0a	15.7a
75% WHC	18.2a	12.9a	15.6a
50% WHC	20.5a	13.7a	17.1a
25% WHC	20.8a	17.7a	19.3b
Mean	19.2a	14.6b	
LSD ($P \leq 0.05$)	Biotype = 1.84; Water regime = 2.60; B × WR = NS		
Total phenolics (mg gallic acid equivalent g^{-1} dry weight)			
100% WHC	19.6a	14.1a	16.8a
75% WHC	14.7a	13.4a	14.1a
50% WHC	17.6a	14.0a	15.8a
25% WHC	16.7a	12.6a	14.6a
Mean	17.1a	13.5b	
LSD ($P \leq 0.05$)	Biotype = 1.92; Water regime = NS; B × WR = NS		

*WHC, Water holding capacity; LSD, Least significant difference; B, Biotype; NS, Not significant; WR, Water regime. Within terms Biotype (B), Water Regime (WR), B × WR, means followed by identical letters are not significantly different at α = 0.05. * indicates means value were compared with LSD of respective factor and thus, letters for each factor are separate.*

stress than the Dalby biotype. At 100% WHC, the St. George biotype produced 9,834 seeds plant^{-1}, while the Dalby biotype produced approximately half of that (4,787 seeds plant^{-1}) (**Table 2**). However, at 25% WHC, the seed production of the Dalby biotype was reduced to only 28 seeds plant^{-1} while the St. George biotype produced 4,061 seeds plant^{-1}. Water regime had no significant effect on the root to shoot biomass ratio; however, the root to shoot ratio was generally higher in the Dalby biotype compared with the St. George biotype (**Table 2**).

Biochemical Attributes

Averaged across all moisture levels, the Dalby biotype had more than double the amount of free proline in leaves compared with the St. George biotype (**Table 3**). The amount steadily increased with increasing water stress and was almost six times higher at 25% compared with 100% WHC, while increasing water stress had no consistent effect on free proline levels in the St. George biotype. On the other hand, water-soluble carbohydrate content was significantly higher in the St. George biotype than the Dalby biotype and it gradually increased in both biotypes with increasing water stress, thus in both biotypes, water-soluble carbohydrate was significantly higher at 25% than at 100% WHC. The amount of soluble phenolics was 27% higher in the St. George biotype relative to the Dalby biotype; however, moisture level had no effect on soluble phenolics content in either biotype (**Table 3**).

Photosynthetic Parameters

Moisture level did not seem to affect net carbon assimilation or conductance on a per leaf area basis, however, averaged across all moisture levels and compared with the Dalby biotype, the St. George biotype had a reduced leaf net carbon assimilation ($P > 0.05$, **Figure 3**), which was accompanied by a trend for lower stomatal conductance (**Figure 4**, $P = 0.066$).

DISCUSSION

In the current study, we exposed two biotypes of *S. thellungii* O. E. Schulz collected from a high (Dalby) and a medium rainfall area (St. George) to different levels of water stress. Significant differences were observed between these two biotypes when grown under varied soil moisture stress. The St. George biotype exhibited more vigorous growth than the Dalby biotype and had higher reproductive output (seed yield) than the Dalby biotype under all levels of water stress. Most importantly, this population still produced high seed yield (4061 seeds plant^{-1}) even under the highest level of water stress while the Dalby biotype yielded less than 30 seeds plant^{-1}.

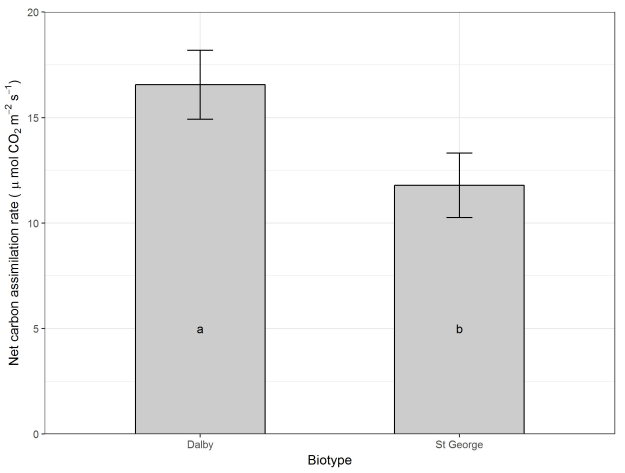

FIGURE 3 | Net carbon assimilation rate (μmol CO_2 m^{-2} s^{-1}) of rosette leaves of two Australian biotypes (St. George and Dalby) of *Sisymbrium thellungii*. There were no significant interactions between biotype and water regime so data shown are means for each biotype across all treatments predicted from the linear mixed model. Vertical lines represent standard error and letters within columns indicate whether differences were significant at $\alpha = 0.5$.

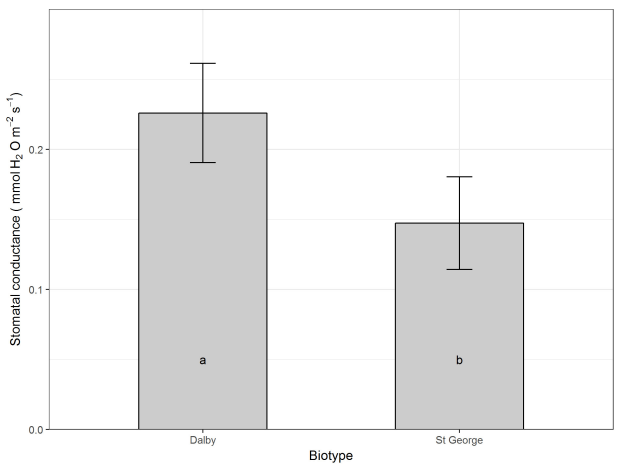

FIGURE 4 | Stomatal conductance (mol H_2O m^{-2} s^{-1}) of rosette leaves of two Australian biotypes (St. George and Dalby) of *Sisymbrium thellungii*. There were no significant interactions between biotype and water regime so data shown are means for each biotype across all treatments predicted from the linear mixed model. Vertical lines represent standard error and letters within columns indicate whether differences were significant at $\alpha = 0.5$.

The increased growth of the St. George biotype was not reflected in increased net carbon assimilation on a per leaf area basis of rosette leaves. Rather, the St. George biotype had low rosette leaf carbon assimilation rates which were accompanied by a trend for lower stomatal conductance compared with the Dalby biotype, which might be a specific adaptation to low soil moisture. Down regulation stomatal conductance and carbon assimilation rates in older large rosette leaves while maintaining persistent whole-plant carbon assimilation and growth via photosynthetic stems and cauline leaves has been found in other weeds that are particularly well adapted to hot and dry environments (Hill and Germino, 2005).

Free proline is known to accumulate in plants as a result of water stress (Bates et al., 1973). The damaging effects of reactive oxygen species might be ameliorated by proline under moisture stress, helping plants to regulate physiological function (Bajwa and Farooq, 2016). Free proline levels were significantly and progressively increased in the Dalby biotype in response to decreasing soil moisture levels, but not in the biotype from St. George. In comparison to the Dalby biotype, the free proline content in the St. George biotype did not increase with increasing moisture stress. At 25% WHC, the proline content in the Dalby biotype was significantly higher than at 100% WHC.

The higher soluble sugar and soluble phenolics content in the St. George biotype in comparison to the Dalby biotype may have helped this biotype alleviate the effects of water stress, resulting in more vigorous growth and greater seed production. Elevated levels of these chemicals have been observed in various weed species in response to multiple abiotic stresses and they have been found to ameliorate the damaging effects of reactive oxygen species produced under moisture stress (Anjum et al., 2011; Bajwa et al., 2016, 2018). Also, soluble phenolics produced by some weeds have been reported to have allelopathic potential which further increases their competitiveness (Kanchan and Jayachandra, 1980; Bajwa et al., 2016).

The present study revealed that *S. thellungii* biotypes selected from high and medium rainfall areas have different growth and reproductive behavior. In the wake of climate change, it is projected that the frequency and severity of droughts in Australia will increase (DEE, 2017). This may have a negative effect on agriculture as water limitation during crop growth may provide weeds a competitive advantage (Patterson, 1995). Weed species or biotypes that have a fast growth habit, high biomass production and high reproductive potential will be more competitive than slow-growing species (Horak and Loughin, 2000); but again the competition might be dependent on level of water stress and needs further investigation.

CONCLUSION

Our results demonstrated that the two Australian *S. thellungii* biotypes differed in growth, physiology, reproduction and biochemical production (free proline, total phenolics, and water-soluble carbohydrates) under well-watered as well as water stress conditions. The St. George biotype of *S. thellungii* had higher reproductive capacity than the Dalby biotype across all the moisture regimes, which suggests greater invasiveness. Overall, the large size and rapid growth of the *S. thellungii* population from the medium rainfall area, together with its physiological response to water stress and its ability to maintain seed production in dry conditions, may enable this biotype to become widespread in Australia.

While it has been known that certain biotypes show differences in competitiveness in different crop production systems, the physiological basis of these differences have not been shown previously. A better understanding of the underlying mechanisms of specific adaptation for each weed species is a prerequisite to develop the best management solutions for each agro-ecological region. With increasing frequencies of droughts, management solutions for biotypes with greater adaptation to drought are particularly important. With climate change, the St. George biotype of *S. thellungii* may expand its invasion range, and knowledge of its response to various soil moisture levels will become important in combating this weed.

Our study forms an excellent basis for such attempts for *S. thellungii*, an emerging and economically important weed in Australia. Information on the biological attributes of both biotypes under water stress conditions may be used to evaluate the effects of water limitation on weed-crop interactions in different areas via crop-modeling.

AUTHOR CONTRIBUTIONS

GM and BC designed the study, ran the experiment and wrote the paper. BG-J took the gas exchange measurements and wrote the physiological part. MW provided help in writing the manuscript. All authors read and approved the paper.

FUNDING

This work was supported by a grant from Grains Research and Development Corporation (GRDC) under Project US00084.

ACKNOWLEDGMENTS

The authors are thankful to Dr. Katherine Raymont for her help with the biochemical analyses.

REFERENCES

Anjum, S. A., Wang, L., Farooq, M., Xue, L., and Ali, S. (2011). Fulvic acid application improves the maize performance under well-watered and drought conditions. *J. Agron. Crop Sci.* 197, 409–417. doi: 10.1111/j.1439-037X.2011.00483.x

Bajwa, A. A., Chauhan, B. S., and Adkins, S. W. (2018). Germination ecology of two Australian biotypes of ragweed parthenium (*Parthenium hysterophorus*) relates to their invasiveness. *Weed Sci.* 66, 62–70. doi: 10.1017/wsc.2017.61

Bajwa, A. A., Chauhan, B. S., Farooq, M., Shabbir, A., and Adkins, S. W. (2016). What do we really know about alien plant invasion? A review of the invasion mechanism of one of the world's worst weeds. *Planta* 244, 39–57. doi: 10.1007/s00425-016-2510-x

Bajwa, A. A., and Farooq, M. (2016). Seed priming with sorghum water extract and benzyl amino purine along with surfactant improves germination metabolism and early seedling growth of wheat. *Arch. Agron. Soil Sci.* 63, 319–329. doi: 10.1080/03650340.2016.1211268

Bates, D., Mächler, M., Bolker, B., and Walker, S. W. (2015). Fitting linear mixed-effects models using lme4. *J. Stat. Softw.* 67, 1–48. doi: 10.18637/jss.v067.i01

Bates, L. S., Waldren, R. P., and Teare, I. D. (1973). Rapid determination of free proline for water-stress studies. *Plant Soil* 39, 205–207. doi: 10.1007/BF00018060

Bernacchi, C. J., Kimball, B. A., Quarles, D. R., Long, S. P., and Ort, D. R. (2007). Decreases in stomatal conductance of soybean under open-air elevation of [CO2] are closely coupled with decreases in ecosystem evapotranspiration. *Plant Physiol.* 143, 134–144. doi: 10.1104/pp.106.089557

Brown, R. (1995). "The water relations of range plants: adaptations to water deficits," in *Wild and plants: Physiological Ecology and Developmental Morphology,* eds J. Donald and R. E. Sosebee Bedunah (Littleton, CO: Society for Range Management), 291–413.

Chauhan, B. S. (2013). Growth response of itchgrass (*Rottboellia cochinchinensis*) to water stress. *Weed Sci.* 61, 98–103. doi: 10.1614/WS-D-12-00060.1

Chauhan, B. S., and Johnson, D. E. (2010). Growth and reproduction of junglerice (*Echinochloa colona*) in response to water stress. *Weed Sci.* 58, 132-135. doi: 10.1614/WS-D-09-00016.1

Chauhan, B. S., and Mahajan, G. (eds). (2014). *Recent Advances in Weed Management.* New York, NY: Springer, doi: 10.1007/978-1-4939-1019-9

Chimenti, C. A., Pearson, J., and Hall, A. J. (2002). Osmotic adjustment and yield maintenance under drought in sunflower. *Field Crops Res.* 75, 235–246. doi: 10.1016/S0378-4290(02)00029-1

Crusciol, C. A. C., Arf, O., Zucareli, C., Sá, M. E., and Nakagawa, J. (2001). Produção e qualidade fisiológica de sementes de arroz de terras altas em função da disponibilidade hídrica. *Rev. Bras. Sementes.* 23, 287–293. doi: 10.17801/0101-3122/rbs.v23n2p287-293

DEE (2017). *Department of the Environment and Energy, Australian Government*. Available at: https://www.environment.gov.au/climate-change/climate-science/impacts/qld [accessed December 18, 2017].

Dubios, M., Giles, K. A., Hamilton, J. K., Roberes, P., and Smith, F. (1956). Colorimetric method for determination of sugars and related substances. *Anal. Chem.* 28, 350–356. doi: 10.1021/ac60111a017

Heap, I. (2018). *International Survey of Herbicide Resistant Weeds*. Available at: http://www.weedscience.org [accessed June 20, 2018].

Hill, J. P., and Germino, M. J. (2005). Coordinated variation in ecophysiological properties among life stages and tissue types in an invasive perennial forb of semiarid shrub steppe. *Can. J. Bot.* 83, 1488–1495. doi: 10.1139/b05-116

Horak, M. J., and Loughin, T. M. (2000). Growth analysis of four *Amaranthus species*. *Weed Sci.* 48, 347–355. doi: 10.1614/0043-1745(2000)048[0347:GAOFAS]2.0.CO;2

Julkenen-Titto, R. (1985). Phenolic constituents in the leaves of northern willows: methods for the analysis of certain phenolics. *J. Agric. Food Chem.* 33, 213–217. doi: 10.1021/jf00062a013

Kanchan, S. D., and Jayachandra. (1980). Allelopathic effects of *Parthenium hysterophorus* L. *Plant Soil* 55, 67–75. doi: 10.1007/BF02149710

Kaur, S., Aulakh, J., and Jhala, A. J. (2016). Growth and seed production of glyphosate-resistant giant ragweed (*Ambrosia trifida* L.) in response to water stress. *Can. J. Plant Sci.* 96, 828–836. doi: 10.1139/cjps-2015-0309

Lee, S. S., and Kim, J. H. (2000). Total sugars, α-amylase activity, and germination after priming of normal and aged rice seeds. *Kor. J. Crop Sci.* 45, 108–111.

Lu, P., Sang, W. G., and Ma, K. P. (2008). Differential responses of the activities of antioxidant enzymes to thermal stresses between two invasive *Eupatorium species* in China. *J. Integ. Plant Biol.* 50, 393–401. doi: 10.1111/j.1744-7909.2007.00583.x

Mahajan, G., Ramesha, M. S., and Chauhan, B. S. (2015). Genotypic differences for water-use efficiency and weed competitiveness in dry direct-seeded rice. *Agron. J.* 107, 1573–1583. doi: 10.2134/agronj14.0508

Mahajan, G., Singh, S., and Chauhan, B. S. (2012). Impact of climate change on weeds in the rice-wheat cropping system. *Curr. Sci.* 102, 1254–1255.

Moran, P. J., and Showler, A. T. (2005). Plant responses to water deficit and shade stresses in pigweed and their influence on feeding and oviposition by the beet armyworm (Lepidoptera: Noctuidae). *Environ. Entomol.* 34, 929–937. doi: 10.1603/0046-225X-34.4.929

Muchow, R. C., and Carberry, P. S. (1989). Environmental control of phenology and leaf growth in a tropically adapted maize. *Field Crops Res.* 20, 221–236. doi: 10.1016/0378-4290(89)90081-6

Mundree, S. G., Baker, B., Mowla, S., Peters, S., Marais, S., Vander Willigen, C., et al. (2002). Physiological and molecular insights into

drought tolerance. *Afr. J. Biotechnol.* 1, 28–38. doi: 10.5897/AJB2002.000-006

Nguyen, T. L. T. (2011). *The Invasive Potential of Parthenium Weed (Parthenium hysterophorus L.) in Australia*. Ph.D. thesis, The University of Queensland, Brisbane.

Parreira, M. C., Barroso, A. A., Portugal, J. M., Da, P. L., and Alves, C. A. (2015). Effect of drought stress on periods prior of weed interference (PPWI) in bean crop using arbitrary and tolerance estimation. *Aust. J. Crop Sci.* 9, 1249–1256.

Patterson, D. T. (1995). Effects of environmental stress on weed/crop interactions. *Weed Sci.* 43, 483–490.

R Core Team (2016). *R: A language and Environment for Statistical Computing*. Vienna: R Foundation for Statistical Computing.

Sarangi, D., Irmak, S., Lindquist, J. L., Knezevic, S. Z., and Jhala, A. J. (2016). Effect of water stress on the growth and fecundity of common waterhemp (*Amaranthus rudis*). *Weed Sci.* 64, 42–52. doi: 10.1614/WS-D-15-00052.1

Stout, D. G., and Simpson, G. M. (1978). Drought resistance of sorghum bicolor. 1. Drought avoidance mechanisms related to leaf water status. *Can. J. Plant Sci.* 58, 213–224. doi: 10.4141/cjps78-031

Sullivan, C. Y., and Ross, W. M. (1979). "Selecting for drought and heat resistance in grain sorghum," in *Stress Physiology in Crop Plants,* eds H. Mussell and R. C. Staples (New York, NY: Willey Interscience), 263–281.

Thomas, A. G., Derksen, D. A., Blackshaw, R. E., Van Acker, R. C., Légère, A., Watson, P. R., et al. (2004). Symposium A multistudy approach to understanding weed population shifts in medium-to long-term tillage systems. *Weed Sci.* 52, 874–880. doi: 10.1614/WS-04-010R1

White, R. H., Engelke, M. C., Morton, S. J., and Ruemmele, B. A. (1992). Competitive turgor maintenance in tall fescue. *Crop Sci.* 32, 251–256. doi: 10.2135/cropsci1992.0011183X003200010050x

Conflict of Interest Statement: The authors declare that the research was conducted in the absence of any commercial or financial relationships that could be construed as a potential conflict of interest.

The reviewer DM and handling Editor declared their shared affiliation.

frontiers in Plant Science

ORIGINAL RESEARCH
published: 05 December 2018
doi: 10.3389/fpls.2018.01767

Resource Reallocation of Two Grass Species During Regrowth After Defoliation

Yanshu Liu[1], Xiaohui Yang[1], Dashuan Tian[2], Richun Cong[1], Xiao Zhang[1], Qingmin Pan[3] and Zhongjie Shi[1]**

[1] Institute of Desertification Studies, Chinese Academy of Forestry, Beijing, China, [2] Institute of Geographical Sciences and Natural Resources Research, Chinese Academy of Sciences, Beijing, China, [3] Inner Mongolia Research Center for Prataculture, Chinese Academy of Sciences, Beijing, China

Defoliation is widely used for grassland management. Our understanding of how grass species adjust their regrowth and regain balance after defoliation remains limited. In the present study, we examined the regrowth processes of two dominant species after defoliation in grasslands in Inner Mongolia. Our results showed that the aboveground biomass and total biomass of both species significantly decreased and did not completely recover to the control level after 30 days of regrowth. The leaf mass ratio of *Leymus chinensis* reached the control level at 15 days, but that of *Stipa grandis* did not recover to the control level. The root mass ratio of these species reached the same levels as that of the control plants within 10 days after defoliation. As indicated by the dynamics of water-soluble carbohydrates (WSCs), protein, and biomass-based shoot: root ratios, both species regained balances of WSCs and protein between above- and below-ground organs at day 10 after defoliation; however, the biomass regained balance 15 days after defoliation. We deduced that the biomass-based shoot:root ratio was regulated by the WSCs and protein concentrations. In conclusion, following defoliation, both grass species first restore their nutrient-based balance between above- and below-ground parts and then regain biomass balance.

Keywords: biomass allocation, grazing, carbohydrates, protein, grassland management

OPEN ACCESS

Edited by:
Yinglong Chen,
The University of Western Australia, Australia

Reviewed by:
Xiao-Tao Lu,
Institute of Applied Ecology (CAS), China
Cameron Ducayet McIntire,
The University of New Mexico, United States

****Correspondence:***
Qingmin Pan
pqm@ibcas.ac.cn
Zhongjie Shi
shizj@caf.ac.cn

Specialty section:
This article was submitted to Plant Abiotic Stress, a section of the journal Frontiers in Plant Science

Received: *21 February 2018*
Accepted: *14 November 2018*
Published: *05 December 2018*

Citation:
Liu Y, Yang X, Tian D, Cong R, Zhang X, Pan Q and Shi Z (2018) Resource Reallocation of Two Grass Species During Regrowth After Defoliation. Front. Plant Sci. 9:1767. doi: 10.3389/fpls.2018.01767

INTRODUCTION

Defoliation caused by animal grazing and hay production has profound impacts on plant growth and development in grassland ecosystems. In general, defoliation decreases the total leaf area, plant photosynthesis, and uptake and assimilation of nutrients, such as carbon and nitrogen, but increases the mobilization of reserved nutrients to develop new leaves and stems (Macduff and Jackson, 1992; Volenec et al., 1996). Previous studies have suggested that defoliation can stimulate plant regrowth (McNaughton, 1983; Muthoni et al., 2014). In fact, plants have evolved a suite of morphological and physiological mechanisms to cope with defoliation. The ability of plants, which use internal stores of carbon and nitrogen, both to rapidly restore photosynthetically active leaf area and to meet the maintenance demands of other organs, is among the key factors that facilitate plant survival during the first 2 weeks of regrowth after defoliation (Volenec et al., 1996).

Numerous studies have highlighted the importance of water-soluble carbohydrate (WSC) reserves of grass species during regrowth following defoliation (Hume, 1991; Donaghy and Fulkerson, 1997). For some grass species, WSCs in the stem stubble (residual stem after defoliation)

constitute the main source for regrowth (Steen and Larsson, 1986); in contrast, other studies have found that WSC reserves in the rhizomes play a critical role in the regrowth of rhizomatous grasses after defoliation (Wang, 2007). For plants subjected to defoliation, WSCs are usually affected by both stubble height (Fulkerson and Slack, 2003; Lee et al., 2009; Jones et al., 2017) and the temporal interval between defoliations (Singh and Sale, 1997; Donaghy and Fulkerson, 2002).

In addition to WSCs, nitrogen reserves also play an important role in plant regrowth (Ourry et al., 1994; Volenec et al., 1996). In herbaceous plants, protein is an important mobile storage form of nitrogen (Staswick, 1994). Thornton et al. (1993) reported that, in support of the growth of new leaves after defoliation, the remobilization of protein reserves and nitrogen uptakes varies among grass species. It has been recognized that the plant root: shoot ratio may function as a balance in terms of resource acquisition and allocation (Agren and Ingestad, 1987). Plants first transport and use their pre-defoliation reserves for maintenance and regrowth within the first 2 weeks after defoliation, after which the newly growing leaves then assimilate new carbohydrates and allocate them to different parts of plants (Detling et al., 1979; Menke and Trlica, 1981; Detling and Painter, 1983). However, WSCs and proteins, during regrowth following defoliation, are often examined separately (Augustine et al., 2011).

Defoliation usually causes a great decline in the plant shoot:root ratio due to the loss of aboveground parts, which disrupts the balance between above- and below-ground parts. To recover from an unbalanced state for biomass loss after defoliation to a plant's original state, in terms of biomass allocation between above- and below-ground parts, a defoliated plant usually exhibits a higher relative growth rate (RGR) of aboveground organs. Such phenomena have been extensively observed (Meyer, 1998; Zhao et al., 2008); however, the rate at which plant species adjust their biomass allocations between above- and below-ground organs after defoliation remains unclear. Moreover, the role of nutrients, such as WSCs and proteins, in the rebalancing process of biomass allocation between above- and below-ground organs has rarely been addressed.

Leymus chinensis (Trin.) Tzvel. and *Stipa grandis* P. Smirn. are two widely distributed species in Inner Mongolia's grasslands (Liu et al., 2012). *L. chinensis*, a rhizomatous grass species, has long, strong rhizomes and exhibits vigorous vegetative propagation; thus, this species usually gives rise to extensively spreading clones and often forms monodominant stands in relatively wet habitats. In contrast, *S. grandis*, a typical bunch grass, usually occupies and dominates relatively dry habitats (Briske and Derner, 1998). The belowground parts of these two species often function as organs for nutrient acquisition and storage, in addition to water absorption from the soil, to address frequent drought stresses. Nutrients stored within roots or rhizomes allow plants to easily overcome fluctuations in nutrient availability. Via the phalanx strategy (producing a compact cluster of closely spaced ramets) (Cheplick, 1997; Chen et al., 2011), *S. grandis* can monopolize and consolidate locally available resources, which is beneficial in a competitive environment. Both species are well-adapted to grazing and periodic drought but differ in terms of functional types (rhizomatous grass vs. bunchgrass). The aim of this study was to answer the following questions: (1) How different is the regrowth between two functional types after defoliation? (2) How do these species reallocate their biomass, WSCs, and proteins between their above- and below-ground parts after defoliation? (3) Does biomass rebalancing between above- and below-ground parts keep pace with the rebalancing of WSCs and proteins? This study will provide a theoretical reference to formulate a wiser grazing system in Inner Mongolia's grasslands.

MATERIALS AND METHODS

This experiment was conducted at the Inner Mongolia Grassland Ecosystem Research Station, Chinese Academy of Sciences (IMGERS), in 2014. The station is located within the Xilin River watershed in the Inner Mongolia Autonomous Region, China (116°40′40″ E, 43°32′45″ N, 1250–1280 m a.s.l.). The area has a semiarid continental temperate steppe climate, which consists of a dry spring season and a humid summer. The average annual temperature is 0.92°C and the average annual precipitation is 337 mm; rainfall occurs mostly within the period from June to August.

Seeds of two species were collected from a permanent fenced grassland plot with an area of 25 ha. To break dormancy, the seeds were immersed in low-temperature water for 12 h and then sown in pots (280 mm in diameter and 260 mm in depth) filled with chestnut soil and arranged in an open field on June 1. A total of 100 pots for each species, with a density of 30 plants per pot, were planted and watered every 3 days during the first 2 weeks and then irregularly depending on the soil conditions. On July 5, 20 uniform seedlings were kept in each pot; other seedlings were removed.

On August 10th, 30 pots for each species were defoliated to a stubble height of 3 cm; another 30 pots for each species were chosen as the controls. To track the regrowth processes of these two species after defoliation, we harvested all the above- and below-ground parts in three pots for each species at 0, 1, 2, 3, 5, 10, 15, 20, 25, and 30 days after defoliation. The aboveground parts were collected and divided into leaves and stems, while the belowground parts were collected via water washing and meshed by a 1 mm × 1 mm screen; *L. chinensis* was further divided into root and rhizome. All plant materials collected were freeze-dried until at a constant weight and then ground with a ball mill (Retsch MM 400; Retsch, Haan, Germany) for WSC and protein analysis. The protein concentration of each organ was analyzed with a Nitrogen Analyzer System (KJELTEC 2300 AUTO SYSTEM II, Foss Tecator AB, Höganäs, Sweden). The protein concentration at plant level was calculated as the biomass weighted average protein concentration of the leaf, stem, root, and rhizome.

The leaf mass ratio (LMR) was calculated as LMR = (leaf weight)/(total biomass), and the root mass ratio (RMR) as RMR = (root weight)/(total biomass). The RGR in terms of the aboveground biomass was calculated as RGR = (lnB2–lnB1)/(t2–t1), where B1 and B2 are the aboveground biomass measured at time 1 and time 2, respectively.

TABLE 1 | *F*-values and *P*-values of repeated measures ANOVA on the effects of defoliation and days after defoliation on height, number of tiller, LWR, RWR, RGR in terms of aboveground biomass, aboveground biomass, total biomass, biomass-based, WSC-based, and protein-based shoot:root ratios of *L. chinensis* and *S. grandis*.

Variable	Days		Defoliation		Days × Defoliation	
	F	*P*	*F*	*P*	*F*	*P*
L. chinensis						
Heigh	43.19	<0.0001	3454.24	0.0108	37.72	< 0.0002
Number of tiller	30.21	<0.0001	1.45	0.2355	1.6	0.148
LWR	6.17	<0.0001	35	<0.0001	8.74	<0.0001
RWR	18.09	<0.0001	149.45	<0.0001	17.98	<0.0001
Aboveground biomass	53.64	<0.0001	53.01	<0.0001	1.03	0.4258
Total biomass	43.33	<0.0001	50.59	<0.0001	2.89	0.0272
Biomass-based shoot:root ratio	14.09	<0.0001	5.26	0.0295	8.84	<0.0001
WSCs-based shoot:root ratio	12.01	<0.0001	0.53	0.4723	1.67	0.1672
Protein-based shoot:root ratio	7.4	<0.0001	0.62	0.437	5.94	0.0004
S. grandis						
Heigh	48.88	<0.0001	4465.21	0.0095	39.6	<0.0002
Number of tiller	1.33	0.2789	0.01	0.9323	0.28	0.9404
LWR	5.36	0.004	17.38	0.0003	0.07	0.9778
RWR	1.13	0.3651	61.68	<0.0001	5.31	<0.0001
Aboveground biomass	11.81	<0.0001	32.15	<0.0001	1.04	0.4218
Total biomass	15.25	<0.0001	27.71	<0.0001	1.51	0.2126
Biomass-based shoot:root ratio	2.65	0.0366	6.28	0.0183	5.46	0.0008
WSCs-based shoot:root ratio	3.77	0.0093	24.21	<0.0001	7.57	0.0001
Protein-based shoot:root ratio	1.38	0.26	5.37	0.0286	7.83	<0.0001

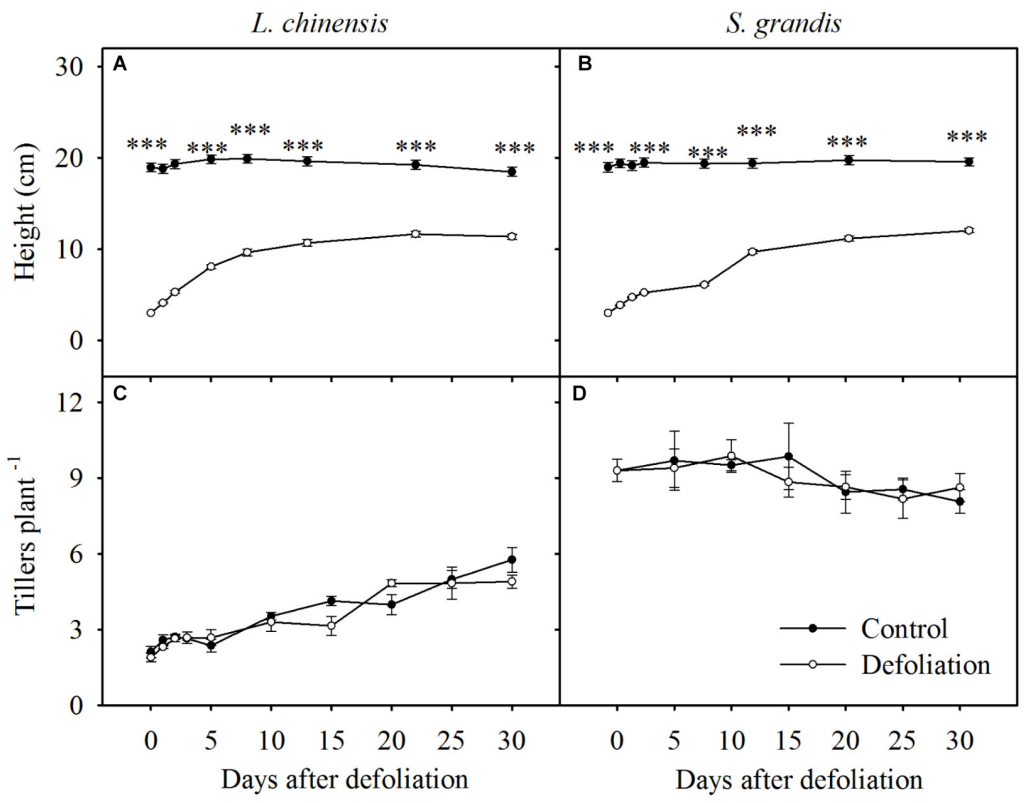

FIGURE 1 | Seedling height and number of tillers per plant of *L. chinensis* **(A,C)** and *S. grandis* **(B,D)** after defoliation. Values are means ± SE (n = 3). ns, *, **, and *** indicate non-significant difference at $P < 0.05$, $P < 0.01$, and $P < 0.001$, respectively.

To determine the WSC concentrations of leaf, stem, root and rhizome for two species, 100 μg of lyophilized plant tissue powder was suspended in 5 ml of distilled water and incubated in 100°C boiling water for 30 min. After the suspensions had cooled to room temperature and been centrifuged (5 min at 10000 *g*), the supernatants were removed and transferred to 50-ml volumetric flasks, after which the pellets were re-extracted one time. The supernatants were subsequently combined in a 50-ml volumetric flask, diluted with water to volume, and mixed (Solution A). Then, 500 μl of Solution A and 1.5 ml of distilled water were added to a new tube, after which 0.5 ml of a throne reagent and concentrated sulfuric acid were added. The contents of the tube were then mixed together, after which the tube was incubated in 100°C boiling water for 1 min. After the tube was cooled to room temperature, the concentration of WSCs was measured by a photoelectric colorimeter (Beckman Coulter DU800, Brea, CA, United States) (Li et al., 2000).

In the current study, we used the shoot:root ratios of the biomass, WSCs, and proteins in the control treatment as references of a balanced state; then, we defined the rebalance of biomass, WSCs, and proteins as the state at which the corresponding shoot:root ratio of a defoliated plant recovered to the level of control treatments, i.e., no significant difference in shoot:root ratio between defoliated treatments and control treatments.

We performed ordinary least squares regressions to examine the relationship between the biomass-based shoot:root ratio with the WSCs concentration, amount of WSCs per plant, protein concentration, and protein amount per plant. The differences between the defoliation and control treatments over regrowth days were measured with repeated measures ANOVA and were compared between two species with a *t*-test. All statistical analyses were performed using SAS version 9.1 (SAS Institute, Cary, NC, United States).

RESULTS

Defoliation Impacts on Plant Height and the Number of Tillers per Plant

Defoliation significantly decreased the height of *L. chinensis* and *S. grandis* during the 30 days of regrowth (**Table 1**).

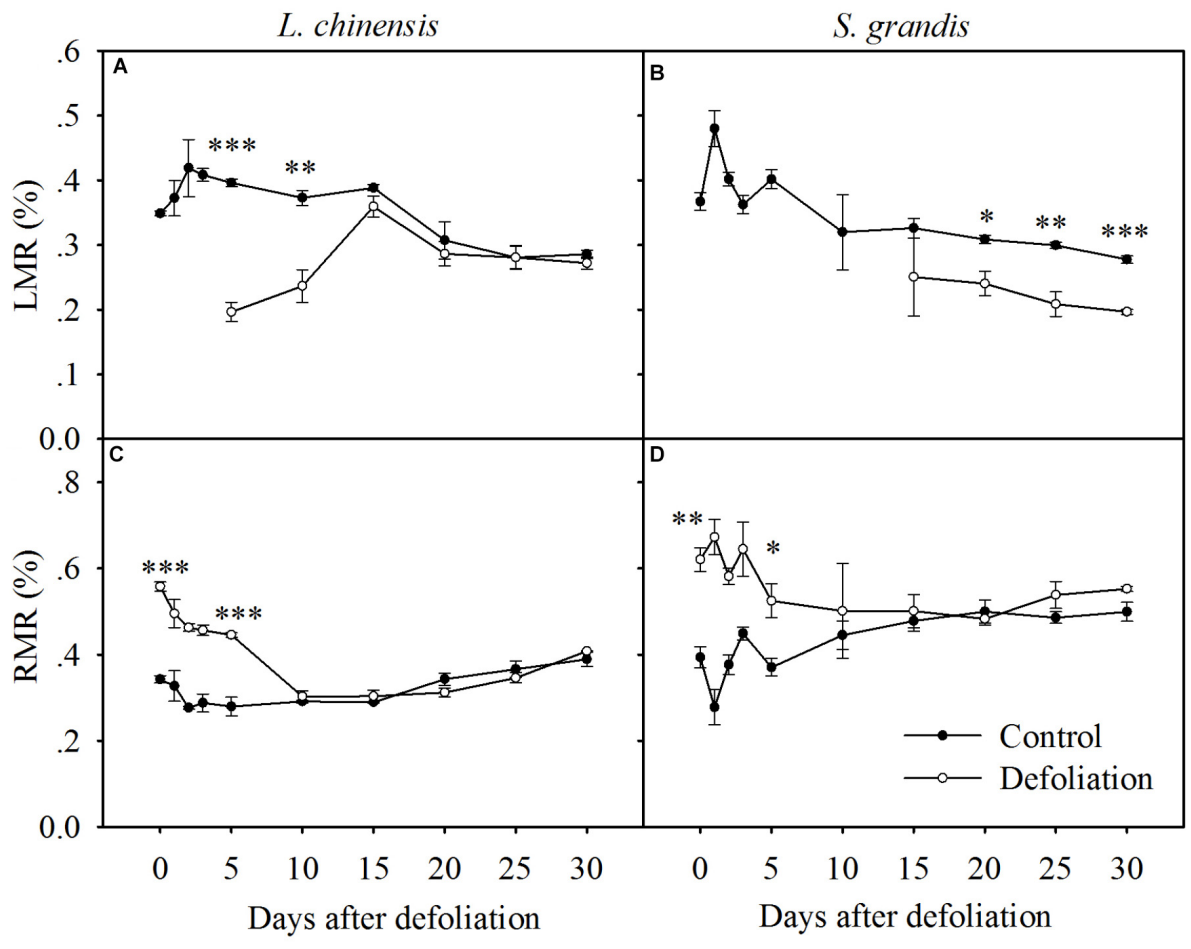

FIGURE 2 | Changes in the LMR and RMR of *L. chinensis* **(A,C)** and *S. grandis* **(B,D)** after defoliation. Values are means ± SE (n = 3). Values and symbols have the same meanings as in **Figure 1** (LMR of first 15 days for *S. grandis* is missing due to no regrowth of leaf).

The height of *L. chinensis* and *S. grandis* plants in the defoliation treatment increased rapidly and reached half that of the control plants within the first 10 days after defoliation, after which the height gradually plateaued (**Figure 1**). No significant effects of defoliation on the number of tillers per plant were observed in either species, but the number of tillers increased in *L. chinensis* regardless of defoliation treatment.

Defoliation Impacts on Leaf Mass Ratio and Root Mass Ratio

The LMR of *L. chinensis* under defoliation treatment was first detected at day 5 after defoliation and then increased rapidly within the following 10 days, reaching the level of the control treatment at day 15. In contrast, the RMR of *L. chinensis* decreased within the first 10 days after defoliation and then reached the level of the control treatment. There was no significant difference in either the LMR or RMR of *L. chinensis* between the control and defoliation treatments from day 10 to day 30 or from day 15 to day 30, respectively (**Figure 2** and **Table 1**).

The LMR of *S. grandis* under the defoliation treatment was first detected at day 5 after defoliation but was significantly lower than that of the control treatments, even after 30 days of regrowth. The RMR of *S. grandis* decreased within the first 10 days after defoliation and then reached the level of the control treatment. There was no significant difference in the RMR of *S. grandis* between the control and defoliation treatments from day 10 to day 30 (**Figure 2** and **Table 1**).

Defoliation Impacts on RGR

For both species, the defoliated plants exhibited a greater RGR in the first 20 days after defoliation, but the RGR of the defoliated plants within 20–30 days was less than that of the control plants (**Figure 3**). However, the magnitude of the increase in RGR was much greater in *L. chinensis* than that in *S. grandis* (**Figures 3**, **7B**). On average, the RGR of *L. chinensis* under the defoliation treatment was 1.8 times that of *S. grandis*.

Defoliation Impacts on Biomass Production

Defoliation significantly reduced the aboveground biomass and total biomass of both species within 30 days of regrowth (**Figures 4**, **7A,B** and **Table 1**). For *L. chinensis*, defoliation removed 74% of the aboveground biomass; as a result, after 30 days of regrowth, the aboveground biomass and total biomass of defoliated individuals were 31 and 39% less than those of the control plants. For *S. grandis*, defoliation removed 61% of the aboveground biomass, and the aboveground biomass and total biomass of defoliated individuals were 39 and 31% less than those of the control plants, respectively (**Figure 5** and **Table 1**).

Defoliation Impacts on Shoot:Root Ratios in Terms of Biomass, WSCs, and Proteins

The biomass-based shoot:root ratios of *L. chinensis* and *S. grandis* increased significantly within 15 days after defoliation; however, there were no significant differences between the defoliated and control plants for either species from day 15 to day 30 (**Figures 5**, **7D** and **Table 1**).

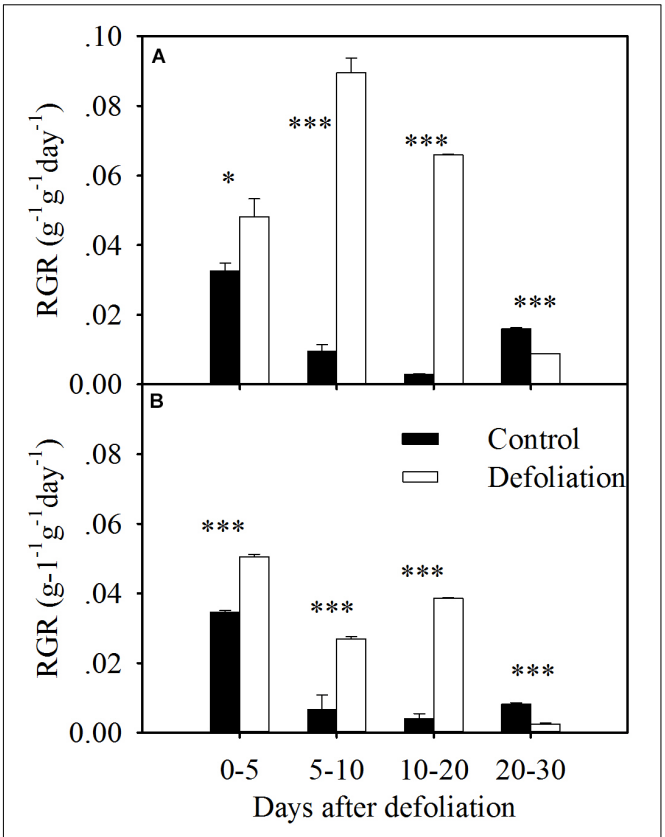

FIGURE 3 | RGR in terms of aboveground biomass of *L. chinensis* **(A)** and *S. grandis* **(B)** after defoliation. Values are means ± SE (n = 3). Values and symbols have the same meanings as in **Figure 1**.

The WSCs- and protein-based shoot:root ratios of *L. chinensis* and *S. grandis* exhibited a significant increase within 10 days after defoliation; however, neither the WSCs-based nor protein-based shoot:root ratio between the defoliated and control plants significantly differed for either species from day 15 to day 30 (**Figures 5**, **7D** and **Table 1**).

Biomass-Based Shoot:Root Ratio With the Amounts per Plant and Concentrations of WSCs and Proteins

Under the control treatment, the biomass-based shoot:root ratio for both species was negatively and linearly related to the amount of WSCs per plant; however, this correlation shifted to a positive linear correlation under the defoliation treatment (**Figures 6A,B**).

For *L. chinensis*, the biomass-based shoot:root ratio was positively and linearly related to the amount of proteins per plant under both the control and defoliation treatments (**Figure 6C**). For *S. grandis*, the biomass-based shoot:root ratio was negatively and linearly related to the amount of proteins per plant under the

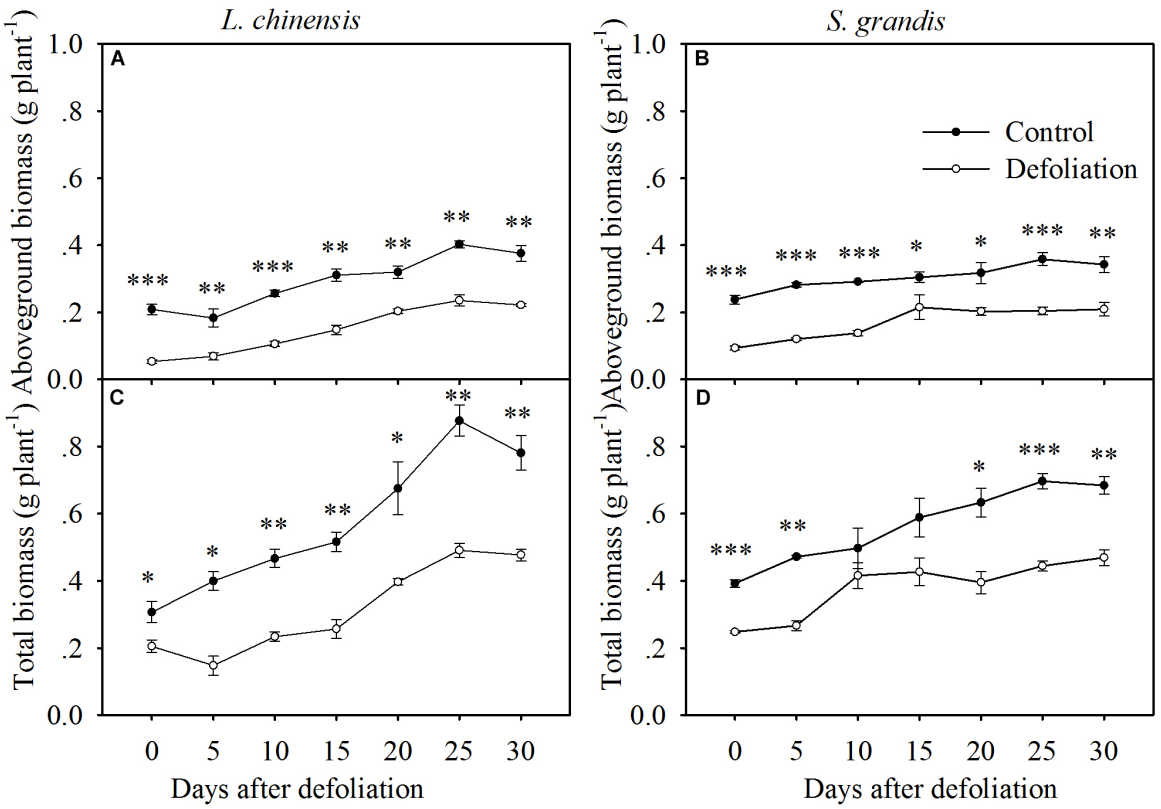

FIGURE 4 | Changes in the aboveground biomass and total biomass of *L. chinensis* **(A,C)** and *S. grandis* **(B,D)** after defoliation. Values are means ± SE (n = 3). Values and symbols have the same meanings as in **Figure 1**.

control treatment but displayed a positive and linear correlation under the defoliation treatment (**Figure 6D**).

For *L. chinensis*, the biomass-based shoot:root ratio was negatively and linearly related to the concentration of WSCs under the control treatment but positively and linearly related to the concentration of WSCs under the defoliation treatment (**Figure 6E**). No relationship was detected between the two for *S. grandis* (**Figure 6F**).

The biomass-based shoot:root ratio for both species generally exhibited a positive linear correlation with the protein concentration (**Figures 6G,H**), except for *L. chinensis* under defoliation treatment, where no relationship was detected between the two (**Figure 6H**).

DISCUSSION

Our experiment demonstrated that the two grassland species displayed both similarities and differences in their regrowth response to defoliation. Generally, both species were damaged by defoliation in plant height and biomass production. However, defoliation stimulated growth in these species, as indicated by a significant increase in the RGR in both species. Such stimulation was much stronger for *L. chinensis* than for *S. grandis*, as the RGR of *L. chinensis* under defoliation treatment was 1.8 times that of *S. grandis*. Though the response strengths in biomass production of the two species differed substantially, balance speeds of these species in terms of resource reallocation between above- and below-ground organs were the same. Specifically, both species achieved a balance of WSCs and proteins at day 10 after defoliation, while biomass was rebalanced at day 15. Moreover, such rebalance processes may be mediated by WSCs and proteins, as our analysis indicated that the biomass-based shoot:root ratio was significantly related to concentrations and the amount per plant of WSCs and protein.

Regrowth After Defoliation

Plants alter their allocation patterns by increasing nutrient allocation to organs responsible for acquiring limited resources (Chu et al., 1992) to maximize their growth. For example, plants limited by carbon often increase their resource partitioning to the photosynthetically active leaf area. Plants suffering from defoliation first maximize their regrowth by increasing the leaf area to capture more carbon per unit of resource and invest in the photosynthetically active leaf area (Chu et al., 1992). In the present study, the LMR of *L. chinensis* increased rapidly and recovered to the control level at day 15 after defoliation, while the LMR of *S. grandis* did not recover (**Figure 2**). These results could be at least partially explained by the lower RGR of *S. grandis* than that of *L. chinensis* in terms of aboveground biomass.

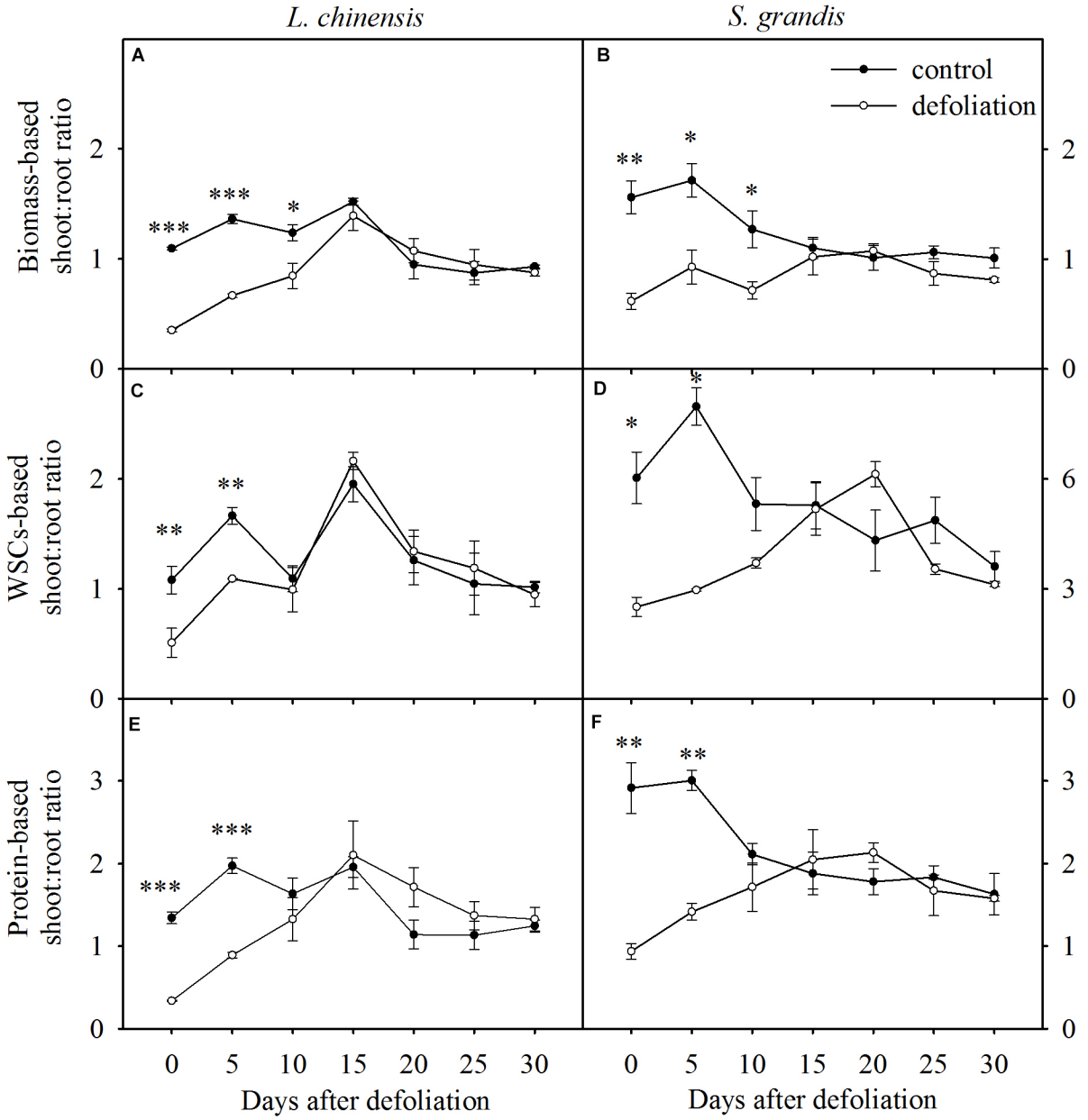

FIGURE 5 | Changes in biomass-based, WSC-based, and protein-based shoot:root ratios of *L. chinensis* (**A,C,E**, respectively) and *S. grandis* (**B,D,F**, respectively) after defoliation. Values are means ± SE (n = 3). Values and symbols have the same meanings as in **Figure 1**.

The heights of *L. chinensis* and *S. grandis* plants, which were reduced to 3 cm with defoliation, rapidly increased during the first 10 days after defoliation (**Figure 1**). The rate of increase slowed over the next 20 days; as a result, the final height after 30 days of defoliation was significantly lower than that of the control treatment. This result is consistent with those of the study of Zhang et al. (2007), who found that defoliation significantly decreased plant height. The lower height of defoliated plants after 30 days of regrowth relative to that of control plants may be due to the lack of sufficient soluble nutrients, such as WSCs or protein. Previous studies have shown that the regrowth of a plant after defoliation in most cases involves replenishing WSCs and proteins from organ reserves to initiate the growth of new tillers (Donaghy and Fulkerson, 1998; Fulkerson and Donaghy, 2001).

The mean RGR in terms of the aboveground biomass of both species significantly increased during the 20 days after defoliation (**Figures 3**, **7**). During the first 5 days of regrowth, translocated WSCs constituted the main nutrients (Morvan-Bertrand et al., 1999), so the mean RGR in the defoliated treatment was slightly higher than that in the control treatment. During the next 15 days, the new leaves, which contained relatively higher nitrogen concentrations, enabled plants to rapidly increase their

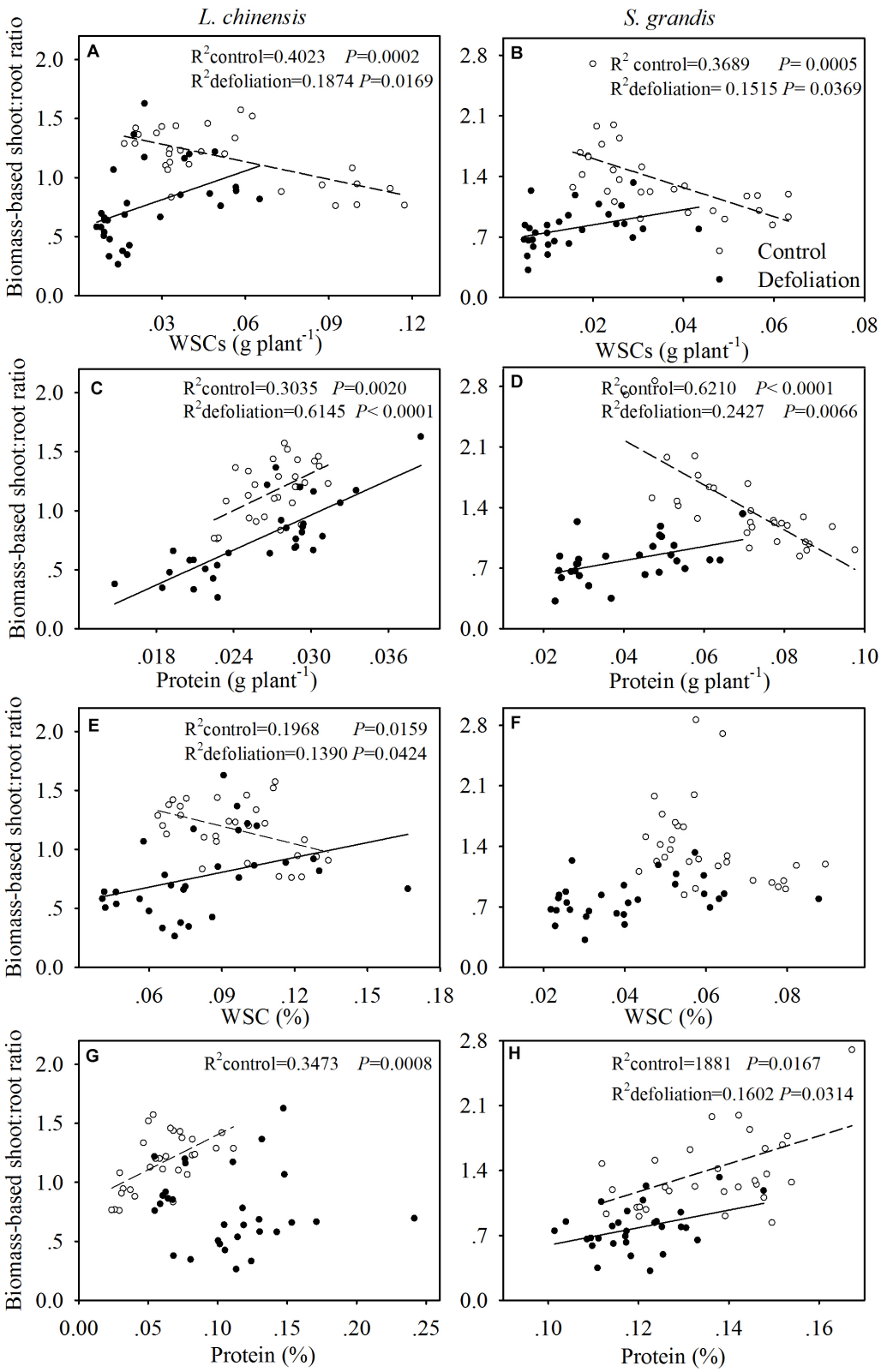

FIGURE 6 | Relationships of the biomass-based shoot:root ratio with the amount of WSCs (g plant^{-1}) and proteins (g plant^{-1}) per plant and with the concentration of WSCs (%) and protein (%) in *L. chinensis* (**A,C,E,G**, respectively) and *S. grandis* (**B,D,F,H**, respectively) subjected to defoliation (filled circles and solid line) and control (open circles and dashed line) treatments.

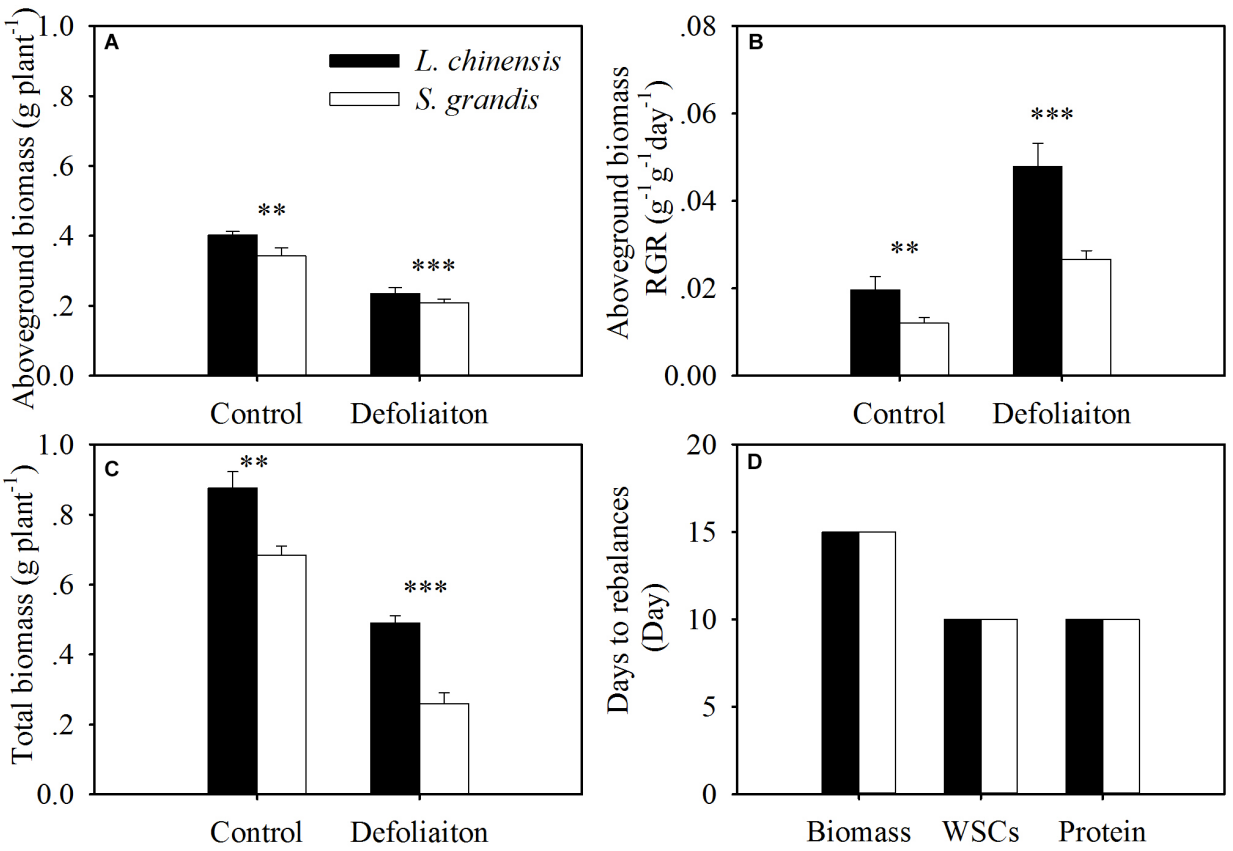

FIGURE 7 | Comparison between *L. chinensis* and *S. grandis* in aboveground biomass **(A)**, aboveground biomass-based RGR **(B)**, total biomass **(C)**, and the days of restoring balance in terms of biomass, WSCs and proteins **(D)**. Values and symbols have the same meanings as in **Figure 1**.

shoot biomass; therefore, the mean RGR was much higher in the defoliation treatment than in the control treatment. As the leaf area enlarges during regrowth, plants experience a trade-off: newly assimilated carbon must be allocated to replenish reserves rather than to increase growth. After 20 days of regrowth, the defoliated plants for both species may partition more assimilates to replenish their nutrient reserves. Therefore, the RGR was lower in the defoliation treatment.

The number of tillers of both species did not significantly change after defoliation. These results are consistent with those of previous studies in that the number of tillers was not affected by defoliation (Hume, 1991; Slack et al., 2000). However, the tiller number of *L. chinensis* did increase during the 30 days in both the defoliation and control treatments, which may result from nutrient storage in rhizomes of *L. chinensis,* promoting the emergence of new tillers (Zhang et al., 2007).

Rebalancing Processes in Biomass, WSCs, and Proteins

In this study, we observed that both species regained the necessary biomass-based rebalance approximately 15 days after defoliation. As defoliation significantly decreased the aboveground biomass and total biomass, the biomass of both plant species in the defoliation treatment did not reach that of the control treatment at 15 days after defoliation; however, the shoot:root ratio in terms of biomass did reach the level of the control. This indicated that plants function as a balanced system between above- and below-ground parts. Previous studies have shown biomass allocation between roots and shoots in response to changes in the balance between carbon and nitrogen (Reynolds and Thornley, 1982). Defoliation removes leaf tissue, which has a high nitrogen concentration and can assimilate carbon. To compensate for this loss, both species can rapidly translocate WSC reserves to support regrowth. Our extended analysis indicated that WSC concentrations in the rhizomes, roots, and stubble of *L. chinensis* decreased by 49, 44, and 41%, respectively, within the first 3 days after defoliation. For *S. grandis*, 53 and 22% of the WSCs reserved in the stubble and roots were translocated. These results highlight the role of rhizomes and stubble as the major reserve organs in perennial grasses for supplying nutrients to produce new leaves after defoliation (Hume, 1991; Donaghy and Fulkerson, 1997; Hikosaka et al., 2005).

Our results demonstrated that both species reestablished the balance in terms of WSCs and proteins between above- and below-ground organs at day 10 after defoliation, while the biomass-based rebalance was achieved at day 15 after defoliation. This suggests that the nutrient-based balances may be reached

earlier than the biomass-based balance. This may be because WSCs and proteins are easier to translocate to the organs that can maximize the regrowth of plants after defoliation. Our regression analysis results show that the shoot:root ratios in terms of biomass were significantly mediated by WSC and protein concentrations and by the amount of WSCs and proteins per plant (**Figure 7**).

CONCLUSION

This study provides us with a clear picture of the dynamic changes in regrowth and in the reallocation of resources of two grass species after defoliation in Inner Mongolia's grasslands. For both species, defoliation impaired plant height and biomass production but increased the RGR. Both species achieved the rebalance of WSCs and proteins earlier than that of biomass, indicating that a balanced system in nutrient allocation between above- and below-ground parts is essential and important for the rebalance of biomass allocation. We deduced that the biomass-based shoot:root ratio was regulated by the concentrations of WSCs and proteins or the amounts of these nutrients per plant. As dominant species in Inner Mongolian grasslands, these two grass species cannot completely recover in terms of biomass production at day 30 after defoliation; hence, the time interval between rotational grazing activities in this area should be longer than 1 month.

AUTHOR CONTRIBUTIONS

YL and QP designed the research. YL, DT, and RC performed the research and analyzed the data. YL wrote the draft paper, which was revised by XY, XZ, and ZS.

FUNDING

This study was supported by the National Key R&D Program of China (Grant No. 2016YFC0500804), the International Science and Technology Cooperation Program of China (Grant No. 2015DFR31130), and the National Natural Science Foundation of China (Grant Nos. 31200350, 41471029, and 41271033).

ACKNOWLEDGMENTS

We thank the staff at the Inner Mongolia Grassland Ecosystem Research Station for their help with field work and laboratory analyses and the reviewers for their constructive comments.

REFERENCES

Agren, G. I., and Ingestad, T. (1987). Root:shoot ratio as a balance between nitrogen productivity and photosynthesis. *Plant Cell Environ.* 10, 579–586. doi: 10.1016/j.plaphy.2011.05.003

Augustine, D. J., Dijkstra, F. A., Hamilton, E. W. I. I. I., and Morgan, J. A. (2011). Rhizosphere interactions, carbon allocation, and nitrogen acquisition of two perennial North American grasses in response to defoliation and elevated atmospheric CO2. *Oecologia* 165, 755–770. doi: 10.1007/s00442-010-1845-4

Briske, D. D., and Derner, J. D. (1998). "Clonal biology of caespitose grasses," in *Population Biology of Grasses*, ed. G. P. Cheplick (Combridge: Combridge University Press), 106–135. doi: 10.1017/CBO9780511525445.006

Chen, X. S., Xie, Y. H., and Deng, Z. M. (2011). A change from phalanx to guerrilla growth form is an effective strategy to acclimate to sedimentation in a wetland sedge species Carexbrevicuspis (Cyperaceae). *Flora* 206, 347–350. doi: 10.1016/j.flora.2010.07.006

Cheplick, G. P. (1997). Responses to severe competitive stress in a clonal plant: differences between genotypes. *Oikos* 79, 581–591. doi: 10.2307/3546902

Chu, C. C., Coleman, J. S., and Mooney, H. A. (1992). Controls of biomass partitioning between roots and shoots-atmospheric CO2 enrichment and the acquisition and allocation of carbon and nitrogen in wild radish. *Oecologia* 89, 580–587. doi: 10.1007/BF00317167

Detling, J., and Painter, E. (1983). Defoliation responses of western wheat grass populations with diverse histories of prairie dog grazing. *Oecologia* 57, 65–71. doi: 10.1007/BF00379563

Detling, J. K., Dyer, M. I., and Winn, D. T. (1979). Net photosynthesis root respiration and regrowth of *Bouteloua gracilis* following simulated grazing. *Oecologia* 41, 127–134. doi: 10.1007/BF00344997

Donaghy, D. J., and Fulkerson, W. J. (1997). The importance of water-soluble carbohydrate reserves on regrowth and root growth of *Lolium perenne* (L.). *Grass Forage Sci.* 52, 401–407. doi: 10.1111/j.1365-2494.1997.tb02372.x

Donaghy, D. J., and Fulkerson, W. J. (1998). Priority for allocation of water-soluble carbohydrate reserves during regrowth of *Lolium perenne*. *Grass Forage Sci.* 53, 211–218. doi: 10.1046/j.1365-2494.1998.00129.x

Donaghy, D. J., and Fulkerson, W. J. (2002). The impact of defoliation frequency and nitrogen fertilizer application in spring on summer survival of perennial ryegrass under grazing in subtropical Australia. *Grass Forage Sci.* 57, 351–359. doi: 10.1046/j.1365-2494.2002.00335.x

Fulkerson, W. J., and Donaghy, D. J. (2001). Plant-soluble carbohydrate reserves and senescence-key criteria for developing an effective grazing management system for ryegrass-based pastures: a review. *Aust. J. Exp. Agric.* 41, 261–275. doi: 10.1071/EA00062

Fulkerson, W. J., and Slack, K. (2003). Effect of defoliation height and redefoliation interval on regrowth and survival of perennial ryegrass (*Lolium perenne*) in subtropical dairy pastures. *Aust. J. Exp. Agric.* 43, 121–125. doi: 10.1071/EA01174

Hikosaka, K., Takashima, T., Kabeya, D., Hirose, T., and Kamata, N. (2005). Biomass allocation and leaf chemical defence in defoliated seedlings of *Quercus serrata* with respect to carbon-nitrogen balance. *Ann. Bot.* 95, 1025–1032. doi: 10.1093/aob/mci111

Hume, D. E. (1991). Effect of cutting on production and tillering in prairie grass (*Bromus-willdenowii* kunth) compared with 2 ryegrass (Lolium) species. 1. vegetative plants. *Ann. Bot.* 67, 533–541. doi: 10.1093/oxfordjournals.aob.a088195

Jones, G. B., Alpuerto, J. B., Tracy, B. F., and Fukao, T. (2017). Physiological effect of cutting height and high temperature on regrowth vigor in orchard grass. *Front. Plant Sci.* 8:805. doi: 10.3389/fpls.2017.00805

Lee, J. M., Donaghy, D. J., Sathish, P., and Roche, J. R. (2009). Interaction between water-soluble carbohydrate reserves and defoliation severity on the regrowth of perennial ryegrass (*Lolium perenne* L.)-dominant swards. *Grass Forage Sci.* 64, 266–275. doi: 10.1111/j.1365-2494.2009.00692.x

Li, H. S., Sun, Q., Zhao, S. J., and Zhang, W. H. (2000). *Physiological and Biochemical Experimental Principles and Techniques*. Beijing: Higher Education Press, 195–197.

Liu, Y. S., Pan, Q. M., Zheng, S. X., Bai, Y. F., and Han, X. G. (2012). Intra-seasonal precipitation amount and pattern differentially affect primary production of two dominant species of Inner Mongolia grassland. *Acta Oecol.* 44, 2–10. doi: 10.1016/j.actao.2012.01.005

Macduff, J. H., and Jackson, S. B. (1992). Influx and efflux of nitrate and ammonium in Italian ryegrass and white clover roots-comparisons between effects of darkness and defoliation. *J. Exp. Bot.* 43, 525–535. doi: 10.1093/jxb/43.4.525

McNaughton, S. J. (1983). Compensatory plant growth as a response to herbivory. *Oikos* 40, 329–336. doi: 10.2307/3544305

Menke, J. W., and Trlica, M. J. (1981). Carbohydrate reserve, phenology, and growth cycles of nine Colorado range species. *J. Range Manage.* 34, 269–277. doi: 10.2307/3897849

Meyer, G. (1998). Mechanisms promoting recovery from defoliation in goldenrod (*Solidago altissima*). *Can. J. Bot.* 76, 450–459. doi: 10.1139/b98-004

Morvan-Bertrand, A., Parvis, N., Boucaud, J., and Prud'Homme, M. (1999). Partitioning of reserve and newly assimilated carbon in the roots and leaf tissues of *Lolium perenne* during regrowth after defoliation: assessment by 13C steady-state labeling and carbohydrate analysis. *Plant Cell Environ.* 22, 1097–1108. doi: 10.1046/j.1365-3040.1999.00485.x

Muthoni, F. K., Groen, T. A., Skidmore, A. K., and van Oel, P. (2014). Ungulate herbivory overrides rainfall impacts on herbaceous regrowth and residual biomass in a key resource area. *J. Arid Environ.* 100, 9–17. doi: 10.1016/j.jaridenv.2013.09.007

Ourry, A., Kim, T. H., and Boucaud, J. (1994). Nitrogen reserve mobilization during regrowth of *Medicago sativa* L. (Relationships between availability and regrowth yield). *Plant Physiol.* 105, 831–837. doi: 10.1104/pp.105.3.831

Reynolds, J. F., and Thornley, J. H. M. (1982). A shoot – root partitioning model. *Ann. Bot.* 49, 585–597. doi: 10.1093/oxfordjournals.aob.a086286

Singh, D. K., and Sale, P. W. G. (1997). Defoliation frequency and the response by white clover to increasing phosphorus supply. 2. Non-structural carbohydrate concentrations in plant parts. *Aust. J. Agric. Res.* 48, 119–124. doi: 10.1071/A96052

Slack, K., Fulkerson, W. J., and Scott, J. M. (2000). Regrowth of prairie grass (*Bromus willdenowii* Kunth) and perennial ryegrass (*Lolium perenne* L.) in response to temperature and defoliation. *Aust. J. Agr. Res.* 51, 555–561. doi: 10.1071/AR99101

Staswick, P. E. (1994). Storage proteins of vegetative plant-tissue. *Annu. Rev.* 45, 303–322. doi: 10.1146/annurev.pp.45.060194.001511

Steen, E., and Larsson, K. (1986). Carbohydrates in roots and rhizomes of perennial grasses. *New Phytol.* 104, 339–346. doi: 10.1111/j.1469-8137.1986.tb02901.x

Thornton, B., Millard, P., Duff, E. I., and Buckland, S. T. (1993). The relative contribution of remobilization and root uptake in supplying nitrogen after defoliation for regrowth of laminae in four grass species. *New Phytol.* 124, 689–694. doi: 10.1111/j.1469-8137.1993.tb03859.x

Volenec, J. J., Ourry, A., and Joern, B. C. (1996). A role for nitrogen reserves in forage regrowth and stress tolerance. *Physiol. Plant.* 97, 185–193. doi: 10.1111/j.1399-3054.1996.tb00496.x

Wang, Z. (2007). Temporal variation of water-soluble WSC in the rhizome clonal grass *Leymus chinensis* in response to defoliation. *J. Plant Ecol.* 31, 673–679. doi: 10.17521/cjpe.2007.0087

Zhang, Z., Wang, S. P., Jiang, G. M., Patton, B., and Nyren, P. (2007). Responses of *Artemisia frigida* Willd. (Compositae) and *Leymus chinensis* (Trin.) Tzvel. (Poaceae) to sheep saliva. *J. Arid Environ.* 70, 111–119. doi: 10.1016/j.jaridenv.2006.12.002

Zhao, W., Chen, S. P., and Lin, G. H. (2008). Compensatory growth responses to clipping defoliation in *Leymus chinensis* (Poaceae) under nutrient addition and water deficiency conditions. *Plant Ecol.* 196, 85–99. doi: 10.1007/s11258-007-9336-3

Conflict of Interest Statement: The authors declare that the research was conducted in the absence of any commercial or financial relationships that could be construed as a potential conflict of interest.

frontiers in Plant Science

REVIEW
published: 15 January 2019
doi: 10.3389/fpls.2018.01965

Bridging Drought Experiment and Modeling: Representing the Differential Sensitivities of Leaf Gas Exchange to Drought

Shuang-Xi Zhou[1,2], I. Colin Prentice[1,3] and Belinda E. Medlyn[1,4]*

[1] Department of Biological Sciences, Macquarie University, Sydney, NSW, Australia, [2] The New Zealand Institute for Plant and Food Research Ltd., Hawke's Bay, New Zealand, [3] AXA Chair of Biosphere and Climate Impacts, Grand Challenges in Ecosystems and the Environment and Grantham Institute – Climate Change and the Environment, Department of Life Sciences, Imperial College London, Ascot, United Kingdom, [4] Hawkesbury Institute for the Environment, Western Sydney University, Penrith, NSW, Australia

Global climate change is expected to increase drought duration and intensity in certain regions while increasing rainfall in others. The quantitative consequences of increased drought for ecosystems are not easy to predict. Process-based models must be informed by experiments to determine the resilience of plants and ecosystems from different climates. Here, we demonstrate what and how experimentally derived quantitative information can improve the representation of stomatal and non-stomatal photosynthetic responses to drought in large-scale vegetation models. In particular, we review literature on the answers to four key questions: (1) Which photosynthetic processes are affected under short-term drought? (2) How do the stomatal and non-stomatal responses to short-term drought vary among species originating from different hydro-climates? (3) Do plants acclimate to prolonged water stress, and do mesic and xeric species differ in their degree of acclimation? (4) Does inclusion of experimentally based plant functional type specific stomatal and non-stomatal response functions to drought help Land Surface Models to reproduce key features of ecosystem responses to drought? We highlighted the need for evaluating model representations of the fundamental eco-physiological processes under drought. Taking differential drought sensitivity of different vegetation into account is necessary for Land Surface Models to accurately model drought responses, or the drought impacts on vegetation in drier environments may be over-estimated.

Keywords: photosynthesis, stomatal and non-stomatal limitation, mesophyll conductance, V_{cmax}, J_{max}, drought acclimation, flux measurement, land surface model

OPEN ACCESS

Edited by:
Zhiyou Yuan,
Northwest A&F University, China

Reviewed by:
Fulai Liu,
University of Copenhagen, Denmark
Mark Andrew Adams,
Swinburne University of Technology, Australia

****Correspondence:***
Shuang-Xi Zhou
shuangxi.zhou@plantandfood.co.nz

Specialty section:
This article was submitted to Plant Abiotic Stress, a section of the journal Frontiers in Plant Science

Received: *22 June 2018*
Accepted: *18 December 2018*
Published: *15 January 2019*

Citation:
Zhou S-X, Prentice IC and Medlyn BE (2019) Bridging Drought Experiment and Modeling: Representing the Differential Sensitivities of Leaf Gas Exchange to Drought. Front. Plant Sci. 9:1965. doi: 10.3389/fpls.2018.01965

INTRODUCTION

Soil water deficit is the main environmental driver that limits aboveground net primary production in land vegetation (Webb et al., 1983; Zeppel et al., 2014), and induces vegetation mortality on all six vegetated continents and for most biomes across the globe (Potts, 2003; Allen et al., 2010; Phillips et al., 2010; Anderegg et al., 2012; Choat et al., 2012; Williams et al., 2013). By

affecting physiological (e.g., leaf gas exchange, canopy conductance), structural (e.g., leaf area, root length, mass distribution) and biogeographic (e.g., forest composition and species distribution) processes at the plant and community levels, extreme drought is expected to cause regional losses of biodiversity and biomass (Phillips et al., 2009) with impacts on ecosystem function and the terrestrial carbon sink (Pitman, 2003; Bonan, 2008; Phillips et al., 2010).

Modeling the quantitative consequences of increased drought for forest ecosystems is challenging (McDowell et al., 2011), and requires unraveling the interaction between drought and plant gas exchange at different time scales, and in different ecosystems with different degrees of adaptation to drought. Reliable model prediction of drought impacts on forest ecosystems must be based on the analysis of observations to identify key traits that promote plant resistance to drought, and process-based modeling to include realistic representation of the ecophysiological mechanisms relating plant gas exchange to water availability and transport. In addition, we need to understand how drought impacts vary among ecosystems. The drought impacts on different ecosystems depend on the drought duration, magnitude, and spatial extent, vegetation type-specific responses to drought at different time scales, and mechanisms affecting the drought resistance and resilience of different vegetation types (Pasho et al., 2011; Vicente-Serrano et al., 2013). Different terrestrial ecosystems are reported to differ in their sensitivity to drought (Knapp and Smith, 2001; Zeppel et al., 2014). For example, conifer forests were found to withstand drought impacts better than broadleaf forests in Canada (Kljun et al., 2006) and in Europe during the extremely dry year of 2003 (Granier et al., 2007). However, the present generation of ecosystem models embody a simplistic representation of drought responses of these ecophysiological properties and processes across forest ecosystems, which makes it difficult to predict the likely extent of drought-induced changes in the function of forest ecosystems.

Current state-of-the-art Earth System models (ESMs), which include dynamic global vegetation models (DGVMs) (Prentice and Cowling, 2013) coupled to physical representations of land-atmosphere exchanges of energy, water vapor and CO_2 (land surface models, LSMs), make widely divergent predictions of drought effects (Prentice et al., 2015). This divergence is partly due to the lack of an established, empirically supported method for the representation of drought effects on plants (Egea et al., 2011). Process-based modeling of the drought impacts on plants and ecosystems must be informed by experiments, which can help us to understand underlying processes. Model evaluation and improvement must include the use of experimental observations, theory to explain the observations, quantitative parameterizations to describe the theory, and model simulations to test the impacts of environmental variables (Bonan et al., 2014; Prentice et al., 2015; see a model-data integration process by Walker et al., 2014). Although thousands of experiments have been done to study the drought responses of plants, relatively few provide information in the quantitative manner required to develop model representations. In particular, work is needed (1) to directly determine how different aspects of plant function respond to experimentally imposed drought and (2) to analyze experimental results in a theoretical framework, suitable for inclusion in ecosystem models.

In particular, current ecosystem models differ greatly in the ways in which they represent drought effects on photosynthesis (Medlyn et al., 2016). Many models simulate the drought effect on photosynthesis in a rough way simply by reducing the slope of the relationship between stomatal conductance (g_s) and net carbon assimilation rate (A_n) (Egea et al., 2011), in a similar way for all plant function types (PFTs). Another specific issue is that the apparent maximum carboxylation rate (V_{cmax}) has usually been attributed to a PFT as a single value, or as a single-valued function of environmental drivers (Haxeltine and Prentice, 1996). It is not known whether the method is adequate to capture the drought response, but there is a strong case to expect that it is not, and it does not account for either differences among species and/or ecosystems of different climatic origins, or for mechanisms of plant acclimation to drought. Emerging modeling evidence points to the importance of representing both stomatal and non-stomatal responses to drought in models (e.g., Egea et al., 2011; De Kauwe et al., 2015b). However, the modeling approach in current LSMs lacks a functionally realistic representation of drought responses of g_s and V_{cmax}, unless the experimentally based and PFT-specific representations of the drought responses of g_s and V_{cmax} have been implemented.

Recently, there are increasingly more model-experiment synthesis studies to improve the representation of photosynthetic responses to environmental drivers in large-scale vegetation models (e.g., Medlyn et al., 2011; Prentice et al., 2014; De Kauwe et al., 2015a,b). In this review, we highlight recent studies which analyze the experimental data of both the short- and long-term drought responses of leaf gas exchange across species of contrasting climatic origins, and which aim at improving the representation of experimentally based and PFT based stomatal and non-stomatal response functions to soil water stress in LSMs and DGVMs.

WHICH PHOTOSYNTHETIC PROCESSES ARE AFFECTED UNDER SHORT-TERM DROUGHT?

Leaf A_n is mainly driven by light, temperature and intercellular CO_2, as represented in the Farquhar-von Caemmerer-Berry leaf-level photosynthesis model for C_3 plants (Farquhar et al., 1980). Intercellular CO_2, in turn, is co-determined by g_s and A_n. Reduction of g_s is one of the foremost, short-term, leaf-scale physiological responses both to atmospheric vapor pressure deficit (the driving force of transpiration, E) and soil water deficit. CO_2 and water vapor exchange are strongly coupled through stomata, because g_s regulates both the CO_2 uptake for photosynthesis, and the loss of water vapor by transpiration (Cowan, 1977) (**Figure 1**). A variant of the Farquhar-von Caemmerer-Berry model was coupled to the empirical Ball–Berry stomatal conductance model (Ball et al., 1987; Collatz et al., 1991) in the land component of climate models already in the mid-1990s, in order to estimate gross primary production on a more mechanistic basis than before

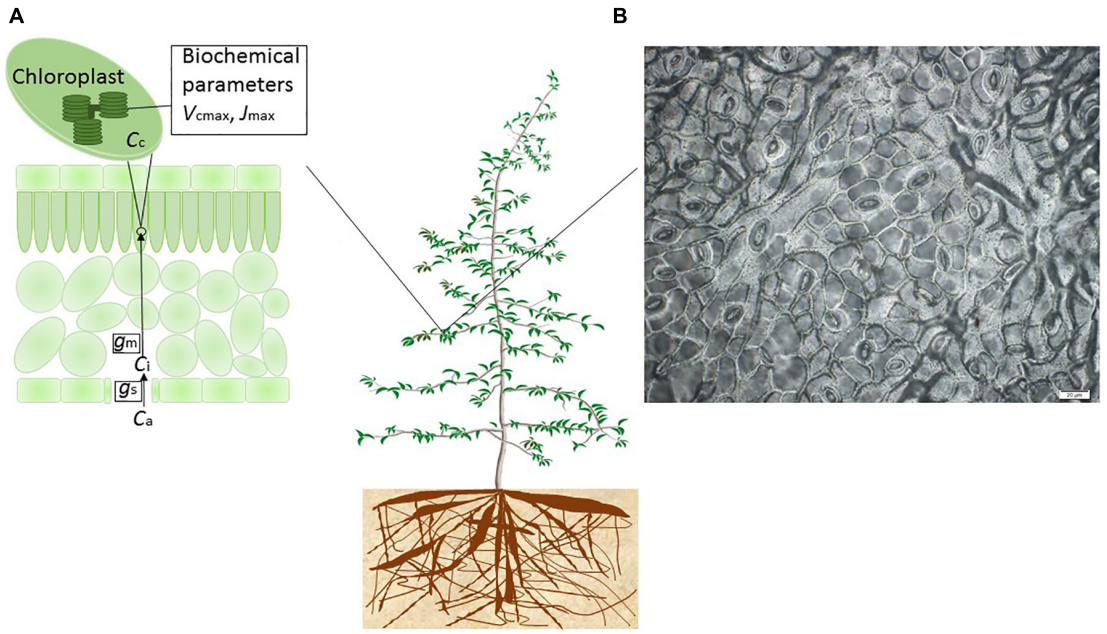

FIGURE 1 | Conceptual diagram of the model-experiment synthesis framework to quantify and model the differential sensitivities of leaf gas exchange to drought. **(A)** During photosynthesis, the CO_2 flux from the air (ambient CO_2 concentration, C_a) to intercellular air spaces (intercellular CO_2 concentration, C_i) through stomata is limited by stomatal conductance (g_s). The CO_2 flux from the intercellular space to the chloroplast site (CO_2 concentration at the chloroplast, C_c) is limited by mesophyll conductance (g_m). The non-stomatal limitation on photosynthesis was attributed to drought effects on g_m, the actual maximum rate of CO_2 consumption by RuBP carboxylation by Rubisco (V_{cmax}) and the actual maximum electron transport rate (J_{max}). **(B)** An impression of the leaf epidermis of *E. camaldulensis* subsp. *camaldulensis* was produced using clear nail polish, which then was mounted for applications of microphotography of the leaf surface. The microscope (Olympus BX53, Olympus America Inc.) was interfaced with a digital camera at ×40 magnification. Photo: Shuang-Xi Zhou.

(Bonan, 1995; Cox et al., 1998). This or other similar formulations are now used widely in state-of-the-art ESMs. Research efforts have also been devoted specifically to the implementation of different modeling approaches for stomatal conductance (e.g., Bonan et al., 2014; De Kauwe et al., 2015a).

Although photosynthesis accounts for the largest CO_2 flux from the atmosphere into ecosystems and is the driving process for terrestrial ecosystem function (Bernacchi et al., 2013), the fundamental component processes of plant gas exchange are still incompletely represented in global models, notably in the area of drought responses, and photosynthetic and morphological acclimation generally (including acclimation to drought) (Prentice and Cowling, 2013). In ecosystem models, drought stress may act either by increasing the marginal water use efficiency, which depends on the ratio of CO_2 concentration inside and outside the leaf (C_i/C_a ratio); by reducing V_{cmax} and/or the maximum rate of electron transport – J_{max} (apparent values implicitly assuming infinite g_m); or both (**Figure 1**). Accurate model prediction of drought impacts on vegetation and global carbon and water cycles requires realistic representation of photosynthetic processes at the leaf level (Baldocchi, 1997; Egea et al., 2011; Verhoef and Egea, 2014).

Stomatal behavior is expected to be related to the marginal carbon cost of water loss ($\lambda = \partial A/\partial E$) (Cowan, 1977; Cowan and Farquhar, 1977; Berninger and Hari, 1993). Cowan and Farquhar (1977) postulated that for any given amount of total water available for transpiration in a period of time, the leaf can achieve the maximum CO_2 uptake if it adjusts leaf scale conductance in the way that the derivative of A_n with respect to the rate of transpiration per unit area of leaf ($\partial A/\partial E$) is maintained constant throughout the period (Cowan, 1977). This criterion amounts to saying that a plant with a given water availability regulates stomata to ensure maximal carbon gain per unit water loss in a finite period of time. Therefore, the constancy of $\partial A/\partial E$ is viewed as an optimality hypothesis (Cowan, 1977; Cowan and Farquhar, 1977). It has also been suggested that the rate at which water stress is imposed might influence the response of $\partial A/\partial E$ to water stress (Hall and Schulze, 1980). The theoretical analysis of Mäkelä et al. (1996) further predicted that the marginal water cost of carbon ($1/\lambda$) should decline exponentially with decreased soil moisture, and that the rate of decline should increase according to the probability of rain.

Medlyn et al. (2011) and Prentice et al. (2014) have proposed re-interpretations of widely used empirical models of stomatal conductance, in terms of optimization theory. Medlyn et al. (2011) derived a simple expression that is a good approximate solution of the Cowan-Farquhar optimization problem, and demonstrated its predictive power for a range of species. The single parameter of the Medlyn et al. (2011) optimal model for stomatal behavior – the stomatal sensitivity parameter (g_1) – is inversely proportional to λ, and thus can be used directly to test the predictions by Mäkelä et al. (1996) (Héroult et al., 2013; see a conceptual modeling framework in Zhou et al., 2013). Prentice et al. (2014) introduced a different derivation

of the same expression, with further empirical support, based on the alternative hypothesis that plants minimize the sum of the unit costs (carbon expended per unit assimilation) of CO_2 uptake and water loss. Different expressions again have been presented by Sperry et al. (2016), Wolf et al. (2016), and Dewar et al. (2018) based on the optimization criterion that plants maximize carbon gain by minimizing carbon costs associated with hydraulic failure.

Besides the stomatal resistance on CO_2 diffusion from the atmosphere to the intercellular air spaces of the leaves, there is now known to be a considerable mesophyll resistance to CO_2 diffusion from the substomatal cavity to the carboxylation sites in the chloroplasts (**Figure 1**). In other words, there is a mesophyll conductance (g_m) which is not infinite and can significantly limit the CO_2 availability and thus the assimilation rate. g_m has been shown to play an important role in determining photosynthetic responses to environmental drivers including temperature and CO_2 (e.g., Niinemets et al., 2011; Evans and von Caemmerer, 2013). Photosynthesis is reported to be limited by decreased g_m – together with g_s – in the initial stages of drought (Bota et al., 2004; Flexas et al., 2004, 2007, 2008, 2012; Grassi and Magnani, 2005; Egea et al., 2011; Zhou et al., 2014). There has been controversy on the magnitude of the g_m effect on photosynthesis under mild to moderate drought conditions, largely due to the methodological issues on estimation of the intercellular or the chloroplastic CO_2 concentration (C_c; **Figure 1**) (Pinheiro and Chaves, 2011). In addition, there is controversy on whether g_m should be included in ecosystem models, and how to include g_m in ecosystem models (Rogers et al., 2017). Some recent studies suggested that the decrease of g_m with increasing soil water deficit could contribute as much as the decrease of g_s to the reduction of A_n under drought (e.g., Flexas et al., 2012; Zhou et al., 2014). However, far less is known on the environmental regulation and interspecific differences in g_m compared to g_s.

As plant water status worsens, there is a further possibility that drought impedes enzyme activity and photosynthetic capacity. In other words, there can be directly drought-induced biochemical limitations on the activity of Rubisco (ribulose-1,5-bisphosphate carboxylase/oxygenase) and the regeneration capacity of RuBP (ribulose-1,5-bisphosphate) (Kanechi et al., 1996; Tezara et al., 1999; Castrillo et al., 2001; Parry et al., 2002; Tezara et al., 2002; Thimmanaik et al., 2002; Grassi and Magnani, 2005). Drought-induced decrease of Rubisco activity is associated with down-regulation of the activation state of the enzyme (e.g., by decarbamylation and/or binding of inhibitory sugar phosphates). In the Farquhar-von Caemmerer-Berry model (Farquhar et al., 1980), the V_{cmax} and J_{max} (apparent values implicitly assuming infinite g_m) are the two key metabolic parameters limiting photosynthetic capacity (**Figure 1**). Varying among leaves within a plant, between plants, among species and seasonally (e.g., Wilson et al., 2000; Xu and Baldocchi, 2003), V_{cmax} plays an important role in linking the carbon fluxes between the leaves and the atmosphere and thus in governing plant productivity and resource use efficiency (Long et al., 2006) and determining large-scale fluxes of CO_2 between vegetation and the atmosphere (Bonan et al., 2011, 2012). The trigger for decreased Rubisco activity is reported to depend on the severity and/or the duration of the stress imposed (Flexas et al., 2006). Ecosystem models commonly assign fixed values of V_{cmax} per PFT, but there is no consistency in the values assigned among different models and, in any case, this approach neglects most of the field-observed variation in V_{cmax} (Kattge et al., 2009; Bonan et al., 2011, 2012; Groenendijk et al., 2011). Recent studies have suggested that it is necessary to represent the effects of climate change on V_{cmax} in models to predict its impact on net primary production (e.g., Bernacchi et al., 2013; Galmés et al., 2013).

It is generally thought that with the increase of drought intensity and/or duration, biochemical limitations on photosynthesis should eventually come to dominate over diffusional (stomatal and mesophyll) limitations (see a review by Lawlor and Tezara, 2009). However, there has been a good deal of debate about the relative importance of photosynthetic limitations of diffusive and biochemical origin, in the context of drought (e.g., Grassi and Magnani, 2005). Reasons for controversy include the use of different measures of drought, the imposition of drought at different rates in experiments, different applied intensities and duration of drought, different experimental designs and growth conditions, and different species with different physiological and structural sensitivities and adaptations to drought.

INTERSPECIFIC VARIATION IN THE SHORT-TERM STOMATAL AND NON-STOMATAL DROUGHT RESPONSES AMONG SPECIES FROM DIFFERENT HYDRO-CLIMATES

The drought responses of different species are likely to depend not only on drought duration and intensity, but also on the species-specific degree of adaptation to the soil water conditions in their native habitat. It is well documented that plants from dry climates can operate better than plants from wet climates down to severe soil water deficits (e.g., Sperry, 2000). However, studies have highlighted that mesic and xeric forest ecosystems are equally vulnerable to drought-induced mortality, based on their functional hydraulic limits (Choat et al., 2012), implying that plants from drier or wetter environments possess some degree of adaptation to the soil conditions encountered in their native habitat. Indeed, xeric species were reported to keep stomata open and maintain photosynthesis down to lower water potential values than mesic species (e.g., Zhou et al., 2014). It is reasonable to assume that this feature of plants from dry climates is adaptive, important for their function under field conditions and shaping their potential geographic ranges (Engelbrecht et al., 2007). Differential drought adaptations among species are presumed to underpin their different levels of sensitivity, resistance, and resilience to soil water deficits (Chaves et al., 2003; McDowell et al., 2008), and differential effectiveness of physiological mechanisms of drought tolerance in the face of decreasing water potential (Engelbrecht et al., 2007). The wide variation of drought adaptations among species is likely to be fundamentally important in determining their different degrees

of vulnerability to biomass loss and mortality (Ciais et al., 2005; Adams et al., 2009; Allen et al., 2010).

Under a drier and hotter climate, the intra- and inter-specific variation in plant traits may provide an important contribution to plants' resistance to drought, with responses characteristic of plants from dry environments promoting persistence and adaptation, reducing risk of mortality and improving chance of survival (Yachi and Loreau, 1999; Clark et al., 2012). Understanding how these effects vary among species from contrasting climates is key to predicting the large-scale consequences of drought on different communities and ecosystems. Very few published experiments have systematically tested how the various components of plant drought response vary across species from contrasting hydro-climates. The response of the stomatal sensitivity parameter (g_1) of the Medlyn stomatal optimality model (Medlyn et al., 2011) to soil water deficit is expected *a priori* to differ among plant functional types and species of different geographical origins (Medlyn et al., 2011; Héroult et al., 2013). Meanwhile, V_{cmax} is expected to be higher in plant species from drier climates (Prentice et al., 2014), in compensation for reduced stomatal conductance. There is also significant variability in the Rubisco specificity factor among closely related C_3 higher plants, which is associated mainly with temperature and water availability (Galmés et al., 2005). Zhou et al. (2013, 2014) fitted quantitative models for species of different origin of climate and PFT membership in their differential g_s and V_{cmax} responses to soil water potential – providing functions that potentially could represent these responses in process-based models.

The decline rates of stomatal and hydraulic function with decreasing water potential levels were reported to be coordinated across species of different climate of origin (Choat et al., 2012; Klein, 2014; Manzoni, 2014; Martin-StPaul et al., 2017; Li et al., 2018; but see Lamy et al., 2014). In this review, we calculated the pre-dawn leaf water potential at which 50% loss of full functions occurred (P_{50}, -MPa) for the photosynthetic parameters reported in Zhou et al. (2014) – 50% loss of net carbon assimilation rate (P_{50An}, -MPa), 50% loss of stomatal conductance (P_{50gs}, -MPa), 50% loss of stomatal sensitivity parameter g_1 (P_{50g1}, -MPa) and 50% loss of RuBP carboxylation by Rubisco ($P_{50Vcmax}$, -MPa) (**Figure 2**). We found P_{50} was more negative for A_n than for g_s, indicating that the reduction in stomatal conductance preceded the reduction in photosynthesis (**Figures 2A,B**). When comparing how stomatal sensitivity parameter g_1 and V_{cmax} contributed to the overall reduction in g_s, we found P_{50g1} and $P_{50Vcmax}$ were correlated, while the $P_{50Vcmax}$ was consistently more negative than P_{50g1} – indicating the reduction in g_1 preceded the reduction in V_{cmax} (**Figures 2E,F**). Moreover,

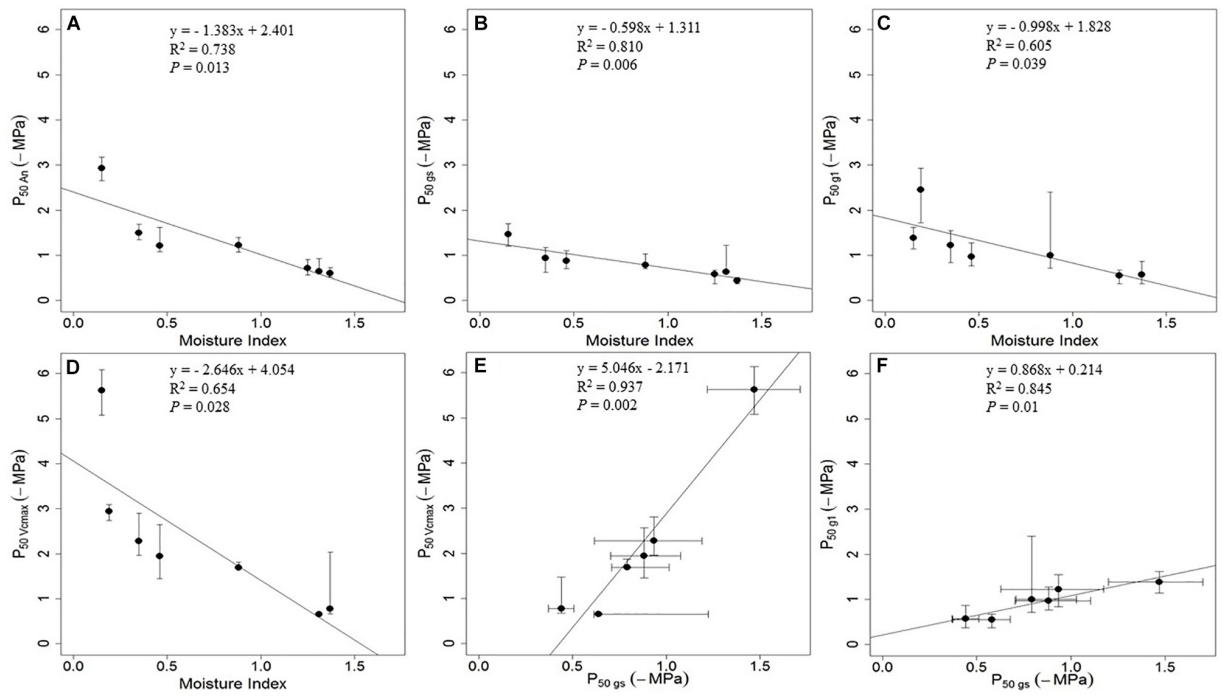

FIGURE 2 | Correlation between the pre-dawn leaf water potential at 50% loss of photosynthetic functions and moisture index for six woody species from contrasting hydroclimates. **(A)** The pre-dawn leaf water potential at 50% loss of net carbon assimilation rate (P_{50An}, -MPa) and moisture index. **(B)** The pre-dawn leaf water potential at 50% loss of stomatal conductance (P_{50gs}, -MPa) and moisture index. **(C)** The pre-dawn leaf water potential at 50% loss of stomatal sensitivity parameter g_1 (P_{50g1}, -MPa) and moisture index. **(D)** The pre-dawn leaf water potential at 50% loss of RuBP carboxylation by Rubisco ($P_{50Vcmax}$, -MPa) and moisture index. **(E)** Correlation between $P_{50Vcmax}$ and P_{50gs}. **(F)** Correlation between P_{50g1} and P_{50gs}. Moisture index is the ratio between mean annual precipitation and mean annual potential evapotranspiration, which can range from zero in the driest regions to higher values in wetter regions (Zhou et al., 2014). Values of P_{50An}, P_{50gs}, P_{50g1} and $P_{50Vcmax}$ (solid circle) – and the bootstrap 2.5% and bootstrap 95% values (bars) to indicate the error in each estimate – were fitted by employing data from Zhou et al. (2014) using the 'fitplc' package in R (Duursma and Choat, 2017).

compared with species from wetter climates, species from drier climates tends to show larger difference between $P_{50Vcmax}$ and P_{50gs} (**Figure 2**). These differences are presumed to have adaptive significance for the survival of plants in dry climates.

INTERSPECIFIC VARIATION IN THE DEGREE OF PLANT PHOTOSYNTHETIC ACCLIMATION TO PROLONGED WATER STRESS

Plants subjected to short-term experimental drought are well documented to experience a decline in photosynthetic capacity. However, plants under prolonged drought may be able to acclimate to drought to some extent, for example through morphological adjustments such as changes in mass allocation to leaves and/or roots (Choat et al., 2018), provided the drought is imposed slowly enough for such changes to take effect. In general, therefore, it is to be expected that the mechanisms underlying plant responses to water stress vary according to time scale (Maseda and Fernández, 2006; Limousin et al., 2010a,b; Martin-StPaul et al., 2012, 2013). Maseda and Fernández (2006) proposed that plants acclimate to drought at the whole-organism level through physiological, anatomical, and morphological adjustments that are adaptive over a time scale of months.

When given time to acclimate to water stress, the photosynthetic response of plants could differ from that of plants in short-term water stress (**Figure 3**). Some longer-term experiments reported higher leaf gas exchange rates for woody plants in the drought treatment (Cinnirella et al., 2002; Ogaya and Peñuelas, 2003; Llorens et al., 2004). Cano et al. (2014) reported xeric species showed significant higher g_m than mesic species under longer-term water stress. Leaves developed during the long-term drought can acclimate by increasing partitioning to total soluble proteins, allowing higher Rubisco activity per unit leaf area (Panković et al., 1999). The Rubisco content could also increase in leaves under prolonged drought, and the increase could be significantly higher in leaves of the drought-tolerant plant taxa than other taxa, conferring the drought-tolerant taxa with better acclimation and higher drought tolerance (Panković et al., 1999).

Despite its importance, the photosynthetic responses of plants to long-term water stress and its variation among species of contrasting climate of origin are poorly understood (Cano et al., 2014). Moreover, long-term studies disagree on whether or not plants can modify the functional relationships between photosynthetic traits and soil water potential to acclimate to long-term water stress (Limousin et al., 2010b; Misson et al., 2010; Martin-StPaul et al., 2012). There could be systematic differences in these functional relationships related to species' climatic origin. Zhou et al. (2016) found the xeric *Eucalyptus* species showed more effective drought acclimation – significantly lower V_{cmax} sensitivity to declined pre-dawn leaf water potential – than the riparian species under prolonged drought. Species-specific physiology may play an importance role in the comparative photosynthetic acclimation of contrasting species under prolonged water stress, leading to the varied findings among these studies (Ogaya and Peñuelas, 2003; Cano et al., 2014).

Intra- and inter- specific variation in drought tolerance and acclimation could have important implications for forest modeling in water-limited ecosystems, particularly in a long-term perspective that takes future climate change into account. Ignoring potentially important acclimation processes in the field could lead to overestimation of the long-term consequences of drought. Changes in forest composition related to drought tolerance and acclimation are already beginning to be observed. For example, the more drought-tolerant *Quercus pubescens* was reported to be replacing *Pinus sylvestris* at low altitudes in Switzerland, where climate change has brought about recurrent water deficits (Eilmann et al., 2006). Reliable prediction of drought effects on contrasting species and forest ecosystems under field conditions requires long-term experiments on the drought-induced limitations on photosynthetic and hydraulic properties, and their potential acclimation to prolonged drought (see a review by Choat et al., 2018). The number of such studies in the literature, however, is surprisingly small, with most published manipulative experiments focusing exclusively on short-term responses to drought.

INCORPORATING EXPERIMENT-DERIVED PFT-SPECIFIC DROUGHT RESPONSE OF g_s AND V_{cmax} TO IMPROVE MODELING ECOSYSTEM RESPONSES TO DROUGHT

Current LSMs treat plant ecophysiological properties simplistically assuming the same drought sensitivity for all vegetation (Prentice and Cowling, 2013; De Kauwe et al., 2015b), disregarding known aspects of trait correlation and trait-environment relationships (Wright et al., 2004; Maire et al., 2013; Prentice et al., 2014) and the considerable variation of drought sensitivity among plant species of different climatic origin highlighted in recent model-oriented experiments and data syntheses (Zhou et al., 2013, 2014). Insufficient attention has been paid to the evaluation of LSMs in their representations of the fundamental eco-physiological responses to drought, in part because their early history of development pre-dates the availability of many relevant measurement data sets (Prentice et al., 2015). It is critical for LSMs to realistically represent the differential drought responses of different vegetation types.

Largely due to the shortage of model-oriented experimental studies describing the separate effects of drought on stomatal and non-stomatal processes, there are large discrepancies in the ways in which current ecosystem models represent the drought effect on plant gas exchange (Powell et al., 2013; Medlyn et al., 2016). There has been a scientific debate on how to represent stomatal closure as soil moisture declines (Bonan et al., 2014). Current state-of-the-art LSMs used in coupled climate models generally treat all PFTs as experiencing similar stomatal and/or non-stomatal limitation during drought (via soil texture and

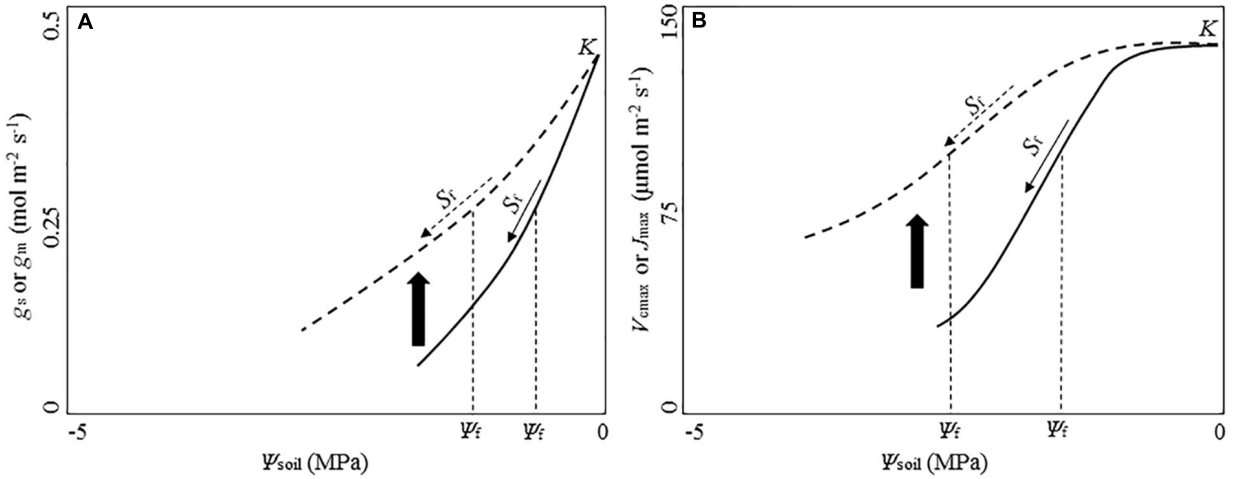

FIGURE 3 | Conceptual diagram of potential acclimation responses of diffusional and biochemical parameters to water stress. Solid lines show the strong short-term sensitivity of parameters to the decreasing soil water potential (Ψ_{soil}) before plants being given time to acclimate to water stress. Dashed lines indicate reduced sensitivity to soil water potential following a period of acclimation to water stress. Upward arrow between the solid and dashed line shows potential shift upward of the drought-response curve during acclimation. **(A)** Exponential function of stomatal conductance (g_s) and mesophyll conductance (g_m) with the decreasing Ψ_{soil} based on Zhou et al. (2013, 2014). **(B)** Logistic function of the maximum rate of CO_2 consumption by RuBP carboxylation by Rubisco (V_{cmax}) and the maximum electron transport rate (J_{max}) with the decreasing Ψ_{soil} based on Zhou et al. (2013, 2014). K is the maximum value of the parameter under moist conditions. S_f indicates the sensitivity of each parameter against the decreasing Ψ_{soil}. Ψ_f is soil water potential at 50% reduction of K.

assumed rooting depths). Many LSMs use an empirical soil moisture stress factor (β) – as a function of volumetric water content (θ) – to impose for down-regulation of stomatal response at decreasing soil moisture, which allowing an abrupt transition in β to take place within a narrow range of θ (Egea et al., 2011; Powell et al., 2013; De Kauwe et al., 2015a,b; but see Medlyn et al., 2016). Powell et al. (2013) reported unrealistic drought responses due to implementing abrupt transitions of this kind in four models [Community Land Model version 3.5 (CLM3.5), Integrated BIosphere Simulator version 2.6.4 (IBIS), Joint UK Land Environment Simulator version 2.1 (JULES), and Simple Biosphere model version 3 (SiB3)], which use different water-stress functions – loosely constrained by data – to down-regulate soil moisture effects on g_s. The sharp shutdown seems to be a common challenge in LSMs whereas the observed fluxes decline much more gradually with water stress (Medlyn et al., 2016). Zhou (2015) compared the θ effect on A_n in the Community Atmosphere Biosphere Land Exchange (CABLE) LSM, and found a rather abrupt transition in A_n from near-normal function to nearly complete shutdown within a narrow range of θ – regardless of PFT or soil type. This modeled abrupt transition is very unlikely under field conditions where the transition from full vegetation function to drought conditions should occur more gradually as a consequence of spatial heterogeneity in plant and soil properties (Liang et al., 1994; Prentice et al., 2015).

Land surface models commonly include generic responses of plant carbon uptake and water loss to soil moisture content. It seems plausible that the performance of LSMs might be improved by including empirically based plant responses to drought, expressed as a function of soil water potential (the key property affecting plant water uptake) and derived from measurements on species of different PFT membership. However, the process of estimation of required model parameters (e.g., quantifying the response functions of photosynthetic and hydraulic traits against drought) for global models is not straightforward and usually not transparent (Choat et al., 2018; Dewar et al., 2018). De Kauwe et al. (2015b) tested whether using the information pertinent to the representation of g_s and V_{cmax} responses in process-based models in Zhou et al. (2013, 2014) would improve the prediction of canopy-atmosphere fluxes during drought in the CABLE model. By estimating soil water potential from dynamically weighted soil layers, De Kauwe et al. (2015b) resolved the modeling challenge in CABLE – the steep drop-off of leaf photosynthesis with soil water content due to the rapid change in soil moisture potential (Zhou, 2015). It is found that CABLE can only accurately reproduce the drought impacts during the 2003 heat wave if the most mesic sites were attributed a high drought sensitivity and the most xeric sites were attributed a lower drought sensitivity (De Kauwe et al., 2015b). These studies demonstrated a practical and effective approach to gain information on drought responses in a form directly applicable to modeling, and highlighted that LSMs will over-estimate the drought impacts in drier climates if the different sensitivity of vegetation to drought were not taken into account (De Kauwe et al., 2015b; Zhou, 2015).

Furthermore, recent efforts to improve model simulation on vegetation dynamics also have highlighted the importance of linking plant traits – especially the correlation among hydraulic and photosynthetic traits (e.g., the water potentials at 50% loss of xylem conductivity and 50% loss of stomatal conductance, respectively) – to forest function under drought (Christoffersen et al., 2016; Xu et al., 2016; see a review by Choat et al., 2018). Christoffersen et al. (2016) represented the correlations between plant hydraulic traits and the leaf and stem economic

traits within a trait-driven model, and found substantial improvement of the model simulations of total ecosystem transpiration fluxes. Xu et al. (2016) updated the Ecosystem Demography model 2 with a novel hydraulics-driven phenology scheme, which incorporated PFT-specific functional traits and allowed alternative photosynthetic and phenological strategies to dominate depending on rainfall seasonality, and found it substantially improved the model simulation of spatiotemporal patterns of vegetation dynamics in seasonally dry tropical forests.

SIGNIFICANCE OF MODEL-EXPERIMENT SYNTHESIS: FUTURE PERSPECTIVES

Increasing research efforts are devoted to improving models through the use of new representations of specific processes based on new data syntheses or experimental findings (e.g., Bonan et al., 2011, 2012; Medlyn et al., 2011, 2016; Prentice et al., 2014; De Kauwe et al., 2015a,b; Christoffersen et al., 2016; Xu et al., 2016; Rogers et al., 2017; see a model-data integration process by Walker et al., 2014). These studies have highlighted the significance of bridging experiment-tested eco-physiological processes and land ecosystem models, through translating empirical findings into improved process representations within models and tested model simulations against carbon and water flux measurements at the ecosystem scale.

Both plant physiologists and modelers should be exposed to the significance of informing process-based models with experimentally derived quantitative information when studying the drought impacts on photosynthetic and hydraulic properties, their variation across forest ecosystems and their interaction underlying short-term and prolonged drought consequences. The model-orientated experimental work would ideally be carried out to identify different drought tolerances in a quantitative modeling context – both in respect of short-term drought responses, and acclimation processes by which plants can adapt to longer-term, lower-level drought – between species from mesic and xeric habitats.

In this review, the new analysis highlights that the drought sensitivities of photosynthesis are consistently higher for species from wetter climates (showing strong diffusional and metabolic limitations earlier during the drying-down process) than species from drier climates (showing more negative pre-dawn leaf water potential at 50% reduction of diffusional and metabolic activities) (**Figure 2**). The positive correlations among the rates of decline of the parameters as the experimental drought progressed define a spectrum of drought adaptations, from more resistant species thriving in dry environments, to more sensitive species thriving in moist environments (**Figure 2**; but see Lamy et al., 2014). These findings support the existence of a co-ordinated spectrum of increasing tolerance in plants from wetter to drier environments, and provide a complementary perspective on the finding by Choat et al. (2012) based on hydraulic traits that trees in mesic habitats – which are not normally considered to be at risk from drought – are actually just as vulnerable to drought as trees in xeric habitats. Meanwhile, these studies have casted light on the general responses of leaf gas exchange to short- and long-term soil water deficits, allowing for realistic model representations of different drought sensitivities among species and PFTs from wetter or drier environments. By providing process-based analytical models of key parameters that define these responses for contrasting species with differential drought sensitivities, these model-oriented experimental studies have offered potentially robust solutions to the problem of representing adaptive differences among PFTs into LSMs.

This review suggests the following priorities to help guide future research to improve modeling on drought compacts upon a firm theoretical and empirical basis:

(1) Plants are subject to Darwinian selection and can adjust genetically or phenotypically to environment to maximize their fitness. Optimality concepts have been proposed and tested on various aspects of plant and ecosystem functions including plant water use, stomatal behavior, photosynthetic capacity, nitrogen uptake and phenology (e.g., Prentice et al., 2014). Covariation of different plant traits is expected to be an expression of optimality principles (Wright et al., 2004; Prentice et al., 2014; Reich, 2014) and should simplify the parameterizations of fundamental eco-physiological responses to environmental drivers, including drought. An explicit theoretical framework is necessary to incorporate the variation, interrelationships and environmental dependencies of plant traits into models. Such quantitative information explaining fundamental plant-level processes and quantifying variability in key plant traits under drought, if gathered on a wider range of species, could allow testing for the existence of a spectrum of drought-response traits, and ultimately a deeper understanding of drought-response strategies (Wright et al., 2004; Prentice et al., 2014; Reich, 2014) and a more comprehensive approach to both trait data analysis and vegetation modeling (Prentice et al., 2014).

(2) Model predictions of future drought impacts on ecosystems, and feedbacks to the atmosphere, should aim to represent drought responses of major plant physiological exchanges (CO_2 and water vapor fluxes between leaf and the atmosphere) realistically, with simple and observationally tested process formulations. They must account for the observed differences between the responses of different PFTs to drought. The realistic model representation of stomatal and non-stomatal responses to short-term and prolonged drought – and their variation among plants of different PFT membership and/or climatic origin – will be fundamental to the prediction of drought-induced mortality at plant scale (due to hydraulic failure, carbon starvation, and/or other mechanisms), or carbon loss at the ecosystem scale. Varied vegetation sensitivity to drought are necessary for LSMs to accurately explain the large-scale patterns of drought response of carbon, water and energy fluxes observed in different environments (De Kauwe et al., 2015b).

(3) Time scale may be of the essence when determining the extent to which climate change is likely to adversely affect forests. Drought acclimation is evidently a real phenomenon in trees adapted to dry climates, and presumably allows such trees to cope with periodic, protracted (but not too severe) droughts. The inherent differences among the species from contrasting climatic origins can be shown not only in their contrasting degree of tolerance to short-term drought (e.g., Zhou et al., 2013, 2014), but also in their contrasting abilities to compensate for long-term drought (e.g., Zhou et al., 2016). Drought-induced mortality of trees, and carbon loss from forests, could be overestimated if such acclimation is not taken into account (Choat et al., 2018). Model projections of drought effects on species distributions and vegetation composition in climate change scenarios should consider the differences in both short-term drought sensitivity and longer-term acclimation potential among species adapted to different climates.

The studies in this review mainly consider short-term dynamics of stomatal behavior and marginal water use efficiency, whose temporal dynamics could differ across seasons and years (Chen et al., 2018). Incorporation of their long-term dynamic patterns – such as the potential difference between dry versus wet seasons and across forest ecosystems – into ecosystem models remains to be improved. Besides, future model-experiment inter-comparison analysis needs to improve the representation of photosynthetic responses to co-occurring environmental stresses, such as drought and heat wave – which usually occur together (Ciais et al., 2005; Granier et al., 2007). High temperature can cause severe impacts on the photosynthetic apparatus, particularly during long-lasting drought events. Meanwhile, forest ecosystems at hot and dry environments – where stomatal closure (contributing to higher leaf temperature) and low C_c are necessary for plants to conserve water and avoid hydraulic failure (see a review by Choat et al., 2018) – could show very different responses of Rubisco characteristics and photosynthetic capacity under drought and high temperature conditions (Delgado et al., 1995; Kent and Tomany, 1995; Galmés et al., 2005). The model-experiment synthesis work in this area will enhance our predictions of environmental change consequences on forestry ecosystems.

CONCLUSION

Investigating the general trends of trait variation with key environmental factors, and translating this variation into improved process representation in vegetation models, are important developments for the improvement of LSMs and DGVMs. The model-oriented data analysis, experiments, and modeling described in this review amount to a new synthesis of information on the responses of different plant functions to drought, and provide a general methodology for systematic study of the relationship between plant processes and drought, allowing the derivation of functions that can be used directly in modeling. They can be seen as part of a wider movement toward the observationally driven parameterization of fundamental vegetation processes. Such work can also contribute to climate-change adaptation, through facilitating more accurate predictions of how forestry systems are likely to respond to projected changes in drought intensity and duration in a rapidly changing world.

AUTHOR CONTRIBUTIONS

S-XZ drafted the work. All authors contributed substantially to the conception of this work and critically revised the work. ICP secured the funding.

FUNDING

The work was financially supported by the International Macquarie University Research Excellence Scholarship. This project has received funding from the European Research Council (ERC) under the European Union's Horizon 2020 Research and Innovation Programme (Grant Agreement No: 787203 REALM).

ACKNOWLEDGMENTS

S-XZ was supported by an International Macquarie University Research Excellence Scholarship. This work is a contribution to the AXA Chair Programme in Biosphere and Climate Impacts and the Imperial College initiative Grand Challenges in Ecosystems and the Environment.

REFERENCES

Adams, H. D., Guardiola-Claramonte, M., Barron-Gafford, G. A., Villegas, J. C., Breshears, D. D., Zou, C. B., et al. (2009). Temperature sensitivity of drought-induced tree mortality portends increased regional die-off under global-change-type drought. *Proc. Natl. Acad. Sci. U.S.A.* 106, 7063–7066. doi: 10.1073/pnas.0901438106

Allen, C. D., Macalady, A. K., Chenchouni, H., Bachelet, D., McDowell, N., Vennetier, M., et al. (2010). A global overview of drought and heat-induced tree mortality reveals emerging climate change risks for forests. *For. Ecol. Manage.* 259, 660–684. doi: 10.1016/j.foreco.2009.09.001

Anderegg, W. R., Berry, J. A., Smith, D. D., Sperry, J. S., Anderegg, L. D., and Field, C. B. (2012). The roles of hydraulic and carbon stress in a widespread climate-induced forest die-off. *Proc. Natl. Acad. Sci. U.S.A.* 109, 233–237. doi: 10.1073/pnas.1107891109

Baldocchi, D. (1997). Measuring and modeling carbon dioxide and water vapor exchange over a temperate broad-leaved forest during the 1995 summer drought. *Plant Cell Environ.* 20, 1108–1122. doi: 10.1046/j.1365-3040.1997.d01-147.x

Ball, J. T., Woodrow, I. E., and Berry, J. A. (1987). "A model predicting stomatal conductance and its contribution to the control of photosynthesis under different environmental conditions," in *Progress in Photosynthesis Research*, ed. J. Biggins (Dordrecht: Martinus-Nijhoff Publishers), 221–224.

Bernacchi, C. J., Bagley, J. E., Serbin, S. P., Ruiz-Vera, U. M., Rosenthal, D. M., and VanLoocke, A. (2013). Modelling C3 photosynthesis from the chloroplast to the ecosystem. *Plant Cell Environ.* 36, 1641–1657. doi: 10.1111/pce.12118

Berninger, F., and Hari, P. (1993). Optimal regulation of gas exchange: evidence from field data. *Ann. Bot.* 71, 135–140. doi: 10.1006/anbo.1993.1017

Bonan, G. B. (1995). Land-atmosphere CO_2 exchange simulated by a land surface process model coupled to an atmospheric general circulation model. *J. Geophys. Res.* 100, 2817–2831. doi: 10.1029/94JD02961

Bonan, G. B. (2008). Forests and climate change: forcings, feedbacks, and the climate benefits of forests. *Science* 320, 1444–1449. doi: 10.1126/science.1155121

Bonan, G. B., Lawrence, P. J., Oleson, K. W., Levis, S., Jung, M., Reichstein, M., et al. (2011). Improving canopy processes in the community land model version 4 (CLM4) using global flux fields empirically inferred from FLUXNET data. *J. Geophys. Res. Biogeosci.* 116:G2. doi: 10.1029/2010JG001593

Bonan, G. B., Oleson, K. W., Fisher, R. A., Lasslop, G., and Reichstein, M. (2012). Reconciling leaf physiological traits and canopy flux data: use of the TRY and FLUXNET databases in the community land model version 4. *J. Geophys. Res. Biogeosci.* 117:G2. doi: 10.1029/2011JG001913

Bonan, G. B., Williams, M., Fisher, R. A., and Oleson, K. W. (2014). Modeling stomatal conductance in the earth system: linking leaf water-use efficiency and water transport along the soil–plant–atmosphere continuum. *Geosci. Model Dev.* 7, 2193–2222. doi: 10.5194/gmd-7-2193-2014

Bota, J., Medrano, H., and Flexas, J. (2004). Is photosynthesis limited by decreased Rubisco activity and RuBP content under progressive water stress? *New Phytol.* 162, 671–681. doi: 10.1111/j.1469-8137.2004.01056.x

Cano, F. J., López, R., and Warren, C. R. (2014). Implications of the mesophyll conductance to CO_2 for photosynthesis and water use efficiency during long-term water stress and recovery in two contrasting *Eucalyptus* species. *Plant Cell Environ.* 37, 2470–2490. doi: 10.1111/pce.12325

Castrillo, M., Fernandez, D., and Calcagno, A. (2001). Responses of ribulose-1,5-bisphosphate carboxylase, protein content, and stomatal conductance to water deficit in maize, tomato, and bean. *Photosynthetica* 39, 221–226. doi: 10.1023/A:1013731210309

Chaves, M. M., Maroco, J. P., and Pereira, J. S. (2003). Understanding plant responses to drought – from genes to the whole plant. *Funct. Plant Biol.* 30, 239–264. doi: 10.1071 /FP02076

Chen, M., Wang, G., Zhou, S., Zhao J., Zhang X., He C., et al. (2018). Studies on forest ecosystem physiology: marginal water-use efficiency of a tropical, seasonal, evergreen forest in Thailand. *J. For. Res.* doi: 10.1007/s11676-018-0804-5

Choat, B., Brodribb, T. J., Brodersen, C. R., Duursma, R. A., López, R., and Medlyn, B. E. (2018). Triggers of tree mortality under drought. *Nature* 558, 531–539. doi: 10.1038/s41586-018-0240-x

Choat, B., Jansen, S., Brodribb, T. J., Cochard, H., Delzon, S., Bhaskar, R., et al. (2012). Global convergence in the vulnerability of forests to drought. *Nature* 491, 752–755. doi: 10.1038/nature11688

Christoffersen, B. O., Gloor, M., Fauset, S., Fyllas, N. M., Galbraith, D. R., Baker, T. R., et al. (2016). Linking hydraulic traits to tropical forest function in a size-structured and trait-driven model (TFS v. 1-Hydro). *Geosci. Model Dev.* 9:4227. doi: 10.5194/gmd-9-4227-2016

Ciais, P., Reichstein, M., Viovy, N., Granier, A., Ogée, J., Allard, V., et al. (2005). Europe-wide reduction in primary productivity caused by the heat and drought in 2003. *Nature* 437, 529–533. doi: 10.1038/nature03972

Cinnirella, S., Magnani, F., Saracino, A., and Borghetti, M. (2002). Response of a mature *Pinus laricio* plantation to a three-year restriction of water supply: structural and functional acclimation to drought. *Tree Physiol.* 22, 21–30. doi: 10.1093/treephys/22.1.21

Clark, J. S., Bell, D. M., Kwit, M., Stine, A., Vierra, B., and Zhu, K. (2012). Individual-scale inference to anticipate climate-change vulnerability of biodiversity. *Philos. Trans. R. Soc. Lond. B Biol. Sci.* 367, 236–246. doi: 10.1098/rstb.2011.0183

Collatz, G. J., Ball, J. T., Grivet, C., and Berry, J. A. (1991). Physiological and environmental regulation of stomatal conductance, photosynthesis and transpiration: a model that includes a laminar boundary layer. *Agric. For. Meteorol.* 54, 107–136. doi: 10.1016/0168-1923(91)90002-8

Cowan, I. R. (1977). Stomatal behaviour and environment. *Adv. Bot. Res.* 4, 117–288. doi: 10.1016/S0065-2296(08)60370-5

Cowan, I. R., and Farquhar, G. D. (1977). Stomatal function in relation to leaf metabolism and environment. *Symp. Soc. Exp. Biol.* 31, 471–505.

Cox, P. M., Huntingford, C., and Harding, R. J. (1998). A canopy conductance and photosynthesis model for use in a GCM land surface scheme. *J. Hydrol.* 21, 79–94. doi: 10.1016/S0022-1694(98)00203-0

De Kauwe, M. G., Kala, J., Lin, Y. S., Pitman, A. J., Medlyn, B. E., Duursma, R. A., et al. (2015a). A test of an optimal stomatal conductance scheme within the CABLE land surface model. *Geosci. Model Dev.* 8, 431–452. doi: 10.5194/gmd-8-431-2015

De Kauwe, M. G., Zhou, S. X., Medlyn, B. E., Pitman, A. J., Wang, Y. P., Duursma, R. A., et al. (2015b). Do land surface models need to include differential plant species responses to drought? Examining model predictions across a mesic-xeric gradient in Europe. *Biogeosciences* 12, 7503–7518. doi: 10.5194/bg-12-7503-2015

Delgado, E., Medrano, H., Keys, A. J., and Parry, M. A. J. (1995). Species variation in Rubisco specificity factor. *J. Exp. Bot.* 46, 1775–1777. doi: 10.1093/jxb/46.11.1775

Dewar, R., Mauranen, A., Mäkelä, A., Hölttä, T., Medlyn, B., and Vesala, T. (2018). New insights into the covariation of stomatal, mesophyll and hydraulic conductances from optimization models incorporating nonstomatal limitations to photosynthesis. *New Phytol.* 217, 571–585. doi: 10.1111/nph.14848

Duursma, R. A., and Choat, B. (2017). fitplc – An R package to fit hydraulic vulnerability curves. *J. Plant Hydraul.* 4:e002. doi: 10.20870/jph.2017.e002

Egea, G., Verhoef, A., and Vidale, P. L. (2011). Towards an improved and more flexible representation of water stress in coupled photosynthesis–stomatal conductance models. *Agric. For. Meteorol.* 151, 1370–1384. doi: 10.1016/j.agrformet.2011.05.019

Eilmann, B., Weber, P., Rigling, A., and Eckstein, D. (2006). Growth reactions of *Pinus sylvestris* L. and *Quercus pubescens* willd. to drought years at a xeric site in Valais, Switzerland. *Dendrochronologia* 23, 121–132. doi: 10.1016/j.dendro.2005.10.002

Engelbrecht, B. M., Comita, L. S., Condit, R., Kursar, T. A., Tyree, M. T., Turner, B. L., et al. (2007). Drought sensitivity shapes species distribution patterns in tropical forests. *Nature* 447, 80–82. doi: 10.1038/nature05747

Evans, J. R., and von Caemmerer, S. (2013). Temperature response of carbon isotope discrimination and mesophyll conductance in tobacco. *Plant Cell Environ.* 36, 745–756. doi: 10.1111/j.1365-3040.2012.02591.x

Farquhar, G. D., von Caemmerer, S., and Berry, J. A. (1980). A biochemical model of photosynthetic CO_2 assimilation in leaves of C_3 species. *Planta* 149, 78–90. doi: 10.1007/BF00386231

Flexas, J., Barbour, M. M., Brendel, O., Cabrera, H. M., Carriquí, M., Díaz-espejo, A., et al. (2012). Mesophyll diffusion conductance to CO_2: an unappreciated central player in photosynthesis. *Plant Sci.* 194, 70–84. doi: 10.1016/j.plantsci.2012.05.009

Flexas, J., Bota, J., Loreto, F., Cornic, G., and Sharkey, T. D. (2004). Diffusive and metabolic limitations to photosynthesis under drought and salinity in C3 plants. *Plant Biol.* 6, 269–279. doi: 10.1055/s-2004-820867

Flexas, J., Diaz-Espejo, A., Galmés, J., Kaldenhoff, R., Medrano, H., and Ribas-Carbo, M. (2007). Rapid variations of mesophyll conductance in response to changes in CO_2 concentration around leaves. *Plant Cell Environ.* 30, 1284–1298. doi: 10.1111/j.1365-3040.2007.01700.x

Flexas, J., Ribas-Carbó, M., Bota, J., Galmés, J., Henkle, M., Martínez-Cañellas, S., et al. (2006). Decreased Rubisco activity during water stress is not induced by decreased relative water content but related to conditions of low stomatal conductance and chloroplast CO_2 concentration. *New Phytol.* 172, 73–82. doi: 10.1111/j.1469-8137.2006.01794.x

Flexas, J., Ribas-Carbó, M., Diaz-Espejo, A., Galmés, J., and Medrano, H. (2008). Mesophyll conductance to CO_2: current knowledge and future prospects. *Plant Cell Environ.* 31, 602–621. doi: 10.1111/j.1365-3040.2007.01757.x

Galmés, J., Aranjuelo, I., Medrano, H., and Flexas, J. (2013). Variation in Rubisco content and activity under variable climatic factors. *Photosynthesis Res.* 117, 73–90. doi: 10.1007/s11120-013-9861-y

Galmés, J., Flexas, J., Keys, A. J., Cifre, J., Mitchell, R. A., and Madgwick, P. J. (2005). Rubisco specificity factor tends to be larger in plant species from drier habitats and in species with persistent leaves. *Plant Cell Environ.* 28, 571–579. doi: 10.1111/j.1365-3040.2005.01300.x

Granier, A., Reichstein, M., Bréda, N., Janssens, I. A., Falge, E., Ciais, P., et al. (2007). Evidence for soil water control on carbon and water dynamics in

European forests during the extremely dry year: 2003. *Agric. For. Meteorol.* 143, 123–145. doi: 10.1016/j.agrformet.2006.12.004

Grassi, G., and Magnani, F. (2005). Stomatal, mesophyll conductance and biochemical limitations to photosynthesis as affected by drought and leaf ontogeny in ash and oak trees. *Plant Cell Environ.* 28, 834–849. doi: 10.1111/j.1365-3040.2005.01333.x

Groenendijk, M., Dolman, A. J., Van der Molen, M. K., Leuning, R., Arneth, A., Delpierre, N., et al. (2011). Assessing parameter variability in a photosynthesis model with and between plant functional types using global Fluxnet eddy covariance data. *Agric. For. Meteorol.* 151, 22–38. doi: 10.1016/j.agrformet.2010.08.013

Hall, A. E., and Schulze, E. D. (1980). Stomatal response to environment and a possible interrelation between stomatal effects on transpiration and CO_2 assimilation. *Plant Cell Environ.* 3, 467–474. doi: 10.1111/1365-3040.ep11587040

Haxeltine, A., and Prentice, I. C. (1996). BIOME3: an equilibrium terrestrial biosphere model based on ecophysiological constraints, resource availability, and competition among plant function types. *Glob. Biogeochem.* 10, 693–709. doi: 10.1029/96GB02344

Héroult, A., Lin, Y.-S., Bourne, A., Medlyn, B. E., and Ellsworth, D. S. (2013). Optimal stomatal conductance in relation to photosynthesis in climatically contrasting *Eucalyptus* species under drought. *Plant Cell Environ.* 36, 262–274. doi: 10.1111/j.1365-3040.2012.02570.x

Kanechi, M., Uchida, N., Yasuda, T., and Yamaguchi, T. (1996). Non-stomatal inhibition associated with inactivation of rubisco in dehydrated coffee leaves under unshaded and shaded conditions. *Plant Cell Physiol.* 37, 455–460. doi: 10.1093/oxfordjournals.pcp.a028967

Kattge, J., Knorr, W., Raddatz, T., and Wirth, C. (2009). Quantifying photosynthetic capacity and its relationship to leaf nitrogen content for global-scale terres- trial biosphere models. *Glob. Change Biol.* 15, 976–991. doi: 10.1111/j.1365-2486.2008.01744.x

Kent, S. S., and Tomany, M. J. (1995). The differential of the ribulose 1,5-bisphosphate carboxylase/oxygenase specificity factor among higher plants and the potential for biomass enhancement. *Plant Physiol. Biochem.* 33, 71–80.

Klein, T. (2014). The variability of stomatal sensitivity to leaf water potential across tree species indicates a continuum between isohydric and anisohydric behaviours. *Funct. Ecol.* 28, 1313–1320. doi: 10.1111/1365-2435.12289

Kljun, N., Black, T. A., Griffis, T. J., Barr, A. G., Gaumont-Guay, D., Morgenstern, K., et al. (2006). Response of net ecosystem productivity of three boreal forest stands to drought. *Ecosystems* 9, 1128–1144. doi: 10.1007/s10021-005-0082-x

Knapp, A. K., and Smith, M. D. (2001). Variation among biomes in temporal dynamics of aboveground primary production. *Science* 291, 481–484. doi: 10.1126/science.291.5503.481

Lamy, J. B., Delzon, S., Bouche, P. S., Alia, R., Vendramin, G. G., Cochard, H., et al. (2014). Limited genetic variability and phenotypic plasticity detected for cavitation resistance in a Mediterranean pine. *New Phytol.* 201, 874–886. doi: 10.1111/nph.12556

Lawlor, D. W., and Tezara, W. (2009). Causes of decreased photosynthetic rate and metabolic capacity in water-deficient leaf cells: a critical evaluation of mechanisms and integration of processes. *Ann. Bot.* 103, 561–579. doi: 10.1093/aob/mcn244

Li, X., Blackman, C. J., Choat, B., Duursma, R. A., Rymer, P. D., Medlyn, B. E., et al. (2018). Tree hydraulic traits are co ordinated and strongly linked to climate of origin across a rainfall gradient. *Plant Cell Environ.* 41, 646–660. doi: 10.1111/pce.13129

Liang, X., Lettenmaier, D. P., Wood, E. F., and Burges, S. J. (1994). A simple hydrologically based model of land surface water and energy fluxes for general circulation models. *J. Geophys. Res.* 99, 14415–14428. doi: 10.1029/94JD00483

Limousin, J. M., Longepierre, D., Huc, R., and Rambal, S. (2010a). Change in hydraulic traits of Mediterranean *Quercus ilex* subjected to long-term throughfall exclusion. *Tree Physiol.* 30, 1026–1036. doi: 10.1093/treephys/tpq062

Limousin, J. M., Misson, L., Lavoir, A. V., Martin, N. K., and Rambal, S. (2010b). Do photosynthetic limitations of evergreen *Quercus ilex* leaves change with long term increased drought severity? *Plant Cell Environ.* 33, 863–875. doi: 10.1111/j.1365-3040.2009.02112.x

Llorens, L., Peñuelas, J., Beier, C., Emmet, B., Estiarte, M., and Tietema, A. (2004). Effects of an experimental increase of temperature and drought on the photosynthetic performance of two ericaceous shrub species along a northsouth European gradient. *Ecosystems* 7, 613–624. doi: 10.1007/s10021-004-0180-1

Long, S. P., Ainsworth, E. A., Leakey, A. B., Nosberger, J., and Ort, D. R. (2006). Food for thought: lower than expected crop yield stimulation with rising CO_2 concentrations. *Science* 312, 1918–1921. doi: 10.1126/science.1114722

Maire, V., Gross, N., Hill, D., Martin, R., Wirth, C., Wright, I. J., et al. (2013). Disentangling coordination among functional traits using an individual-centred model: impact on plant performance at intra- and inter-specific levels. *PLoS One* 8:e77372. doi: 10.1371/journal.pone.0077372

Mäkelä, A., Berninger, F., and Hari, P. (1996). Optimal control of gas exchange during drought: theoretical analysis. *Ann. Bot.* 77, 461–467. doi: 10.1006/anbo.1996.0056

Manzoni, S. (2014). Integrating plant hydraulics and gas exchange along the drought-response trait spectrum. *Tree Physiol.* 34, 1031–1034. doi: 10.1093/treephys/tpu088

Martin-StPaul, N., Delzon, S., and Cochard, H. (2017). Plant resistance to drought depends on timely stomatal closure. *Ecol. Lett.* 20, 1437–1447. doi: 10.1111/ele.12851

Martin-StPaul, N. K., Limousin, J. M., Rodríguez-Calcerrada, J., Ruffault, J., Rambal, S., Letts, M. G., et al. (2012). Photosynthetic sensitivity to drought varies among populations of *Quercus ilex* along a rainfall gradient. *Funct. Plant Biol.* 39, 25–37. doi: 10.1071/FP11090

Martin-StPaul, N. K., Limousin, J. M., Vogt-Schilb, H., Rodríguez-Calcerrada, J., Rambal, S., Longepierre, D., et al. (2013). The temporal response to drought in a Mediterranean evergreen tree: comparing a regional precipitation gradient and a throughfall exclusion experiment. *Glob. Chang. Biol.* 19, 2413–2426. doi: 10.1111/gcb.12215

Maseda, P. H., and Fernández, R. J. (2006). Stay wet or else: three ways in which plants can adjust hydraulically to their environment. *J. Exp. Bot.* 57, 3963–3977. doi: 10.1093/jxb/erl127

McDowell, N., Pockman, W. T., Allen, C. D., Breshears, D. D., Cobb, N., Kolb, T., et al. (2008). Mechanisms of plant survival and mortality during drought: why do some plants survive while others succumb to drought? *New Phytol.* 178, 719–739. doi: 10.1111/j.1469-8137.2008.02436.x

McDowell, N. G., Beerling, D. J., Breshears, D. D., Fisher, R. A., Raffa, K. F., and Stitt, M. (2011). The interdependence of mechanisms underlying climate-driven vegetation mortality. *Trends Ecol. Evol.* 26, 523–532. doi: 10.1016/j.tree.2011.06.003

Medlyn, B. E., De Kauwe, M. G., Zaehle, S., Walker, A. P., Duursma, R. A., Luus, K., et al. (2016). Using models to guide field experiments: a priori predictions for the CO_2 response of a nutrient and water limited native Eucalypt woodland. *Glob. Change Biol.* 22, 2834–2851. doi: 10.1111/gcb.13268

Medlyn, B. E., Duursma, R. A., Eamus, D., Ellsworth, D. S., Prentice, I. C., Barton, C. V., et al. (2011). Reconciling the optimal and empirical approaches to modelling stomatal conductance. *Glob. Change Biol.* 17, 2134–2144. doi: 10.1111/j.1365-2486.2010.02375.x

Misson, L., Limousin, J. M., Rodriguez, R., and Letts, M. G. (2010). Leaf physiological responses to extreme droughts in Mediterranean *Quercus ilex* forest. *Plant Cell Environ.* 33, 1898–1910. doi: 10.1111/j.1365-3040.2010.02193.x

Niinemets, U., Penuelas, J., and Flexas, J. (2011). Evergreens favored by higher responsiveness to increased CO_2. *Trends Ecol. Evol.* 26, 136–142. doi: 10.1016/j.tree.2010.12.012

Ogaya, R., and Peñuelas, J. (2003). Comparative field study of *Quercus ilex* and *Phillyrea latifolia*: photosynthetic response to experimental drought conditions. *Environ. Exp. Bot.* 50, 137–148. doi: 10.1016/S0098-8472(03)00019-4

Panković, D., Sakač, Z., Kevrešan, S., and Plesničar, M. (1999). Acclimation to long-term water deficit in the leaves of two sunflower hybrids: photosynthesis, electron transport and carbon metabolism. *J. Exp. Bot.* 50, 127–138. doi: 10.1093/jxb/50.330.128

Parry, M. A., Andralojc, P. J., Khan, S., Lea, P. J., and Keys, A. J. (2002). Rubisco activity: effects of drought stress. *Ann. Bot.* 89, 833–839. doi: 10.1093/aob/mcf103

Pasho, E., Camarero, J. J., de Luis, M., and Vicente-Serrano, S. M. (2011). Impacts of drought at different time scales on forest growth across a wide climatic gradient in north-eastern Spain. *Agric. For. Meteorol.* 151, 1800–1811. doi: 10.1016/j.agrformet.2011.07.018

Phillips, O. L., Aragão, L. E., Lewis, S. L., Fisher, J. B., Lloyd, J., and López-González, G. (2009). Drought sensitivity of the Amazon rainforest. *Science* 323, 1344–1347. doi: 10.1126/science.1164033

Phillips, O. L., Van Der Heijden, G., Lewis, S. L., López González, G., Aragão, L. E., Lloyd, J., et al. (2010). Drought-mortality relationships for tropical forests. *New Phytol.* 187, 631–646. doi: 10.1111/j.1469-8137.2010.03359.x

Pinheiro, C., and Chaves, M. M. (2011). Photosynthesis and drought: can we make metabolic connections from available data? *J. Exp. Bot.* 62, 869–882. doi: 10.1093/jxb/erq340

Pitman, A. J. (2003). The evolution of, and revolution in, land surface schemes designed for climate models. *Int. J. Climatol.* 23, 479–510. doi: 10.1002/joc.893

Potts, M. (2003). Drought in a Bornean everwet rain forest. *J. Ecol.* 91, 467–474. doi: 10.1046/j.1365-2745.2003.00779.x

Powell, T. L., Galbraith, D. R., Christoffersen, B. O., Harper, A., Imbuzeiro, H., Rowland, L., et al. (2013). Confronting model predictions of carbon fluxes with measurements of Amazon forests subjected to experimental drought. *New Phytol.* 200, 350–365. doi: 10.1111/nph.12390

Prentice, I. C., and Cowling, S. A. (2013). "Dynamic global vegetation models," in *Encyclopedia of Biodiversity*, 2nd Edn, ed. S. A. Levin (Cambridge: Academic Press), 607–689.

Prentice, I. C., Dong, N., Gleason, S. M., Maire, V., and Wright, I. J. (2014). Balancing the costs of carbon gain and water loss: testing a new quantitative framework for plant functional ecology. *Ecol. Lett.* 17, 82–91. doi: 10.1111/ele.12211

Prentice, I. C., Liang, X., Medlyn, B. E., and Wang, Y. P. (2015). Reliable, robust and realistic: the three R's of next-generation land-surface modelling. *Atmos. Chem. Phys.* 15, 5987–6005. doi: 10.5194/acp-15-5987-2015

Reich, P. B. (2014). The world-wide 'fast-slow' plant economics spectrum: a traits manifesto. *J. Ecol.* 102, 275–301. doi: 10.1111/1365-2745.12211

Rogers, A., Medlyn, B. E., Dukes, J. S., Bonan, G., Caemmerer, S., Dietze, M. C., et al. (2017). A roadmap for improving the representation of photosynthesis in Earth system models. *New Phytol.* 213, 22–42. doi: 10.1111/nph.14283

Sperry, J. S. (2000). Hydraulic constraints on plant gas exchange. *Agric. For. Meteorol.* 104, 13–23. doi: 10.1016/S0168-1923(00)00144-1

Sperry, J. S., Wang, Y., Wolfe, B. T., Mackay, D. S., Anderegg, W. R., McDowell, N. G., et al. (2016). Pragmatic hydraulic theory predicts stomatal responses to climatic water deficits. *New Phytol.* 212, 577–589. doi: 10.1111/nph.14059

Tezara, W., Mitchell, V., Driscoll, S. P., and Lawlor, D. W. (2002). Effects of water deficit and its interaction with CO_2 supply on the biochemistry and physiology of photosynthesis in sunflower. *J. Exp. Bot.* 53, 1781–1791. doi: 10.1093/jxb/erf021

Tezara, W., Mitchell, V. J., Driscoll, S. D., and Lawlor, D. W. (1999). Water stress inhibits plant photosynthesis by decreasing coupling factor and ATP. *Nature* 401, 914–917. doi: 10.1038/44842

Thimmanaik, S., Kumar, S. G., Kumari, G. J., Suryanarayana, N., and Sudhakar, C. (2002). Photosynthesis and the enzymes of photosynthetic carbon reduction cycle in mulberry during water stress and recovery. *Photosynthetica* 40, 233–236. doi: 10.1023/A:1021397708318

Verhoef, A., and Egea, G. (2014). Modeling plant transpiration under limited soil water: comparison of different plant and soil hydraulic parameterizations and preliminary implications for their use in land surface models. *Agric. For. Meteorol.* 191, 22–32. doi: 10.1016/j.agrformet.2014.02.009

Vicente-Serrano, S. M., Gouveia, C., Camarero, J. J., Beguería, S., Trigo, R., López-Moreno, J. I., et al. (2013). Response of vegetation to drought time-scales across global land biomes. *Proc. Natl. Acad. Sci. U.S.A.* 110, 52–57. doi: 10.1073/pnas.1207068110

Walker, A. P., Hanson, P. J., De Kauwe, M. G., Medlyn, B. E., Zaehle, S., Asao, S., et al. (2014). Comprehensive ecosystem model data synthesis using multiple data sets at two temperate forest free air CO_2 enrichment experiments: model performance at ambient CO_2 concentration. *J. Geophys. Res. Biogeosci.* 119, 937–964. doi: 10.1002/2013JG002553

Webb, W. L., Lauenroth, W. K., Szarek, S. R., and Kinerson, R. S. (1983). Primary production and abiotic controls in forests, grasslands, and desert ecosystems in the United States. *Ecology* 64, 134–151. doi: 10.2307/1937336

Williams, A. P., Allen, C. D., Macalady, A. K., Griffin, D., Woodhouse, C. A., Meko, D. M., et al. (2013). Temperature as a potent driver of regional forest drought stress and tree mortality. *Nat. Clim. Change* 3, 292–297. doi: 10.1038/nclimate1693

Wilson, K. B., Baldocchi, D. D., and Hanson, P. J. (2000). Quantifying stomatal and non-stomatal limitations to carbon assimilation resulting from leaf aging and drought in mature deciduous tree species. *Tree Physiol.* 20, 787–797. doi: 10.1093/treephys/20.12.787

Wolf, A., Anderegg, W. R., and Pacala, S. W. (2016). Optimal stomatal behavior with competition for water and risk of hydraulic impairment. *Proc. Natl. Acad. Sci. U.S.A.* 113, E7222–E7230. doi: 10.1073/pnas.1615144113

Wright, I. J., Reich, P. B., Westoby, M., Ackerly, D. D., Baruch, Z., Bongers, F., et al. (2004). The worldwide leaf economics spectrum. *Nature* 428, 821–827. doi: 10.1038/nature02403

Xu, L., and Baldocchi, D. D. (2003). Seasonal trends in photosynthetic parameters and stomatal conductance of blue oak (*Quercus douglasii*) under prolonged summer drought and high temperature. *Tree Physiol.* 23, 865–877. doi: 10.1093/treephys/23.13.865

Xu, X., Medvigy, D., Powers, J. S., Becknell, J. M., and Guan, K. (2016). Diversity in plant hydraulic traits explains seasonal and inter annual variations of vegetation dynamics in seasonally dry tropical forests. *New Phytol.* 212, 80–95. doi: 10.1111/nph.14009

Yachi, S., and Loreau, M. (1999). Biodiversity and ecosystem productivity in a fluctuating environment: the insurance hypothesis. *Proc. Natl. Acad. Sci. U.S.A.* 96, 1463–1468. doi: 10.1073/pnas.96.4.1463

Zeppel, M. B., Wilks, J. V., and Lewis, J. D. (2014). Impacts of extreme precipitation and seasonal changes in precipitation on plants. *Biogeosciences* 11:3083. doi: 10.5194/bg-11-3083-2014

Zhou, S. (2015). *Quantifying and Modelling the Responses of Leaf Gas Exchange to Drought*, PhD thesis, Macquarie University, Sydney.

Zhou, S., Duursma, R. A., Medlyn, B. E., Kelly, J. W., and Prentice, I. C. (2013). How should we model plant responses to drought? An analysis of stomatal and non-stomatal responses to water stress. *Agric. For. Meteorol.* 182, 204–214. doi: 10.1016/j.agrformet.2013.05.009

Zhou, S., Medlyn, B. E., Santiago, S., Sperlich, D., and Prentice, I. C. (2014). Short-term water stress impacts on stomatal, mesophyll, and biochemical limitations to photosynthesis differ consistently among tree species from contrasting climates. *Tree Physiol.* 34, 1035–1046. doi: 10.1093/treephys/tpu072

Zhou, S.-X., Medlyn, B. E., and Prentice, I. C. (2016). Long-term water stress leads to acclimation of drought sensitivity of photosynthetic capacity in xeric but not riparian *Eucalyptus* species. *Ann. Bot.* 117, 133–144. doi: 10.1093/aob/mcv161

Conflict of Interest Statement: The authors declare that the research was conducted in the absence of any commercial or financial relationships that could be construed as a potential conflict of interest.

frontiers in Plant Science

ORIGINAL RESEARCH
published: 26 February 2019
doi: 10.3389/fpls.2019.00224

Drought-Induced Carbon and Water Use Efficiency Responses in Dryland Vegetation of Northern China

*Chengcheng Gang[1,2,3], Yi Zhang[2], Liang Guo[1,2], Xuerui Gao[1,2], Shouzhang Peng[1,2], Mingxun Chen[4] and Zhongming Wen[1,2]**

[1] Institute of Soil and Water Conservation, Northwest A&F University, Yangling, China, [2] Institute of Soil and Water Conservation, Chinese Academy of Sciences and Ministry of Water Resources, Yangling, China, [3] International Center for Climate and Global Change Research, School of Forestry and Wildlife Sciences, Auburn University, Auburn, AL, United States, [4] College of Agronomy, Northwest A&F University, Yangling, China

Given the context of global warming and the increasing frequency of extreme climate events, concerns have been raised by scientists, government, and the public regarding drought occurrence and its impacts, particularly in arid and semi-arid regions. In this paper, the drought conditions for the forest and grassland areas in the northern region of China were identified based on 12 years of satellite-based Drought Severity Index (DSI) data. The impact of drought on dryland vegetation in terms of carbon use efficiency (CUE) and water use efficiency (WUE) were also investigated by exploring their correlations with DSI. Results indicated that 49.90% of forest and grassland experienced a dry trend over this period. The most severe drought occurred in 2001. In general, most forests in the study regions experienced near normal and wet conditions during the 12 year period. However, grasslands experienced a widespread drought after 2006. The forest CUE values showed a fluctuation increase from 2000 to 2011, whereas the grassland CUE remained steady over this period. In contrast, WUE increased in both forest and grassland areas due to the increasing net primary productivity (NPP) and descending evapotranspiration (ET). The CUE and WUE values of forest areas were more sensitive to droughts when compared to the values for grassland areas. The correlation analysis demonstrated that areas of DSI that showed significant correlations with CUE and WUE were 17.24 and 10.37% of the vegetated areas, respectively. Overall, the carbon and water use of dryland forests was more affected by drought than that of dryland grasslands.

Keywords: carbon use efficiency, drought severity index, dryland vegetation, northern China, water use efficiency

OPEN ACCESS

Edited by:
Zhiyou Yuan,
College of Forestry, Northwest A&F University, China

Reviewed by:
Zhaoqi Wang,
Peking University, China
Jinsong Wang,
Institute of Geographic Sciences and Natural Resources Research (CAS), China
Wen Yang,
Shaanxi Normal University, China

***Correspondence:**
Zhongming Wen
zmwen@ms.iswc.ac.cn

Specialty section:
This article was submitted to Plant Abiotic Stress, a section of the journal Frontiers in Plant Science

Received: *15 October 2018*
Accepted: *11 February 2019*
Published: *26 February 2019*

Citation:
Gang C, Zhang Y, Guo L, Gao X, Peng S, Chen M and Wen Z (2019) Drought-Induced Carbon and Water Use Efficiency Responses in Dryland Vegetation of Northern China. Front. Plant Sci. 10:224. doi: 10.3389/fpls.2019.00224

INTRODUCTION

Recently, droughts have been frequently recorded due to climatic warming from elevated concentrations of greenhouse gasses. This warming exacerbates water resource stress and poses a significant threat to food security and the sustainability of human activities in these areas (Vorosmarty et al., 2000; Rosegrant et al., 2003). The reports of the Intergovernmental Panel on Climate Change suggest that drought frequency will likely increase by the end of 21st century, particularly in regions that are currently dry (IPCC, 2014). At the ecosystem scale, drought

will reduce the carbon sequestration ability of vegetation and aggravate the water evaporation rate of ecosystems (Ciais et al., 2005; Zhao and Running, 2010). The ecosystem-scale carbon use efficiency (eCUE), which is defined as the ratio of net primary productivity (NPP) to gross primary productivity (GPP), describes the capacity of an ecosystem to transfer the carbon from the atmosphere to vegetation biomass (DeLucia et al., 2007). The ecosystem-scale water use efficiency (eWUE), a ratio of NPP to evapotranspiration (ET), measures the net carbon uptake per amount of water lost from the ecosystem (Beer et al., 2009; Gang et al., 2016a,b). The eCUE and eWUE are two vital indicators for addressing the ecosystem function in terms of carbon and water cycles (Webb et al., 1978; LeHouerou, 1984; DeLucia et al., 2007). The satellite-based imageries provide an effective way in monitoring drought severity and vegetation responses in term of carbon and water cycles (AghaKouchak et al., 2015; Liu Y. et al., 2015). The impacts of droughts on CUE and WUE have been widely reported in multiple scales (Webb et al., 1978; DeLucia et al., 2007; Liu Y. et al., 2015; Gang et al., 2016a). However, the occurrence of drought and its subsequent influences on ecosystem-scale CUE and WUE have not been extensively investigated, especially in the arid and semi-arid regions. Therefore, further research is needed on the extent and duration of droughts as well as their impacts on the carbon and water cycles of dryland vegetation.

Precipitation is a primary input data in most drought indices, which have been widely used in monitoring drought conditions at different levels, such as the Standardized Precipitation Index (SPI) (McKee et al., 1995), the Palmer Drought Severity Index (PDSI) (Palmer, 1965), the Temperature-Vegetation Dryness Index (TVDI) (Sandholt et al., 2002), the Vegetation, Water and Thermal Stress Index (VWTCI) (Shakya and Yamaguchi, 2010), and the Percentage of Precipitation Anomaly (PPA). The large-scale effects of drought on vegetation are detectable with the help of remote sensing technology, which avoids the deficiencies of filed-based metrological observation (Rhee et al., 2010; Rojas et al., 2011). The Normalized Difference Vegetation Index (NDVI), which can reflect the growth status of plants, has been widely used for evaluating the effects of drought on vegetation growth (Cunha et al., 2015; Klisch and Atzberger, 2016). Many NDVI-based drought indicators have also been developed, such as the Anomaly Vegetation Index (AVI) (Chen et al., 1994), the Temperature Vegetation Drought Index (TVDI) (Sandholt et al., 2002), and the Standardized Vegetation Index (SVI) (Peters et al., 2002). ET, an important component of terrestrial water cycles, is a more direct and effective indicator for reflecting ecosystem moisture status (Mu et al., 2007a, 2011). Remote sensing technology can provide spatially explicit ET information for terrestrial ecosystems (Jackson et al., 2005). Combining the MODIS-derived NDVI and evapotranspiration/potential evapotranspiration (ET/PET) data, Mu et al. (2013) developed a satellite-based drought index with fine resolution at the global scale. This index is known as Drought Severity Index (DSI). The DSI dataset has been proven to be capable of monitoring droughts over the last decade worldwide (Zhao and Running, 2011; Mu et al., 2013; Zhang and Yamaguchi, 2014).

The northwest regions of China and Inner Mongolia (NWIM), which are mainly situated in the northern inland of China, are characterized with a dry climate, scarce precipitation, intensive evaporation, and a fragile environment (Gou et al., 2015). The unique location and climate make these regions vulnerable to climate change and human disturbance. Previous research has demonstrated that Ningxia, Gansu, and Xinjing provinces have experienced different drought conditions in the past decade, and these conditions exerted great influence on environment and agricultural production (Gou et al., 2015; Huang et al., 2015; Wang et al., 2015; Zhang et al., 2016). However, most of these studies mainly focused on the regional scale. The extent and severity of drought occurrences as well as the effects of droughts on carbon and water cycles at the ecosystem scale are still open questions that require further study.

The first decade of the 21st century has been estimated as the warmest period since the 1880s. These extreme temperatures highlight the importance of identifying the drought condition for the dryland vegetation during this particular period (Zhao and Running, 2010). The primary objectives of this study are: (i) to examine the extent and duration of drought events in the forests and grasslands of the NWIM from 2000 to 2011 via remotely sensed DSI data; (ii) to quantify the annual changes of ecosystem-scale CUE and WUE for forests and grasslands during this period; and (iii) to explore the correlations between vegetation CUE, WUE, and climate variables to reveal the environment drivers of vegetation carbon and water utilization. The outcomes of this study will elucidate the extent and duration of drought occurrence in the forests and grasslands of the NWIM region, and the results provide guidance for the initiation of adaptation strategies to respond to the climate extremes.

MATERIALS AND METHODS

Study Area

The NWIM region covers three provinces (Shaanxi, Gansu, and Qinghai) and three autonomous regions (Ningxia Hui Autonomous Region, Inner Mongolia Autonomous Region, and Xinjiang Uygur Autonomous Region) between the latitudes of 37–53°N and the longitudes of 73–126°E (**Figure 1**). The total area of NWIM is approximately 4.15×10^6 km^2, occupying approximately 45% of the land area of China and supporting 10% of the population. Most of this region is characterized by arid and semi-arid climates with mean annual temperatures (MAT) ranging from −7 to 16°C. The mean annual precipitation (MAP) ranges from 10 to 1100 mm (Shi et al., 2007; Mu et al., 2013; Wang H. et al., 2013). The MAP exhibits an obvious latitudinal distribution. Xinjiang and northern Inner Mongolia exhibit lower values and the southern areas of Shaanxi, Gansu, and Qinghai present higher MAP values (Shi et al., 2007).

Land Use and Land Cover Data

The land use and land cover map of the NWIM region was derived from the International Geosphere-Biosphere Project (IGBP) land cover dataset, which contains 17 land cover classes (Loveland et al., 2000). In this study, closed

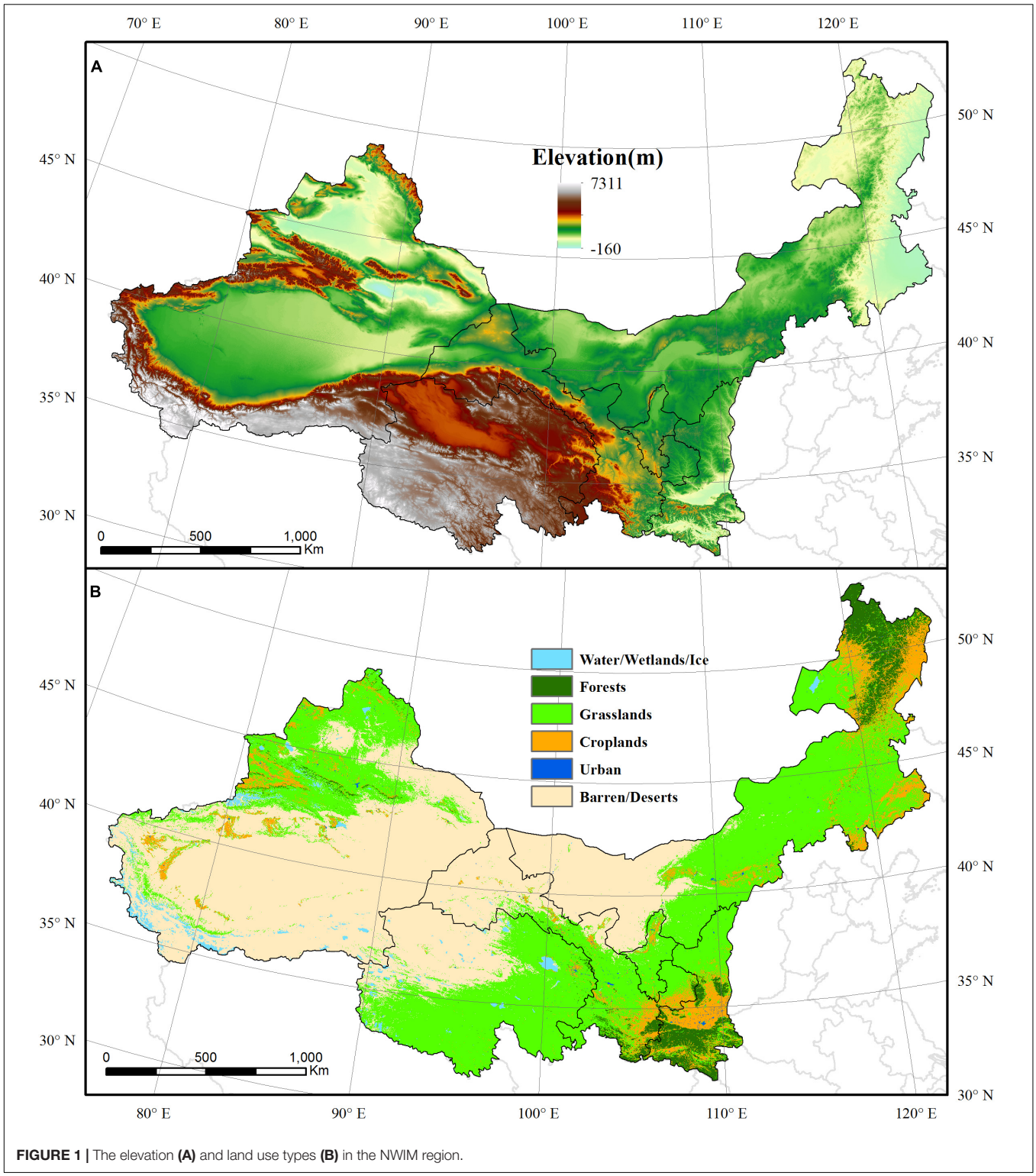

FIGURE 1 | The elevation **(A)** and land use types **(B)** in the NWIM region.

shrublands, open shrublands, woody savannas, savannas, and non-woody grasslands were regrouped as grasslands. The NWIM region has the largest typical steppe grassland in China, covering more than 41.00% of the total region. Evergreen needle forest, evergreen broadleaf forest, deciduous needle forest, and mixed forests were reclassified as forests, and these areas account for 4.70% of the total NWIM region. Barren/deserts, occupying 44.80% of the region, is the mostly widely distributed land use type in the NWIM region. Water bodies, croplands, and urban area made

up to 1.52, 7.69, and 0.24% of total area, respectively. Only the grassland and forest areas were included in the following analyses.

MODIS DSI, GPP, NPP, and ET Data

The annual MODIS DSI, GPP, NPP, and ET data from 2000 to 2011 for the NWIM region were obtained from the Numerical Terra dynamic Simulation Group at the University of Montana[1]. The DSI (0.05° spatial resolution) was based on the basis of ET/PET and snow-free growing season MODIS NDVI products for all vegetated land areas(Atkinson et al., 2011; Mu et al., 2013). The NDVI has been widely used to monitor the global vegetation photosynthetic activities due to its sensitivity to vegetation drought responses and associated water stress, especially in the water-limited regions (Huete et al., 2002; Justice et al., 2002). DSI is calculated as a standardized value, and its equation is expressed as follows:

$$SA_{\mathrm{NDVI}} = \frac{NDVI - \overline{NDVI}}{\delta_{\mathrm{NDVI}}} \quad (1)$$

$$SA_{\mathrm{EVA}} = \frac{(ET/PET) - \overline{(ET/PET)}}{\delta_{(\mathrm{ET/PET})}} \quad (2)$$

$$SA = SA_{\mathrm{NDVI}} + SA_{\mathrm{EVA}} \quad (3)$$

$$DSI = \frac{SA - \overline{SA}}{\delta_{\mathrm{SA}}} \quad (4)$$

where SA_{NDVI}, the standardized anomaly of the NDVI, is calculated using the long-term mean value of $\overline{NDVI}$ and the standard deviation δ_{NDVI} during the period 2000–2011; SA_{EVA}, the standardized anomaly of *ET/PET,* is calculated as the long-term mean value of $\overline{ET/PET}$ and a standard deviation $\delta_{(\mathrm{ET/PET})}$; ET/PET means the ratio of ET to PET; *SA* is a sum of SA_{NDVI} and SA_{EVA}; the DSI is a standardized anomaly of *SA*; $\overline{SA}$ is the long-term mean value of SA_{NDVI} and $SA_{(\mathrm{ET/PET})}$; δ_{SA} is the standardized deviation. The DSI value can be reclassified into 11 categories to indicate different drought conditions, which is shown in **Table 1** (Mu et al., 2013; Zhang and Yamaguchi, 2014).

The new version of MODIS productivity products have been improved by matching the spatial resolution of metrological data to that of MODIS pixel, filling the missing value of FPAR/LAI data due to cloud contamination and malfunction of MODIS sensor, and updating the biome parameter look-up table according to the productivity data from flux tower measurements (Zhao et al., 2005; Gang et al., 2016a). GPP values are calculated as follows:

$$GPP = \varepsilon_{\max} \times 0.45 \times SWrad \times FPAR \times fVPD \times fT_{\min} \quad (5)$$

where $\varepsilon_{\max}$ is the maximum light use efficiency under optimal conditions; SW_{rad} is the incoming short-wave solar radiation, of which 45% is Photosynthetically Active Radiation (PAR); FPAR is the fraction of PAR absorbed by the plant canopy; *fVPD* is vapor pressure deficits scalar, and $fT_{\min}$ is the daily minimum temperature ($T_{\min}$, °C) scalar.

TABLE 1 | The categories for drought conditions of the global DSI (Mu et al., 2013).

Category	Description	DSI
D5	Extremely drought	<−1.50
D4	Severe drought	−1.49 to −1.20
D3	Moderate drought	−1.99 to −0.9
D2	Mild drought	−0.89 to −0.60
D1	Incipient drought	−0.59 to −0.30
WD	Near normal	−0.29 to 0.29
W1	Incipient wet	0.30 to 0.59
W2	Slightly wet	0.60 to 0.89
W3	Moderately wet	0.90 to 1.19
W4	Very wet	1.20 to 1.50
W5	Extremely wet	>1.50

NPP is calculated by subtracting the maintenance and growth respiration from GPP. It is calculated as follows:

$$NPP = \sum_{1}^{365} GPP - R_{\mathrm{m\_lr}} - R_{\mathrm{m\_w}} - R_{\mathrm{g}} \quad (6)$$

where $R_{\mathrm{m\_lr}}$ is the maintenance respiration from living leaves and fine roots, and $R_{\mathrm{m\_w}}$ is the annual maintenance respiration from living wood, R_{g} is annual growth respiration. Detailed description for modeling MODIS GPP and NPP can be found in Zhao et al. (2005, 2006). Ecosystem-scale CUE for vegetation was calculated as the ratio of annual NPP to GPP in each grid.

The ET represents transpiration by vegetation and evaporation from canopy and soil surfaces. Based on the Penman-Monteith equation, the new version of MODIS ET dataset improved in many aspects, including the recalculation of the fraction of vegetation cover, the soil heat flux, and boundary layer resistance (Mu et al., 2007a,b, 2011). The ET algorithm is computed as follows:

$$\lambda E = \lambda E_{\mathrm{wet\_C}} + \lambda E_{\mathrm{trans}} + \lambda E_{\mathrm{SOIL}} \quad (5)$$

Where λE is the total daily ET, $\lambda E_{\mathrm{wet\_C}}$ refers to evaporation from the wet canopy surface, $\lambda E_{\mathrm{trans}}$ means the transpiration from the dry canopy surface, and $\lambda E_{\mathrm{SOIL}}$ is the evaporation from the soil surface (Mu et al., 2007a,b, 2011). The MODIS ET product has been validated and widely used in regional and global research (Mu et al., 2011; Gang et al., 2016a). The ecosystem-scale WUE for vegetation was calculated as the ratio of annual NPP to ET in each grid. The MODIS GPP, NPP, and ET performed reliable estimation accuracy on vegetation in northern China (Wang X. et al., 2013; Xiao, 2014; Liu Z. et al., 2015).

Climate Factor Data

Meteorological data, including temperature and precipitation, from 2000 to 2011 were obtained from the China Meteorological Data Service Center[2]. The monthly data, interpolated by using ANUSPLIN, were used to generate the gridded MAT and MAP.

[1]http://www.ntsg.umt.edu/

[2]http://data.cma.cn/

Analysis of Temporal Dynamic

Equation 6 was used to quantify the linear trend of variables (including DSI, CUE, WUE, NPP, GPP, ET, MAT, and MAP) via the ordinary least square estimation:

$$Slope = \frac{n \times \sum_{i=1}^{n} i \times Va_i - \left(\sum_{i=1}^{n} i\right)\left(\sum_{i=1}^{n} Va_i\right)}{n \times \sum_{i=1}^{n} i^2 - \left(\sum_{i=1}^{n} i\right)^2} \quad (6)$$

where i starts 1 for the year 2000, 2 for year 2001, and goes up to 12 for 2011; and Va_i refers to the annual value of variable at time i, i = 1,. . ..n, n = 12. The positive value of *Slope* in Eq. (6) indicates an increasing trend of variable, while the negative value connotes a decreasing trend during the 12-year period.

Correlation Analysis of Climate Variables With Vegetation CUE and WUE

The correlations of vegetation CUE and WUE with climate variables, including DSI, MAP, and MAT, were calculated to reveal the controlling of climate variables that impact CUE and WUE. If the correlation coefficient passes the significance test, then an extremely significant (at 99% confidence level) or significant (at 95% confidence level) linear correlation is indicated.

RESULTS

Drought Characteristics of Forest and Grassland in the NWIM Region

During the period of 2000–2011, the area of regions that became increasingly dry accounted for 49.90% of the total area of forest and grassland. These areas were mainly located in eastern Inner Mongolia and northern Xinjiang. The total area of regions that exhibited increasingly wetness was a little larger than the area exhibiting aridity. There regions with increasing wetness were mainly distributed within the 30–40°N, including the northern Shaanxi, Ningxia, Gansu, and Qinghai (**Figure 2A**). Nearly 3.73×10^4 km^2 of the forest regions that were dry in 2000 became wet in 2011. The areas under near normal conditions underwent the most obvious changes. Meanwhile, the forest regions that changed from wet to dry conditions reached an area of 15.56×10^4 km^2. This is far larger than the regions that became wet over the same period (**Figure 2B**). In contrast, 86.08×10^4 km^2 of the dry regions of grassland became wet during the 12-year period. Regions under D3 conditions were the largest contribution to this trend. The wet grassland area that became dry was relatively smaller, with the D2 condition making the largest contribution to such change.

In 2001, 62.66% of forest regions were under dry conditions, and 38.90% were under extremely dry conditions (**Figure 3**). Meanwhile, 71.61% of grassland regions experienced drought, in which 32.51% were under D4 and D5 conditions. Most of forest and grassland regions were under wet conditions between 2002 and 2005. Both forest and grassland regions experienced an obvious drought in 2006. During 2006, 78.59% of the forest area and 55.49% of the grassland area were under dry conditions. Despite the widespread of dry conditions in 2006, most of regions were under D1-D3 conditions. After 2006, most of the forest regions were in wet conditions except in 2008 and 2011. Different drought levels occurred in most of the grassland regions until 2010. Overall, regions under wet conditions expanded gradually during the first half of the study period, and the dry spells expanded gradually in the grassland regions thereafter.

The Spatiotemporal Dynamics of Vegetation CUE and WUE

The spatial dynamics of CUE and WUE for forest and grassland were firstly evaluated. 53.74% of forest and grassland regions showed an overall increasing trend of CUE over the entire study period, which mainly distributed in eastern Mongolia, and southern Shaanxi. Regions showing decreased CUE mainly occurred in the mid-west of Inner Mongolia, northern Shaanxi, and Tianshan Mountains region. In contrast, WUE increased in 85.98% of forest and grassland regions. Regions showing a decreased WUE mainly distributed in southern Gansu and northwestern Qinghai (**Figure 4**).

The annual CUE, WUE, and DSI during this period were plotted against time. The average CUE of grassland during the 12-year period was 0.60, higher than that of forest (0.41) for the same period (**Figure 5**). The value of grassland CUE remained steady over the past 12 years. WUE of forest exhibited fluctuating increase from 2000 to 2011, and the minimum and maximum values exhibited in 2001 and 2009, respectively. The range of change for grassland WUE was less drastic than that for forest. The WUE of grassland also peaked in 2009. The overall variation in forest and grassland DSI can be divided into three stages: the wetting trend from 2000 to 2004, the drying trend from 2004 to 2009, and the wet recovery from 2009 to 2011. The most severe drought occurred in 2001. Averagely, the forest and grassland experienced wet conditions in 3 years, while drought occurred in forest and grassland areas in 2001, 2006, and 2008. In all other years, forest and grassland regions were under near normal conditions. The spatiotemporal dynamics of GPP, NPP, and ET were presented in the **Supplementary Material**.

The Controlling of Climatic Variables on Vegetation CUE and WUE

The correlations of vegetation CUE and WUE with DSI, MAP, and MAT were calculated to reveal the sensitivity of the vegetation carbon and water use to drought and climate variables. Regions with significant correlations (at 95 and 99% confidence level) between CUE and DSI amounted to 17.24% of the total study area. Area of forest regions that showed significant correlations (at 95 and 99% confidence level) between CUE and DSI reached 29.68% of the total forest regions, and 28.96% of this area exhibited positive correlations. For grassland, regions presenting significant positive and negative correlations between CUE and DSI accounted

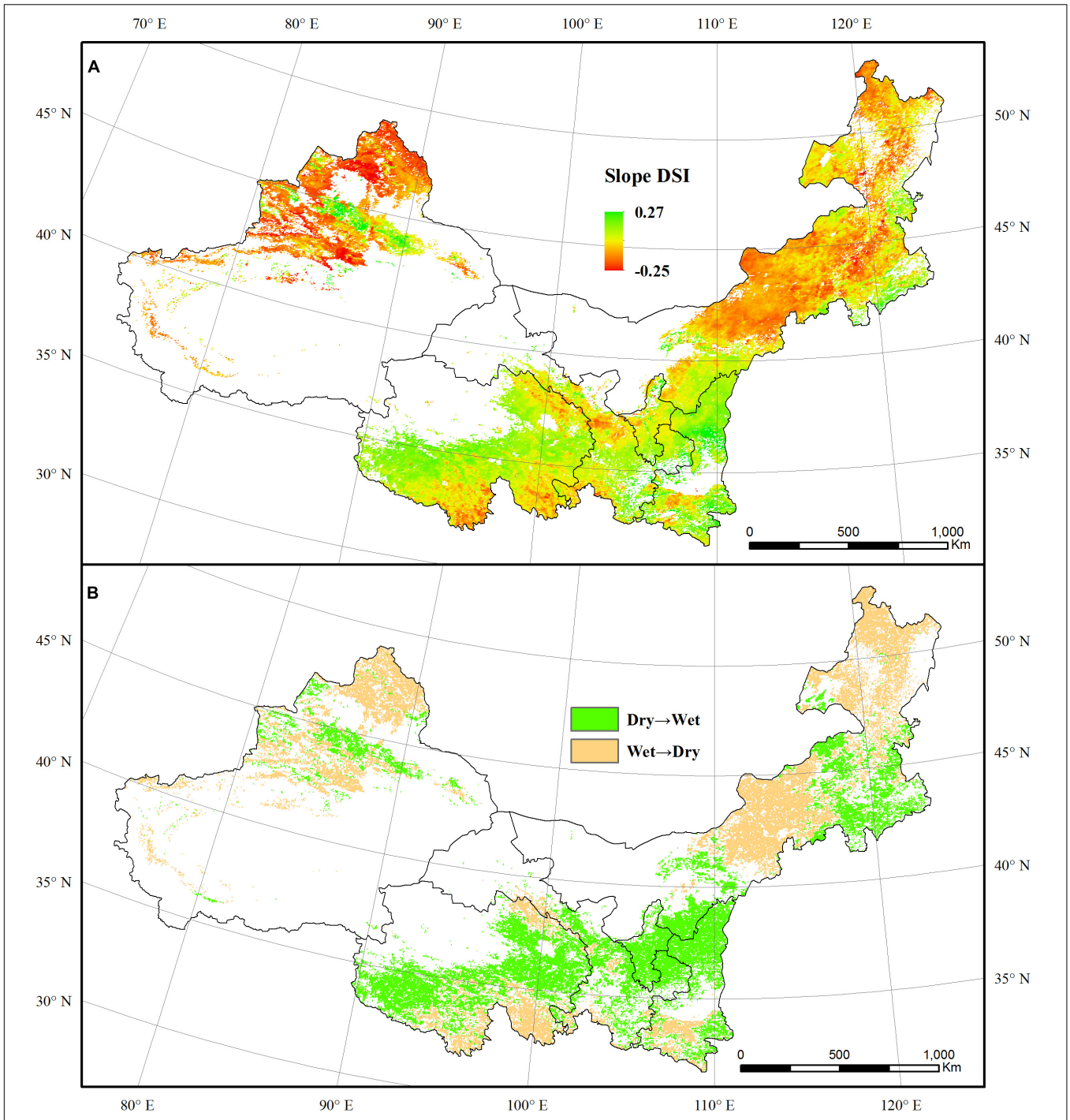

FIGURE 2 | The spatial pattern of Drought Severity Index (DSI) dynamic **(A)**, the wetting and drying trend **(B)** of vegetation in the NWIM region from 2000 to 2011.

for 5.23 and 3.04% of total grassland area, respectively. Regions showing significant correlations (at 95 and 99% confidence level) between CUE and MAP accounted for 10.52% of the total area. These regions were mainly located in eastern Inner Mongolia, southern Shaanxi, and Qinghai (**Figure 6**). For forest, 15.20% of the area showed significant correlations between CUE and MAP, with 11.09% exhibiting positive correlations and 4.11% exhibiting negative correlation. In contrast, 17.47% of grassland regions showed significant correlations (at 95 and 99% confidence level) between CUE and MAP, in which 7.85% were positive correlations and 9.62% were negatively correlations. There were significant correlations between CUE and MAT in 7.79% of forest regions and 9.92% of grassland regions (at 95 and 99% confidence level), respectively.

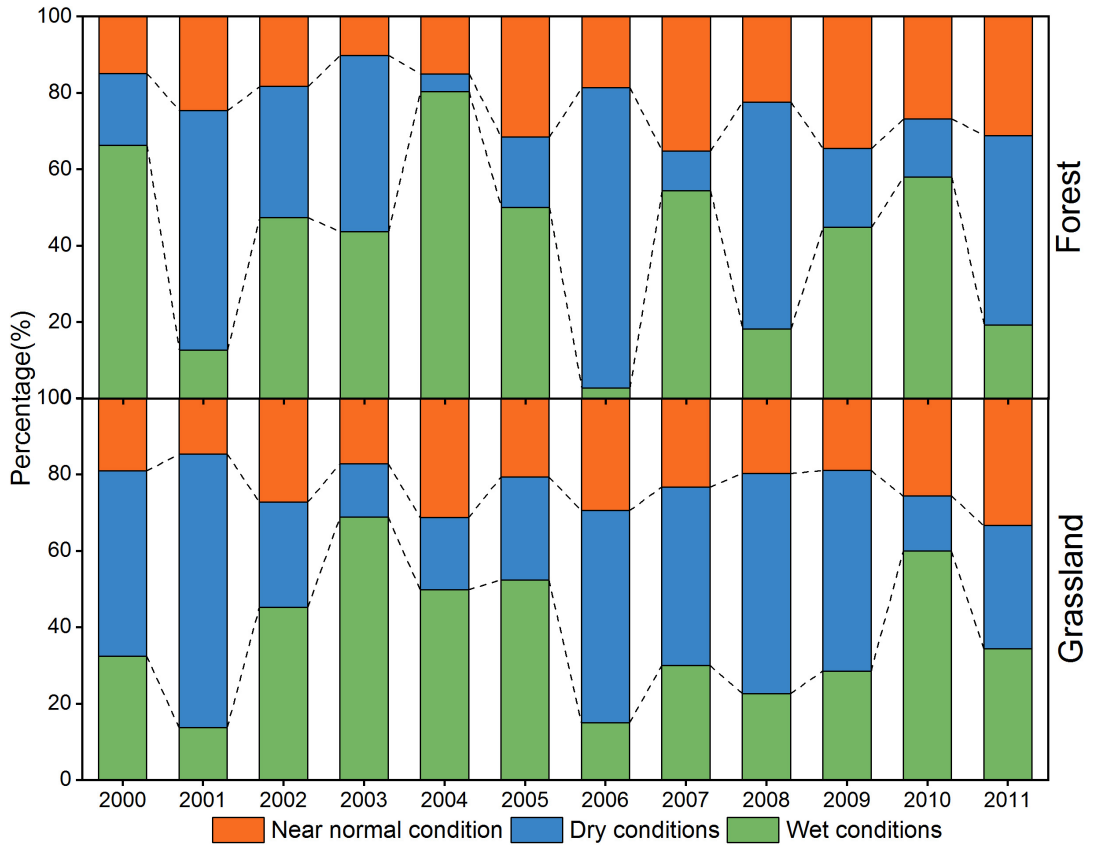

FIGURE 3 | The percentage change of dry, wet, near normal conditions for forest and grassland during 2000–2011.

Grassland regions showing significant positive and negative correlations (at 95 and 99% confidence level) between CUE and MAT accounted for 5.99 and 3.94% of total grassland areas, respectively.

Regions with significant correlations (at 95 and 99% confidence level) between WUE and DSI, MAP, and MAT accounted for 10.37, 12.48, and 8.67% of the total study area, respectively. These regions were mainly located in eastern Inner Mongolia, Ningxia, and southern Qinghai (**Figure 7**). Regions that showed a significant correlation (at 95 and 99% confidence level) between WUE and DSI accounted for 15.89% of the forest area and 9.70% of the grassland area. The forest area with significant positive correlations (at 95 and 99% confidence level) between WUE and DSI was larger than the area with significant negative correlations (11.33% vs. 4.56%). Forest WUE was more correlated with MAP. Regions with significant correlations (at 95 and 99% confidence level) between WUE and MAP amounted to 35.68% of the total forest area, and 34.17% of these regions exhibited positive correlation. Forest WUE exhibited significant negative correlation (at 95 and 99% confidence level) with MAT over 4.23% of the forest area, and 1.02% of the forest region exhibited significant positive correlation. For grassland, regions showing significant positive correlations (at 95 and 99% confidence level) between WUE and DSI, MAP, and MAT were larger than those showing the negative correlations. WUE exhibited positive correlations with DSI, MAP, and MAT in 5.91, 5.53, and 7.58% of total grassland area, respectively, and showed negative correlations in 3.78, 4.13 and 1.52% of total grassland area, respectively.

DISCUSSION

In this study, the drought status and its impacts on dryland vegetation in northern China was evaluated by exploring the satellite-based data. Drought severity in forest and grassland as well as its influence on CUE and WUE at the ecosystem scale were investigated. During the period of 2000–2011, most of the forest and grassland in the NWIM region were in near normal and wet conditions. The widespread droughts mainly occurred in 2001 and 2006, and the drought in 2001 was the most severe across the entire study period. Previous studies have demonstrated that widespread and large droughts were frequently recorded in northern China since the late 1990s, and they intensified after 2000. The 2001 drought is considered to be one of the most severe droughts in terms of distribution and duration, which led to extensive agricultural and economical losses (Zhang et al., 2016). The strength of the East Asian summer monsoon in the developing and decaying

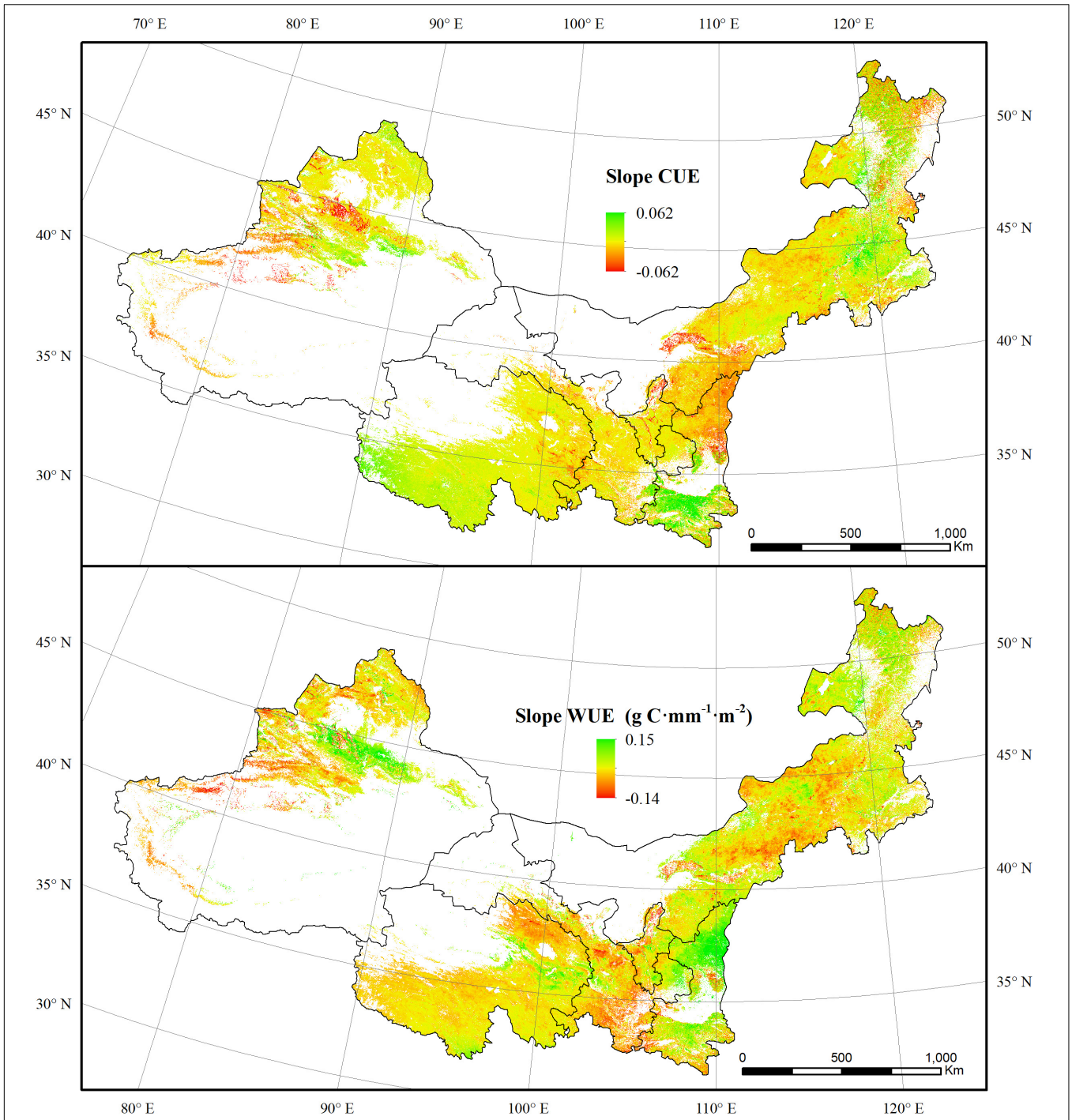

FIGURE 4 | The spatial dynamics of CUE and WUE for forest and grassland from 2000 to 2011.

phases of El Niño and La Niña events is probably one of the reasons that precipitated the recent drought in northern China (Yu et al., 2014).

Drought affects the vegetation carbon and water utilization mainly through influencing the photosynthesis and ET processes, particularly in regions where water supply is limited (Gang et al., 2016a). In this study, both the NPP and GPP for grassland increased during the 2000–2011 period. This synchronic changing pattern led to a steady state of grassland CUE during this period. In contrast, forest CUE was more sensitive to drought. The forest CUE presented a weak increasing trend with a curve similar to that of NPP. This was probably caused by the different sensitivities of forest NPP and GPP to the drought conditions (Zhang et al., 2014). In contrast,

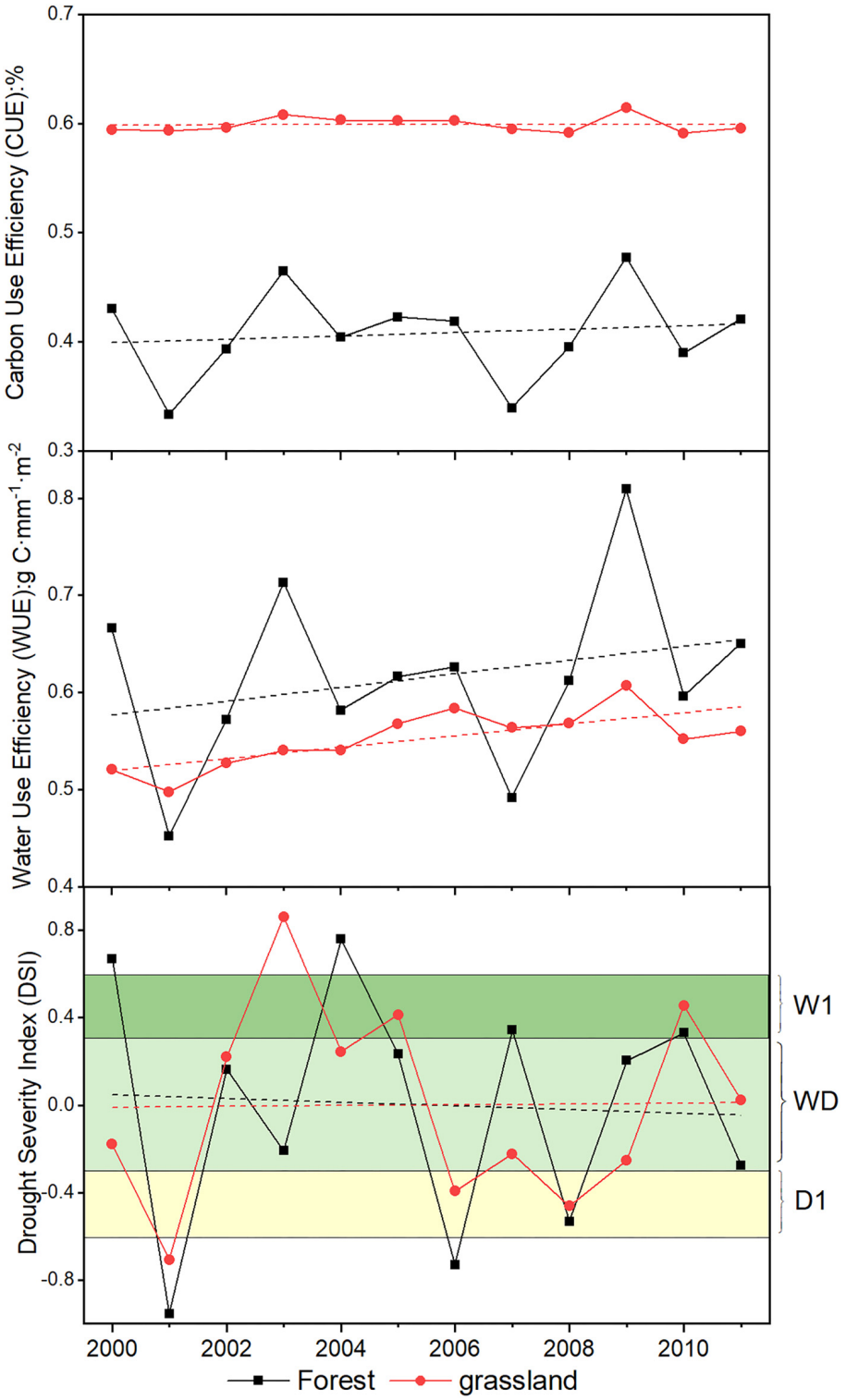

FIGURE 5 | The temporal dynamics of CUE, WUE, and DSI for forest and grassland from 2000 to 2011.

the rising NPP and decreasing ET both contributed to the overall ascending trend of WUE for forest and grassland. The WUE increased obviously in the Tianshan Mountains region and northern Shaanxi (**Figure 4**). The revegetation due to the "Grain for Green" project in the Loess Plateau has significantly increased the vegetation NPP during the past several decades

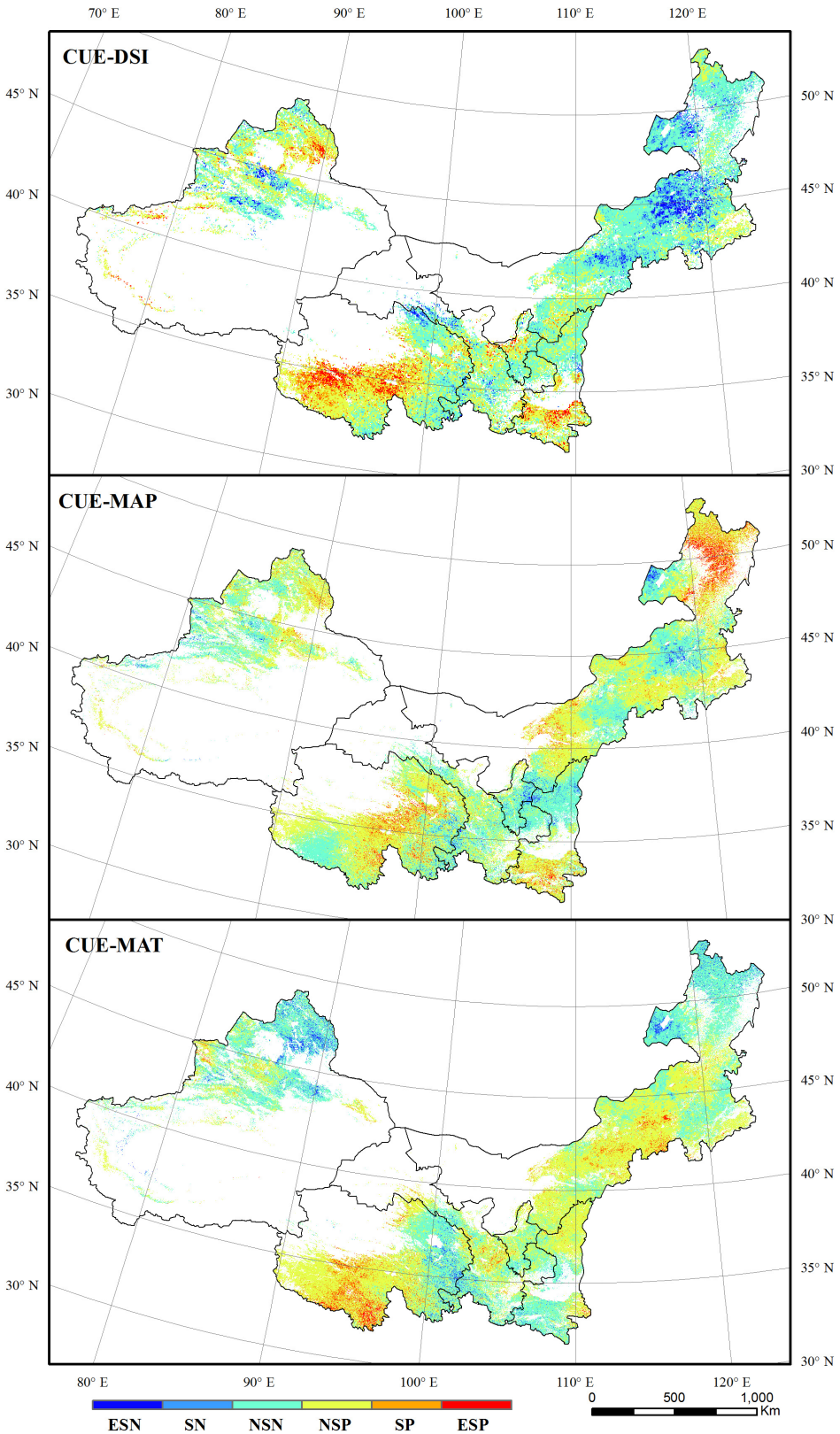

FIGURE 6 | The correlations between grassland CUE and DSI, MAP, and MAT. ESN, extremely significant negative; SN, significant negative; NSN, non-significant negative; NSP, non-significant positive; SP, significant positive; ESP, extremely significant positive.

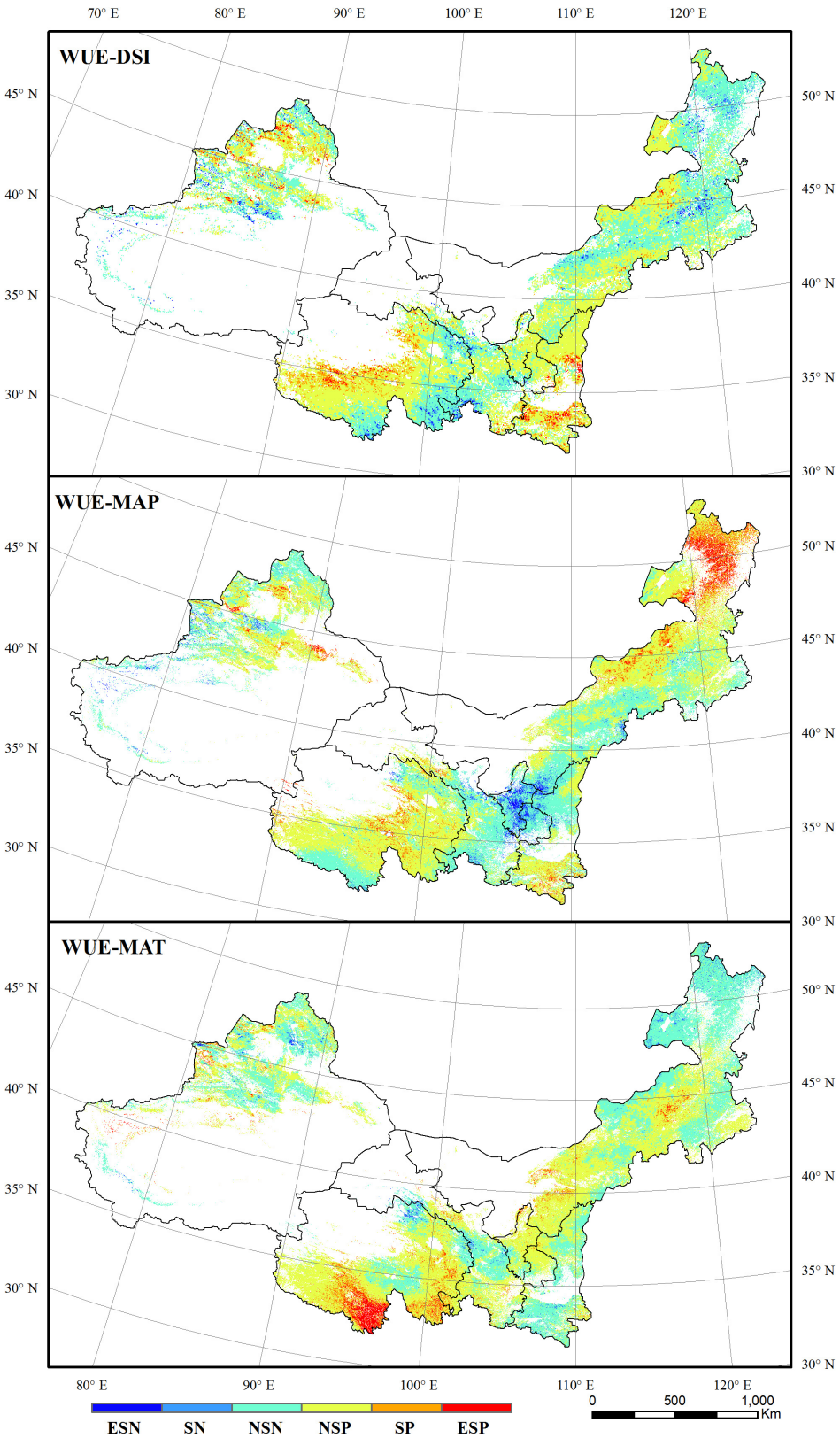

FIGURE 7 | The correlations between grassland WUE and DSI, MAP, and MAT. ESN, extremely significant negative; SN, significant negative; NSN, non-significant negative; NSP, non-significant positive; SP, significant positive; ESP, extremely significant positive.

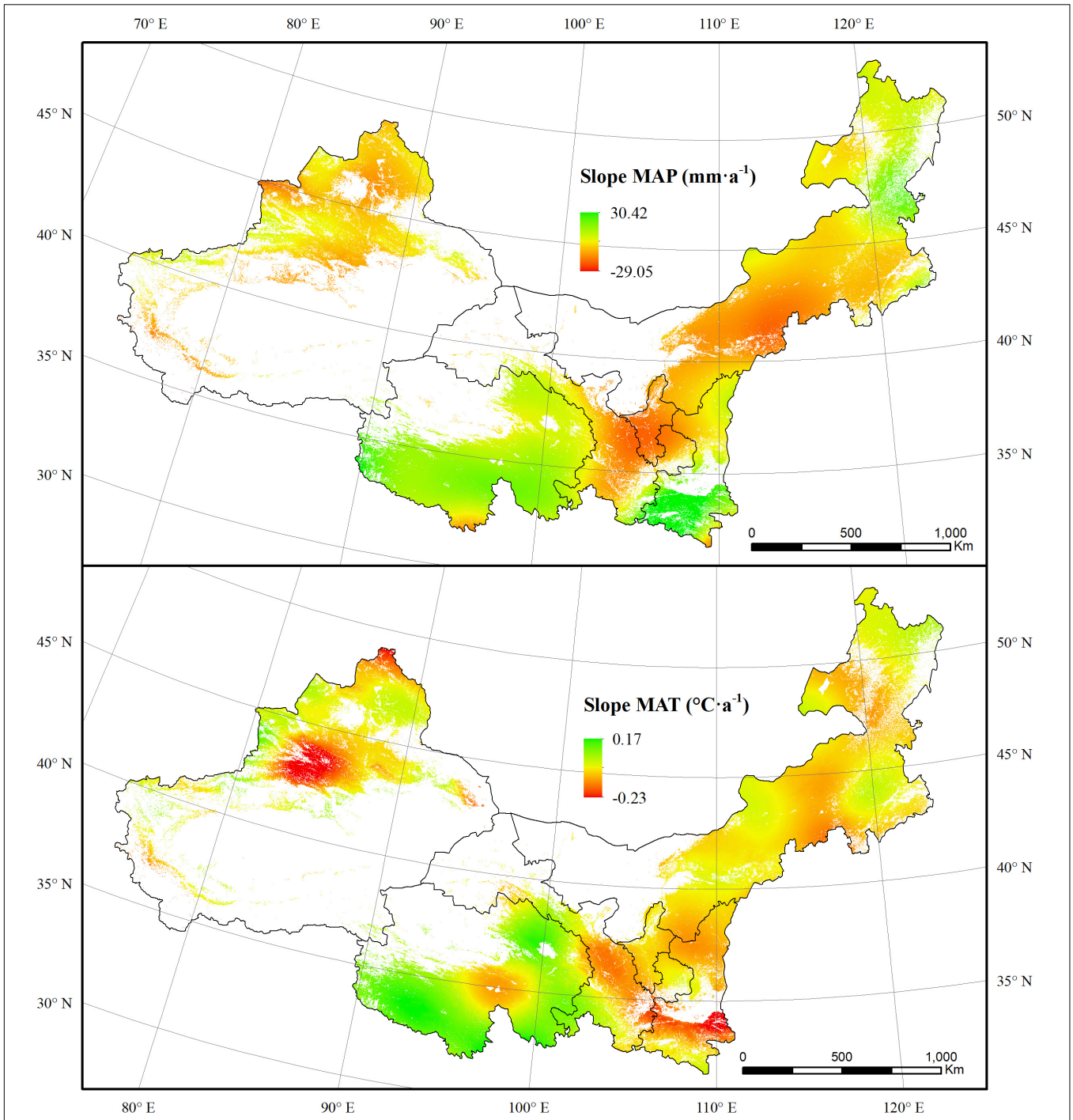

FIGURE 8 | The spatial dynamics of MAP and MAT for forest and grassland from 2000 to 2011.

(Xiao, 2014; Deng et al., 2017). The Tianshan Mountains region experienced a cooling trend, which probably is the leading reason for the WUE increase (**Figure 8**) (Guan et al., 2015). The canopy transpiration, net photosynthesis, and CO_2 exchange were constrained by soil moisture (Mu et al., 2013). Soil moisture status affects the responses of heterotrophic respiration and photosynthesis to temperature. When experiencing a slight drought, the net photosynthesis rate of plants would decreases due to the reduced activity of ribulose diphosphate carboxylase and reduced photosynthetic capacity of mesophyll cells (Zhou et al., 2009). The widespread drought that occurred in 2006 did not lead to sudden drops in CUE and WUE values in 2006. However, there were drops in 2007. This indicates that the effects of drought might accumulate and appear in the

following years. However, the photosynthetic organs of plants would be damaged under severe drought conditions. This would reduce plant water loss and photosynthesis (Arneth et al., 1998; Tian et al., 2009). This effect explains the obvious decreases of CUE and WUE in the 2001, when a widespread severe drought was recorded.

The correlation between vegetation WUE and DSI was relatively lower than the correlation between CUE and DSI. This implies that WUE was less sensitive to droughts than CUE for dryland vegetation in northern China. Drought affects the vegetation CUE mainly via the photosynthesis process (Gang et al., 2016b). Regions in eastern Inner Mongolia that are primarily vegetated by meadow showed significant negative correlations between CUE and DSI. The CUE increased in these regions despite a drying trend that was observed during 2000–2011. This increasing trend of CUE was probably caused by human interference, such as fencing or irrigation (Zhang et al., 2015; Yan et al., 2018). Regions showing significant positive correlations between CUE and DSI were mainly located in the northern fringe of Qinghai where became wet during the 12 years. The rising precipitation promotes the increase of both NPP and GPP in these regions (Bai et al., 2013). WUE can be affected by both the photosynthesis and ET process (Tian et al., 2010). Under slight and moderate drought conditions, the vegetation WUE would increase to mitigate the negative effects of water loss to some extent. This study found that area with significant positive correlations between WUE with MAP was larger than the area exhibiting significant positive correlations between WUE and DSI. This implies that rainfall more directly affected the vegetation WUE. Regions presenting the significant positive correlations between WUE and MAP were mainly distributed in eastern Inner Mongolia, Greater Khingan regions, where coniferous forests were mostly vegetated. Trees, such as *Larix gmelinii*, *Pinus tabulaeformis*, and *Abiescephalonica*, have higher WUE values because of low photosynthesis rates, ET rates, and stomatal conductance values (Lefi et al., 2004; Otieno et al., 2005). The photosynthesis ability can be maintained at a certain level even when a severe drought occurred (Maroco et al., 2000; Ogaya and Peñuelas, 2003; Lefi et al., 2004). Regions with a significant positive correlation between WUE and MAT were mainly distributed in the Three Rivers Source regions. This region is primarily characterized by alpine meadow. Temperature is reported as the primary factor affecting the growth of plants in this region (Xu et al., 2011; Guo et al., 2016).

CONCLUSION

The dryland vegetation in northern China was deeply influenced by the drought during the 2000–2011 period, and forest and grassland reacted differently to drought conditions. Nearly half of the NWIM region became dry in 2000–2011. The areas of forest that experienced a drying trend was more than four times larger than the areas that became wet, whereas the area of grassland regions presenting a drying trend was closer to the area showing a wetting trend. The most widespread droughts occurred in 2001 and 2006, and the drought severity was higher in 2001 than 2006. In general, most of the vegetation was under wet conditions during the first half of the study period, and grassland subsequently experienced more frequent drought than forest. The forest CUE increased slightly, whereas the CUE of grassland remained steady over the 12-year period. Meanwhile, the decreased ET values of forest and grassland led to the overall increases in WUE values for forest and grassland. The DSI variation adequately explains the temporal dynamics of forest CUE and WUE over this period. In contrast, the CUE and WUE values for grassland were less sensitive to the recent drought conditions. Although there are a few uncertainties, our results suggest that the carbon and water use of forest in northern China suffered more from the recent droughts than that of grassland. Due to the data availability, only the 12 years of DSI and CUE, and WUE data were evaluated in this study. Given the complexity of drought events and the warming climate, it is important to continuously monitor various drought impacts on ecosystem-scale carbon and water use in dryland vegetation under future climate change.

DATA AVAILABILITY

All datasets generated for this study are included in the manuscript and/or the **Supplementary Files**.

AUTHOR CONTRIBUTIONS

CG and ZW conceived and designed the research. CG, YZ, and MC collected the data and performed the research. LG, XG, and SP contributed data analysis and validation. CG wrote the manuscript.

FUNDING

This work was supported by the National Key Research and Development Program of China (Grant No. 2016YFC0501707), the National Natural Science Foundation of China (Grant No. 31602004), the CAS "Light of West China" program (Grant No. XAB2016B05), and the Fundamental Research Funds for the Central Universities (Grant No. 2452017184), the Special Foundation for State Basic Research Program of China (No. 2014YF210100), the Key cultivation project of Chinese Academy of Sciences "The promotion and management of ecosystem functions of restored vegetation in Loess Plateau, China." We also appreciate the China Meteorological Data Service Center and the NTSG for sharing dataset.

SUPPLEMENTARY MATERIAL

The Supplementary Material for this article can be found online at: https://www.frontiersin.org/articles/10.3389/fpls.2019.00224/full#supplementary-material

REFERENCES

AghaKouchak, A., Farahmand, A., Melton, F. S., Teixeira, J., Anderson, M. C., Wardlow, B. D., et al. (2015). Remote sensing of drought: progress, challenges and opportunities. *Rev. Geophys.* 53, 452–480. doi: 10.1002/2014RG000456

Arneth, A., Kelliher, F. M., McSeveny, T. M., and Byers, J. N. (1998). Net ecosystem productivity, net primary productivity and ecosystem carbon sequestration in a Pinus radiata plantation subject to soil water deficit. *Tree Physiol.* 18, 785–793. doi: 10.1093/treephys/18.12.785

Atkinson, P. M., Dash, J., and Jeganathan, C. (2011). Amazon vegetation greenness as measured by satellite sensors over the last decade. *Geophys. Res. Lett.* 38, 1–6. doi: 10.1029/2011GL049118

Bai, S., Shi, J., Xiang, D., and Wang, G. (2013). Spatiotemporal pattern change of precipitation in Qinghai in the last 50 years. *J. Arid Land Resourc. Environ.* 27, 148–153.

Beer, C., Ciais, P., Reichstein, M., Baldocchi, D., Law, B. E., Papale, D., et al. (2009). Temporal and among-site variability of inherent water use efficiency at the ecosystem level. *Glob. Biogeochem. Cycles* 23:GB2018. doi: 10.1029/2008GB003233

Chen, W. Y., Xiao, Q. G., and Sheng, Y. W. (1994). Application of the anomaly vegeta-tion index to monitor heavy drought in 1992. *Remote Sens. Environ. China* 9, 106–112.

Ciais, P., Reichstein, M., Viovy, N., Granier, A., Ogee, J., Allard, V., et al. (2005). Europe-wide reduction in primary productivity caused by the heat and drought in 2003. *Nature* 437, 529–533. doi: 10.1038/nature03972

Cunha, A. P. M., Alvala, R. C., Nobre, C. A., and Carvalho, M. A. (2015). Monitoring vegetative drought dynamics in the Brazilian semiarid region. *Agr. For. Meteorol.* 214, 494–505. doi: 10.1016/j.agrformet.2015.09.010

DeLucia, E. H., Drake, J. E., Thomas, R. B., and Gonzalez-Meler, M. (2007). Forest carbon use efficiency: is respiration a constant fraction of gross primary production? *Glob. Chang. Biol.* 13, 1157–1167. doi: 10.1111/j.1365-2486.2007.01365.x

Deng, L., Liu, S., Kim, D. G., Peng, C., Sweeney, S., and Shangguan, Z. (2017). Past and future carbon sequestration benefits of China's grain for green program. *Glob. Environ. Chang.* 47, 13–20. doi: 10.1016/j.gloenvcha.2017.09.006

Gang, C., Wang, Z., Chen, Y., Yang, Y., Li, J., Cheng, J., et al. (2016a). Drought-induced dynamics of carbon and water use efficiency of global grasslands from 2000 to 2011. *Ecol. Indic.* 67, 788–797. doi: 10.1016/j.ecolind.2016.03.049

Gang, C., Wang, Z., Zhou, W., Chen, Y., Li, J., Chen, J., et al. (2016b). Assessing the spatiotemporal dynamic of global grassland water use efficiency in response to climate change from 2000 to 2013. *J. Agron. Crop Sci.* 202, 343–354. doi: 10.1111/jac.12137

Gou, X., Gao, L., Deng, Y., Chen, F., Yang, M., and Still, C. (2015). An 850-year tree-ring-based reconstruction of drought history in the western Qilian Mountains of northwestern China. *Int. J. Climatol.* 35, 3308–3319. doi: 10.1002/joc.4208

Guan, Y., Wang, R., Li, C., Yao, J., Zhang, M., and Zhao, J. (2015). Spatial-temporal characteristics of land surface temperature in Tianshan Mountains area based on MODIS data. *Chin. J. Appl Ecol.* 26, 681–688.

Guo, B., Zhou, Y., Zhu, J., Liu, W., Wang, F., Wang, L., et al. (2016). Spatial patterns of ecosystem vulnerability changes during 2001-2011 in the three-river source region of the Qinghai-Tibetan Plateau. *China. J. Arid Land* 8, 23–35. doi: 10.1007/s40333-015-0055-7

Huang, J., Xue, Y., Sun, S., and Zhang, J. (2015). Spatial and temporal variability of drought during 1960-2012 in inner Mongolia, north China. *Quatern. Int.* 355, 134–144. doi: 10.1016/j.quaint.2014.10.036

Huete, A., Didan, K., Miura, T., Rodriguez, E. P., Gao, X., and Ferreira, L. G. (2002). Overview of the radiometric and biophysical performance of the MODIS vegetation indices. *Remote Sens. Environ.* 83, 195–213. doi: 10.1016/S0034-4257(02)00096-2

IPCC (2014). *Climate change 2014: Impacts, Adaptation and Vulnerability. Part A: Global and Sectoral Aspects. Contribution of Working Group II to the Fifth Assessment Report of the IPCC*. Cambridge: Cambridge University Press.

Jackson, R. B., Jobbágy, E. G., Avissar, R., Roy, S. B., Barrett, D. J., Cook, C. W., et al. (2005). Trading water for carbon with biological carbon sequestration. *Science* 310, 1944–1947. doi: 10.1126/science.1119282

Justice, C. O., Townshend, J., Vermote, E. F., Masuoka, E., Wolfe, R. E., Saleous, N., et al. (2002). An overview of MODIS land data processing and product status. *Remote Sens. Environ.* 83, 3–15. doi: 10.1016/S0034-4257(02)00084-6

Klisch, A., and Atzberger, C. (2016). Operational drought monitoring in kenya using MODIS NDVI time series. *Remote Sens.* 8:267. doi: 10.3390/rs8040267

Lefi, E., Medrano, H., and Cifre, J. (2004). Water uptake dynamics, photosynthesis and water use efficiency in field-grown *Medicago arborea* and *Medicago citrina* under prolonged Mediterranean drought conditions. *Ann. Appl. Biol.* 144, 299–307. doi: 10.1111/j.1744-7348.2004.tb00345.x

LeHouerou, H. N. (1984). Rain use efficiency: a unifying concept in arid-land ecology. *J. Arid Environ.* 7, 213–247.

Liu, Y., Xiao, J., Ju, W., Zhou, Y., Wang, S., and Wu, X. (2015). Water use efficiency of China's terrestrial ecosystems and responses to drought. *Sci. Rep.* 5:13799. doi: 10.1038/srep13799

Liu, Z., Shao, Q., and Liu, J. (2015). The performances of MODIS-GPP and-ET products in China and their sensitivity to input data (FPAR/LAI). *Remote Sens.* 7, 135–152. doi: 10.3390/rs70100135

Loveland, T. R., Reed, B. C., Brown, J. F., Ohlen, D. O., Zhu, Z., Yang, L., et al. (2000). Development of a global land cover characteristics database and IGBP DISCover from 1 km AVHRR data. *Int. J. Remote Sens.* 21, 1303–1330. doi: 10.1080/014311600210191

Maroco, J. P., Pereira, J. S., and Chaves, M. M. (2000). Growth, photosynthesis and water-use efficiency of two C4Sahelian grasses subjected to water deficits. *J. Arid Environ.* 45, 119–137. doi: 10.1006/jare.2000.0638

McKee, T. B., Doesken, N. J., and Kleist, J. (1995). "Drought monitoring with multiple time scales," in *Proceeding of the Ninth Conference on Applied Climatology*, (Boston, MA: American Meteorological Society), 233–236.

Mu, Q., Heinsch, F. A., Zhao, M., and Running, S. W. (2007a). Development of a global evapotranspiration algorithm based on MODIS and global meteorology data. *Remote Sens. Environ.* 111, 519–536. doi: 10.1016/j.rse.2007.04.015

Mu, Q., Zhao, M., Heinsch, F. A., Liu, M., Tian, H., and Running, S. W. (2007b). Evaluating water stress controls on primary production in biogeochemical and remote sensing based models. *J. Geophys. Res.* 112:G01012. doi: 10.1029/2006JG000179

Mu, Q., Zhao, M., Kimball, J. S., McDowell, N. G., and Running, S. W. (2013). A remotely sensed global terrestrial drought severity index. *Bull. Am. Meteorol. Soc.* 94, 83–98. doi: 10.1175/BAMS-D-11-00213.1

Mu, Q., Zhao, M., and Running, S. W. (2011). Improvements to a MODIS global terrestrial evapotranspiration algorithm. *Remote Sens. Environ.* 115, 1781–1800. doi: 10.1016/j.rse.2011.02.019

Ogaya, R., and Peñuelas, J. (2003). Comparative field study of *Quercus ilex* and *Phillyrea latifolia*: photosynthetic response to experimental drought conditions. *Environ. Exp. Bot.* 50, 137–148. doi: 10.1016/S0098-8472(03)00019-4

Otieno, D. O., Schmidt, M., Kinyamario, J. I., and Tenhunen, J. (2005). Responses of *Acacia tortilis* and *Acacia xanthophloea* to seasonal changes in soil water availability in the savanna region of Kenya. *J. Arid Environ.* 62, 377–400. doi: 10.1016/j.jaridenv.2005.01.001

Palmer, W. C. (1965). *Meteorological Drought*. Washington, DC: Weather Bureau.

Peters, A. J., Walter-Shea, E. A., Ji, L., Vina, A., Hayes, M., and Svoboda, M. D. (2002). Drought monitoring with NDVI-based standardized vegetation index. *Photogramm. Eng. Remote Sens.* 68, 71–75.

Rhee, J. Y., Im, J. H., and Carbone, G. J. (2010). Monitoring agricultural drought for arid and humid regions using multi-sensor remote sensing data. *Remote Sens. Environ.* 114, 2875–2887. doi: 10.1016/j.rse.2010.07.005

Rojas, O., Vrieling, A., and Rembold, F. (2011). Assessing drought probability for agricultural areas in Africa with coarse resolution remote sensing imagery. *Remote Sens. Environ.* 115, 343–352. doi: 10.1016/j.rse.2010.09.006

Rosegrant, M. W., Cai, X., and Cline, S. A. (2003). Will the world run dry? Global water and food security. *Environ. Sci. Policy Sustain. Dev.* 45, 24–36. doi: 10.1080/00139150309604555

Sandholt, I., Rasmussen, K., and Andersen, J. (2002). A simple interpretation of the surface temperature/vegetation index space for assessment of surface moisture status. *Remote Sens. Environ.* 79, 213–224. doi: 10.1016/S0034-4257(01)00274-7

Shakya, N., and Yamaguchi, Y. (2010). Vegetation, water and thermal stress index for study of drought in Nepal and central northeastern India. *Int. J. Remote Sens.* 31, 903–912. doi: 10.1080/01431160902902617

Shi, Y., Shen, Y., Kang, E., Li, D., Ding, Y., Zhang, G., et al. (2007). Recent and future climate change in northwest China. *Clim. Chang.* 80, 379–393. doi: 10.1007/s10584-006-9121-7

Tian, H., Chen, G., Liu, M., Zhang, C., Sun, G., Lu, C., et al. (2010). Model estimates of net primary productivity, evapotranspiration, and water use efficiency in the

terrestrial ecosystems of the southern United States during 1895-2007. *For. Ecol. Manag.* 259, 1311–1327. doi: 10.1016/j.foreco.2009.10.009

Tian, Y. Q., Gao, Q., Zhang, Z. C., Zhang, Y., and Zhu, K. (2009). The advances in study on plant photosynthesis and soil respiration of alpine grasslands on the Tibetan Plateau. *Ecol. Environ. Sci.* 18, 711–721. doi: 10.1016/j.foreco.2009.10.009

Vorosmarty, C. J., Green, P., Salisbury, J., and Lammers, R. B. (2000). Global water resources: vulnerability from climate change and population growth. *Science* 289, 284–288. doi: 10.1126/science.289.5477.284

Wang, H., Chen, Y., and Pan, Y. (2015). Characteristics of drought in the arid region of northwestern China. *Clim. Res.* 62, 99–113. doi: 10.3354/cr01266

Wang, H., Chen, Y., Xun, S., Lai, D., Fan, Y., and Li, Z. (2013). Changes in daily climate extremes in the arid area of northwestern China. *Theor. Appl. Climatol.* 112, 15–28. doi: 10.1007/s00704-012-0698-7

Wang, X., Ma, M., Li, X., Song, Y., Tan, J., Huang, G., et al. (2013). Validation of MODIS-GPP product at 10 flux sites in northern China. *Int. J. Remote Sens.* 34, 587–599. doi: 10.1080/01431161.2012.715774

Webb, W., Szarek, S., Lauenroth, W., Kinerson, R., and Smith, M. (1978). Primary productivity and water-use in native forest, grassland, and desert ecosystems. *Ecology* 59, 1239–1247. doi: 10.2307/1938237

Xiao, J. (2014). Satellite evidence for significant biophysical consequences of the "Grain for Green" Program on the Loess Plateau in China. *J. Geophys. Res. Biogeosci.* 119, 2261–2275. doi: 10.1002/2014JG002820

Xu, W., Gu, S., Zhao, X., Xiao, J., Tang, Y., Fang, J., et al. (2011). High positive correlation between soil temperature and NDVI from 1982 to 2006 in alpine meadow of the three-river source region on the qinghai-tibetan plateau. *Int. J. Appl. Earth Obs.* 13, 528–535. doi: 10.1016/j.jag.2011.02.001

Yan, Y., Wan, Z., Chao, R., Ge, Y., Chen, Y., Gu, R., et al. (2018). A comprehensive appraisal of four kinds of forage under irrigation in Xilingol, Inner Mongolia, China. *Rangel. J.* 40, 171–178. doi: 10.1071/RJ16084

Yu, M., Li, Q., Hayes, M. J., Svoboda, M. D., and Heim, R. R. (2014). Are droughts becoming more frequent or severe in China based on the standardized precipitation evapotranspiration index: 1951-2010? *Int. J. Climatol.* 34, 545–558. doi: 10.1002/joc.3701

Zhang, J., Huang, Y., Chen, H., Gong, J., Qi, Y., and Yang, F. (2015). Effects of grassland management on the community structure, aboveground biomass and stability of a temperate steppe in Inner Mongolia. *China. J. Arid Land* 8, 422–433. doi: 10.1007/s40333-016-0002-2

Zhang, J., Mu, Q., and Huang, J. (2016). assessing the remotely sensed drought severity index for agricultural drought monitoring and impact analysis in North China. *Ecol. Indic.* 63, 296–309. doi: 10.1016/j.ecolind.2015.11.062

Zhang, X. Q., and Yamaguchi, Y. (2014). Characterization and evaluation of MODIS-derived Drought Severity Index (DSI) for monitoring the 2009/2010 drought over southwestern China. *Nat. Hazards* 74, 2129–2145. doi: 10.1007/s11069-014-1278-1

Zhang, Y., Yu, G., Yang, J., Wimberly, M. C., Zhang, X., Tao, J., et al. (2014). Climate-driven global changes in carbon use efficiency. *Glob. Ecol. Biogeogr.* 23, 144–155. doi: 10.1111/geb.12086

Zhao, M., Heinsch, F. A., Nemani, R. R., and Running, S. W. (2005). Improvements of the MODIS terrestrial gross and net primary production global data set. *Remote Sens. Environ.* 95, 164–176. doi: 10.1016/j.rse.2004.12.011

Zhao, M., and Running, S. W. (2010). Drought-induced reduction in global terrestrial net primary production from 2000 through 2009. *Science* 329, 940–943. doi: 10.1126/science.1192666

Zhao, M., and Running, S. W. (2011). Response to comments on "Drought-induced reduction in global terrestrial net primary production from 2000 through 2009". *Science* 333, 1093–1093. doi: 10.1126/science.1199169

Zhao, M., Running, S. W., and Nemani, R. R. (2006). Sensitivity of Moderate Resolution Imaging Spectroradiometer (MODIS) terrestrial primary production to the accuracy of meteorological reanalyses. *J. Geophys. Res.* 111:G01002. doi: 10.1029/2004JG000004

Zhou, Q., Cheng, J., Wan, H., and Yu, J. (2009). Study on the diurnal variations of photosynthetic characteristics and water use efficiency of Stipa bungeana Trin. under drought stress. *Acta Agrestia Sin.* 17, 510–514.

Conflict of Interest Statement: The authors declare that the research was conducted in the absence of any commercial or financial relationships that could be construed as a potential conflict of interest.

frontiers in Plant Science

ORIGINAL RESEARCH
published: 05 March 2019
doi: 10.3389/fpls.2019.00220

Shelterbelt Poplar Forests Induced Soil Changes in Deep Soil Profiles and Climates Contributed Their Inter-site Variations in Dryland Regions, Northeastern China

Yan Wu[1], *Qiong Wang*[3], *Huimei Wang*[3], *Wenjie Wang*[3]* *and Shijie Han*[2]*

[1] Department of Biological Engineering, Da Qing Normal University, Daqing, China, [2] Department of Life Science, Henan University, Kaifeng, China, [3] Key Laboratory of Forest Plant Ecology, Northeast Forestry University, Harbin, China

The influence of shelterbelt afforestation on soils in different-depth profiles and possible interaction with climatic conditions is important for evaluating ecological effects of large-scale afforestation programs. In the Songnen Plain, northeastern China, 720 soil samples were collected from five different soil layers (0–20, 20–40, 40–60, 60–80, and 80–100 cm) in shelterbelt poplar forests and neighboring farmlands. Soil physiochemical properties [pH, electrical conductivity (EC), soil porosity, soil moisture and bulk density], soil carbon and nutrients [soil organic carbon (SOC), N, alkaline-hydrolyzed N, P, available P, K and available K], forest characteristics [tree height, diameter at breast height (DBH), and density], climatic conditions [mean annual temperature (MAT), mean annual precipitation (MAP), and aridity index (ARID)], and soil texture (percentage of silt, clay, and sand) were measured. We found that the effects of shelterbelt afforestation on bulk density, porosity, available K, and total P were observed up to 100 cm deep; while the changes in available K and P were several-fold higher in the 0–20 cm soil layer than that in deeper layers ($p < 0.05$). For other parameters (soil pH and EC), shelterbelt-influences were mainly observed in surface soils, e.g., EC was 14.7% lower in shelterbelt plantations than that in farmlands in the 0–20 cm layer, about 2.5–3.5-fold higher than 60–100 cm soil inclusion. For soil moisture, shelterbelt afforestation decreased soil water by 7.3–8.7% in deep soils ($p < 0.05$), while no significant change was in 0–20 cm soil. For SOC and N, no significant differences between shelterbelt and farmlands were found in all five-depth soil profiles. Large inter-site variations were found for all shelterbelt-induced soil changes ($p < 0.05$) except for total K in the 0–20 cm layer. MAT and silt content provided the greatest explanation powers for inter-site variations in shelterbelt-induced soil properties changes. However, in deeper soils, water (ARID and MAP) explained more of the variation than that in surface soils. Therefore, shelterbelt afforestation in northeastern China could affect aspects of soil properties down to 100 cm deep, with inter-site variations mainly controlled by climate and soil texture, and greater contribution from water characteristics in deeper soils.

Keywords: poplar shelterbelt, farmlands, soil properties change, deep-layer soil, analysis of causes

OPEN ACCESS

Edited by:
Zhiyou Yuan,
College of Forestry, Northwest A&F University, China

Reviewed by:
Lu-Jun Li,
Northeast Institute of Geography and Agroecology (CAS), China
Guofan Shao,
Purdue University, United States

***Correspondence:**
Wenjie Wang
wwj225@nefu.edu.cn
Shijie Han
hansj@iae.ac.cn

Specialty section:
This article was submitted to Plant Abiotic Stress, a section of the journal Frontiers in Plant Science

Received: *28 September 2018*
Accepted: *08 February 2019*
Published: *05 March 2019*

Citation:
Wu Y, Wang Q, Wang H, Wang W and Han S (2019) Shelterbelt Poplar Forests Induced Soil Changes in Deep Soil Profiles and Climates Contributed Their Inter-site Variations in Dryland Regions, Northeastern China. Front. Plant Sci. 10:220. doi: 10.3389/fpls.2019.00220

INTRODUCTION

Globally, ecological shelterbelt engineering projects, such as the Great Plains Shelterbelt Project (Roosevelt Engineering) in the USA, the Great Plan for the Transformation of Nature in the former Soviet Union, forestry and water conservation projects in Japan, the Green Dam Engineering Project in the five countries of North Africa, and the Three-North Shelterbelt Program in China, have increased the scientific study of shelterbelt forests (Zhang et al., 2016). There are numerous forest plantations worldwide, many of which were planted in degraded or abandoned farmlands and are used as agricultural protection forests or bioenergy forests in China (Wang G. Y. et al., 2018; Zhang et al., 2018) and worldwide (Deniz and Paletto, 2018; Jha, 2018). The area of shelterbelt forests used for protecting soil and water increased to 330 million ha globally by 2010, accounting for 8% of all forest areas. The largest proportion of shelterbelt forests is in Asia (26%), 33% of which are in East Asia, and China's shelterbelt forests account for most of that area (60 million ha of the total 83 million ha) (Obschatko et al., 2010). There are approximately 6.67 million ha of poplar plantations that are widely distributed in China. The large shelterbelt forest area in China makes it a good example for studying the ecological functions of shelterbelt forests, and underground soil changes are an important issue to fully understand the functions of forests (Zhu, 2013; Wang et al., 2015, 2017b; Wu and Wang, 2016; Wang Q. et al., 2017; Zhong et al., 2017; Nan et al., 2018).

Black soils in northeastern China are mainly located in the Songnen Plain and Sanjiang Plain, which contain one of the three global black soil belts, and over 45% of the total grain output in northeastern China is produced in this region (Wang et al., 2009b). Although the black soils in northeastern China contain abundant soil organic matter and have high fertility compared with other soils (Cas, 1980; Hljtr, 1992), excessive historical reclamation has led to sharp decreases in soil fertility since the establishment of the People's Republic of China in 1949 (Wang et al., 1996) and nearly half of the nitrogen and soil organic matter has been lost from the black soils in northeastern China (Ding and Liu, 1980; Wang, 2002; Wang et al., 2011b). Several studies have shown that afforestation in cultivated farmland soils induced changes in most soil properties and soil fertility, contributing to soil improvement in different cases (Li and Cui, 2000; Wang Q. et al., 2014; Wang et al., 2017a). Shelterbelts of different ages and tree species could effectively reduce nitrate nitrogen by 22–60% (Jaskulska and Jaskulska, 2017), and also regulate soil physiochemical properties, fertility, and carbon sequestration (Wang et al., 2017a). In addition, soil physical properties could be altered from afforestation practices, including increases in soil bulk density and decreases in total porosity, water retention, and ventilation capacity (Wang, 2002; Wang et al., 2011b, 2017a). However, other studies also found that fast-growing plantations, such as larch, poplar, or eucalyptus, require more soil nutrients, and water (Chen, 1998; Mendham et al., 2003; Merino et al., 2004; Zhang et al., 2004; Li Y. et al., 2018), which is possibly induced by deep soil changes in various soil properties (Wang H. M. et al., 2014; Wang W. J. et al., 2014). Most of these studies have been undertaken in surface soils <40 cm deep with the assumption of neglectable changes in deep soils relative to surface soils. However, other studies have found that deep soils can sensitively react to land use changes (Fontaine et al., 2010; Rukshana et al., 2011), especially for tree species that have relatively longer roots compared to crops (Wang Q. et al., 2014; Wang S. et al., 2017).

Songnen Plain was named after the Songhua and Nenjiang Rivers running through this region. This plain has been recognized as the northern-most region of the Three-North Shelterbelt Program (Wu and Wang, 2016). Songnen Plain is about 18.28 million ha and locates in the transitional region between the semi-moist and semi-arid region, featured as saline-alkalinization and heavy farmland soil degradation (Li, 2000; Wang et al., 2011a) as well as natural forest degradation (Dai et al., 2018). Our previous study has shown that poplar shelterbelt afforestation in northeastern China slightly changed SOC sequestration and N nutrients in the surface (20 cm) soils, with sharp decreases in bulk density (Wu et al., 2018), with no consideration in deep soils (>20 cm). Moreover, glomalin-related soil carbon sequestration was higher in deep soils than that in surface soils, with more response to climatic changes in the farmlands of this region (Wang et al., 2017b). Most poplar roots concentrated in the 0–60 cm soils, and the influence of vegetation growth and microbial activities on soils may extend over the depth of the roots (Jobbágy and Jackson, 2000). Annual precipitation in Songnen Plain ranges from 300 to 500 mm, with a 2–3-fold higher annual evaporation (1,000–1,500 mm) (Li, 2000). This natural background, heavy pressure from farming and grazing, and fast saline-alkalinization in soil are important challenges for social development and livelihood in this region (Li, 2000; Wang et al., 2011a). The evaluation of shelterbelt afforestation on underground soils in this region must fully consider the variations in the widespread plain, and fully understanding of the underlying mechanisms needs more consideration on forest characteristics, climatic conditions including the aridity index (ARID), soil texture both at surface and deep soils (Wang W. J. et al., 2014; Wu et al., 2018).

In the present study, we alleged that deep soils at 100 cm depth should be included in the evaluation of various soil changes in poplar afforestation, and large inter-site variation in the shelterbelt forest-induced soil changes were related to local climatic differences, soil texture, and forest growth. We posed several research questions as follows: (1) Should deep soil layers be included in the evaluations of soil improvements from degraded farmlands to poplar forests and did these improvements differ in different soil parameters? (2) How great a difference among locations occurred in the shelterbelt-induced soil changes, and which factors of climatic condition, soil texture, and tree growth parameter were responsible for these variations? By evaluating the shelterbelt-induced soil changes in various properties in different soil layers, our data assisted the evaluation of underground soil changes in large scale shelterbelt programs, such as the Three-North Shelterbelt Program, particularly the quantification of the importance of deep soils for afforestation practices in degraded farmlands.

MATERIALS AND METHODS

Study Sites and Sample Collection

The Three-North Shelterbelt Program established tree plantations around farmlands in northern China, northwestern China, and northeastern China in 1978 (Zhu, 2013). The general design was to plant 4–10 rows of poplars around 500 × 500 m of farmland, and large areas of shelterbelts around farmlands are found everywhere throughout the Songnen Plain of northeastern China (**Figure 1**). Nowadays, the most-used poplar variety in northeast regions (young forests) is Yinzhong poplar (*Populus alba* × *Populus berolinensis*), while historically, the most-planted poplars were *Populus simonii, Populus* × *xiaohei*, and *Populus deltoides* ×*P. canadensis*, etc. (Wu et al., 2018).

Six study sites (Dumeng, Fuyu, Lanling, Mingshui, Zhaodong, and Zhaozhou) distributed in the Songnen Plain in the middle of northeastern China were selected as study sites (**Figure 1**). The soil types in the study region are typical black soils, including Chernozem (Fuyu, Lanling), Phaeozem (Mingshui), Cambosols (Dumeng), and some degraded soil, such as Solonetz (Zhaozhou, Zhaodong). This region has a continental monsoon climate, with MAT of 2.9–4.4°C, MAP of 350–500 mm, and ARID of 0.4–0.7.

Soil samples were collected from 72 paired shelterbelt plantations and farmland plots in the six study sites. Five soil profiles were collected from each paired plot. After the exclusion of the A0 layer, we sampled 100 cm of soil from 0 to 20, 20 to 40, 40 to 60, 60 to 80, and 80 to 100 cm depths. Additionally, we obtained a composite sample by mixing five samples from the same soil layers from each of the five soil profiles. In total, 720 soil samples (6 regions × 2 (farmland and shelterbelt) × 12 sites/region × 5 depths/site = 720 samples) were collected.

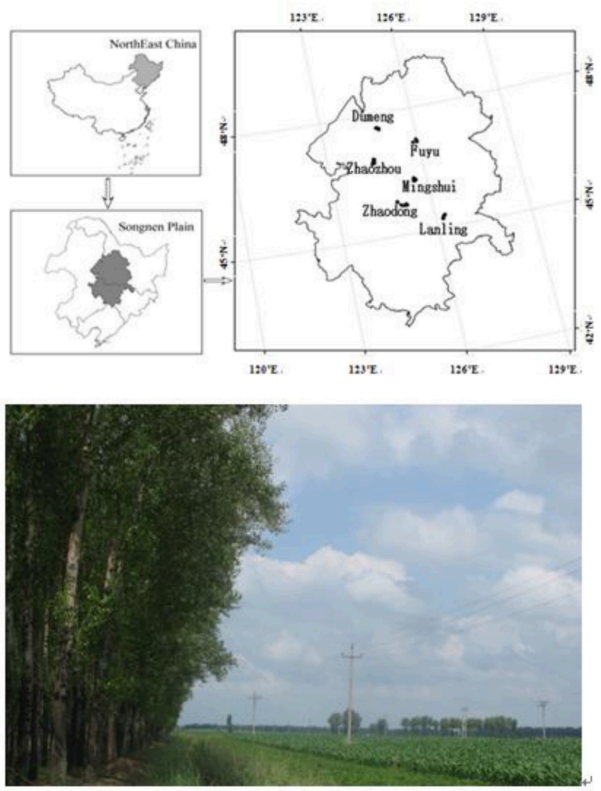

FIGURE 1 | Six study sites in the Songnen Plain, Northeastern China, and a typical poplar shelterbelt-farmland paired site. Parts of this figures was adapted from our previous publication (Wu et al., 2018).

Determination of Soil Parameters

Sample preparation details and some of the soil parameters analysis (e.g., bulk density, soil moisture, SOC, total N, available N, total K, available K, total P, available P, and soil texture) have been described previously by Wu et al. (2018). Soil porosity was calculated by the following formula: soil porosity = (1−bulk density/specific gravity) × 100%. The pH of the soil solution (one-part soil to five-parts water) was measured with an acidity meter (Sartorius PT-21, Shanghai, China). Soil electrical conductivity (EC) was determined with an EC meter (DDS-307, Shanghai Precision Scientific Instruments Co., Ltd., Shanghai, China) (Bao, 2000). Soil carbon or nutrient storage were computed as:

Farmland soil carbon or nutrient storage $= \alpha_f \times \rho_f \times 0.2 \times (1-V_{gravel})$

Poplar soil carbon or nutrient storage $= \alpha_p \times \rho_p \times 0.2 \times \rho_f/\rho_p \times (1-V_{gravel})$

where, α_f and α_p are the concentrations of farmland and poplar SOC (g kg^{-1}); ρ_f and ρ_p are farmland and poplar soil bulk densities (Mg m^{-3}), respectively; 0.2 is the soil thickness (0.2 m); and V_{gravel} is the proportion of gravel. Details regarding the bulk density correction can be found in Wuest (2009) and Wu et al. (2018).

Forest Characteristics, Soil Texture, and Climatic Data Collection

Poplar forest characteristics of tree density, tree height, and DBH were measured at each plot site. Regarding the distance between forest and farmland, 42% (30 plots) of plots were <3.4 m from neighboring farmland, while 47% (34 plots) were 3.4 to 6.7 m away. To reduce the influence of roots on neighboring farmlands, ditches of about 2 m in width and 2 m in depth were excavated between shelterbelt and farmland by local farmers. Forest characteristics data of 72 plots can be found in Wu et al. (2018).

The soil texture was the relative amount of sand, silt, and clay in the bulk soil, measured using a rapid and simple method described by Kettler et al. (2001) and Wu et al. (2018).

MAT and MAP at the six sites were obtained from the meteorological scientific data sharing service network of China (http://cdc.cma.gov.cn/) and the ARID was computed as the MAP over the mean annual reference evapotranspiration (Huo et al., 2013).

Data Analysis

Calculation of storage at different soils depth, such as 0–20 cm, 0–40 cm, 0–60 cm, 0–80 cm, and 1 m soil profiles, is a general rule for many previous studies for ease of comparison among studies (Wang et al., 2011b; Wei et al., 2014; Wang H. M. et al., 2017a; Deng et al., 2018). In this paper, in order to compare soil carbon or nutrient storage with other studies, we have re-grouped

our data from 0 to 20, 20 to 40, 40 to 60, 60 to 80, and 80 to 100 cm into 0 to 20, 0 to 40, 0 to 60, 0 to 80, and 0 to 100 cm by combining the corresponding soil layer's measured data. For example, 0–20 and 20–40 cm were combined into one set of 0–40 cm by average of two data; Similarly, combining 0–40 and 40–60 cm into 0–60 cm, combining 0–60 and 60–80 cm into 0–80 cm, and combining 0–60 and 80–100 cm into 0–100 cm during dada analysis in order to evaluate the effects of afforestation on soil properties in five soil-depth profiles.

Multivariate analysis of variance (MANOVA) was used to determine the influence of land use type (shelterbelt forest and neighboring farmland), sampling location (Dumeng, Fuyu, Lanling, Mingshui, Zhaodong, and Zhaozhou), and their interaction on various soil parameters. The 19 parameters (soil bulk density, soil porosity, soil moisture, pH, EC, SOC concentration, total N concentration, alkaline hydrolyzed N concentration, total P concentration, available P concentration, total K concentration, available K concentration, SOC storage, total N storage, alkaline hydrolyzed storage, total P storage, available P storage, total K storage, and available K storage) were used as dependent variables.

A paired *t*-test was used to determine the difference in soil properties between shelterbelt plantations and farmlands at different soil depths, and the Duncan's test was used for multiple comparisons among different soil-depth profiles for all shelterbelt-induced soil changes. In the present study, the relative change [(forest—farmland)/farmland] of each soil parameter was treated as a dependent variable for the following analysis.

Redundancy analysis (RDA) was conducted to ordinate the complex associations between shelterbelt-induced variations in various soil properties and climatic conditions, soil texture, and forest characteristics (Canoco 5.0 software program). Ordination was performed in all five soil-depth profile, as we wanted to find the differences in different soil depths. Conditional term effects (excluding collinear effects among different dependent parameters) were derived from the RDA, and the possible factors contributing to the dependent variables (e.g., shelterbelt-forest-induced changes in soil properties as a whole). In conditional term effects, the significant factor with the highest explanation percentage showed the strongest contribution to the variation of soil properties. Details explaining the RDA ordination can be found in previous studies (Wang et al., 2017b, 2018b).

Stepwise regression analysis was used to explore the factors responsible for the poplar-induced changes in various soil properties in the five soil layers. Statistical significance was evaluated at $p = 0.05$, unless otherwise stated. Three groups of parameters, forest characteristics (tree height, DBH, and tree density), soil texture (sand, silt, and clay), and climatic conditions (MAT, MAP, and ARID), were tested as independent parameters. The more entering times, and more frequent parameter into the stepwise models indicate the stronger influence from these parameters for explaining the variations of soil properties from shelterbelt afforestation. By using this criteria, stepwise regression models were analyzed for simplifying the presentation of the data and facilitate data interpretation.

RESULTS

Land Use Type and Sampling Location Affect All Soil Parameters: Manova Results

Table 1 showed the influences of soil use type, sampling location, and their interaction on the soil parameters at five depths. Significant land use effects (farmland and poplar forest) were observed in bulk density, porosity, and total P storage for all five depths. Significant differences between the two land uses on pH, EC, available K concentration, and available K storage were found in the 0–20 cm depth, whereas others, such as soil moisture, total K, total P, available P concentration, and available P storage were statistically different among the two land uses in the deeper soil layers (>20 cm).

Compared with land use differences, there were even larger significant location-related differences among all parameters in all five soil depths. Moreover, significant interactions existed among the influence of land use and sampling location on some soil parameters in different layers (**Table 1**). For example, the influence of shelterbelt plantations on porosity, total K concentration, and available P concentration significantly interacted with location in the five depths, indicating that these shelterbelt-induced changes significantly differed among the six locations in all soil layers.

Changes in Soil Properties Between Shelterbelt Plantations and Farmlands at Five Soil-Depth Profiles: Overall Patterns

The effects of shelterbelt construction on soil properties in the five soil-depth profiles and the differences in shelterbelt-induced soil changes in various parameters among the five profiles were shown in **Table 2**.

The effects of shelterbelt construction on soil properties varied in five soil depth layers. Some indicators, such as bulk density, porosity, available K concentration, and total P storage, had significant difference at five soil depth. However, some indicators, such as SOC concentration (storage), total N concentration (storage), and available N concentration (storage) had no significant change on five profiles following shelterbelt establishment. Moreover, the effects of afforestation on the surface soils were more obvious than at depth for pH and EC. On the contrary, the effect of soil moisture was seen mainly in the deeper soil profiles (**Table 2**).

The significances among the five soil-depth profiles were distinct for different shelterbelt-induced soil properties changes. First, opposite trends ($p < 0.05$) were observed in shelterbelt-induced soil moisture and EC changes between surface and deeper soil layers. A 6.2% increase in soil moisture (poplar compared with farmland) was observed in the 0–20 cm layer, whereas there was a 7.3–8.7% decrease in the deep soil profiles. Contrary to soil moisture, EC was 14.7% lower in shelterbelt plantations than that in farmlands in the surface layer, but was 4.1, 6.2, and 4.2% higher in the 0–60, 0–80, 0–100 cm layers, respectively (**Table 2**). Second, the changes in available K and P were several-fold higher in the 0–20 cm soil profiles than that in the deeper profiles ($p < 0.05$). For

TABLE 1 | Shelterbelt plantation establishment, sampling regions, influences various soil parameters, and possible interacts at different depths.

Dependent Variable	0–20 cm			0–40 cm			0–60 cm			0–80 cm			0–100 cm		
	T	L	T *L	T	L	T *L	T	L	T *L	T	L	T *L	T	L	T *L
PHYSIOCHEMICAL PROPERTIES															
Bulk density (g/cm^3)	**	***	*	***	***	*	***	***	ns	***	***	**	***	***	**
Porosity (%)	*	***	**	*	***	*	*	***	***	**	***	**	**	***	**
Soil moisture (%)	ns	***	***	ns	***	ns	*	***	ns	*	***	ns	*	***	ns
pH	***	***	**	*	***	ns	ns	***	ns	ns	***	ns	ns	***	ns
EC(μS/cm)	***	***	***	ns	***	***	ns	***	***	ns	***	**	ns	***	ns
SOIL CARBON AND NUTRIENT IN CONCENTRATION															
SOC concentration(g/kg)	ns	***	ns	ns	***	ns	ns	***	ns	ns	***	ns	ns	***	ns
Total N (g/kg)	ns	***	ns	ns	***	ns	ns	***	ns	ns	***	ns	ns	***	ns
Alkaline hydrolyzed N (mg/kg)	ns	**	ns	ns	***	ns	ns	***	ns	ns	***	ns	ns	***	ns
Total K (g/kg)	ns	ns	**	ns	*	***	*	**	***	***	***	***	ns	***	***
Available K(mg/kg)	***	*	ns	ns	**	ns	ns	**	ns	ns	***	ns	ns	***	ns
Total P (g/kg)	ns	***	ns	*	***	ns	*	***	ns	*	***	ns	ns	***	ns
Available P (mg/kg)	ns	***	*	ns	***	*	*	***	**	*	***	**	ns	***	***
SOIL CARBON AND NUTRIENT IN STORAGE															
SOC (kg/m^2)	ns	***	ns	ns	***	ns	ns	***	ns	ns	***	ns	ns	***	ns
Total N (kg/m^2)	ns	***	*	ns	***	ns	ns	***	ns	ns	***	***	ns	***	ns
Alkaline hydrolyzed N (g/m^2)	ns	**	ns	ns	***	ns	ns	***	ns	ns	***	ns	ns	***	ns
Total K (kg/m^2)	**	ns	***	*	***	***	ns	***	***	*	***	ns	ns	***	***
Available K(g/m^2)	***	**	ns	ns	**	ns	ns	***	ns	ns	***	ns	ns	***	ns
Total P (kg/m^2)	*	***	ns	***	***	ns	***	***	ns	***	***	ns	*	***	ns
Available P (g/m^2)	ns	***	*	ns	***	ns	**	***	*	**	***	**	*	***	***

$^{***}p < 0.001$, $^{**}p < 0.01$, $^{*}p < 0.05$, ns, no significant difference ($p > 0.05$) T, Type; L, Location.

TABLE 2 | A comparison in soil properties between shelterbelt plantation and farmland at five depths and the differences in shelterbelt-induced soil changes among five profiles.

	Type	0–20 cm	0–40 cm	0–60 cm	0–80 cm	0–100 cm
PHYSIOCHEMICAL PROPERTIES						
Bulk density (g/cm^3)	Farmland	1.42	1.44	1.45	1.46	1.47
	Poplar	1.37*	1.38***	1.37***	1.40***	1.41***
	Change (%)	−3.1a	−4.1 a	−5.5 a	−4.2a	−4.3a
Porosity (%)	Farmland	42.30	41.13	39.99	39.03	38.87
	Poplar	45.33*	43.46*	42.08*	41.41**	40.76**
	Change (%)	13.7a	8.2a	8.0a	8.4a	6.7a
Soil moisture (%)	Farmland	12.56	13.41	13.16	12.67	12.35
	Poplar	12.92 ns	12.60*	12.19**	11.75**	11.42***
	Change (%)	6.2a	−7.3b	−8.7b	−8.0b	−7.9b
pH	Farmland	7.83	7.89	8.00	8.08	8.11
	Poplar	8.08***	8.04***	8.07 ns	8.14*	8.18*
	Change (%)	3.2a	2.0ab	0.9b	0.9b	0.9b
EC (μS/cm)	Farmland	159.85	127.78	116.87	112.16	108.39
	Poplar	105.22***	112.71 ns	113.07 ns	112.34 ns	108.45 ns
	Change (%)	−14.7b	−0.1ab	4.1a	6.2a	4.2a
NUTRIENT CONCENTRATION						
Total K (g/kg)	Farmland	44.38	48.28	47.17	48.36	50.84
	Poplar	40.34 ns	46.86 ns	49.26 ns	53.21 ***	52.55 ns
	Change (%)	27.6a	0.9a	7.3a	12.6a	5.5a
Available K (mg/kg)	Farmland	82.92	72.89	69.05	85.56	61.78
	Poplar	135.23***	89.34***	78.83**	99.16***	71.77***
	Change (%)	117.4a	39.2b	29.5b	26.3b	24.6b
Total P (g/kg)	Farmland	0.47	0.41	0.37	0.34	0.31
	Poplar	0.42 ns	0.37*	0.33*	0.31*	0.30 ns
	Change (%)	1.9a	−2.4a	−3.2a	−3.5a	0.6a
Available P (mg/kg)	Farmland	5.36	4.68	6.10	5.90	6.14
	Poplar	4.88 ns	4.15 ns	5.21 ns	5.16 ns	5.68 ns
	Change (%)	28.3a	6.1b	1.0b	−0.2b	3.5b
NUTRIENT STORAGE						
Total K (kg/m^2)	Farmland	12.86	13.97	13.72	14.2	15.01
	Poplar	11.03*	12.97*	13.64 ns	14.92 ns	14.81 ns
	Change (%)	−0.7a	−2.8a	2.8a	8.1a	1.1a
Available K (g/m^2)	Farmland	22.74	20.07	20.15	24.89	18.09
	Poplar	36.77***	24.46**	21.80 ns	27.53*	20.04*
	Change (%)	108.3a	33.6b	24.0b	21.1b	19.0b
Total P (kg/m^2)	Farmland	0.13	0.12	0.11	0.10	0.09
	Poplar	0.11*	0.10***	0.09**	0.09***	0.08*
	Change (%)	−2.8a	−8.7a	−7.4a	−7.7a	−3.7a
Available P (g/m^2)	Farmland	1.51	1.35	1.76	1.72	1.80
	Poplar	1.34 ns	1.14 ns	1.44*	1.44*	1.59 ns
	Change (%)	22.9a	2.1b	−3.0b	−4.3b	−0.5b

**** indicates significant differences between shelterbelt plantation and farmland at different profiles at $p < 0.001$, ** indicates the significant differences at $p < 0.01$, * indicates the significant differences at $p < 0.05$. ns indicates no significant difference ($p > 0.05$). The same letters denoted not significant difference among five profiles in shelterbelt-induced soil properties change ($p > 0.05$), while different letters denoted significant difference ($p < 0.05$). In addition, those parameters, which are not significant differences between shelterbelt plantation and farmland at different profiles and not significant difference among five profiles in shelterbelt-induced change among five profiles at the same time, are not shown in **Table 2** (such as SOC, total N, and Alkaline hydrolyzed N).*

example, a 117.4% increase in available K concentration was observed in the surface layer, whereas only a 24.6–39.2% increase was observed in the deeper layers. A 28.3% increase in available P concentration in shelterbelt plantations was observed in the surface layer, whereas a −0.2–6.1% change was found in the deeper layers. Third, no significant changes ($p > 0.05$) were found among the five soil profiles for the other properties.

Shelterbelt-Induced Soil Parameter Changes: Large Inter-site Variations Differed With Soil Depth

All soil parameters except total K concentration and total K storage showed marked location-related differences in the five depths among the different sites (**Table 1**). The vertical pattern and magnitude of differences are shown in **Figure 2** and **Table A1**.

The location differences were soil-depth dependent, i.e., in most cases, the surface soil layer showed much larger location differences in the poplar forest-induced changes in various soil properties (**Figure 2**). For example, inter-site differences in soil bulk density and soil water were −10 to 5% and −25 to 60% respectively, whereas those in deep soils (0–100 cm) were, respectively −9 to −1% and −20 to 0%. However, for other parameters, similar inter-site differences were found among surface and deep soils, with even larger variation in deep soils, for example, soil available P and SOC for both concentration and storage (**Figure 2**).

Depth-induced significant differences were observed in soil moisture, pH, EC, available K concentration and storage, and available P concentration and storage (**Table 2**), with large inter-site variations found among the different sites (**Figure 2** and **Table A1**). There was a higher amount of available K concentration in the surface layer than that in the other four soil layers (**Table 2**). This trend mainly occurred in Dumeng, Fuyu, Mingshui, and Zhaodong ($p < 0.05$), with a 221.8% increase in the 0–20 cm layer and an average 0–20 cm layer and an average 46.8% increase in the other four profiles at Dumeng, whereas there was a 79.9% increase in the surface layer and an average 15.9% increase in the deeper profiles at Mingshui (**Table A1**). Moreover, although no significant differences were observed in three of the soil parameters (porosity, total K concentration, and total K storage) among the five soil layers (**Table 2**), inter-site differences were found among the different sites. For example, there were significant differences ($p < 0.05$) among the five soil profiles in total K concentration and storage at Dumeng, Fuyu, and Mingshui, with a 24.1% decrease in the 0–20 cm layer and an average 1.8% increase in the deeper profiles at Dumeng, and a 42.8% decrease in the surface and an average 17.5% decrease in the deeper profiles at Mingshui (**Table A1**).

RDA Ordination: Climatic, Soil Texture and Forest Controls on the Inter-site Variations and Differences Between Surface and Deep Soils

As shown in **Table 3**, in general, climatic conditions provided the largest explaining power for the inter-site variations of

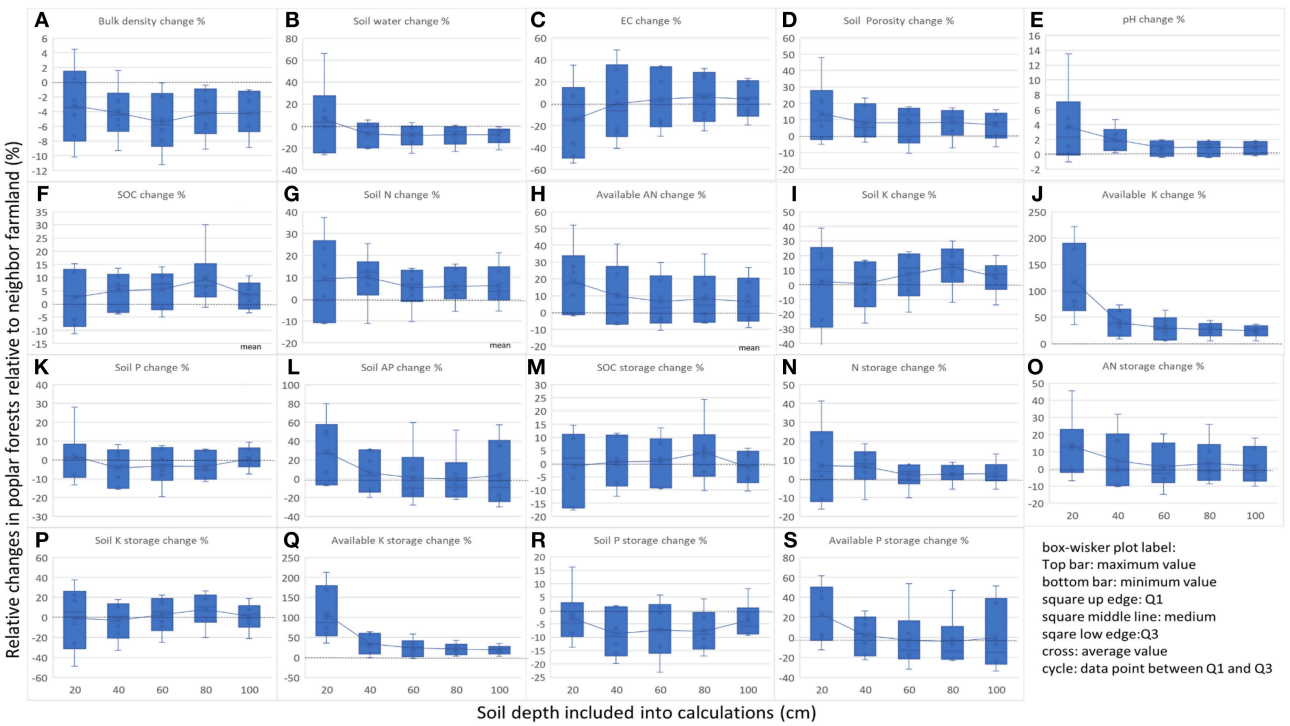

FIGURE 2 | Changes of various soil properties in poplar forests compared with neighbor farmland, and differences at 1 m profiles. Dash line in the figure showed the zero line, indicating that no changes relative to neighbor farmland. Statistics of the mean values had shown in **Table 2** and **Table A1**. **(A)** Soil bulk density change %; **(B)** Soil water change %; **(C)** Soil EC change %; **(D)** Soil porosity change %; **(E)** Soil pH change %; **(F)** Soil organic carbon concentration change %; **(G)** Soil total N concentration change %; **(H)** Soil alkaline hydrolyzed N concentration change %; **(I)** Soil total K concentration change %; **(J)** Soil alkaline K concentration change %; **(K)** Soil total P concentration change %; **(L)** Soil alkaline P concentration change %; **(M)** Soil organic carbon storage change %; **(N)** Soil total N storage change %; **(O)** Soil alkaline hydrolyzed N storage change %; **(P)** Soil total K storage change %; **(Q)** Soil alkaline K storage change %; **(R)** Soil total P storage change %; **(S)** Soil alkaline P storage change %.

TABLE 3 | Comparison on the explaining power from climatic condition, soil texture, and forest characteristics for the forest-induced soil changes at different locations from the RDA ordination-related conditional term effects excluding their collinear effects.

Soil inclusion		Explains %	pseudo-F	*P*	RDA ordination figure
0–20 cm	Silt	7.8	5.9	0.002	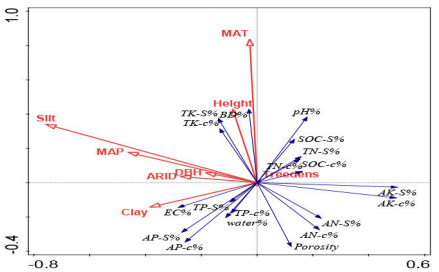
	MAT	4.9	3.9	0.004	
	DBH	3.1	2.6	0.028	
	MAP	2.8	2.2	0.042	
	ARID	1.4	1.2	0.276	
	Treedensity	1.3	1.1	0.374	
	Height	1.1	0.9	0.51	
0–40 cm	MAT	5.1	3.9	0.004	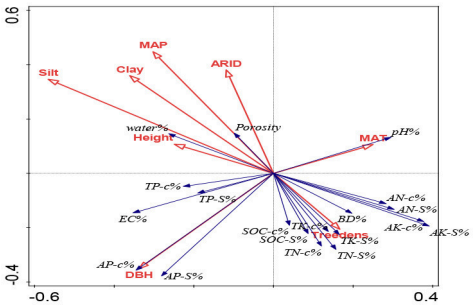
	Silt	4.5	3.3	0.004	
	Height	2.5	2	0.05	
	MAP	2.4	1.9	0.08	
	DBH	2.4	1.9	0.086	
	Treedensity	2	1.6	0.15	
	ARID	1	0.8	0.612	
	Clay	0.8	0.7	0.682	
0–60 cm	MAT	4.4	3.2	0.004	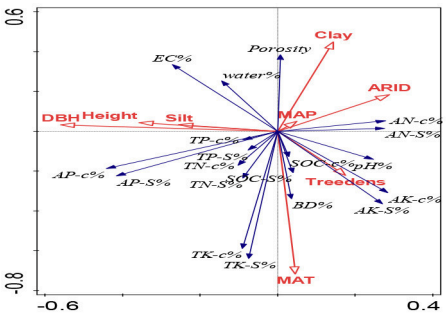
	DBH	3.6	2.8	0.008	
	Silt	3.3	2.5	0.01	
	ARID	3	2.2	0.036	
	Clay	1.8	1.4	0.182	
	Height	1.4	1.1	0.338	
	Treedensity	1	0.8	0.574	
	MAP	1	0.8	0.608	
0–80 cm	ARID	3.9	2.9	0.008	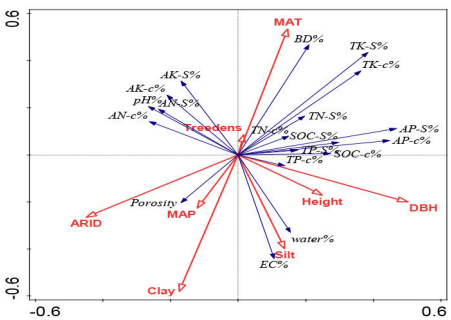
	DBH	3.5	2.7	0.01	
	Silt	3.5	2.7	0.018	
	MAT	3	2.1	0.036	
	Height	1.3	1	0.394	
	Treedensity	0.8	0.6	0.73	
	Clay	0.6	0.5	0.842	
	MAP	0.6	0.5	0.852	
0-100cm	MAP	6.9	5.3	0.002	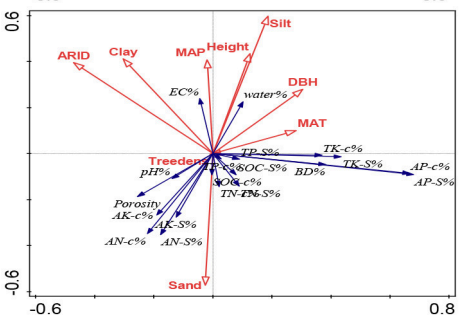
	ARID	4.6	3.4	0.006	
	MAT	3.5	2.8	0.01	
	DBH	2.7	2.2	0.034	
	Silt	2.1	1.7	0.124	
	Sand	1.5	1.2	0.276	
	Clay	1.4	1.2	0.308	
	Height	1.2	1	0.378	

shelterbelt-induced soil changes. Moreover, at different soil layers, MAT was the most influential parameter, providing the highest explanation percentage. For example, MAT explained 4.9, 5.1, 4.4, 3.0, and 3.5% of the forest-induced soil variations for 20, 40, 60, 80, and 100 cm depth soils, respectively (**Table 3**). In deeper soils, ARID and MAP explained much more of the variation than that in the surface soil layer. For example, ARID in 20 cm, 40 cm soils did not show significant explanation for the variations, while in 60, 80, and 100 cm soils, ARID showed significant explaining powers ranged from 3.0–4.6% ($p < 0.05$); and MAP explained 6.9% of the variations for 100 cm soil layers ($p < 0.01$) (**Table 3**).

Following the climatic conditions, soil texture gave the next largest explanation power for the location-related variations and silt showed significant explanation percentage in four out of five soil layers ($p < 0.05$) (**Table 3**). In general, the deep soils, the less explaining power from soil texture of silt percentage. In 20 and 40 cm soils, silt's explaining percentage was 4.5–7.8% ($p < 0.001$), and this percentage was 3.3–3.5% in 60 and 80 cm soils ($p < 0.05$), and no significant explaining percentage was found in 100 cm soil ($p = 0.124$) (**Table 3**).

In addition, tree growth traits (DBH and height) also significantly explained the shelterbelt-induced soil variations at different locations, and their explaining powers ranged from 2.5 to 3.6% at different soil layers ($p < 0.05$) (**Table 3**).

Stepwise Regression Statistics: Factors Related to the Inter-site Variations and Differences Between Surface and Deep Soils

As a further step to decouple the association, stepwise regression analysis was used to determine the most possible parameters for the large inter-site variations (**Table A2**).

For each soil properties, we found different associations with climatic conditions. For example, positive correlations were observed between shelterbelt-induced soil bulk density change and MAT in all layers expect for the 0–40 cm depth. Although soil texture and tree growth significantly accounted for shelterbelt-induced porosity change in the 0–20 cm layer, MAT was the leading factor that determined the porosity change in the other four soil depths ($r^2 = 0.10$–0.18, $p < 0.05$). The pH change was significantly related to MAT in the 0–20 and 0–40 cm depth layers, and the shelterbelt-induced EC decrease was accompanied with higher MAT in all five soil profiles. Significant positive correlations were found between SOC storage change, total K concentration (storage) changes, and MAT ($p < 0.05$). In the deep soil layers (0–80 and 0–100 cm), ARID was the significant affecting factor ($r^2 = 0.32$, $p < 0.001$) for bulk density changes compared with the surface soil layer. Similar significant negative correlations were found between available P (concentration and storage) and ARID in the deeper soil profiles. Higher ARID accounted for the poplar-induced total K decrease in the five soil profiles ($r^2 = 0.15$–0.46, $p < 0.001$), whereas the available K (concentration and storage) changes in the 0–100 cm depth could be explained by ARID and MAP ($r^2 = 0.39$ and $r^2 = 0.40$, respectively) (**Table A2**).

For soil silt percentage, significant positive correlations were found among silt percentage and EC, available P concentration, whereas marked negative correlations were found in the shelterbelt-induced differences in seven soil parameters in the different soil depths (including porosity, total N concentration, alkaline hydrolyzed N concentration, available K concentration, total N storage, alkaline hydrolyzed N storage, and available K storage) (**Table A2**). For tree growth parameters, DBH, Tree height, and Tree density have been found in different stepwise regression models in different soil layers; However, their appearances were not as often as that of climatic parameters and soil textures (**Table A2**).

By counting the entering times for each tested parameter observed in all stepwise regression models, we want to confirm the findings in RDA ordination, and the basic criteria is that the more entering times mean the more influences on soils from this parameter (**Figure 3**). Comparison among climate, soil texture and tree growth, we found the most entering times from climatic factors (10–12 entering times), followed by soil texture (3–7 entering times), and tree growth factors (0–7 entering times); This is the similar to those observed in RDA ordination (**Table 3**). In the case of different climatic parameters, we found that MAT showed the most influences (5–8 entering times), followed by ARID (2–5 entering times) and MAP (1–2 entering times) (**Figure 3**). At the vertical soil profiles, MAT's influences decreased from surface to deep soils, as shown by eight entering times in 20 cm soils and five entering times in 100 cm soils. However, ARID's influences showed a contrary pattern, i.e., lower influences were at surface soils (two entering times in 20 cm), while much stronger influences were in deep soils (five entering times) in 80 cm and 100 cm soils (**Figure 3**).

Soil texture showed the similar entering times at the surface (5–7 entering times) and deep (3–7 entering times) soils, and 2–4 times entering into stepwise models were observed from silt percentage at five depths soil (**Figure 3**). In the case of DBH, two entering times were found in 100 cm soil, while 0–1 time entering to the stepwise models was found in other soils (**Figure 3**).

DISCUSSION

Higher Water Consumption in Deep Soils, Saline-Alkalinization in Surface Soils, and Better Physical Structure in the Entire 100 cm Soil Profile Following Shelterbelt Plantations

Our study highlighted significant water consumption in deeper soil layers in poplar forests in northeast China. There were significant decreases (7.3–8.7%) in 0–40 cm and deeper soils ($p < 0.05$), while a slight increase was found in 0–20 cm layer (**Table 2**). Artificial afforestation can decrease soil moisture because of leaf interception and root uptake (Jin et al., 2011). Divergent hydrological response to large-scale afforestation has been found on a national scale throughout China (Li Y. et al., 2018). Previous studies have shown that soil moisture differed significantly between traditional farmland and introduced woody vegetation (Wang et al., 2009a, 2011b; Liu et al., 2010; Li Y. et al., 2018). In north and southeast China, the increased

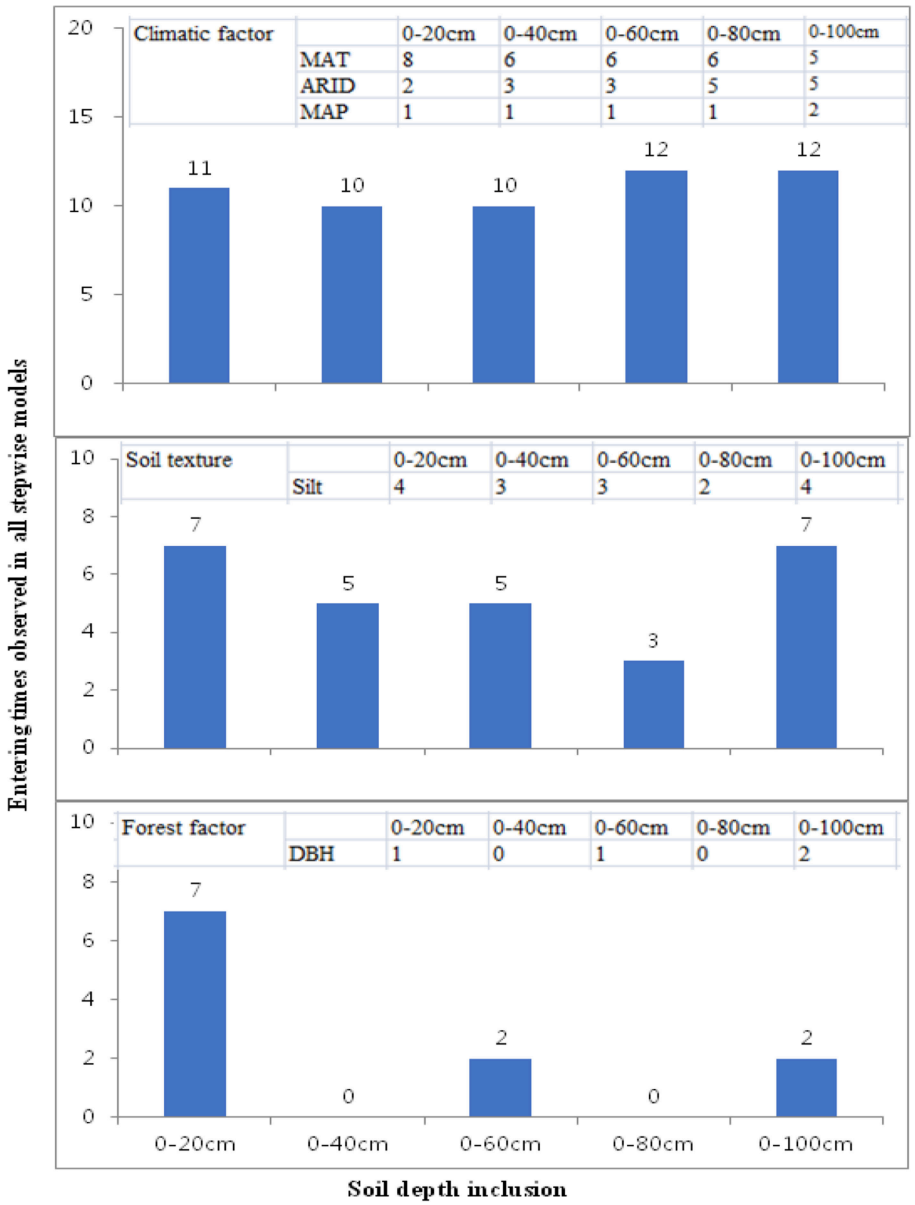

FIGURE 3 | Differences of entering times of climatic factors (upper), soil texture (middle), and forest traits (lower) observed in the all stepwise regression models at different depths. Inset tables are the most observed parameters (MAT, ARID, MAP, Silt, and DBH) and their entering times all stepwise models at different soil depths. All the stepwise regression models were shown in **Table A2**. The more inclusion of the parameters into the stepwise models indicates their stronger contribution at that soil layers for explaining the forest-farmland differences in the studied soil properties.

precipitation and increased forest area were not statistically significant, and had only a weak influence on soil moisture content (Li Y. et al., 2018). In southwest China, however, the afforestation practices have been shown to significantly reduce soil moisture in combination with decreased precipitation (Li Y. et al., 2018). In northeastern China (the same region as in the present study), soil moisture has been shown to be significantly decreased by -8.1 mm decade^{-1} (Li Y. et al., 2018). High water consumption following afforestation has been reported as an important feature of fast-growth tree species afforestation (Yang et al., 2012; Jia et al., 2017; Liang et al., 2018). Songnen Plain (the central part of northeastern China) is characterized as experiencing land degradation with a shortage of precipitation (Li, 2000), and the high water consumption from poplar shelterbelt plantations possibly intensifies the degree of drought in the deeper soil depths, with an average precipitation of 400–500 mm and a large area of saline-alkalinization land (Zhang et al., 2013). Currently, measures used by local people to prevent this water consumption include digging a root-cutting ditch to hinder root invasion into farmland. Possible

other measures to counteract the over-consumption of water by plantations forests have been proposed (Ferraz et al., 2013); for example, the selection of suitable tree species with low water utilization, such as *Picea* spp. (e.g., *P. jezoensis*), plays an important role in the reduction and regulation of water use (Wang et al., 2017a), and an increased proportion of native forests and mosaic management could also stabilize water flow across plantation landscapes.

Saline-alkalinization is an important feature of local land degradation in the Songnen Plain (Li, 2000) and different methods have been invented for soil improvement and afforestation practices in this region (Wang et al., 2011a). Our study found that, compared to farmland, the establishment of shelterbelts increased soil pH in the 0–20 cm and 0–40 cm soil layers ($p < 0.001$) (**Table 2**), whereas there were no significant differences in the deeper soil layers. Therefore, poplar afforestation resulted in surface soil saline-alkalinization in the Songnen Plain of China. Previous meta-analyses have found site-scale soil acidification globally (Berthrong et al., 2009) or afforestation-induced soil neutralizing pH that favored acidifying alkaline soils (Hong et al., 2018). Our findings were different from these meta-analyses, which may be related to the following. First, the addition of plant residues can increase, decrease, or have little effect on soil pH (Tang and Yu, 1999; Marschner and Noble, 2000; Xu et al., 2006; Rukshana et al., 2011), and are mainly dependent on the amount of returning organic materials. In poplar shelterbelt plantations, the relatively smaller area (i.e., several rows) could result in limited litter decomposition and rhizospheric processes following afforestation. Second, the increases in evapotranspiration (Yao et al., 2016) caused by poplar afforestation reduces the leaching loss of base cations (Slessarev et al., 2016), and thus increases soil pH. Third, the upward vertical movement of water by deep-rooted trees (compared with crops) could generally induce the upward movement of soluble salts from the deep soils to the surface soils, resulting in soil saline-alkalinization (Li, 2000; Lu et al., 2017; Wang et al., 2017a).

Planting shelterbelts with fast-growing species such as poplar causes soil bulk density to be significantly reduced in the 0–20 cm soil layer (Wu et al., 2018), and similar significant improvement in soil physics (e.g., bulk density decreasing and porosity increasing) were observed over the entire 100 cm soil profile including 0–40, 0–60, 0–80, and 0–100 cm soil layers (**Tables 1**, **2**, $p < 0.05$). Soil physical structure is very important for soil function (Han et al., 2018) and previous studies have found surface soil improvements, for example, Marta and Halina (2008) observed that total porosity, on average, in the entire 20 cm horizon of the studied afforested soils was 1.08 and 1.12 times higher (for soils of young and older stands, respectively) than that in the arable soils. Our results are in agreeance with previous findings, emphasizing the importance of shelterbelt afforestation to deep soil layers. The long-term farmland cultivation in northeastern China has seriously degraded black soils, with one important aspect being the degradation of the soil physics (Li, 2000; Wang, 2002). Our results clearly show that shelterbelt afforestation could strongly improve soil physics and suggests a possible way for local soil improvement, such as returning degraded farmland to forests, with such policy being implemented in China over the past years (Wang et al., 2011b).

Non-accrual of SOC Both in Surface and Deep Soil Layers Following Shelterbelt Forest Establishment

Results from various studies on the effects of afforestation on SOC are inconsistent. Some studies have found that afforestation increased SOC accumulation (Lemma et al., 2006; Wang et al., 2011b; Wei et al., 2012; Cukor et al., 2017), whereas other studies have shown that afforestation decreased SOC (Farley et al., 2004; Mao et al., 2010) or there was more initial loss than SOC gain (Paul et al., 2002; Wang et al., 2006; Ritter, 2007). In this paper, we did not find any significant changes between poplar shelterbelt plantations and neighboring farmlands.

According to our survey (data not shown here), 28 mg cm^{-3} poplar root system was in 1 m depth, and 95% of the root was distributed in 0–60 cm soil layer, especially in 20–40 cm (57%). Previous studies have also highlighted the possible differences in different soil layers, owing to the root differences between trees (long roots) and crops (short roots) (Wang H. M. et al., 2014). For example, Hooker and Compton (2003) found that SOC linearly accumulated in the subsoil (20–70 cm), but did not differ in the top 20 cm after afforestation. Wang H. M. et al. (2014) reported that, in larch forest plantations, the rate of change in SOM in the surface soil was 262.1 g $kg^{-1}year^{-1}$; however, a different trend in deeper soils resulted in no evident changes in the overall 80 cm soil profile. Our previous paper found no shelterbelt-induced SOC accumulation in the 0–20 cm soil layer (Wu et al., 2018). In the present study, we confirmed a similar finding (i.e., no significant SOC changes) in the 0–40, 0–60, 0–80, and 0–100 cm soil layers (**Tables 1**, **2**, **Table A1**).

Possible reasons for the above-mentioned patterns include the following. First, the shelterbelt poplar planting area was generally 4–6 rows of poplars around large farmlands of ∼25 ha in size (**Figure 1**). In this type of shelterbelt forest, the canopy litter is usually deposited on both farmland and forest simultaneously, which reduces the influence of shelterbelt poplar to forest soils with reference to neighboring farmlands. Second, high productive crops and tillage practices diminish the differences between farmland and forests. It is generally assumed that forests can improve soil carbon sequestration; however, different crops and tillage practices change this sequestration. In the present study, the high productive C4 crop (maize) was the main crop in this region and soybean was the second largest crop with high N-fixation ability (this N fixation favors SOC sequestration) (Lian et al., 2017; You et al., 2017). Proper chemical fertilizer utilization together with straw returning, which has been strongly implemented by the local government, improves the stabilization and accumulation of SOC (Li and Han, 2016). No chemical fertilization or organic manure were applied in the management of the shelterbelt forest, which was different from the neighboring farmlands. Third, microbial priming-induced SOC loss possibly also contributed to the patterns (Li L. J. et al., 2018). The root-exudate inputs in the deep soil could stimulate the decomposition

of SOC by priming soil microbial activity (Marie-Anne et al., 2014), and the SOC mineralization might stimulate loss of the deeper SOC pool (Fontaine et al., 2007), which possibly resulted in the non-accrual of SOC storage in the deeper profiles in the poplar shelterbelts.

Non-evident Changes in all Nutrients Except Available K Recovery in 5 Soil Layers and Total P Depletion in Deep Soils Following Shelterbelt Afforestation

Shelterbelt-induced available K recovery was found in all five soil depths ($p < 0.05$) (**Table 2**), showing that K accumulation was not only in the surface soils but was also in the deeper soils. Returning farmland to forest could rehabilitate the soil K fertility in different areas worldwide using different tree species (Likens et al., 1994; Romanowicz et al., 1996). In China, Jiao et al. (2012) observed that available K was significantly higher in afforested sites than that in degraded croplands in the Loess Plateau. In the case of farmland fertilization practices, more K fertilizer together with N (the favorite fertilizer of local people) should be applied to ensure soil nutrient supply for crop productivity.

In the present study, shelterbelt-induced total P depletion was observed mainly in the deeper soil layers ($p < 0.05$) (**Table 2**). In large areas of larch plantations in northeastern China, Wang W. J. et al. (2014) observed that more P was stored in deeper soil layers, and >70% of P (total and extractable) was found in deeper soil layers (20–80 cm) during larch reforestation. The development of larch plantations could result in a general uplifting of SOM, N, and P based on vertical distribution data and this redistribution was accompanied by the depletion of N and P. The soil nutrient depletion could be related to the biological uplifting function and possible absorption related to tree growth (Jobbágy and Jackson, 2004). In addition, the differences in microbial decomposability between deep and surface soils might strengthen the depletion in deep soil layers (Fontaine et al., 2007; Xiang et al., 2008).

All tested nutrients including N, available N, available P, and total K did not significantly change throughout the entire 100 cm soil profile in shelterbelt poplar forests with reference to neighboring farmlands in a large-scale field in this paper (**Table 2**). A general observation from field surveys is that the growth of crops near the shelterbelt poplar is smaller and general assumptions are that shelterbelt afforestation can decrease soil nutrients owing to nutrient competition between poplar and crops. By the entire soil profile measurements in the present study, we updated this assumption and found that the most likely nutrient depletion was that of P depletion. However, for almost all other nutrients, such depletion was not found either in surface soils or deeper soils. This should be taken into consideration in future shelterbelt forest evaluations.

Large Inter-site Variations Closely Associated With Climatic Conditions and Deep Soils Showed Greater Dependence on Arid and Map: Implications

To determine the differences between plantation forest and neighboring farmlands, many previous studies have looked at a relatively smaller region to minimize the inferences of inter-site variation on the forest effects (Mao et al., 2010; Wang et al., 2011b; Wei et al., 2012; Cukor et al., 2017). In the present study, large-scale sampling was undertaken in Songnen Plain (at least 33,000 km^2) to determine the general soil change patterns in a 100 cm soil profile. Large inter-site variations in the shelterbelt-induced soil changes were found (**Figure 2** and **Table A1**). Currently, global climatic changes strongly affect local development including natural processes in farmlands, pastures, and forests (Li, 2000; Li Y. et al., 2018) and new developments has been reported in tree inventory methods (Wang et al., 2018a) and complex association analysis (Lv et al., 2018; Wang et al., 2018b; Yang et al., 2019). Decoupling the contribution of different components on inter-site variations of the shelterbelt-induced soil changes will favor the mechanical understanding of underlying processes, and is a possible strategy for large scale evaluation of shelterbelt poplar ecological functions (Wang et al., 2018b; Yang et al., 2019).

To identify the possible contributions from climatic conditions, soil texture, and tree growth that affected soil property changes following afforestation, statistical methods including RDA and stepwise regression analysis were applied, which have been proven as beneficial for determining the causal relationship between patterns (Eisenhauer et al., 2015; Wang et al., 2018b; Yang et al., 2019). Accordingly, we found that the inter-site variations in the shelterbelt-induced soil changes in surface soils were different from those in deeper soils.

In general, MAT was the most important parameter with the highest explanation powers, and changes in seven parameters (bulk density, porosity, soil moisture, pH, EC, SOC stock, and total K in different soil layers) were significantly accounted for by the variations in MAT (**Figure 3**, **Table 3, Table A2**). This is related to the fact that temperature is one of the main factors limiting soil nutrients following the planting of plantations (Wiesmeier et al., 2013). Similar to our conclusion, climate warming has been strongly associated with a decrease in the accumulation of glomalin proportion to total soil carbon in soils (Wang et al., 2017b). Moreover, RDA and stepwise regression analysis indicated that ARID and MAP gave greater explanation percentages in deeper soils than those in surface soils (**Figure 3**, **Table 3, Table A2**).

Potential evapotranspiration (PE) and aridity index (ARID) based on the observational data from 1961 to 2004 from 94 meteorological stations showed a general increasing trend in MAT, MAP, PE, and ARID (Zhao et al., 2007). Moreover, increases were more significant in MAT and PE than that in MAP and ARID (Zhao et al., 2007), showing that northeastern China is the most serious region experiencing global changes, especially for temperature warming. The ARID range of the six locations in Songnen plain is 0.49–0.67 and the semi-arid climate possibly affects the shelter-induced soil properties changes. Our findings indicate that global changes will shift the shelterbelt-induced soil changes with reference to neighboring farmlands. Moreover, different changes have been found between surface and deep soils. Compared with surface soils, the drying trends will give more influences in deep soils owing to the large explanation powers compared with the surface soils (**Figure 3**, **Table 3**, **Table A2**).

The Three-North Shelterbelt Program has been evaluated as the most important natural environmental rehabilitation program in China (Bryan et al., 2018), and our findings highlight that soil changes should be carefully considered during any evaluation and divergent responses to climatic changes should be included in risk assessments.

CONCLUSION

By analyzing 720 soil samples from 72 paired sites of poplar shelterbelts and farmlands in Songnen Plain in northeastern China, we concluded the following: (1) Shelterbelt poplar plantations significantly improved soil physical properties by decreasing bulk density and increasing porosity down into the 100 cm depth; however, higher water consumption was mainly found in the deep soils and soil saline-alkalinization was mainly in the surface soils. (2) There were no evident changes in all nutrients except for available K recovery following shelterbelt afforestation in all five soil depths and shelterbelt-induced total P depletion occurred mainly in deep soils. (3) Large inter-site variations were found for all shelterbelt-induced soil changes ($p < 0.05$) except for total K in the 0–20 cm soil layer, and MAT and soil texture were the largest explanation powers for soil property changes in the different soil layers. However, in deeper soils, soil drought (ARID and MAP) gave more explanation percentages than that in surface soils. Our findings highlight that shelterbelt poplar plantations could divergently change different soil properties in different soil depths, and inter-site variation was strongly associated with climatic changes. Our findings favor shelterbelt poplar forest evaluation and the underlying reasons for the large inter-site variation could help find suitable parameters to reduce the uncertainty of future evaluations.

AUTHOR CONTRIBUTIONS

WW, SH, YW, QW, and HW conceived and designed the experiments. WW and YW contributed reagents, materials, and analysis tools. QW, YW performed the experiments. WW, SH, QW, and YW analyzed the data. WW and YW wrote the paper. All authors approved the submitted and final versions.

ACKNOWLEDGMENTS

This study was supported financially by China's National Foundation of Natural Sciences (41877324, 41730641), Fundamental Research Funds for the Central Universities (2572017DG04, 2572017EA03), 13–5 Key Research and Development Project from China Ministry of Science and Technology (2016YFA0600802), Heilongjiang Province for Distinguished Young Scholars (JC201401), and Doctoral Scientific Fund Project of Da Qing Normal University (17ZR03). Thanks are due to Mr. Zhong Zhaoliang and other students (Mr. Du Hongju and Ms. Zhang Jianyu) for their help in laboratory analysis and field sampling.

SUPPLEMENTARY MATERIAL

The Supplementary Material for this article can be found online at: https://www.frontiersin.org/articles/10.3389/fpls.2019.00220/full#supplementary-material

REFERENCES

Bao, S. D. (2000). *The Method of the Soil and Agriculture Chemical Analysis.* Beijing: China Agriculture Press.

Berthrong, S. T., Jobbagy, E. G., and Jackson, R. B. (2009). A global meta-analysis of soil exchangeable cations, pH, carbon, and nitrogen with afforestation. *Ecol. Appli.* 19, 2228–2241. doi: 10.1890/08-1730.1

Bryan, B. A., Gao, L., Ye, Y., Sun, X., and Connor, J. D. (2018). China's response to a national land-system sustainability emergency. *Nature* 559, 193–204. doi: 10.1038/s41586-018-0280-2

Cas, F. S. G. O. (1980). *Forest Soil in Northeast China.* Beijing: Science Press.

Chen, L. X. (1998). Larch litter and soil fertility. *Chin. J. Appl. Ecol.* 9, 581–586.

Cukor, J., Vacek, Z., Linda, R., and Bílek, L. (2017). Carbon sequestration in soil following afforestation of former agricultural land in the Czech Republic. *Central Eur. Forest. J.* 63, 74–104. doi: 10.1515/forj-2017-0011

Dai, L. M., Li, S. L., Lewis, B. J., Wu, J., Yu, D. P., et al. (2018). The influence of land use change on the spatial–temporal variability of habitat quality between 1990 and 2010 in Northeast China. *J. Forest. Res.* 1–10. doi: 10.1007/s11676-018-0771-x

Deng, L., Wang, K. B., Zhu, G. Y., Liu, Y. L., Chen, L., et al. (2018). Changes of soil carbon in five land use stages following 10 years of vegetation succession on the Loess Plateau, China. *Catena* 171, 185–192. doi: 10.1016/j.catena.2018.07.014

Deniz, T., and Paletto, A. (2018). Effects of bioenergy production on environmental sustainability: a preliminary study based on expert opinions in Italy and Turkey. *J. Forest. Res.* 29, 1611–1626. doi: 10.1007/s11676-018-0596-7

Ding, R. X., and Liu, S. T. (1980). A study on the fertility of black soil after reclamation. *Acta Pedol. Sin.* 1, 20–32.

Eisenhauer, N., Bowker, M. A., Grace, J. B., and Powell, J. R. (2015). From patterns to causal understanding: structural equation modeling (SEM) in soil ecology. *Pedobiol. J. Soil Ecol.* 58, 65–72. doi: 10.1016/j.pedobi.2015.03.002

Farley, K. A., Kelly, E. F., and Hofstede, R. G. M. (2004). Soil organic carbon and water retention following conversion of grasslands to pine plantations in the Ecuadorian Andes. *Ecosystems* 7, 729–739. doi: 10.1007/s10021-004-0047-5

Ferraz, S. F. B., Lima, W. D. P., and Rodrigues, C. B. (2013). Managing forest plantation landscapes for water conservation. *Forest Ecol. Manage.* 301, 58–66. doi: 10.1016/j.foreco.2012.10.015

Fontaine, S., Bardoux, G., Abbadie, L., and Mariotti, A. (2010). Carbon input to soil may decrease soil carbon content. *Ecol. Lett.* 7, 314–320. doi: 10.1111/j.1461-0248.2004.00579.x

Fontaine, S., Barot, S., Barré, P., Bdioui, N., Mary, B., and Rumpel, C. (2007). Stability of organic carbon in deep soil layers controlled by fresh carbon supply. *Nature* 450, 277–280. doi: 10.1038/nature06275

Han, Q. L., Zhou, X. B., Liu, L., Zhao, Y. D., and Zhao, Y. (2018). Three-dimensional visualization of soil pore structure using computed tomography. *J. Forest. Res*. doi: 10.1007/s11676-018-0834-z

Hljtr (1992). *Soil of Heilongjiang Province, P.R.* China. Harbin: Science and Technology press of Heilongjiang Province.

Hong, S., Piao, S., Chen, A., Liu, Y., Liu, L., Peng, S., et al. (2018). Afforestation neutralizes soil pH. *Nat. Commun.* 9:520. doi: 10.1038/s41467-018-02970-1

Hooker, T. D., and Compton, J. E. (2003). Forest ecosystem carbon and nitrogen accumulation during the first century afterag ricultural abandonment. *Ecol. Appli.* 13, 299–313. doi: 10.1890/1051-0761(2003)013[0299:FECANA]2.0.CO;2

Huo, Z. L., Dai, X. Q., Feng, S. Y., Kang, S. Z., and Huang, G. H. (2013). Effect of climate change on reference evapotranspiration and aridity index in arid region of China. *J. Hydrol.* 492, 24–34. doi: 10.1016/j.jhydrol.2013.04.011

Jaskulska, R., and Jaskulska, J. (2017). Efficiency of old and young shelterbelts in reducing the contents of nutrients in Luvisols. *Agric. Ecosyst. Environ.* 240, 269–275. doi: 10.1016/j.agee.2017.02.033

Jha, K. K. (2018). Biomass production and carbon balance in two hybrid poplar (Populus euramericana) plantations raised with and without agriculture in southern France. *J. Forest. Res.* 29, 1689–1701. doi: 10.1007/s11676-018-0590-0

Jia, X. X., Shao, M. A., Zhu, Y. J., and Luo, Y. (2017). Soil moisture decline due to afforestation across the Loess Plateau, China. *J. Hydrol.* 546, 113–122. doi: 10.1016/j.jhydrol.2017.01.011

Jiao, J. Y., Zhang, Z. G., Bai, W. J., Jia, Y. F., and Wang, N. (2012). Assessing the ecological success of restoration by afforestation on the Chinese Loess Plateau. *Restor. Ecol.* 20, 240–249. doi: 10.1111/j.1526-100X.2010.00756.x

Jin, T. T., Fu, B. J., Liu, G. H., and Wang, Z. (2011). Hydrologic feasibility of artificial forestation in the semi-arid Loess Plateau of China. *Hydrol. Earth Syst. Sci. Discuss.* 8, 2519–2530. doi: 10.5194/hess-15-2519-2011

Jobbágy, E. G., and Jackson, R. B. (2000). The vertical distribution of soil organic carbon and its relation to climate and vegetation. *Ecol. Applic.* 10, 423–436. doi: 10.1890/1051-0761(2000)010[0423:TVDOSO]2.0.CO;2

Jobbágy, E. G., and Jackson, R. B. (2004). The uplift of soil nutrients by plants: biogeochemical consequences across scales. *Ecol. Evol.* 85, 2380–2389. doi: 10.1890/03-0245

Kettler, T. A., Doran, J. W., and Gilbert, T. L. (2001). Simplified method for soil particle-size determination to accompany soil-quality analyses. *Soil Sci. Soc. Am. J.* 65, 849–852. doi: 10.2136/sssaj2001.653849x

Lemma, B., Dan, B. K., Nilsson, I., and Olsson, M. (2006). Soil carbon sequestration under different exotic tree species in the southwestern highlands of Ethiopia. *Geoderma* 136, 886–898. doi: 10.1016/j.geoderma.2006.06.008

Li, J. Q., and Cui, G. (2000). On nature forest protection and degraded ecosystem restoration in Northwest China. *J. Beijing Forest. Univ.* 22, 1–7. doi: 10.13332/j.1000-1522.2000.04.001

Li, L. J., and Han, X. Z. (2016). Changes of soil properties and carbon fractions after long-term application of organic amendments in Mollisols. *Catena* 143, 140–144. doi: 10.1016/j.catena.2016.04.007

Li, L. J., Xia, Z. B., Ye, R., Doane, T. A., and Horwath, W. R. (2018). Soil microbial biomass size and soil carbon influence the priming effect from carbon inputs depending on nitrogen availability. *Soil Biol. Biochem.* 119, 41–49. doi: 10.1016/j.soilbio.2018.01.003

Li, X. J. (2000). The alkili-saline land and agricultural sustainable development of the Western songnen plain in China. *Sci. Geogr. Sin.* 20, 51–55.

Li, Y., Piao, S., Li, L. Z. X., Chen, A., Wang, X., Ciais, P., et al. (2018). Divergent hydrological response to large-scale afforestation and vegetation greening in China. *Sci. Adv.* 4:eaar4182. doi: 10.1126/sciadv.aar4182

Lian, T. X., Jian, J., Wang, G. H., Tang, C. X., Yu, Z. H., Li, Y., et al. (2017). The fate of soybean residue-carbon links to changes of bacterial community composition in Mollisols differing in soil organic carbon. *Soil Biol. Biochem.* 109, 50–58. doi: 10.1016/j.soilbio.2017.01.026

Liang, H. B., Xue, Y. Y., Li, Z. S., Shuai, W., Xing, W., Gao, G., et al. (2018). Soil moisture decline following the plantation of *Robinia* pseudoacacia forests: evidence from the Loess Plateau. *Forest Ecol. Manage.* 412, 62–69. doi: 10.1016/j.foreco.2018.01.041

Likens, G. E., Driscoll, C. T., Buso, D. C., Siccama, T. G., Johnson, C. E., Lovett, G. M., et al. (1994). The biogeochemistry of potassium at Hubbard Brook. *Biogeochemistry* 25, 61–125. doi: 10.1007/BF00000881

Liu, W. Z., Zhang, X. C., Dang, T. H., Ouyang, Z., Li, Z., Wang, J., et al. (2010). Soil water dynamics and deep soil recharge in a record wet year in the southern Loess Plateau of China. *Agric. Water Manage.* 97, 1133–1138. doi: 10.1016/j.agwat.2010.01.001

Lu, J. L., Shen, G., Wang, Q., Pei, Z. X., Ren, M. L., et al. (2017). Larch, ash, Scots pine, and farmland-induced differences on 17 soil parameters and their comprehensive analyses. *Acta Ecol. Sin.* 37, 1–10. doi: 10.1016/j.chnaes.2016.09.003

Lv, H. L., Wang, W., He, X., Wei, C., and Xiao, L., Zhang, B (2018). Association of urban forest landscape characteristics with biomass and soil carbon stocks in Harbin City, Northeastern China. *PeerJ* 6:e5825. doi: 10.7717/peerj.5825

Mao, R., Zeng, D. H., Hu, Y. L., Li, L. J., and Yang, D. (2010). Soil organic carbon and nitrogen stocks in an age-sequence of poplar stands planted on marginal agricultural land in Northeast China. *Plant Soil* 332, 227–287. doi: 10.1007/s11104-010-0292-7

Marie-Anne, D. G., Jastrow, J. D., Gilette, S., Johns, A., and Wullschleger, S. D. (2014). Differential priming of soil carbon driven by soil depth and root impacts on carbon lability. *Soil Biol. Biochem.* 69, 147–156. doi: 10.1016/j.soilbio.2013.10.047

Marschner, B., and Noble, A. D. (2000). Chemical and biological processes leading to the neutralisation of acidity in soil incubated with litter materials. *Soil Biol. Biochem.* 32, 805–813. doi: 10.1016/S0038-0717(99)00209-6

Marta, O., and Halina, S. (2008). The effect of afforestation with Scots pine (Pinus silvestris L.) of sandy post-arable soils on their selected properties. *I. Physical and sorptive properties. Plant Soil* 305, 157–169. doi: 10.1007/s11104-008-9537-0

Mendham, D. S., O'connell, A. M., Grove, T. S., and Rance, S. J. (2003). Residue management effects on soil carbon and nutrient contents and growth of second rotation eucalypts. *Forest Ecol. Manage.* 181, 357–372. doi: 10.1016/S0378-1127(03)00007-0

Merino, A. N., Solla-Gullón, F., and Edeso, J. M. (2004). Soil changes and tree growth in intensively managed Pinus radiata in northern Spain. *Forest Ecol. Manage.* 196, 393–404. doi: 10.1016/j.foreco.2004.04.002

Nan, H., Liu, X. X., Jumpponen, A., Setälä, H., Kotze, D. J., Biktasheva, L., et al. (2018). Over twenty years farmland reforestation decreases fungal diversity of soils, but stimulates the return of ectomycorrhizal fungal communities. *Plant Soil* 427, 231–244. doi: 10.1007/s11104-018-3647-0

Obschatko, E. S. D., Foti, M. P., Román, M. E., Cuenca Capa, P. R., Chinchilla, O., et al. (2010). *Global Forest Resources Assessment 2010: Main Report*. Fao Forestry Paper.

Paul, K. I., Polglase, P. J., Nyakuengama, J. G., and Khanna, P. K. (2002). Change in soil carbon following afforestation. *Forest Ecol. Manage.* 168, 241–257. doi: 10.1016/S0378-1127(01)00740-X

Ritter, E. (2007). Carbon, nitrogen and phosphorus in volcanic soils following afforestation with native birch (*Betula pubescens*) and introduced larch *(Larix sibirica*) in Iceland. *Plant Soil* 295, 239–251. doi: 10.1007/s11104-007-9279-4

Romanowicz, R. B., Driscoll, C. T., Fahey, T. J., Johnson, C. E., Likens, G. E., Siccama, T. G., et al. (1996). Changes in the biogeochemistry of potassium following a whole-tree harvest. *Soil Sci. Soc. Am. J.* 60, 1664–1674. doi: 10.2136/sssaj1996.03615995006000060009x

Rukshana, F., Butterly, C. R., Baldock, J. A., and Tang, C. (2011). Model organic compounds differ in their effects on pH changes of two soils differing in initial pH. *Biol. Fertil. Soils* 47, 51–62. doi: 10.1007/s00374-010-0498-0

Slessarev, E. W., Lin, Y., Bingham, N. L., Johnson, J. E., Dai, Y., Schimel, J. P., et al. (2016). Water balance creates a threshold in soil pH at the global scale. *Nature* 540, 567–569. doi: 10.1038/nature20139

Tang, C., and Yu, Q. (1999). Impact of chemical composition of legume residues and initial soil pH on pH change of a soil after residue incorporation. *Plant Soil* 215, 29–38. doi: 10.1023/A:1004704018912

Wang, C. M., Ouyang, H., Shao, B., Tian, Y. Q., Zhao, J. G., and Xu, H.-Y. (2006). Soil carbon changes following afforestation with Olga Bay Larch (*Larix olgensis Henry*) in Northeastern China. *J. Integr. Plant Biol.* 48, 503–512. doi: 10.1111/j.1744-7909.2006.00264.x

Wang, G. Y., Ma, O. Z., Wang, L. G., Shrestha, A., Chen, B. Z., Mi, F., et al. (2018a). Local perceptions of the conversion of cropland to forestland program in Jiangxi, Shaanxi, and Sichuan, China. *J. Forest. Res.* doi: 10.1007/s11676-018-0870-8

Wang, H. M., Wang, W., Chen, H., Zhang, Z., Mao, Z., and Zu, Y. G. (2014). Temporal changes of soil physic-chemical properties at different soil depths during larch afforestation by multivariate analysis of covariance. *Ecol. Evolu.* 4, 1039–1048. doi: 10.1002/ece3.947

Wang, H. M., Wang, W. J., and Chang, S. (2017a). Sampling Method and Tree-Age Affect Soil Organic C and N Contents in Larch Plantations. *Forests* 8, 28. doi: 10.3390/f8010028

Wang, J. G., Liu, H. X., and Meng, K. (1996). *Songnen Plain Agricultural Ecosystem Research*. Harbin: Harbin Engineering University Press.

Wang, J. K. (2002). An approach to the changes of black soil quality (I)—changes of the indices of black soil with the year(s) of reclamation. *J. Shenyang Agric. Univ.* 33, 43–47.

Wang, Q., Wang, W., He, X., Zhang, W., Song, K., Han, S., et al. (2015). Role and variation of the amount and composition of glomalin in soil properties in farmland and adjacent plantations with reference to a primary forest in north-eastern China. *PLoS ONE* 10:e0139623. doi: 10.1371/journal.pone.0139623

Wang, Q., Wang, W., He, X., Zheng, Q., Wang, H., Wu, Y., et al. (2017). Changes in soil properties, X-ray-mineral diffractions and infrared-functional groups in bulk soil and fractions following afforestation of farmland, Northeast China. *Sci. Rep.* 7:12829. doi: 10.1038/s41598-017-12809-2

Wang, Q., Wu, Y., Wang, W., Zhong, Z., Pei, Z., Ren, J., et al. (2014). Spatial variations in concentration, compositions of glomalin related soil protein in poplar plantations in northeastern China, and possible relations with soil physicochemical properties. *Sci. World J.* 2014:160403. doi: 10.1155/2014/160403

Wang, S., Wang, Z., and Gu, J. (2017). Variation patterns of fine root biomass, production and turnover in Chinese forests. *J. Forest. Res.* 28, 1185–1194. doi: 10.1007/s11676-017-0386-7

Wang, W., Xiao, L., Zhang, J., Yang, Y., Tian, P., Wang, H., et al. (2018). Potential of Internet street-view images for measuring tree sizes in roadside forests. *Urban Forest. Urban Green.* 35, 211–220. doi: 10.1016/j.ufug.2018.09.008

Wang, W., Zhang, B., Xiao, L., Zhou, W., Wang, H., and He, X.(2018b). Decoupling forest characteristics and background conditions to explain urban-rural variations of multiple microclimate regulation from urban trees. *PeerJ* 6:e5450. doi: 10.7717/peerj.5450

Wang, W. J., He, H. S., Zu, Y. G., Guan, Y., Liu, Z. G., Zhang, Z.-H., et al. (2011a). Addition of HPMA affects seed germination, plant growth and properties of heavy saline-alkali soil in northeastern China: comparison with other agents and determination of the mechanism. *Plant Soil* 339, 177–191. doi: 10.1007/s11104-010-0565-1

Wang, W. J., Lu, J. L., Du, H. J., Wei, C. H., Wang, H. M., Fu, Y., et al. (2017a). Ranking thirteen tree species based on their impact on soil physiochemical properties, soil fertility, and carbon sequestration in Northeastern China. *Forest Ecol. Manage.* 404, 214–229. doi: 10.1016/j.foreco.2017.08.047

Wang, W. J., Qiu, L., Zu, Y. G., Su, D. X., An, J., Hong-Yan, W., et al. (2011b). Changes in soil organic carbon, nitrogen, pH and bulk density with the development of larch (Larix gmelinii) plantations in China. *Glob. Change Biol.* 17, 2657–2676. doi: 10.1111/j.1365-2486.2011.02447.x

Wang, W. J., Wang, H. M., and Zu, Y. G. (2014). Temporal changes in SOM, N, P, K, and their stoichiometric ratios during reforestation in China and interactions with soil depths: importance of deep-layer soil and management implications. *Forest Ecol. Manage.* 325, 8–17. doi: 10.1016/j.foreco.2014.03.023

Wang, W. J., Zhong, Z. L., Wang, Q., Wang, H., Fu, Y., He, X., et al. (2017b). Glomalin contributed more to carbon, nutrients in deeper soils, and differently associated with climates and soil properties in vertical profiles. *Sci. Rep.* 7:13003. doi: 10.1038/s41598-017-12731-7

Wang, Z. Q., Liu, B. Y., Gang, L., and Zhang, Y. X. (2009a). Soil water depletion depth by planted vegetation on the Loess Plateau. *Sci. China* 52, 835–842. doi: 10.1007/s11430-009-0087-y

Wang, Z. Q., Liu, B. Y., and Wang, X. (2009b). Erosion effect on the productivity of black soil in Northeast China. *Sci. China* 52, 1005–1021. doi: 10.1007/s11430-009-0093-0

Wei, X., Qiu, L., Shao, M. G., Zhang, X., and Gale, W. (2012). The accumulation of organic carbon in mineral soils by afforestation of abandoned farmland. *PLoS ONE* 7:e32054. doi: 10.1371/journal.pone.0032054

Wei, X., Shao, M., Gale, W., and Li, L. (2014). Global pattern of soil carbon losses due to the conversion of forests to agricultural land. *Sci. Rep.* 4:4062. doi: 10.1038/srep04062

Wiesmeier, M., Prietzel, J., Barthold, F., Spörlein, P., Geuß, U., Hangen, E., et al. (2013). Storage and drivers of organic carbon in forest soils of southeast Germany (Bavaria) – Implications for carbon sequestration. *Forest Ecol. Manage.* 295, 162–172. doi: 10.1016/j.foreco.2013.01.025

Wu, Y., Wang, W., Wang, Q., Zhong, Z., Pei, Z., Wang, H., et al. (2018). Impact of poplar shelterbelt plantations on surface soil properties in northeast China. *Can. J. Forest Res.* 48, 559–567. doi: 10.1139/cjfr-2017-0294

Wu, Y., and Wang, W. J. (2016). "Poplar forests in NE China and possible influences on soil properties: ecological importance and sustainable development," in *Poplars and Willows, Cultivation, Applications and Environmental Benefits*, ed M. V. Desmond (Hauppauge, NY: Novapublishers), 1–29.

Wuest, S. B. (2009). Correction of bulk density and sampling method biases using soil mass per unit area. *Soil Sci. Soc. Am. J.* 73, 3647–3654. doi: 10.2136/sssaj2008.0063

Xiang, S., Doylec, A., Holdenad, P. A., and Schimelc, J. P. (2008). Drying and rewetting effects on C and N mineralization and microbial activity in surface and subsurface California grassland soils. *Soil Biol. Biochem.* 40, 2281–2289. doi: 10.1016/j.soilbio.2008.05.004

Xu, J. M., Tang, C., and Chen, Z. L. (2006). The role of plant residues in pH change of acid soils differing in initial pH. *Soil Biol. Biochem.* 38, 709–719. doi: 10.1016/j.soilbio.2005.06.022

Yang, L., Wei, W., Chen, L. D., and Mo, B. R. (2012). Response of deep soil moisture to land use and afforestation in the semi-arid Loess Plateau, China. *J. Hydrol.* 475, 111–122. doi: 10.1016/j.jhydrol.2012.09.041

Yang, Y. B., Lv, H. L., Fu, Y. J., He, X. Y., and Wang, W. J. (2019). Associations between road density, urban forest landscapes, and structural-taxonomic attributes in northeastern china: decoupling and implications. *Forests* 10:58. doi: 10.3390/f10010058

Yao, Y., Wang, X., Zeng, Z., Liu, Y., and Peng S. (2016). The effect of afforestation on soil moisture content in Northeastern China. *PLoS ONE* 11:e0160776. doi: 10.1371/journal.pone.0160776

You, M. Y., Li, N., Zou, W. X., Han, X., and Burger, M. (2017). Increase in soil organic carbon in a Mollisol following simulated initial development from parent material: dynamics of SOC stocks at initial stage of soil restoration. *Eur. J. Soil Sci.* 68, 39–47. doi: 10.1111/ejss.12400

Zhang, G. Q., Zhang, P., and Cao, Y. (2018). Ecosystem carbon and nitrogen storage following farmland afforestation with black locust (Robinia pseudoacacia) on the Loess Plateau, China. *J. Forest. Res.* 29, 761–771. doi: 10.1007/s11676-017-0479-3

Zhang, H. Q., Wang, L. X., Sun, G. Y., and Yang, Y. (2013). Evaluation of saling-alkali land resource and development potential in low songnen plains. *Chin. J. Agric. Resour. Region. Plan.* 34, 6–11.

Zhang, X. Q., Kirschbaum, M. U. F., Hou, Z., and Guo, Z. (2004). Carbon stock changes in successive rotations of Chinese fir (Cunninghamia lanceolata (lamb) hook) plantations. *Forest Ecol. Manage.* 202, 131–147. doi: 10.1016/j.foreco.2004.07.032

Zhang, Y., Peng, C. H., Li, W. Z., Tian, L. X., Zhu, Q. A., Chen, H., et al. (2016). Multiple afforestation programs accelerate the greenness in the 'Three North' region of China from 1982 to 2013. *Ecol. Indicat.* 61, 404–412. doi: 10.1016/j.ecolind.2015.09.041

Zhao, Q., Zeng, D. H., Lee, D. K., He, X. Y., Fan, Z. P., and Jin, Y. H. (2007). Effects of *Pinus sylvestris* var. *mongolica* afforestation on soil phosphorus status of the Keerqin Sandy Lands in China. *J. Arid Environ.* 69, 569–582. doi: 10.1016/j.jaridenv.2006.11.004

Zhong, Z. L., Wang, W. J., Wang, Q., Wu, Y., Wang, H. M., and Pei, Z. (2017). Glomalin amount and compositional variation, and their associations with soil properties in farmland, northeastern China. *J. Plant Nutri. Soil Sci.* 180, 1–13. doi: 10.1002/jpln.201600579

Zhu, J. J. (2013). A review of the present situation and future prospect of science of protective forest. *Chin. J. Plant Ecol.* 37, 872–888. doi: 10.3724/SP.J.1258.2013.00091

Conflict of Interest Statement: The authors declare that the research was conducted in the absence of any commercial or financial relationships that could be construed as a potential conflict of interest.

frontiers in Plant Science

ORIGINAL RESEARCH
published: 18 March 2019
doi: 10.3389/fpls.2019.00085

The Latitudinal Patterns of Leaf and Soil C:N:P Stoichiometry in the Loess Plateau of China

Zhao Fang[1,2], Dong-Dong Li[2,3], Feng Jiao[1,2], Jing Yao[1] and Hao-Tian Du[1]*

[1] State Key Laboratory of Soil Erosion and Dryland Farming on the Loess Plateau, Institute of Soil and Water Conservation, Northwest A&F University, Yangling, China, [2] Institute of Soil and Water Conservation, Chinese Academy of Sciences and Ministry of Water Resources, Yangling, China, [3] University of Chinese Academy of Sciences, Beijing, China

Understanding the spatial patterns and the driving factors of plant leaf and soil stoichiometry are critical for improving the parameterization of future ecological models and to predict the responses of ecosystems to environmental changes. This study aimed to determine how the latitudinal patterns of leaf and soil C:N:P stoichiometry are affected by climate and vegetation types in the dryland ecosystems. The concentrations of leaf C, N, and P in herb community as well as soil nutrient concentrations along a 500–km–long latitudinal gradient in Northern Shaanxi of the Loess Plateau, were measured. The results showed that the soil C, N, P and C:N:P ratios at all three depths (0–10, 10–20, and 20–40 cm) showed significant latitudinal trends (except for soil C:N ratios) ($P < 0.01$). In general, the soil C, N and C:N:P ratios decreased exponentially while soil P increased first and then decreased with the latitude. The soil C, N, C:P, and N:P ratios at all three depths (0–10, 10–20 and 20–40 cm) were positively correlated with MAT and MAP ($P < 0.05$), while soil P and C:N ratios at all three depths were weakly correlated with MAT and MAP ($P > 0.05$). In addition, leaf C:N:P stoichiometry was significantly correlated with the latitude, MAT, and MAP (except for N:P ratios) ($P < 0.01$), such that, leaf C, C:N, and C:P ratios decreased as the latitude increased and MAT and MAP decreased, and leaf N, P concentrations increased as the latitude increased and MAT and MAP decreased, while leaf N:P ratios were weakly correlated with the latitude, MAT, and MAP ($P > 0.05$). Furthermore, the leaf C:N:P stoichiometry of herbaceous communities was related to the soil properties (except for soil P), and we found that the C:P ratios between the soil and leaves were strongly correlated. Compared with the global scale, the relatively high N:P ratios indicated that the vegetation growth of the herb community in the dryland of the Loess Plateau was more susceptible to P limitation.

Keywords: ecological stoichiometry, climatic factors, herb community, vegetation types, leaves, soil, Loess Plateau

OPEN ACCESS

Edited by:
Zhiyou Yuan,
Northwest A&F University, China

Reviewed by:
Hui Shi,
Xi'an University of Architecture and Technology, China
Guanghui Zhang,
Beijing Normal University, China
Juying Huang,
Ningxia University, China

***Correspondence:**
Feng Jiao
Jiaof@ms.iswc.ac.cn

Specialty section:
This article was submitted to Plant Abiotic Stress, a section of the journal Frontiers in Plant Science

Received: *12 October 2018*
Accepted: *21 January 2019*
Published: *18 March 2019*

Citation:
Fang Z, Li D-D, Jiao F, Yao J and Du H-T (2019) The Latitudinal Patterns of Leaf and Soil C:N:P Stoichiometry in the Loess Plateau of China. Front. Plant Sci. 10:85. doi: 10.3389/fpls.2019.00085

INTRODUCTION

The terrestrial ecosystem consists of above- and belowground ecological components, and their strong interactions greatly affect the material cycle and energy flow in the terrestrial ecosystem (Wardle and Peltzer, 2007). In general, plants on the ground affect the soil properties by inputting litter and root exudates, while the intense activity of the microorganisms in the soil provides the

mineralized nutrients and suitable environmental conditions needed for plant growth (Lambers et al., 2009; van der Heijden et al., 2010). A considerable body of evidence has suggested that the aboveground and belowground ecological components of ecosystems are tightly linked and are susceptible to environmental factors. Besides, the feedback between the above- and belowground components have important implications for the community structure and the ecosystem function (Bardgett et al., 2005; van der Putten et al., 2009; Laurel, 2013).

Ecological stoichiometry is a discipline that studies the balance of the various elements that are required by organisms and provides new perspectives for understanding the ecosystem structure and processes (Elser et al., 2000b; Yang and Luo, 2011). As essential components of organisms, carbon, nitrogen, and phosphorus play a vital role in studying nutrient cycling and the ecosystem structure and function (Koerselman, 1996; Sterner and Elser, 2002). Furthermore, the nutrient cycling of carbon, nitrogen, and phosphorus in the plant-soil system would tightly couple (Elser et al., 2000b). Nitrogen and phosphorus are generally considered to be the main limiting elements for terrestrial ecosystem productivity (Güsewell, 2010). Leaf N:P ratios have been a practical and important tool for detecting vegetation composition, dynamics and nutrient limitation in different ecosystems (Koerselman, 1996; Cernusak et al., 2010). Recently, the geographical pattern of plant and soil nutrient elements and its relationship with environmental factors has been studied extensively at global and regional scales (Reich et al., 1999; Han et al., 2005; He et al., 2006; Thompson et al., 2010; Wright et al., 2010; Wang et al., 2015), but the results have been inconsistent. For example, Tian et al. (2010) and Han et al. (2005) found that the C:N ratios of leaf, litter, and mineral soil in forests are well constrained at a national scale in China. Reich and Oleksyn (2004) revealed that global leaf N and P concentrations increased and N:P ratios decreased with increasing latitude (or decreasing mean annual temperature, MAT). In contrast, Han et al. (2005) and Ren et al. (2007) revealed similar research findings in China at the regional scale, but the differences were that N:P ratio was weakly correlated with the latitude and the MAT. In addition, Zheng and Shangguan (2007) found that C:N and C:P ratios in the leaves of the Loess Plateau were not related to the latitude and the MAT, but N:P ratio increased with the increasing latitude and was not correlated with MAT. Furthermore, Chen et al. (2016) found that the soil N and P concentrations both decreased significantly with the increasing MAT and the mean annual precipitation (MAP), while the soil N:P ratio did not vary in a systematic way with the latitude. Han et al. (2005) and Zheng and Shangguan (2007) concluded that this inconsistency may be attributed to the different research scales. So far, very little work has been done at the regional scale, especially in the Loess Plateau. To further confirm biogeographic patterns of leaf and soil nutrients at regional scales are more and more important for increasing the basic data of relevant research in the Loess Plateau and providing new materials to solve that inconsistent views.

The Loess Plateau in China, with an area of 6.2 km $\times$ 10^5 km, is famous for having the highest rate of erosion in the world (Fu et al., 2000). For this reason, the Chinese government has launched a series of nationwide conservation projects to improve this dilemma, which is caused by the population pressure that has been increasing since the last century (An et al., 2013). These projects, such as the "Grain for Green" project, will inevitably have a major impact on regional soil nutrient cycling, and will in turn cause changes in the surface vegetation. Notably, the natural environment of the Loess Plateau varies greatly, and features such as rainfall, temperature, soil, and vegetation show regular changes from southeast to northwest (Yamanaka et al., 2014). This climatic variation at a regional scale along latitudinal gradients provides an excellent natural laboratory for investigating the formation mechanism and the relationship of the spatial distribution pattern of plant leaves and soil elements. According to the hydro-thermal conditions of the Loess Plateau, Cheng and Wan (2002) classified the vegetation of the Loess Plateau into five vegetation subzones: the forest zone (FO), the forest steppe zone (FS), the steppe zone (ST), the desert steppe, and the desert zone. Differences in the environmental conditions (temperature, moisture, etc.) are often linked to varying latitudes and, in turn could be used to explain the distribution of vegetation types across the Loess Plateau. In recent years, considerable research efforts have been devoted to surveying the effects of different vegetation restoration years, succession stages, and land use on the soil and plant ecological stoichiometry characteristics of the Loess Plateau (Jiao et al., 2011; Chai et al., 2015; Zhao et al., 2015). However, there are still few studies on the relationships between the soil and plant C:N:P stoichiometry and the latitudinal patterns of leaf and soil C:N:P stoichiometry.

In this study, a field survey was conducted on 15 subplots of different vegetation zones in the Loess Plateau to examine the changes in the soil and in the plant C:N:P stoichiometry and their relationships along latitudinal gradients, to reveal the limiting conditions of nutrient restrictions and provide a reference and basis for ecological restoration on the Loess Plateau. Our objectives were: (1) to determine the latitudinal patterns of leaf and soil C:N:P stoichiometry; (2) to quantify the relationships of the spatial variations of leaf and soil nutrients with climatic variables (MAT and MAP); (3) to quantify the relationships of the leaf nutrients traits with the soil nutrients traits; (4) to compare the patterns of leaf nutrients in the Loess Plateau with those of other scales.

MATERIALS AND METHODS

Study Sites

This study was conducted in fifteen sites along a 500–km–long latitudinal gradient in Northern Shaanxi of the Loess Plateau, which were located in the FO, FS, ST, and steppe-desert zone (SD), consistent with previous studies (Yamanaka et al., 2014) (**Figure 1**). The study area is located at N35°95′–38°36′ and E107°97′–109°87′ and belongs to the temperate zone. All sites were selected on flat terrain away from the human activity area, with minimal microclimate differences caused by the microtopography and grazing disturbance. This area was characterized by a temperate

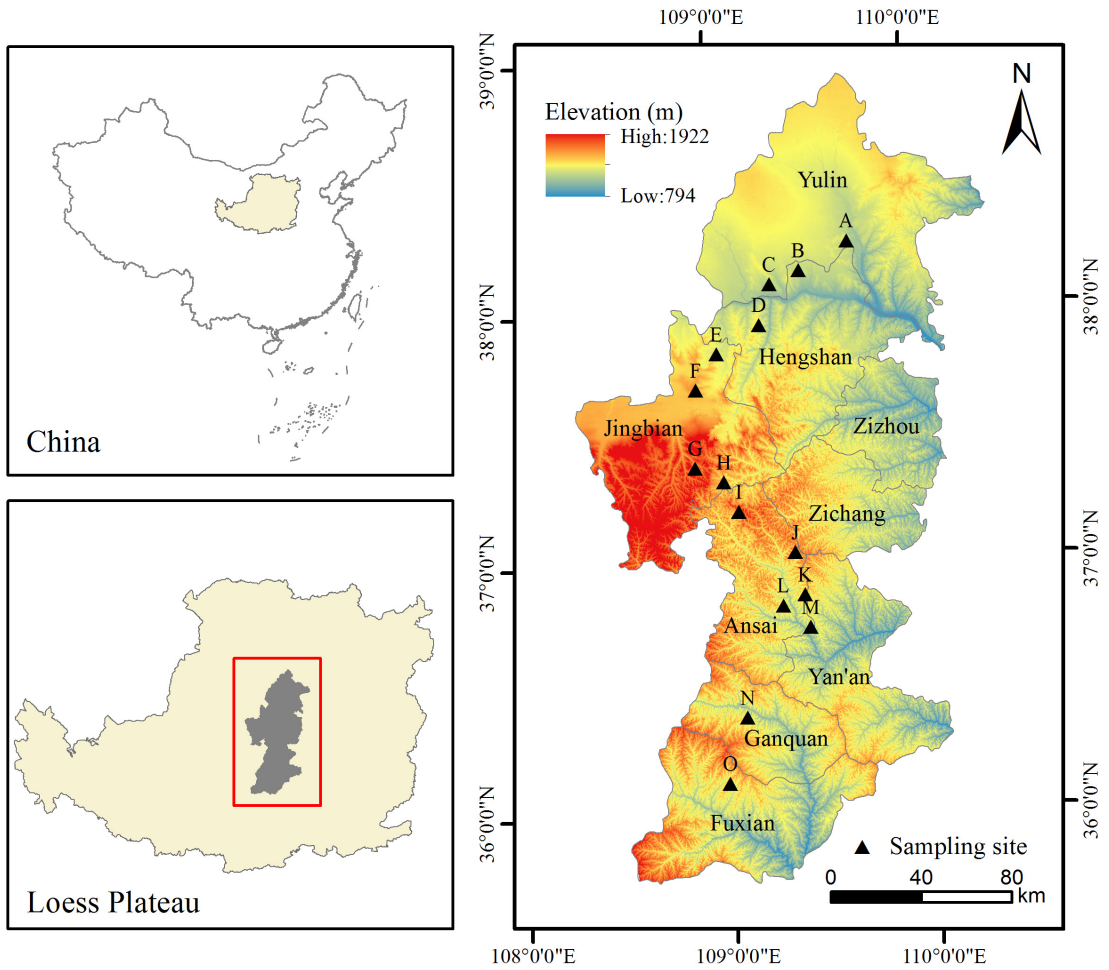

FIGURE 1 | Sample arrangement diagram of study area.

semi-arid climate with an annual mean temperature ranking of 8.87°C >7.99°C >6.80°C > 6.32°C and a MAP ranking of 590.0 mm > 469.3 mm > 408.8 mm > 355.7 mm for the four vegetation type zones (FO, FS, ST, and SD) (**Figure 2**) (1990–2010 data), which occurred during May to October in the growing season and most intensely in fall. The elevation of the study area ranged from 1,015 to 1,600 m above sea level. The zonal soil in this region was classified as Loessoal soils according to the Genetic Soil Classification of China (Shi et al., 2010). In this area, the main types of herb species were dominated by *Bothriochloa ischaemum*, *Stipa bungeana*, *Cleistogenes caespitosa*, *Lespedeza davurica*, *Astragalus melilotoides*, *Artemisia sacrorum*, *Heteropappus altaicus*, *Potentilla tanacetifolia*, etc.

Soil and Plant Sampling and Analyses

Each vegetation zone type was represented by three to four subplots (30 m × 30 m); in total, there were 15 subplots. The spatial geographical coordinates (longitude and latitude) and altitude of each site were obtained by GPS. The basic information of the sample plots is shown in **Table 1**. Five 1 m × 1 m quadrats were surveyed at random in each subplot to represent the plot heterogeneity. Apparently, the species diversity and productivity of herb communities decreasing with the environmental gradients are shown in **Table 2**. And 23 herbaceous species (nine families) were selected based on the following criteria: the target species should be the dominant species and relatively abundant at each site. We selected healthy and mature leaves for each target species and collected them for about 30 g to bring them back to the laboratory in every 1 m × 1 m quadrat at the community level as well as in the community characteristics survey. The plant samples were dried at 75°C for 72 h to the appropriate constant mass.

Five soil samples were collected randomly from each quadrat with use of a soil drilling sampling corer (9 cm in diameter) in accordance with serpents sampling and litter was cleared before soil sampling. The samples in the soil layer were collected at intervals of 0–10, 10–20, and 20–40 cm with a soil core (5 cm in diameter), and the samples from the same layer were mixed into a composite sample. All soil samples were naturally air-dried in the laboratory and were sieved thoroughly through a 2–mm screen, and other debris were removed by hand for an analysis of the soil chemical properties. The organic C concentrations

TABLE 1 | Descriptions of the sampling site.

Vegetation zone	Site	Latitude	Slope/(°)	Altitude/(m)	Target dominant species	Position
FO	A	35.95	28	1100	*Stipabungeana; Rubia cordifolia; Phragmites australis; Taraxacum mongolicum*	Southern Yanan
	B	36.22	17	1105	*Stipabungeana; Dracocephalum moldavica; Patrinia scabiosaefolia; Phragmites australis*	
	C	36.35	13	1015	*Stipabungeana; Lespedeza davurica; Taraxacum mongolicum; Incarvillea sinensis*	
	D	36.72	21	1100	*Stipabungeana; Lespedeza davurica; Taraxacum mongolicum; Phragmites australis*	
FS	E	36.88	19	1300	*Stipabungeana; Melilotus officinalis; Artemisia gmelinii; Lespedeza davurica*	Northern Yanan and Southern Ansai
	F	36.89	11	1330	*Stipabungeana; Melilotus officinalis; Saussurea amurensis; Lespedeza davurica*	
	G	37.03	15	1300	*Lespedeza davurica; Artemisia gmelinii; Bidens pilosa*	
	H	37.2	8	1277	*Artemisia gmelinii; Phragmites australis; Stipabungeana; Heteropappus altaicus*	
ST	I	37.33	11	1500	*Stipabungeana; Artemisia capillary; Dracocephalum moldavica; Lespedeza davurica*	Central Ansai and Southern Jingbian
	J	37.46	16	1500	*Stipabungeana; Lespedeza davurica; Artemisia desertorum; Scorzoneradivaricata*	
	K	37.67	12	1600	*Polygala tenuifolia; Erodium stephanianum; Dracocephalum moldavica; Vicia sepium*	
	L	37.79	12	1400	*Artemisia ordosica; Stipabungeana; Setaria viridis; Artemisia scoparia*	
SD	M	37.95	23	1100	*Artemisia desertorum; Heteropappus altaicus; Artemisia scoparia; Lespedeza davurica*	Northern Jingbian and Southern Yulin
	N	38.13	27	1148	*Artemisia desertorum; Artemisia scoparia; Astragalus adsurgens*	
	O	38.36	29	1205	*Artemisia desertorum; Artemisia scoparia; Lespedeza davurica*	

FO, Forest zone; FS, Forest steppe zone; ST, Steppe zone; SD, Steppe-desert zone.

TABLE 2 | The species diversity index of the herb communities in different vegetation zones.

Vegetation zone	Species number	Shannon-Wiener index	Pielou index	Community productivity (g/m^2)
FO	11.5 ± 1.21a	2.71 ± 0.21a	0.87 ± 0.02a	178.80 ± 14.7ab
FS	8.75 ± 0.98*bc*	2.47 ± 0.14b	0.76 ± 0.03ab	191.21 ± 13.5a
ST	9.55 ± 1.03b	2.43 ± 0.16ab	0.74 ± 0.05ab	144.86 ± 10.4b
SD	6 ± 0.77*d*	2.23 ± 0.25*c*	0.54 ± 0.11*c*	98.35 ± 9.5*c*

Values are the means ± SE in the above table. Within each column, means with different letters are significantly different based on ANOVA and LSD ($P < 0.05$).

of the soil and plant samples were analyzed by the classical potassium dichromate external heating method, and the total N concentrations of the soil and plant samples were measured via the semi-micro Kjeldahl method; in addition, the total P concentration was analyzed colorimetrically by the ammonium molybdate method (Bao, 2000).

Statistical Analyses

All variables were described by the mean and standard error (SE), and SPSS 18.0 software (SPSS Inc., Chicago, IL, United States) was used for the statistical analysis. All of the data were checked for the normality and homogeneity of the variances before applying the parametric tests. One-way ANOVA and multiple comparisons (LSD) were used to test the differences between the plant leaves and the soil nutrients and the stoichiometric characteristics in different vegetation zones. Regressions were linear for the latitudinal patterns of leaf C:N:P stoichiometry, while nonlinear fits were used for the latitudinal patterns of soil C:N:P stoichiometry. The Pearson coefficient test was used to measure the correlation between leaf and soil C:N:P stoichiometry and climatic variables. The figures were conducted using Origin 9.0. The plant leaf and soil nutrients concentrations were expressed as mg·g^{-1} on a dry mass basis, and all of the C:N:P stoichiometric ratios in leaves and soil were mass ratios.

RESULTS

Patterns of Soil C, N, and P Concentrations and Ratios Along Latitudinal Gradients

As seen from parts A and B of **Figure 3**, the concentrations of the soil C and the soil N at all three depths tended to decline exponentially along the latitudinal gradients, and all of the regression equations reached significant levels ($P < 0.01$). In

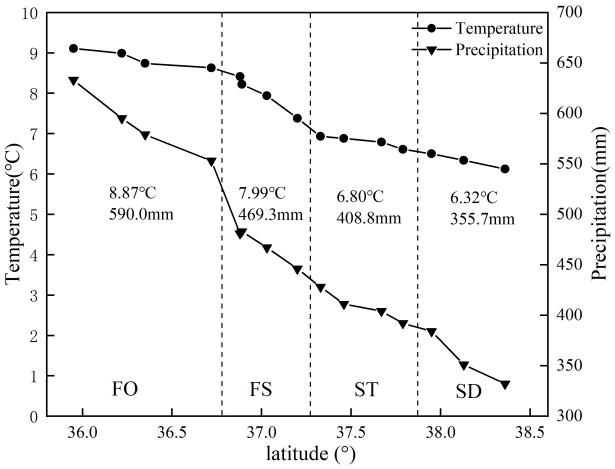

FIGURE 2 | Climatic features of the sampling sites.

contrast, with increasing latitude, the concentrations of soil P in the three soil layers were significantly diminished by the binomial approach ($P < 0.01$) (**Figure 3C**). The patterns for the soil C:N ratios showed poor performance; however, only the 20–40 cm soil layers significantly decreased along the latitudinal gradients ($P < 0.01$) (**Figure 3D**). The patterns for the soil C:P and N:P ratios were similar to those of the soil C and N concentrations (**Figures 3E,F**), and an exponential regression equation was suitable for the trend of the soil C:P and N:P ratios variations in all three soil depths, while the soil N:P ratio (20–40 cm) was not noticeable in the exponential regression ($P > 0.05$).

To further explore this difference, we compared the differences in the soil nutrients between the four different vegetation zones in the 0–40 cm soil layer (**Table 3**). The soil C and N concentrations of the three soil layers in the FO were the highest, while the soil P concentrations of the three soil layers in the FS were the highest among the four vegetation zones. The concentrations of total soil C and total soil N in the 0–10 cm soil layer varied with a ranking of FO > FS > ST ≈ SD; similarly, a ranking of FO > FS ≈ ST > SD was presented in the 20–40 cm soil layer for the concentrations of the total soil C and the total soil N. Furthermore, the concentrations of total soil P in all three soil layers had the same varied trend in all four vegetation zones: FS > FO ≈ ST > SD. The C:N ratio of 20–40 cm and the N:P ratio of 0–10 cm showed obvious differences in the four vegetation zones, but the ratios of C:P showed a significant difference in the 0–10 and 20–40 cm soil layers of the four vegetation zones.

Patterns of Leaf C, N, and P Concentrations and Ratios Along Latitudinal Gradients

The leaf C, N, and P nutrient patterns in **Figure 4** show that the latitudinal gradient had a significant effect on the leaf total C, total N and total P concentrations. There was an obviously different trend between the leaf C concentrations and the leaf N, P concentrations along the latitudinal gradient. With the increase of latitude, the leaf C concentrations remarkably decreased ($r^2 = 0.794$, $P < 0.001$) (**Figure 4A**), while the leaf N, P concentrations apparently increased ($r^2 = 0.845$, $P < 0.001$; $r^2 = 0.850$, $P < 0.001$) (**Figures 4B,C**). Furthermore, the patterns for the leaf C:N ratios (**Figure 4D**) and C:P ratios (**Figure 4E**) were similar to that for the leaf C concentrations (**Figure 4A**). The relationship between the leaf N:P and the latitude, however, was not significant ($r^2 = 0.085$, $P = 0.723$) (**Figure 4F**). Furthermore, our analysis of variance on the leaf nutrients and the C:N:P characteristics stoichiometry was consistent with the observation results above (**Table 4**).

Relationships Between the Soil Nutrients and the Leaf Stoichiometry

There were significant differences in the correlations among different soil layer C, N, P concentrations, the leaf C, N, P concentrations and the C:N:P stoichiometric characteristics (**Table 5**). Overall, the different soil layers of the C, N, P concentrations were positively correlated with the leaf C concentrations, while being negatively correlated with the leaf N, P concentrations (except the soil P concentrations). The correlation between the leaf N:P and the different soil layer C, N, P nutrient concentrations was weakly ($P > 0.05$), while the different soil layer C, N, P nutrient concentrations and leaf C:N, and C:P stoichiometric characteristics showed a significant or extremely significant positive correlation. More interestingly, a significantly positive correlation with the soil total phosphorus concentration in different soil layers, the leaf C concentrations ($P < 0.01$), and the leaf N, P concentrations were not significant ($P > 0.01$). The correlation analysis between the soil and leaf stoichiometric characteristics in **Figure 5** shows that the soil C:N ratio of 20–40 cm was significantly correlated with the leaf C:N ratio ($P < 0.01$), and the ratios of soil C:P at all three depths were significantly correlated with the leaf C:P ratio. In contrast, there was no significant correlation between the soil N:P ratios at all three depths and the leaf N:P ratio.

Relationships Between Leaf and Soil Nutrient Traits With Climatic Variables

Leaf C, C:N, and C:P ratios were positively correlated with MAT ($r = 0.783$, $P < 0.01$; $r = 0.918$, $P < 0.01$; $r = 0.887$, $P < 0.01$) and MAP ($r = 0.693$, $P < 0.01$; $r = 0.922$, $P < 0.01$; $r = 0.820$, $P < 0.01$), leaf N and P were negatively correlated with MAT ($r = -0.876$, $P < 0.01$; $r = -0.871$, $P < 0.01$) and MAP ($r = -0.915$, $P < 0.01$; $r = -0.851$, $P < 0.01$), while leaf N:P ratios were weakly correlated with MAT and MAP ($P > 0.05$). For soil nutrient traits, the soil C, N, C:P, and N:P ratios at all three depths (0–10, 10–20, and 20–40 cm) were positively correlated with MAT ($r = 0.592$–0.842, $P < 0.05$) and MAP ($r = 0.592$–0.814, $P < 0.05$), while the soil P and C:N ratios at all three depths were weakly correlated with MAT and MAP ($P > 0.05$) (**Table 6**).

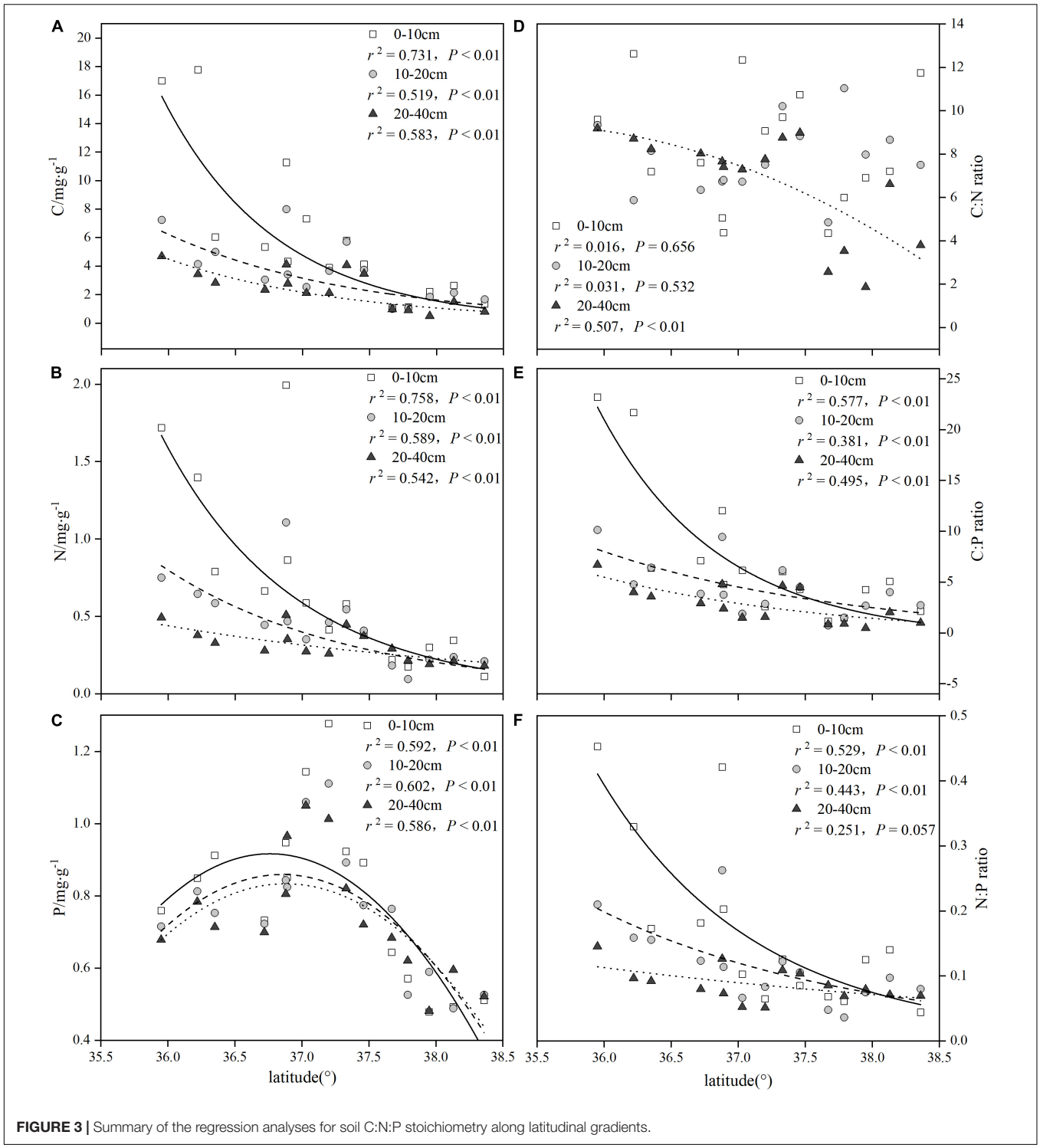

FIGURE 3 | Summary of the regression analyses for soil C:N:P stoichiometry along latitudinal gradients.

DISCUSSION

The Latitudinal Patterns of Soil C:N:P Stoichiometry in Response to Climate

In the current study, the soil C and soil N concentrations in different soil layers showed an exponential decrease as latitude increased, which was consistent with previous findings (Wu et al., 2003; Yang et al., 2007; Zhu et al., 2013). Nitrogen in the soil mainly depends on the accumulation and decomposition of organic matter, which was positively correlated with the soil organic matter, and consequently, the soil N and soil C showed consistent spatial distribution patterns. A possible explanation for the pattern of the C:N ratios were weakly correlations with

TABLE 3 | The concentrations of soil nutrients and the soil ecological stoichiometry.

Soil layer	Vegetation zone types	C content (g/kg)	N content (g/kg)	P content (g/kg)	C:N ratio	C:P ratio	N:P ratio
0–10 cm	FO	11.53 ± 3.38a	1.14 ± 0.25a	0.81 ± 0.04b	9.57 ± 1.16a	14.31 ± 4.26a	1.42 ± 0.33a
	FS	6.70 ± 1.70ab	0.96 ± 0.36ab	1.05 ± 0.10a	8.13 ± 1.74a	6.61 ± 1.89ab	0.99 ± 0.40ab
	ST	3.04 ± 1.16b	0.34 ± 0.09b	0.76 ± 0.09b	8.12 ± 1.41a	3.65 ± 1.10b	0.42 ± 0.72b
	SD	2.06 ± 0.38b	0.25 ± 0.07b	0.49 ± 0.09c	8.98 ± 1.46a	4.20 ± 0.82b	0.52 ± 0.15ab
10–20 cm	FO	4.86 ± 0.89a	0.61 ± 0.06a	0.75 ± 0.22b	7.87 ± 0.75a	6.52 ± 1.30a	0.81 ± 0.89a
	FS	4.41 ± 1.22a	0.60 ± 0.17a	0.96 ± 0.07a	7.42 ± 0.18a	4.83 ± 1.59a	0.66 ± 0.22a
	ST	2.89 ± 1.14a	0.31 ± 0.10ab	0.74 ± 0.77b	9.08 ± 1.28a	3.64 ± 1.19a	0.39 ± 0.11a
	SD	1.89 ± 0.14a	0.22 ± 0.01c	0.53 ± 0.30c	8.44 ± 0.31a	3.56 ± 0.41a	0.42 ± 0.03a
20–40 cm	FO	3.33 ± 0.51a	0.37 ± 0.46a	0.72 ± 0.02b	8.91 ± 0.24a	4.65 ± 0.78a	0.52 ± 0.07a
	FS	2.78 ± 0.47ab	0.35 ± 0.57ab	0.96 ± 0.54a	7.96 ± 0.10ab	3.02 ± 0.72ab	0.38 ± 0.09a
	ST	2.36 ± 0.83ab	0.33 ± 0.05ab	0.71 ± 0.04b	6.50 ± 1.58ab	3.17 ± 1.00ab	0.46 ± 0.05a
	SD	0.94 ± 0.29c	0.19 ± 0.01c	0.53 ± 0.03c	4.75 ± 1.29c	1.72 ± 0.43b	0.37 ± 0.02a

Means with different small letters were significantly different at the 0.05 level for different vegetation zones at the same soil layer.

the latitude in that the trends for the soil N with respect to the latitude were general similar to the trends for soil C, which also verified the relative stability of the soil C:N ratios in different ecosystems (Tian et al., 2010). Previous findings have suggested that the concentrations of soil C and soil N were determined by the relative size of the input and output quantities of soil organic matter and nitrogen (Trumbore et al., 1996); meanwhile, the climate (temperature and precipitation) and the soil formation are main factors that affect the characteristics of the soil ecological chemometrics (Tian et al., 2010). The results of correlation analysis showed that the concentrations of soil C and N in all three soil depths (0–10, 10–20, and 20–40 cm) were significantly correlated with MAP and MAT ($P < 0.05$) (**Table 6**), which indicated that the soil C and N were influenced by biological action under natural conditions. In this area, the temperature and rainfall showed a significant downward trend with increasing latitude, which resulted in high P leaching rate and weathering rate. At the same time, the high species diversity and productivity of the FO and the FS maintained relatively high soil C and N concentrations (**Table 2**), which gave these regions higher C:P and N:P ratios. However, the dry and cool climate regime in the ST and in the SD resulted in low species diversity and productivity (**Table 2**), lower soil C and N concentrations and low P leaching rate. Hence, the soil organic carbon and the total nitrogen displayed a decreasing trend with the latitudinal gradients. In addition, this was demonstrated in a number of studies that showed that the soil C and N concentrations decreased with the increase in soil depth (Drahorad et al., 2013; Gao and Cheng, 2013).

In contrast, the spatial variability of soil P is relatively smaller than that of soil C and N in our study. As mentioned above, high P leaching rate in the FO and the FS resulted in decreasing of soil P concentrations and high productivity and abundant litter transported more nutrients for the soil, promoting accumulation of the soil C, N, and P (Muller, 2014). Lower productivity in the ST and in the SD led to reduced nutrient input, which gave these regions relatively low soil P concentrations. Based on an inventory data set of 2,384 soil profiles, Tian et al. (2010) found that the soil P concentrations were affected by a series of factors such as the parent material, climate, biology, and geochemical processes in the soil. Our previous studies suggested that the soil P concentrations at all three depths were weakly correlated with MAT and MAP ($P > 0.05$) which this weak relationship probably be attributed to the smaller scale in this study.

The Latitudinal Patterns of Leaf C:N:P Stoichiometry in Response to Climate

Considerable research efforts have been devoted to investigate the geographical pattern of plant nutrient elements and its relationship with environmental factors at local, regional, or global scales. The leaf C concentrations sharply decreased with the increasing latitude. A better explanation for this decline is that the plants overcame stress conditions (the temperature increase aggravates soil aridity with the decline of latitude) by increasing their structural carbon compounds (cellulose, lignin, cutin, and waxes) (Bussotti et al., 2000). Reich and Oleksyn (2004) revealed that global leaf N and P concentrations increased and N:P ratios decreased with increasing latitude (or decreasing mean annual temperature, MAT). The concentrations of leaf N and P showed an increasing trend along the latitudinal gradients, which is a phenomenon that can be explained well by the Temperature-Plant Physiological Hypothesis (Reich and Oleksyn, 2004). In contrast, Han et al. (2005) and Ren et al. (2007) revealed similar research findings in China at the regional scale, but the differences were that N:P ratio was weakly correlated with the latitude and the MAT. In addition, Zheng and Shangguan (2007) found that C:N and C:P ratios in the leaves of the Loess Plateau were not related to the latitude and the MAT, but N/P increased with the increasing latitude and was not correlated with MAT. In this study, leaf C, C/N, and C/P ratios decreased as the latitude increased and MAT and MAP decreased, and leaf N, P concentrations increased as the latitude increased and MAT and MAP decreased, while leaf N/P ratio was unrelated to

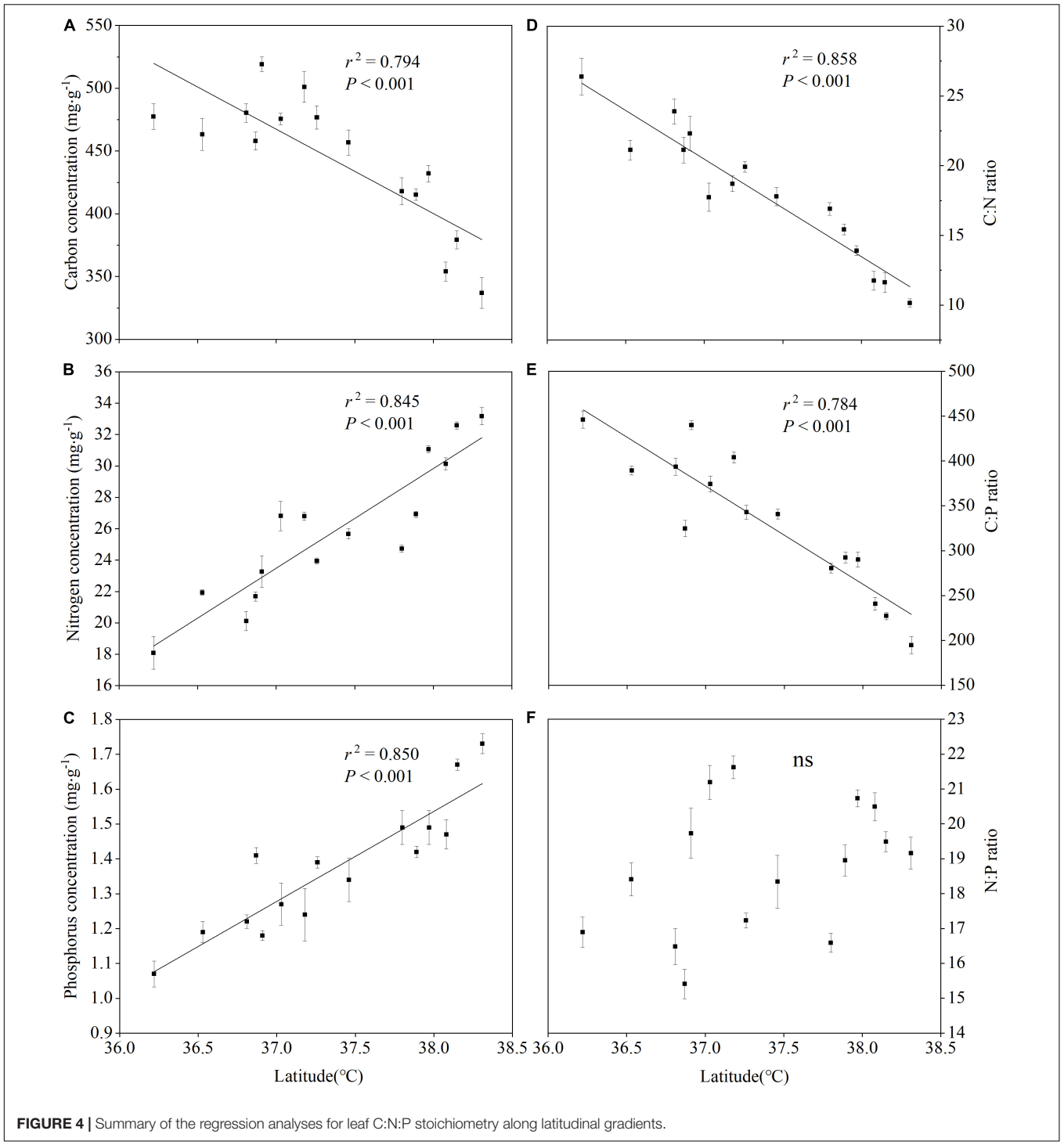

FIGURE 4 | Summary of the regression analyses for leaf C:N:P stoichiometry along latitudinal gradients.

TABLE 4 | The concentrations of the leaf nutrients and the leaf ecological stoichiometry.

Vegetation zone types	C content (g/kg)	N content (g/kg)	P content (g/kg)	C:N ratio	C:P ratio	N:P ratio
FO	469.70 ± 5.41a	20.45 ± 0.88*c*	1.22 ± 0.07*c*	23.1 ± 1.27a	388.46 ± 24.85a	16.80 ± 0.62*c*
FS	493.06 ± 10.49a	25.20 ± 0.93b	1.27 ± 0.04*bc*	19.67 ± 0.99b	390.31 ± 20.72a	19.94 ± 0.99a
ST	430.47 ± 9.50b	27.10 ± 1.40b	1.44 ± 0.04b	16.00 ± 0.85*c*	300.92 ± 13.56b	18.65 ± 0.85ab
SD	356.76 ± 12.30*c*	31.96 ± 0.93a	1.62 ± 0.08a	11.2 ± 0.51*d*	220.91 ± 13.65*c*	19.71 ± 0.40a

Means with different small letters were significantly different at the 0.05 level for different vegetation zones.

TABLE 5 | Correlation coefficients between the leaf stoichiometry characteristics and the soil nutrients.

	0–10 cm			10–20 cm			20–40 cm		
	Soil C	**Soil N**	**Soil P**	**Soil C**	**Soil N**	**Soil P**	**Soil C**	**Soil N**	**Soil P**
Leaf C	0.567*	0.671*	0.782**	0.653*	0.710**	0.723**	0.685*	0.675*	0.775**
Leaf N	−0.668*	−0.648*	−0.511	−0.691*	−0.696*	−0.48	−0.757**	−0.630*	−0.36
Leaf P	−0.736**	−0.637*	−0.458	−0.684*	−0.714**	−0.514	−0.712**	−0.772**	−0.456
Leaf C:N	0.749**	0.771**	0.609	0.777**	0.784**	0.532*	0.791**	0.746**	0.468
Leaf C:P	0.756**	0.823**	0.659*	0.755**	0.794**	0.619*	0.758**	0.771**	0.629*
Leaf N:P	−0.127	−0.078	0.053	−0.267	−0.194	−0.007	−0.338	−0.209	0.223

*Correlation is significant at the 0.05 level (2-tailed), **Correlation is significant at the 0.01 level (2-tailed).

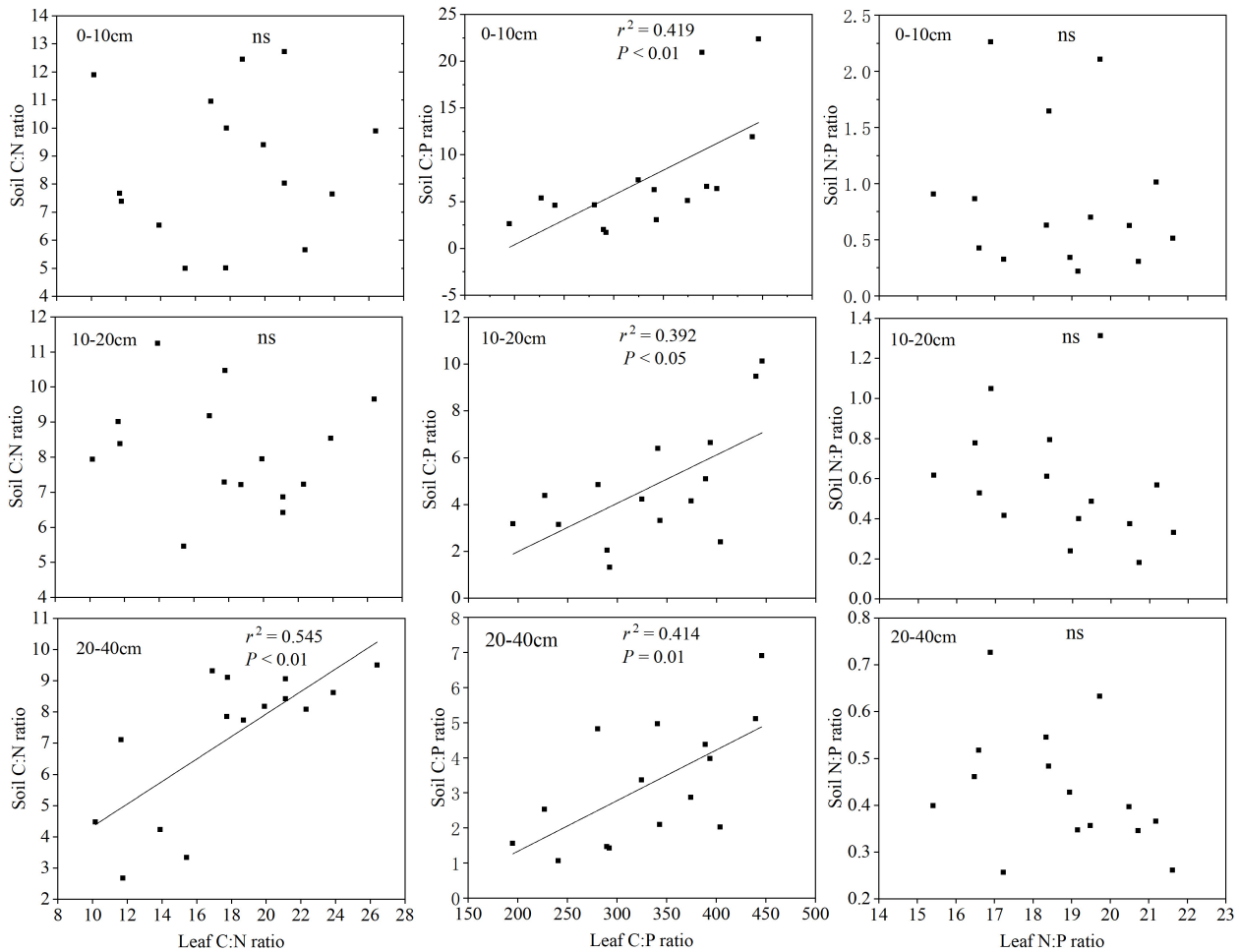

FIGURE 5 | Relationships between the soil and leaf C:N:P stoichiometry.

the latitude, MAT. and MAP (**Figure 4** and **Table 6**). Possible reasons for this inconsistency may be attributed to the difference of research scales and sample size. Our study had a smaller geographical range with its latitudes ranging from 36 to 39°N and its sample size was much smaller than that in other scholars' studies.

Furthermore, to deeply reveal the level of the leaf nutrients and the leaf C:N:P characteristics of the herbaceous vegetation of the Loess Plateau, we compared the results of this study with other scholars' findings and found that the leaf C concentrations of herbaceous plants in the Loess Plateau were significantly lower than that of the average global level of Elser et al. (2000a), which was consistent with the results of Zheng and Shangguan (2007) for the leaf C concentrations in the Loess Plateau. Furthermore, the leaf N concentrations of herbaceous plants on the Loess Plateau were significantly higher than the

TABLE 6 | Correlation coefficients between leaf, soil nutrient traits, and climatic variables in the Loess Plateau of China.

Leaf	MAT	MAP	0–10cm Soil	MAT	MAP	10–20cm Soil	MAT	MAP	20–40cm Soil	MAT	MAP
C	0.783**	0.693**	C	0.842**	0.814**	C	0.646**	0.619**	C	0.678**	0.672**
N	−0.876**	−0.915**	N	0.802**	0.734**	N	0.730**	0.649**	N	0.625*	0.604*
P	−0.871**	−0.851**	P	0.465	0.39	P	0.412	0.339	P	0.427	0.308
C/N	0.918**	0.922**	C/N	0.066	0.131	C/N	−0.298	−0.182	C/N	0.335	0.526
C/P	0.877**	0.820**	C/P	0.778**	0.774**	C/P	0.592*	0.592*	C/P	0.629*	0.666**
N/P	−0.342	−0.464	N/P	0.759**	0.724**	N/P	0.697**	0.640*	N/P	0.434*	0.492*

*Correlation is significant at the 0.05 level (2-tailed), **Correlation is significant at the 0.01 level (2-tailed).

level at the global scale (Reich et al., 1999; Elser et al., 2000a), but were also slightly higher than that found on the Loess Plateau by Zheng and Shangguan (2007). Herbs generally absorb highly mobile mineral nitrogen (such as nitrate nitrogen and ammonium nitrogen), which can be used to improve the level of leaf N nitrogen concentrations directly. The influence of hydrothermal factors increased the mineralization rate of soil N on the Loess Plateau, thereby increasing the leaf N concentrations of herbaceous plants (Heerwaarden et al., 2010). In recent years, the soil available nitrogen increased due to the increase of nitrogen deposition (Galloway et al., 2008), and it also promoted the leaf N concentrations of herbaceous plants. Furthermore, the leaf P concentrations of herbaceous plants on the Loess Plateau were significantly lower than that at the global scale (Reich et al., 1999; Elser et al., 2000a), but were also slightly lower than that at the Loess Plateau (Zheng and Shangguan, 2007) scale and at the China national scale (Han et al., 2005). This reveals that the P concentrations of herbaceous plants on the Loess Plateau scale and even on the China national scale were still kept at a fairly low level. Studies have showed that, serious soil erosion causes great losses of plant nutrients, which may lead to herbaceous plants on the Loess Plateau to be at low phosphorus levels (Zheng and Shangguan, 2007). In brief, compared with the global scale, the Loess Plateau is characterized by lower C, P concentrations and higher N concentrations for herbaceous leaves, which results in lower leaf C:N ratio and higher C:P and N:P ratios than those of the global scale.

Relationships Between Leaf and Soil C:N:P Stoichiometry

Plant and soil, as different components in the biogeochemical cycle, are closely linked and interact with each other; however, a few examples have been reported to show how the concentrations of C, N, and P in soil were related to their concentrations in plants (Jobbágy and Jackson, 2001; Yu et al., 2010). Our results show that there was strong links between leaf C:N:P stoichiometry and soil properties (except for soil P), which is consistent with previous studies (Han et al., 2005; Zeng et al., 2016). Generally, the absorption and utilization of soil nutrients is the main purpose for the output of soil available nutrients. The soil and herbaceous plants achieve and maintain a balanced proportion of elements through the dynamic exchange of nutrient supply and demand. In this report, the soil P concentrations were not positively related to the leaf N, P concentrations, which confirmed to the results of Yang et al. (2018). According to the correlation analysis between the soil and leaf stoichiometric characteristics, we found that the soil C:P ratios in all three depths were significantly related to the leaf C:P ratios. This observation is mainly related to an extremely significant positive correlation between the soil P concentrations in all three depths and the leaf C concentrations (**Table 5**). Moreover, the dynamics of the plant leaf nutrients are primarily restricted by the soil P supply on the Loess Plateau, which we will discuss below. Furthermore, the soil C:N ratio of 20–40 cm was significant correlated with the leaf C:N ratios, probably because the soil C and N concentrations in the 0–10 and 10–20 cm soil layers varied greatly.

The leaf N:P ratios were used as an indicator of the N-limitation or P-limitation in the ecosystems; i.e., N:P ratios <14 suggest N limitation, and N:P ratios >16 suggest P limitation (Güsewell, 2010). In this study, the average N:P ratios of the four vegetation zones were all higher than 16 (**Table 4**), which also suggested an increase in the P limitation in the Loess Plateau compared with the results of a global scale study (Elser et al., 2000a; Reich and Oleksyn, 2004). Therefore, further research should pay more attention to the transformation of the soil nutrient-limited elements and the interactions among the C:N:P stoichiometry in the plant-soil systems, especially for large-scale vegetation restoration projects on the Loess Plateau.

CONCLUSION

Our study provided a complete picture of the spatial patterns of the C, N, and P elements of leaves and the soil stoichiometry along the latitude of the Loess Plateau. The results suggested that the soil C, N, P, and C:N:P ratios at all three depths (0–10, 10–20, and 20–40 cm) showed significant latitudinal trends (except for soil C:N ratios) ($P < 0.01$). In general, the soil C, N, and C:N:P ratios decreased exponentially while soil P increased first and then decreased with the latitude. The soil C, N, C:P, and N:P ratios at all three depths (0–10, 10–20, and 20–40 cm) were positively correlated with MAT and MAP ($P < 0.05$), while soil P and C:N ratios at all three depths were weakly correlated with MAT and MAP ($P > 0.05$). In addition, leaf C:N:P stoichiometry was significantly correlated with the latitude, MAT, and MAP (except for N:P ratios) ($P < 0.01$), such that, leaf C, C:N, and C:P ratios decreased as the latitude increased and MAT and MAP decreased, and leaf N, P concentrations increased as the latitude increased and MAT and MAP decreased, while leaf N:P ratios were weakly correlated with the latitude, MAT, and

MAP ($P > 0.05$). In addition, the leaf C:N:P stoichiometry of the herbaceous communities is related to the soil properties (except for soil P), and we found that the soil and plant C:P ratios are strongly related, which indicated strong links among the C:N:P stoichiometry in leaves and the soil properties. Compared with the vegetation of global scale, the vegetation of the Loess Plateau is more susceptible to P limitation.

DATA AVAILABILITY

All datasets generated for this study are included in the manuscript and/or the supplementary files.

AUTHOR CONTRIBUTIONS

FJ contributed to study design, statistical analyses, and data management. D-DL, JY, and H-TD performed the experiments. ZF wrote the manuscript.

FUNDING

This study was supported by the National Key Research and Development Program of China (2016YFA0600801) and the National Special Program on Basic Works for Science and Technology of China (2014FY210130).

REFERENCES

An, S. S., Darboux, F., and Cheng, M. (2013). Revegetation as an efficient means of increasing soil aggregate stability on the Loess Plateau (China). *Geoderma* 209, 75–85. doi: 10.1016/j.geoderma.2013.05.020

Bao, S. D. (2000). *Soil Agrochemical Analysis*. Beijing: China Agriculture Press.

Bardgett, R. D., Bowman, W. D., Kaufmann, R., and Schmidt, S. K. (2005). A temporal approach to linking aboveground and belowground ecology. *Trends Ecol. Evol.* 20, 634–641. doi: 10.1016/j.tree.2005.08.005

Bussotti, F., Borghini, F., Celesti, C., Leonzio, C., and Bruschi, P. (2000). Leaf morphology and macronutrients in broadleaved trees in central Italy. *Trees* 14, 361–368. doi: 10.1007/s004680000056

Cernusak, L. A., Winter, K., and Turner, B. L. (2010). Leaf nitrogen to phosphorus ratios of tropical trees: experimental assessment of physiological and environmental controls. *New Phytol.* 185, 770–779. doi: 10.1111/j.1469-8137.2009.03106.x

Chai, Y. F., Liu, X., Yue, M., Guo, J. C., Wang, M., Wan, P., et al. (2015). Leaf traits in dominant species from different secondary successional stages of deciduous forest on the Loess Plateau of northern China. *Appl. Veg. Sci.* 18, 50–63. doi: 10.1111/avsc.12123

Chen, L. Y., Li, P., and Yang, Y. H. (2016). Dynamic patterns of nitrogen: phosphorus ratios in forest soils of China under changing environment. *J. Geophys. Res. Biogeosci.* 121, 2410–2421. doi: 10.1002/2016jg003352

Cheng, J. M., and Wan, H. E. (2002). *Vegetation Construction and Soil and Water Conservation in the Loess Plateau of China*. Beijing: China Forestry Publishing House.

Drahorad, S., Felix-Henningsen, P., Eckhardt, K. U., and Leinweber, P. (2013). Spatial carbon and nitrogen distribution and organic matter characteristics of biological soil crusts in the Negev desert (Israel) along a rainfall gradient. *J. Arid. Environ.* 94, 18–26. doi: 10.1016/j.jaridenv.2013.02.006

Elser, J. J., Fagan, W. F., Denno, R. F., Dobberfuhl, D. R., Folarin, A., Huberty, A., et al. (2000a). Nutritional constraints in terrestrial and freshwater food webs. *Nature* 408, 578–580. doi: 10.1038/35046058

Elser, J. J., Sterner, R. W., Gorokhova, E., Fagan, W. F., Markow, T. A., Cotner, J. B., et al. (2000b). Biological stoichiometry from genes to ecosystems. *Ecol. Lett.* 3, 540–550. doi: 10.1046/j.1461-0248.2000.00185.x

Fu, B. J., Chen, L. D., Ma, K. M., Zhou, H. F., and Wang, J. (2000). The relationships between land use and soil conditions in the hilly area of the loess plateau in northern Shaanxi. *Catena* 39, 69–78. doi: 10.1016/S0341-8162(99)00084-3

Galloway, J. N., Townsend, A. R., Erisman, J. W., Bekunda, M., Cai, Z., Freney, J. R., et al. (2008). Transformation of the nitrogen cycle: recent trends, questions, and potential solutions. *Science* 320, 889–892. doi: 10.1126/science.1136674

Gao, Y., and Cheng, J. M. (2013). Spatial and temporal variations of grassland soil organic carbon and total nitrogen following grazing exclusion in semiarid Loess Plateau, Northwest China. *Acta Agric. Scand. Sect. B Soil Plant Sci.* 63, 704–711. doi: 10.1080/09064710.2013.854828

Güsewell, S. (2010). N:P ratios in terrestrial plants: variation and functional significance. *New Phytol.* 164, 243–266. doi: 10.1111/j.1469-8137.2004.01192.x

Han, W. X., Fang, J. Y., Guo, D. L., and Zhang, Y. (2005). Leaf nitrogen and phosphorus stoichiometry across 753 terrestrial plant species in China. *New Phytol.* 168, 377–385. doi: 10.1111/j.1469-8137.2005.01530.x

He, J. S., Fang, J. Y., Wang, Z. H., Guo, D. L., Flynn, D. F. B., and Geng, Z. (2006). Stoichiometry and large-scale patterns of leaf carbon and nitrogen in the grassland biomes of China. *Oecologia* 149, 115–122. doi: 10.1007/s00442-006-0425-0

Heerwaarden, L. M. V., Toet, S., and Aerts, R. (2010). Nitrogen and phosphorus resorption efficiency and proficiency in six sub-arctic bog species after 4years of nitrogen fertilization. *J. Ecol.* 91, 1060–1070. doi: 10.1046/j.1365-2745.2003.00828.x

Jiao, F., Wen, Z. M., and An, S. S. (2011). Changes in soil properties across a chronose quence of vegetation restoration on the Loess Plateau of China. *Catena* 86, 110–116. doi: 10.1016/j.catena.2011.03.001

Jobbágy, E. G., and Jackson, R. B. (2001). The distribution of soil nutrients with depth: global patterns and the imprint of plants. *Biogeochemistry* 53, 51–77. doi: 10.1023/A:1010760720215

Koerselman, W. (1996). The vegetation n:p ratio: a new tool to detect the nature of nutrient limitation. *J. Appl. Ecol.* 33, 1441–1450. doi: 10.2307/2404783

Lambers, H., Mougel, C., Jaillard, B., and Hinsinger, P. (2009). Plant-microbe-soil interactions in the rhizosphere: an evolutionary perspective. *Plant Soil.* 321, 83–115. doi: 10.1007/s11104-009-0042-x

Laurel, J. A. (2013). Aboveground-belowground linkages: biotic interactions, ecosystem processes, and global change. *Q. Rev. Biol.* 86, 340–340. doi: 10.1086/662483

Muller, R. N. (2014). "Nutrient relation of the herbaceous layer in deciduous forest ecosystems," in *The Herbaceous Layer in Forests of Eastern North America*, ed. F. S. Gilliam (New York, NY: Oxford University Press), 13–34.

Reich, P. B., Ellsworth, D. S., Walters, M. B., Vose, J. M., Gresham, C., Volin, J. C., et al. (1999). Generality of leaf trait relationships: a test across six biomes. *Ecology* 80, 1955–1969. doi: 10.2307/176671

Reich, P. B., and Oleksyn, J. (2004). Global patterns of plant leaf N and P in relation to temperature and latitude. *Proc. Natl. Acad. Sci. U.S.A.* 101, 11001–11006. doi: 10.1073/pnas.0403588101

Ren, S. J., Yu, G. R., Tao, B., and Wang, S. Q. (2007). Leaf nitrogen and phosphorus stoichiometry across 654 terrestrial plant species in NSTEC. *J. Environ. Sci.China* 28, 2665–2673. doi: 10.13227/j.hjkx.2007.12.007

Shi, X. Z., Yu, D. S., Xu, S. X., Warner, E. D., Wang, H. J., Sun, W. X., et al. (2010). Cross-reference for relating genetic soil classification of China with WRB at different scales. *Geoderma* 155, 344–350. doi: 10.1016/j.geoderma.2009.12.017

Sterner, R. W., and Elser, J. J. (2002). *Ecological Stoichiometry: The Biology of Elements from Molecules to the Biosphere*. New Jersey: Princeton University Press.

Thompson, K., Parkinson, J. A., Band, S. R., and Spencer, R. E. (2010). A comparative study of leaf nutrient concentrations in a regional herbaceous flora. *New Phytol.* 136, 679–689. doi: 10.1046/j.1469-8137.1997.00787.x

Tian, H. Q., Chen, G. S., Zhang, C., Melillo, J. M., and Hall, C. A. S. (2010). Pattern and variation of C:N:P ratios in China's soils: a synthesis of observational data. *Biogeochemistry* 98, 139–151. doi: 10.1007/s10533-009-9382-0

Trumbore, S. E., Chadwick, O. A., and Amundson, R. (1996). Rapid exchange between soil carbon and atmospheric carbon dioxide driven by temperature change. *Science* 272, 393–396. doi: 10.1126/science.272.5260.393

van der Heijden, M. G. A., Bardgett, R. D., and van Straalen, N. M. (2010). The unseen majority: soil microbes as drivers of plant diversity and productivity in terrestrial ecosystems. *Ecol. Lett.* 11, 296–310. doi: 10.1111/j.1461-0248.2007.01139.x

van der Putten, W. H., Bardgett, R. D., de Ruiter, P. C., Hol, W. H. G., Meyer, K. M., Bezemer, T. M., et al. (2009). Empirical and theoretical challenges in aboveground–belowground ecology. *Oecologia* 161, 1–14. doi: 10.1515/9781400847297.105

Wang, L. L., Zhao, G. X., Li, M., Zhang, M. T., Zhang, L. F., Zhang, X., et al. (2015). C:n:p stoichiometry and leaf traits of halophytes in an arid saline environment, northwest china. *PLoS One* 10:e0119935. doi: 10.1371/journal.pone.0119935

Wardle, D. A., and Peltzer, D. A. (2007). "Aboveground-belowground linkages, ecosystem development, and ecosystem restoration," in *The Linking Restoration and Ecological Succession*, eds L. Walker, J. Walker, and R. J. Hobbs (New York, NY: Springer Press), 45–68. doi: 10.1007/978-0-387-35303-6_3

Wright, I. J., Reich, P. B., Cornelissen, J. H. C., Falster, D. S., Garnier, E., Hikosaka, K., et al. (2010). Assessing the generality of global leaf trait relationships. *New Phytol.* 166, 485–496. doi: 10.1111/j.1469-8137.2005.01349.x

Wu, H. B., Guo, Z. T., and Peng, C. H. (2003). Land use induced changes of organic carbon storage in soils of China. *Glob. Change Biol.* 9, 305–315. doi: 10.1046/j.1365-2486.2003.00590.x

Yamanaka, N., Hou, Q. C., and Du, S. (2014). "Vegetation of the Loess Plateau," in *Restoration and Development of the Degraded Loess Plateau, China*, eds A. Tsunekawa, G. B. Liu, N. Yamanaka, and S. Du (Tokyo: Springer Press), 49–60. doi: 10.1007/978-4-431-54481-4_4

Yang, Y., Liu, B. R., and An, S. S. (2018). Ecological stoichiometry in leaves, roots, litters and soil among different plant communities in a desertified region of Northern China. *Catena* 166, 328–338. doi: 10.1016/j.catena.2018.04.018

Yang, Y. H., and Luo, Y. Q. (2011). Carbon:nitrogen stoichiometry in forest ecosystems during stand development. *Glob. Ecol. Biogeogr.* 20, 354–361. doi: 10.1111/j.1466-8238.2010.00602.x

Yang, Y. H., Mohammat, A., Feng, J. M., Zhou, R., and Fang, J. Y. (2007). Storage, patterns and environmental controls of soil organic carbon in China. *Biogeochemistry* 84, 131–141. doi: 10.1007/s10533-007-9109-z

Yu, Q., Chen, Q. S., Elser, J. J., He, N. P., Wu, H. W., Zhang, G., et al. (2010). Linking stoichiometric homoeostasis with ecosystem structure, functioning and stability. *Ecol. Lett.* 13, 1390–1399. doi: 10.1111/j.1461-0248.2010.01532.x

Zeng, Q. C., Li, X., Dong, Y. H., An, S. S., and Darboux, F. (2016). Soil and plant components ecological stoichiometry in four steppe communities in the Loess Plateau of China. *Catena* 147, 481–488. doi: 10.1016/j.catena.2016.07.047

Zhao, F. Z., Sun, J., Ren, C. J., Kang, D., Deng, J., Xinhui, H., et al. (2015). Land use change influences soil c, n, and p stoichiometry under 'grain-to-green program' in china. *Sci. Rep.* 5:10195. doi: 10.1038/srep10195

Zheng, S. X., and Shangguan, Z. P. (2007). Spatial patterns of leaf nutrient traits of the plants in the loess plateau of china. *Trees* 21, 357–370. doi: 10.1007/s00468-007-0129-z

Zhu, Q. L., Xing, X. Y., Zhang, H., and An, S. S. (2013). Soil ecological stoichiometry under different vegetation area on loess hilly-gully region. *Acta Ecol. Sin.* 33, 4674–4682. doi: 10.5846/stxb201212101772

Conflict of Interest Statement: The authors declare that the research was conducted in the absence of any commercial or financial relationships that could be construed as a potential conflict of interest.

frontiers in Plant Science

ORIGINAL RESEARCH
published: 26 March 2019
doi: 10.3389/fpls.2019.00356

The Growth and N Retention of Two Annual Desert Plants Varied Under Different Nitrogen Deposition Rates

Xiaoqing Cui[1,2†], Ping Yue[3,4†], Wenchao Wu[3,5], Yanming Gong[3], Kaihui Li[3], Tom Misselbrook[6], Keith Goulding[7] and Xuejun Liu[1]*

[1] Key Laboratory of Plant-Soil Interactions of the Ministry of Education, Beijing Key Laboratory of Farmland Soil Pollution Prevention and Remediation, College of Resources and Environmental Sciences, China Agricultural University, Beijing, China, [2] Sino-France Institute of Earth Systems Science, Laboratory for Earth Surface Processes, College of Urban and Environmental Sciences, Peking University, Beijing, China, [3] State Key Laboratory of Desert and Oasis Ecology, Xinjiang Institute of Ecology and Geography, Chinese Academy of Sciences, Ürümqi, China, [4] Urat Desert-Grassland Research Station, Northwest Institute of Eco-Environment and Resources, Chinese Academy of Sciences, Lanzhou, China, [5] College of Life Sciences, University of the Chinese Academy of Sciences, Beijing, China, [6] Department of Sustainable Soils and Grassland Systems, Rothamsted Research, Devon, United Kingdom, [7] Department of Sustainable Soils and Grassland Systems, Rothamsted Research, Harpenden, United Kingdom

OPEN ACCESS

Edited by:
Zhiyou Yuan,
Northwest A&F University, China

Reviewed by:
Juying Huang,
Ningxia University, China
Guo Ziwu,
Chinese Academy of Forestry, China
Xiaobing Zhou,
Xinjiang Institute of Ecology and Geography (CAS), China

***Correspondence:**
Xuejun Liu
liu310@cau.edu.cn

[†] These authors have contributed equally to this work as co-first authors

Specialty section:
This article was submitted to Plant Abiotic Stress, a section of the journal Frontiers in Plant Science

Received: *27 September 2018*
Accepted: *07 March 2019*
Published: *26 March 2019*

Citation:
Cui X, Yue P, Wu W, Gong Y, Li K, Misselbrook T, Goulding K and Liu X (2019) The Growth and N Retention of Two Annual Desert Plants Varied Under Different Nitrogen Deposition Rates. Front. Plant Sci. 10:356. doi: 10.3389/fpls.2019.00356

Nitrogen (N) partitioning between plant and soil pools is closely related to biomass accumulation and allocation, and is of great importance for quantifying the biomass dynamics and N fluxes of ecosystems, especially in low N-availability desert ecosystems. However, partitioning can differ among species even when growing in the same habitat. To better understand the variation of plant biomass allocation and N retention within ephemeral and annual species we studied the responses of *Malcolmia Africana* (an ephemeral) and *Salsola affinis* (an annual) to N addition, including plant growth, N retention by the plant and soil, and N lost to the environment using ^{15}N (double-labeled $^{15}NH_4{}^{15}NO_3$ (5.16% abundance) added at 0, 0.8, 1.6, 3.2, and 6.4 g pot^{-1}, equivalent to 0, 15, 30, 60, and 120 kg N ha^{-1}) in a pot experiment. Higher N addition (N120) inhibited plant growth and biomass accumulation of the ephemeral but not the annual. In addition, the aboveground:belowground partitioning of N (the R:S ratio) of the ephemeral decreased with increasing N addition, but that of the annual increased. The N input corresponding to maximum biomass and ^{15}N retention of the ephemeral was significantly less than that of the annual. The aboveground and belowground retention of N in the ephemeral were significantly less than those of the annual, except at low N rates. The average plant–soil system recovery of added ^{15}N by the ephemeral was 70%, significantly higher than that of the annual with an average of 50%. Although the whole plant–soil ^{15}N recovery of this desert ecosystem decreased with increasing N deposition, our results suggested that it may vary with species composition and community change under future climate and elevated N deposition.

Keywords: desert plants, annual, ephemeral, ^{15}N tracer, biomass, ^{15}N retention, N deposition

INTRODUCTION

Nitrogen (N) limitation of net primary productivity in terrestrial ecosystems is globally distributed, including desert ecosystems (LeBauer and Treseder, 2008; Yahdjian et al., 2011). A meta-analysis showed that N addition could significantly increase aboveground net productivity of water-limited, i.e., desert and semi-arid ecosystems (Yahdjian et al., 2011). However, the critical loads for N deposition in desert ecosystems are thought to be lower than those for other ecosystems due to their N-poor status and low biomass (Fenn et al., 2010). It has been suggested that desert ecosystems are particularly susceptible to small increases in N inputs due to the sensitivity of desert plants to N. However, different desert plant species or plant-functional types have different growth responses to N. In the Mojave Desert, for example, increased N input from atmospheric deposition or from other sources at a rate of 3.2 g N m^{-2} yr^{-1} decreased the biomass of native annual plants but increased the density and biomass of alien annual plants (Brooks, 2003). In a pot and field experiment in the Gurbantuggut Desert, ephemeral biomass significantly increased and its allocation to roots significantly decreased with N application compared with annuals (Zhou et al., 2011, 2014). In response to chronic N addition in a temperate desert ecosystem, biomass change was non-linear and N rate-dependent: low and intermediate levels of N increased biomass but high levels (24 g N m^{-2} yr^{-1}) suppressed biomass, mainly through suppressing the composition of annuals in the community (Zhou et al., 2018). Although research has concluded that an increase in N deposition would favor ephemeral composition in a temperate desert community, it is still difficult to know whether high levels of N have a positive or negative effect on growth and biomass allocation of fast-growing ephemerals and slow-growing annuals if growing separately rather than in a mixed community. Since plant growth and biomass allocation is closely related to N remaining in the plant–soil system and the N allocation between plant and soil pools (Templer et al., 2012), knowledge of biomass accumulation and allocation in desert plants under different N additions is crucial to quantifying ecosystem dynamics and ecosystem N fluxes.

Excess N addition can cause nutrient imbalance and reduce ecosystem productivity, once N supply exceeds the amount needed for plant growth (Homyak et al., 2014). A recent ^{15}N labeled experiment showed that the total added N recovery of a *Haloxylon ammodendron* dominated desert ecosystem in the Gurbantunggut desert was on average 52%; ephemerals contained almost 86% of the N retained in the herbaceous layer (which included ephemerals, annuals and perennials) (Cui et al., 2017). Another study also demonstrated that ephemerals retained more N than summer annuals due to their relatively higher density and biomass in a temperate desert ecosystem (Huang et al., 2016). The higher ^{15}N retention of ephemerals might be due to their higher capacity for N uptake or their domination in the community, or to their larger biomass than annuals. In N-limited grassland soils, fast-growing species can take up more N than slow-growing species (Harrison et al., 2008). Plant–soil ^{15}N retention was found to be determined by the proportion of herbs, dominant plant traits, and the phenology of the plants by Mauritz et al. (2014) and De Vries and Bardgett (2016). However, the relationship of plant N retention and plant–soil recovery of N in desert plants with different growth strategies under certain N addition levels is not clear.

The Gurbantunggut Desert, located in Northwest China in Central Asia, is a typical temperate desert. Shrubs and densely distributed herbs are the dominant species (Angert et al., 2007). Ephemerals are the main species in the herbaceous layer (which includes ephemerals, ephemeroids, annuals and perennials), accounting for more than 80% of the plant biomass (Huang et al., 2016). Due to increased anthropogenic activities, especially farming, the area surrounding the Gurbantunggut Desert has received large amounts of N from atmospheric deposition (Li et al., 2012; Liu et al., 2013; Xu et al., 2015). We hypothesize that ephemerals and annuals will respond differently to this extra N because of their differing growth strategies. To test our hypotheses, we chose two of the most typical native species of Central Asian Desert ecosystems, *Malcolmia africana* and *Salsola affinis* to compare. *M. Africana* is a fast-growing and "opportunistic" ephemeral species; in contrast, *S. affinis* is a slow-growing and "conservative" annual species. We hypothesized that (1) high N addition would inhibit the growth and biomass accumulation of the ephemeral, and decrease the aboveground:belowground partitioning of N (the R:S ratio) of the ephemeral; (2) the ephemeral, with a shorter growing cycle and higher relative growth rate, would take up and retain significantly more N than the annual with its longer growing cycle; (3) the plant–soil recovery of N in the ephemeral would be significantly higher than that of the annual.

MATERIALS AND METHODS

Plant Material

Malcolmia Africana is an ephemeral belonging to the family *Brassicaceae*, an "opportunistic" C3 species, whose germination, growth, flowering and fruiting and entire life cycle is highly dependent on precipitation and temperature (Yuan and Tang, 2010). In general, ephemerals can take advantage of water and available nutrients to complete their growing cycles before high temperature and drought can restrict growth, and reach peak biomass in late May (Yuan and Tang, 2009). *S. affinis* is an annual and "conservative" species belonging to the family *Chenopodiaceae*. It is a C4 species whose photosynthetic and water utilization pathway is more favorable for survival and growth and has evolved in plants under the stresses of high temperature and drought conditions (Su and Xie, 2011). Annuals generally have slower growth rates and a longer growing season (from March to October), with peak biomass in mid-August (Wang et al., 2006). Seeds of *M. africana* and *S. affinis* were collected in June and October in 2015, respectively, from the southern edge of the Gurbantunggut Desert. After air-drying, the seeds were stored at ambient temperature (20–25°C) until the experiment began in April 2016.

Experimental Site and Design

The experiment was carried out at Fukang Station of Desert Ecology, Chinese Academy of Sciences, on the southern edge of the Gurbantunggut Desert (44°30′ N, 87°45′ E and 460 m a.s.l.). To compare the effect of N addition on the growth and N retention of ephemeral and annual herbs, a pot experiment was conducted, focusing on the two typical desert plant species described above. The experiment comprised five N rates [no N (N0), 15 kg N ha^{-1} (N15), 30 kg N ha^{-1} (N30), 60 kg N ha^{-1} (N60) and 120 kg N ha^{-1} (N120)] with ten replicates of each treatment. The N30 rate approximated to the current N deposition in the study area (35.4 kg N ha^{-1} yr^{-1}) (Li et al., 2012; Song, 2015). N15 simulated a low N deposition; N60 and N120 higher depositions, following the prediction that global N deposition will double by 2050 relatively to the early 1990s (Galloway et al., 2008).

Surface soil (0–20 cm) from where the seeds were collected was used as the growth substrate. The soil samples were combined and thoroughly mixed. Soil physical and chemical properties are described in **Supplementary Table S1**. Fifty plastic pots (26 cm diameter and 19 cm depth) were filled with 8 kg soil for each species, and 20 seeds sown in each pot on 9 April 2016, maintaining the same seeding and germination schedule as in the field. All pots were placed in a controlled-environment greenhouse at Fukang Station at 30/11°C day/night temperature regime and a photosynthetic photo flux density of 1600 μmol^{-1} s^{-1} m^{-2} at midday. The relative air humidity ranged from 35 to 60%.

The pots were well watered with distilled water to achieve field capacity before the seeds sprouted. After establishment, some 25 days after sowing, the seedlings were thinned to 6 plants per pot to reduce competition for nutrients. The corresponding amount of $^{15}NH_4{}^{15}NO_3$ fertilizer (5.16% abundance, Shanghai Research Institute of Chemical Industry) was calculated for each treatment based on the pot soil surface area and 0, 0.8, 1.6, 3.2, and 6.4 g N pot^{-1} added for the N0, N15, N30, N60, and N120 treatments, respectively. The fertilizer was dissolved in 100 mL distilled water and the solution applied once with an injector inserted into soil at 5 cm depth at the four corners of the pot. Soil in all pots was then maintained at 60–70% of field capacity and the pots moved randomly each week to minimize any effects of position.

Sampling and Analysis

Six plants from each pot were harvested shortly after flowering (time of peak biomass) to measure plant growth and biomass allocation. The samplings were at 72 and 149 days after sowing *M. africana* and *S. affinis*, respectively, and were taken to represent the growing season length of the plants. Prior to harvest, the aboveground plant growth parameters including height, number of leaves and branches of each plant were recorded. The aboveground parts were then clipped with scissors and separated into stems and leaves. Following harvest, soil samples to 16.5 cm were carefully collected away from the taproot with a miniature auger (1 cm diameter). These samples were stored at <4°C in a refrigerator before analysis. All the soil samples from the pots were then washed with water to obtain coarse and fine roots, and the length of the longest root was measured and the number of lateral roots recorded. To calculate the biomass of stem, leaf, coarse roots and fine roots, all plant materials were oven-dried at 105°C for half an hour and then at 65°C for 48 h to a constant weight. After weighing, stems and leaves were mixed as the aboveground parts and ground to <0.25 mm in a high speed ball mill for analysis of total aboveground N content on an elemental analyzer (Vario Max CN, Elementar, Germany) and ^{15}N abundance by mass spectrometry (Delta Plus XP, Thermo Finnigan, Pittsburg, PA, United States). The coarse and fine roots were combined as the belowground parts and analyzed in the same way. The fresh soil samples were air-dried, finely ground and sieved through <0.25 mm to measure total N content by elemental analysis as above and ^{15}N abundance by mass spectrometry as above.

The percentage of N applied recovered in the aboveground and belowground parts of the plants and in the soil were calculated using the following equations (De Vries and Bardgett, 2016; Cui et al., 2017), with ^{15}N atom% excess corrected for background abundance (0.3663%; Cabrera and Kissel, 1989).

(1) Applied N (Ndff) in the plant (kg N ha^{-1}) = (plant N (g kg^{-1}) × biomass (g pot^{-1}) × 10^{-2}/0.053 (m^2 pot^{-1})) × $^{15}N_{plant}$ atom% excess/$^{15}N_{fertilizer}$ atom% excess
(2) Applied N (Ndff) in soil (kg N ha^{-1}) = (soil N (g kg^{-1}) × soil weight (g pot^{-1}) × 10^{-2}/0.053 (m^2 pot^{-1})) × $^{15}N_{soil}$ atom% excess/$^{15}N_{fertilizer}$ atom% excess
(3) Fertilizer N recovery (%) = Ndff/^{15}N rate × 100

Statistical Analysis

The effects of N on plant growth characteristics, biomass production and allocation, N content, ^{15}N abundance, N retention and recovery in *M. africana* and *S. affinis* were examined by two-way ANOVA with SAS V8 software (Version 8.0, SAS Institute Inc., Cary, NC, United States). A significant effect was determined as LSD at $P < 0.05$. Biomass and plant N retention response curves to N rates, and N input values at which maximum values of biomass and N retention occurred, were calculated using a quadratic-plateau model in R 3.3.1 (R Core Team, 2016) with packages "easyreg" and "er1" function (R Core Team, 2016) (**Supplementary R code**). Structural equation modeling (SEM) was used to test the direct and indirect effects of growing season length and N rate on ecosystem N retention (**Supplementary R code**). The model was constructed based on the theoretical knowledge and criterion described by De Vries and Bardgett (2016). SEM was performed with the "specifyModel" function in the "SEM" package of R 3.3.1 (R Core Team, 2016). All figures were drawn with Origin software 2015 (Origin Lab, Northampton, MA, United States).

RESULTS

Plant Growth

Plant height, branch number, leaf number, root length and lateral root number were significantly different between *M. africana*

TABLE 1 | Two-way ANOVA analyses of species and N treatment on plant morphology and biomass partitioning.

Dependent variable	Independent variable	Df	*F*-value	*P*-value
Plant height	Species	1	4024.42	< 0.0001
	Treatment	4	115.08	< 0.0001
Branch number	Species	1	841.52	< 0.0001
	Treatment	4	96.3	< 0.0001
Leaf number	Species	1	832.26	< 0.0001
	Treatment	4	13.57	< 0.0001
Root length	Species	1	134.88	< 0.0001
	Treatment	4	2.69	0.03
Lateral root number	Species	1	470.72	< 0.0001
	Treatment	4	5.52	0.0002
Leave biomass	Species	1	608.64	< 0.0001
	Treatment	4	42.57	< 0.0001
Stem biomass	Species	1	568.84	< 0.0001
	Treatment	4	35.92	< 0.0001
Coarse root biomass	Species	1	28.13	< 0.0001
	Treatment	4	27.53	< 0.0001
Fine root biomass	Species	1	70.6	< 0.0001
	Treatment	4	34.09	< 0.0001
Aboveground biomass	Species	1	657.32	< 0.0001
	Treatment	4	44.32	< 0.0001
Belowground biomass	Species	1	73.16	< 0.0001
	Treatment	4	35.85	< 0.0001
R:S	Species	1	371.29	< 0.0001
	Treatment	4	9.96	< 0.0001

and *S. affinis* at each N rate (**Table 1**). Plant height, branch number and leaf number of *S. affinis* were significantly higher than those of *M. Africana*, whereas root length and lateral root number of *S. affinis* were significantly lower than those of *M. Africana* (**Figure 1** and **Table 1**). For *M. Africana*, except for root length, low and moderate amounts of N (N15 and N30) significantly enhanced plant height, branch number, leaf number and lateral root number compared with the control, but high N rates (especially N120) significantly inhibited plant growth compared with low and moderate N rates (N15 and N30) (**Figures 1A,C,E,G,I**). For *S. affinis*, all plant growth parameters increased with N addition (**Figures 1B,D,F,H,J**).

Biomass and Biomass Partitioning

All measured plant biomass fractions of *S. affinis* were significantly higher than those of *M. Africana* (**Table 1** and **Figure 2**). The mean aboveground biomass of *M. Africana* and *S. affinis* ranged from 7.7 to 19.1 g m^{-2}, and from 36.2 to 115.4 g m^{-2}, respectively. The mean belowground biomass of *M. Africana* and *S. affinis* ranged from 9.2 to 12.0 g m^{-2}, and from 6.2 to 29.7 g m^{-2}, respectively (**Figures 2A,B**). For *M. Africana*, low and moderate N addition (N15 and N30) significantly increased leaf, stem, fine root, coarse root biomass, aboveground biomass and belowground biomass; however, compared to the moderate N rate (N30), high N addition (especially N120) significantly inhibited stem and coarse root biomass (**Figure 2A**). For *S. affinis*, leaf, stem, coarse root, fine root, aboveground biomass and belowground biomass were all significantly enhanced by N addition (**Figure 2B**). The R:S ratio of *M. Africana* decreased significantly with N addition (**Figure 2C**); in contrast the R:S ratio of *S. affinis* increased with N addition (**Figure 2D**).

Aboveground and belowground biomass N response curves are shown in **Figure 3**. All curves fitted the quadratic-plateau model well. The aboveground biomass and belowground biomass of *M. Africana* were positively correlated with N addition up to a threshold of 25.5 and 48.9 kg N ha^{-1} added, respectively. Similarly, the aboveground biomass and belowground biomass of *S. affinis* were also positively correlated with N addition up to significantly higher thresholds of 37.5 and 77.0 kg N ha^{-1} added, respectively. The maximum aboveground biomass and belowground biomass for *M. Africana* were 18.3 and 11.6 g m^{-2}, and for *S. affinis* were 115.9 and 26.4 g m^{-2}, respectively.

N Retention Added ^{15}N

ANOVA analysis showed that ^{15}N retention in the aboveground and belowground parts of the plants, in the soil and that lost, significantly differed between *M. Africana* and *S. affinis* as well as between treatments (**Table 2**). Except at low N addition (N15), aboveground and belowground retentions of ^{15}N in *S. affinis* were significantly higher than those in *M. Africana*. Response curves of aboveground and belowground ^{15}N retention of *M. Africana* and *S. affinis* are illustrated in **Figure 4**, showing a good fit to the quadratic-plateau model. For *M. Africana*, the relationships between aboveground retention and belowground ^{15}N retention and N addition had maxima of 6.4 and 0.9 kg N ha^{-1}, respectively, at N additions of 42.1 and 37.3 kg N ha^{-1}, respectively. Similarly, *S. affinis* had maximum ^{15}N retentions of 21.6 and 2.0 kg N ha^{-1} in aboveground and belowground parts at N applications of 114.9 and 21.6 kg N ha^{-1}, respectively. *M. Africana* retained significantly more N in its aboveground and belowground components under moderate and high N additions than under low N addition. However, there were no significant differences between the N30, N60 and N120 treatments. ^{15}N retained in the soil and lost from the plant–soil system of *M. Africana* increased significantly with increasing N applied (**Table 2**). For *S. affinis*, N retention in the aboveground and belowground components of the plant, in the soil, and the amount lost, significantly increased with increasing N rate (**Table 2**).

Application of the SEM suggested that the plant–soil ^{15}N retention was directly and indirectly affected by N rate and the length of the growing season of the plants [χ^2 = 1.57, Df = 2, Pr ($>\chi^2$) = 0.457, AIC = 27.6, BIC = −5.81] (**Figure 5**). Nitrogen addition can directly and indirectly affect plant–soil ^{15}N retention through the ^{15}N excess that remains in the soil (the standardized indirect effect of excess ^{15}N remaining in the soil = 0.75 × 0.58 = 0.435). In addition, the length of the growing season can also directly and indirectly affect plant–soil ^{15}N retention through the aboveground biomass (the standardized indirect effect of aboveground biomass on ecosystem ^{15}N retention = 0.95 × 0.52 = 0.494), and the ^{15}N remaining in the soil (the standardized indirect effect of ^{15}N excess remaining in

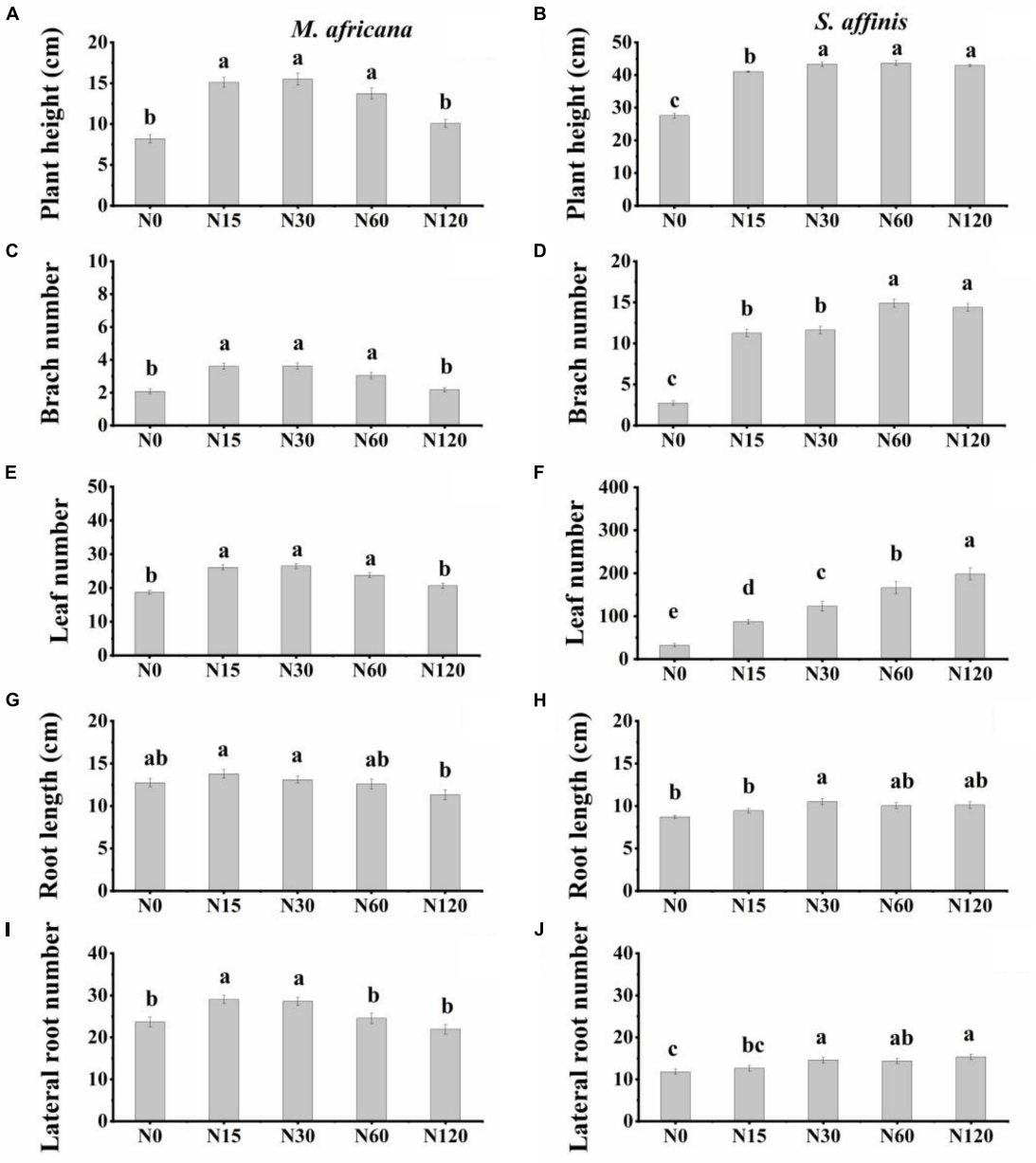

FIGURE 1 | Plant height, number of branches, number of leaves, root length, and number of lateral roots of *M. africana* **(A,C,E,G,I)** and *S. affinis* **(B,D,F,H,J)** for each treatment. Bars represent means ± standard error (n = 10). Columns with different lowercase letters differ significantly at P = 0.05.

the soil on ecosystem ^{15}N retention = −0.47 × 0.58 = −0.273). In general, the N addition rate was positively related to plant–soil ^{15}N retention, whereas the length of growing season was negatively related to plant–soil ^{15}N retention.

N Recovery of Added ^{15}N

The mean ^{15}N recovery in the *M. Africana* and *S. affinis* plant–soil systems was 70.1 and 50.2%, respectively. For *M. Africana*, most of the ^{15}N was retained in the soil or lost, whereas for *S. affinis* most of the ^{15}N was in the aboveground part of the plants or lost (**Figure 6**). The recovery of ^{15}N in the soil under *M. Africana* was 52.0%, significantly higher than that of *S. affinis*. In contrast, the recovery of ^{15}N in the aboveground and belowground parts of the plant and the loss from *M. Africana* was significantly lower than that of *S. affinis*. Recovery in the whole plant–soil system of *M. Africana* was significantly higher than that of *S. affinis* at the same N rate. Except for retention in the soil under *M. Africana*, the recovery of ^{15}N in the different components of the two plant–soil systems significantly decreased with increasing ^{15}N addition, whereas losses significantly increased with ^{15}N addition.

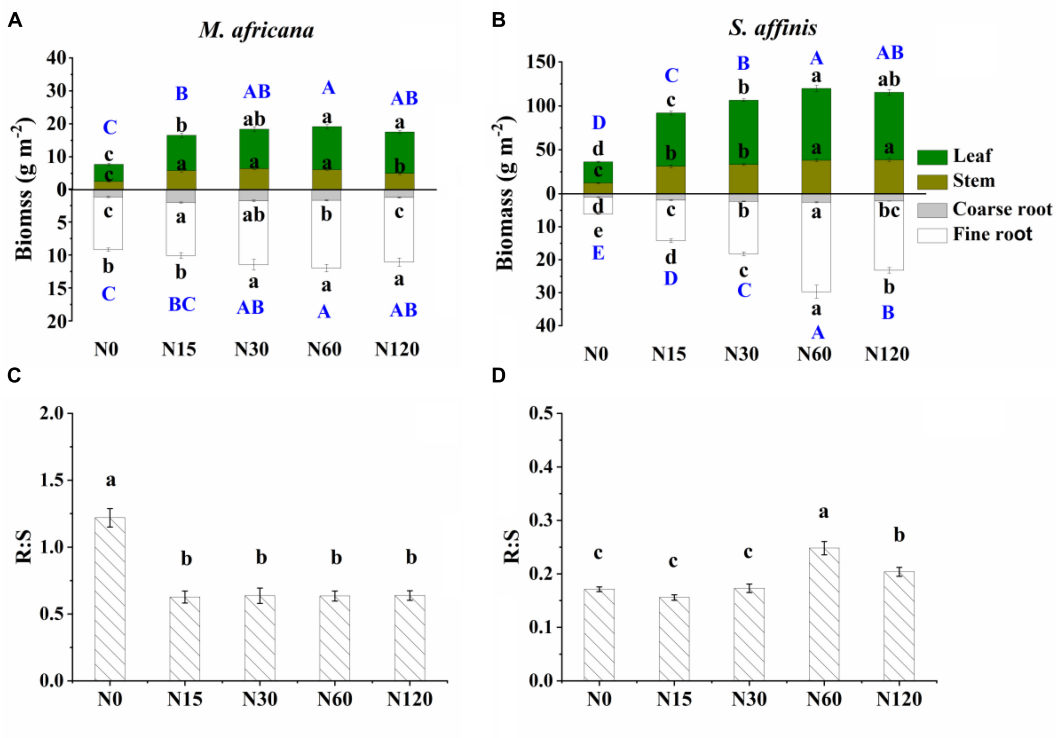

FIGURE 2 | Biomass partitioning (including leaf biomass, shoot biomass, coarse root biomass and fine root biomass) and R:S ratio of *M. africana* **(A,C)** and *S. affinis* **(B,D)** at each N treatment. Bars represent means ± standard error (n = 10). Different lowercase letters above each column show values differ significantly at P = 0.05, and different uppercase letters (with blue color) indicate that the total aboveground biomass (the sum of leaf biomass and shoot biomass) or belowground biomass (the sum of coarse root biomass and fine root biomass) differ significantly at P = 0.05.

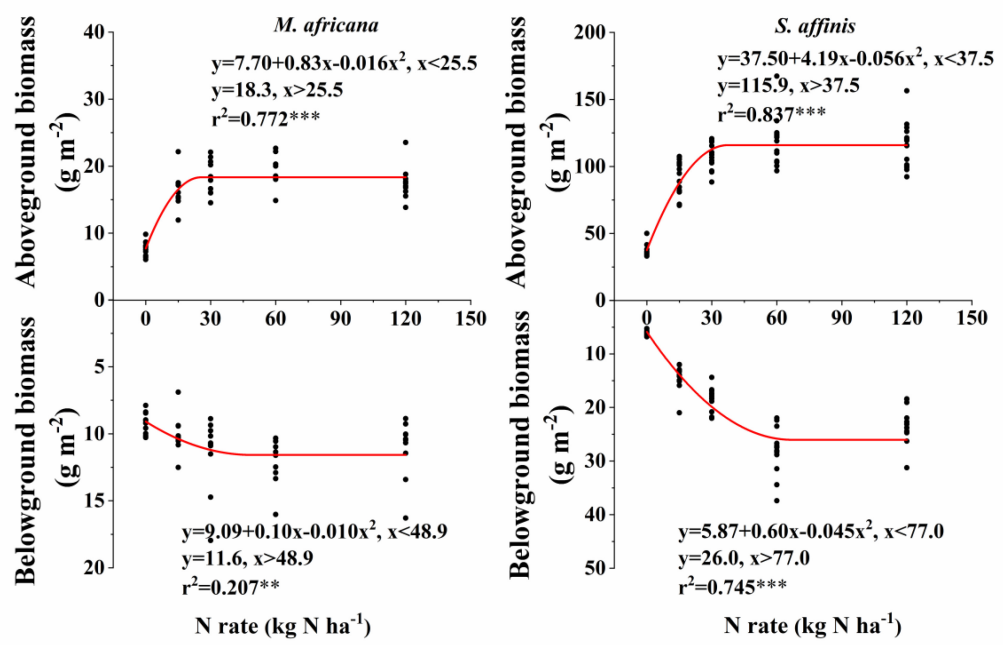

FIGURE 3 | Responses of aboveground and belowground biomass of *M. africana* **(left)** and *S. affinis* **(right)** to increasing N addition. The asterisks on the panel represent the statistical results of the relationship, in which *, **, ***, represent statistical significance at $P < 0.05$, $P < 0.01$, and $P < 0.001$, respectively.

TABLE 2 | Fate of ^{15}N applied to the plant–soil system of *M. africana* (ephemeral) and *S. affinis* (annual), and two-way ANOVA analyses of the effects of species and N treatment on ^{15}N partitioning in the plant–soil system.

Species	Treatment	^{15}N addition (kg ha^{-1})	Aboveground (kg ha^{-1})	Belowground (kg ha^{-1})	Soil (kg ha^{-1})	Loss (kg ha^{-1})
M. africana	N15	15	4.09 ± 0.37b	0.57 ± 0.08b	7.87 ± 0.9*c*	2.47 ± 0.58*c*
	N30	30	5.96 ± 0.27a	0.85 ± 0.09ab	13.85 ± 1.38c	9.33 ± 1.38bc
	N60	60	6.47 ± 0.41a	0.9 ± 0.12a	33.92 ± 3.68b	18.71 ± 3.65b
	N120	120	6.39 ± 0.18a	0.88 ± 0.11a	63.51 ± 6.94a	49.23 ± 7.12a
S. affinis	N15	15	4.06 ± 0.29d	0.65 ± 0.08c	4.52 ± 0.24c	5.78 ± 0.31d
	N30	30	7.79 ± 0.56c	1.39 ± 0.14b	6.7 ± 0.62c	14.13 ± 1.05c
	N60	60	16.55 ± 1.06b	2.28 ± 0.29a	11.31 ± 0.5b	29.86 ± 1.41b
	N120	120	21.5 ± 2.41a	1.8 ± 0.19ab	19.91 ± 1.77a	76.8 ± 3.94a
Source (*P*-values)	Species		<0.0001	<0.0001	<0.0001	<0.0001
	Treatment		<0.0001	<0.0001	<0.0001	<0.0001

DISCUSSION

Growth and Biomass Responses to N Addition

In arid and semi-arid ecosystems, water availability is the main factor limiting plant growth, community composition and community productivity (Yahdjian and Sala, 2006; Miranda et al., 2009; Robertson et al., 2009). Nitrogen can become the main limiting factor if drought stress is alleviated, and extra N combined with enough water can then promote plant growth and increase community productivity (Ladwig et al., 2012; Fan et al., 2013). Our study confirmed this in both the ephemeral and annual plants, as the pot experiment was conducted with adequate water. However, the effect of N on the growth and biomass of the ephemeral and annual differed. High N addition had little effect or even inhibited plant growth and biomass accumulation of *M. Africana* compared to *S. affinis*. Wu et al. (2008) reported that adding large amounts of N did not affect the height, basal diameter, leaf number, leaf area and biomass of *Sophora davidii* (a shrub) seedlings, but root length decreased with increasing N supply. Moderate amounts of extra N promoted aboveground growth and root development, but excess N decreased root growth or even damaged roots (Salih et al., 2005; Wu et al., 2008). Similarly, the response curves also provided direct evidence of the different response of the two species to N addition (**Figure 3**). The N rate at which maximum growth of the ephemeral was observed was significantly less than that of the annual, which indicates that the ephemeral was more sensitive to N than the annual. Similar results were found between Japanese red pine and Japanese cedar: generally species grown in nutrient-poor habitats were more sensitive to high N deposition and its growth were significantly reduced under the highest N treatment (Nakaji et al., 2001).

The allocation of biomass between aboveground and belowground components of plants (the R:S ratio) is determined by species, ontogenetic development and environmental change (Poorter and Nagel, 2000). We found that the R:S ratio of the ephemeral was significantly higher than that of the annual. This difference was most likely due to the phenological differences and the relative ability to adapt to growing conditions, i.e., the environment. We found that the R:S ratio of the ephemeral decreased with N input in accordance with the "functional equilibrium" model (Poorter and Nagel, 2000; Poorter et al., 2012), consistent with our original hypothesis. However, the response of the R:S ratio of the annual plant to N addition did not fit with the "functional equilibrium" model. In a study of 27 herbaceous species, Muller et al. (2000) found that the R:S ratio of "opportunistic" species fitted the general relationship, decreasing with nutrient input, whereas "conservative" species from nutrient-poor habitats increased their R:S ratio under higher nutrient inputs. Similarly, in the current study, the ephemeral is an "opportunistic" and resource-exploitative species whose adaptive capacity was less than that of "conservative" and resource-conservative species. Therefore, the growth of the ephemeral was inhibited under high N addition. Adaptive responses in physiology and morphology may be the main mechanism by which different species deal with environmental change in their habitats (Patterson et al., 1997; Poorter et al., 2012). The positive response of the R:S ratio of *S. affinis* to N also supported our finding that the root morphology of the annual could adapt to high N addition by increasing the number of lateral roots as N input increased.

Response of Plant–Soil ^{15}N Retention to N Addition Rate

Added N significantly increased ^{15}N retention in aboveground and belowground parts of the plant, but this varied between the species. In N-limited ecosystems, grassland species with different growth strategies also showed species-specific differences in the amount of N retained. Fast-growing and resource-exploitative species usually retained more N than slow-growing and resource-conservative species (Bardgett et al., 2003; Weigelt et al., 2005; Harrison et al., 2007, 2008; Grassein et al., 2015; De Vries and Bardgett, 2016). However, contrary to our original hypothesis, the difference in ^{15}N retention between the two species was dependent on the amount of ^{15}N added. It has been suggested that the species-specific ^{15}N retention in plants is related to the plant relative growth rate (Weigelt et al., 2005). Alternatively, it has been pointed out that plant traits rather than plant growth rate or trait functional

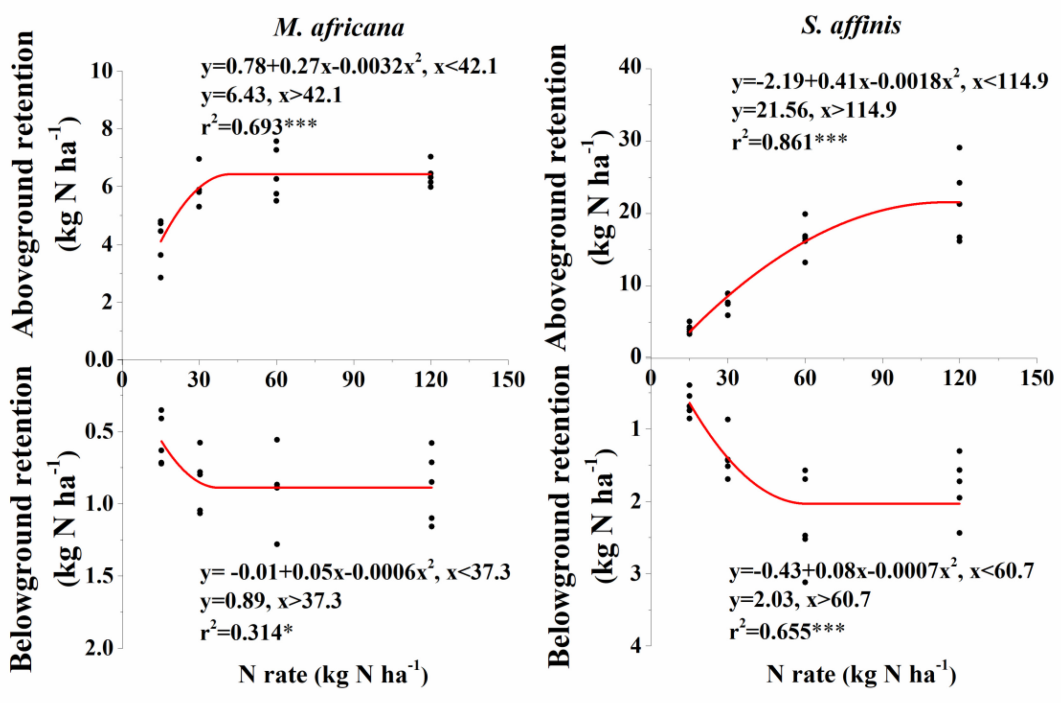

FIGURE 4 | Aboveground and belowground ^{15}N retention of *M. africana* **(left)** and *S. affinis* **(right)** in response to increasing N addition. The asterisks on the panel represent the statistical results of the relationship, in which *, **, ***, represent statistical significance at $P < 0.05$, $P < 0.01$, and $P < 0.001$, respectively.

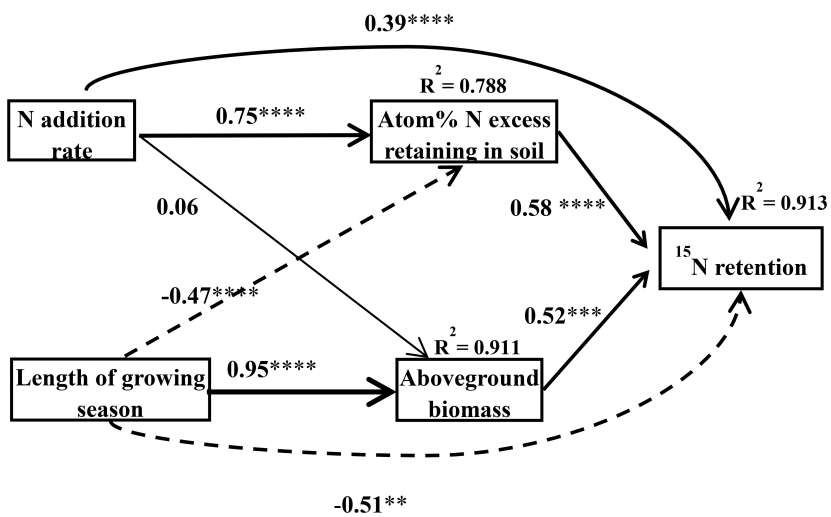

FIGURE 5 | Final structural equation models describing the effects of the N treatment and the length of growing season on N retention in the plant–soil system as separated into aboveground biomass and atom% ^{15}N in the soil. Boxes contain measured variables. Arrows indicate the hypothesized causal relationship (paths), and the width of the arrow denotes the strength of the relationship. The number and asterisks on the arrows represent the path coefficients and the statistical results of the relationship, in which *, **, ***, **** represent statistical significance at $P < 0.05$, $P < 0.01$, $P < 0.001$, $P < 0.0001$, respectively. Solid arrows represent positive effects, dashed arrows represent negative effects. R^2 values represent the proportion of variance explained by the model for the response variables. This model fitted well [$\chi^2 = 1.57$, Df = 2, Pr (>Chisq) = 0.457, AIC = 27.6, BIC = −5.81].

diversity could determine the inter-specific plant ^{15}N retention (Harrison et al., 2008; De Vries and Bardgett, 2016). In our experiment, especially in the low N treatment, although the aboveground and belowground biomass of *M. Africana* were significantly less than that of *S. affinis* (**Figures 2A,B**; $P < 0.0001$; $P < 0.0001$), we did not find significant differences in the ^{15}N retained in the aboveground and belowground components between *M. Africana* and *S. affinis* due to the

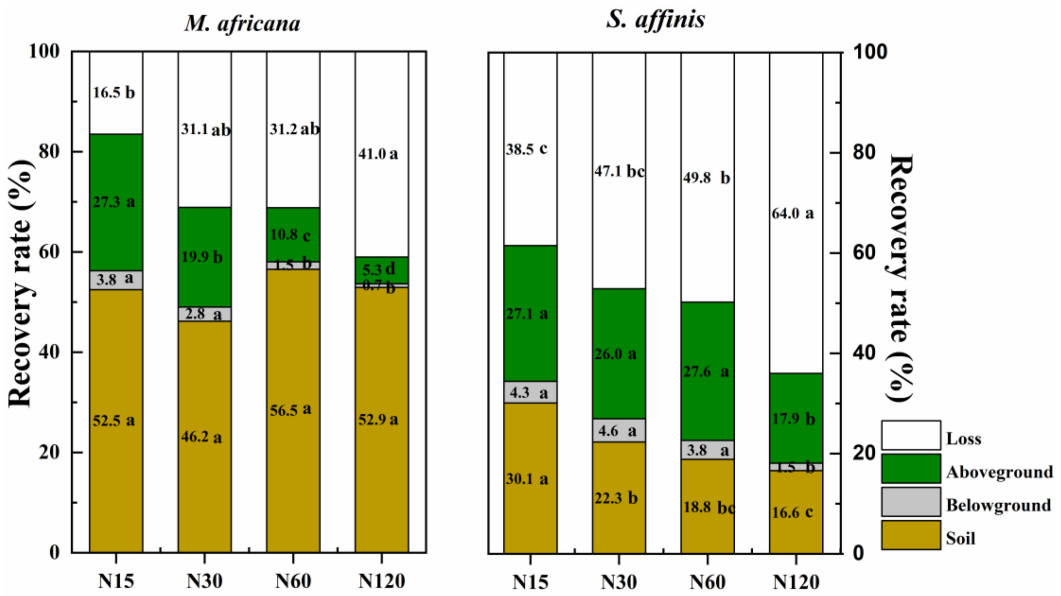

FIGURE 6 | The percentage of added ^{15}N recovered in the soil, the belowground and aboveground parts of the plants, and that lost to air or water in *M. africana* **(left)** and *S. affinis* **(right)** under the different N treatments. Values with different letters differ significantly between treatments at $P = 0.05$.

higher aboveground and belowground ^{15}N uptake of *M. Africana* (**Supplementary Figures S1A,B**). Under moderate and high N additions, both the ability to take up ^{15}N and the growth of the ephemeral aboveground and belowground were suppressed, causing ^{15}N retention in the aboveground and belowground parts of the ephemeral to be less than those of the annual (**Figure 2** and **Supplementary Figure S1**). Therefore, it can be inferred that the higher retention of N by the ephemeral in the community compared to that of the annual in the field experiment of Cui et al. (2017) was not due to the higher uptake ability of ^{15}N of the ephemeral under moderate (N30) and high N (N60) addition. Clearly, species differences in the N-retention of plants at different N rates can be explained by plant growth, shoot and root uptake capacity.

The SEM results also showed that N rate and the length of the growth season can directly affect N retention in the whole plant–soil system, and also indirectly affect it through the aboveground biomass and the amount of excess N that remains in the soil (**Figure 5**). De Vries and Bardgett (2016) pointed out that root biomass and the dominant plant trait, and the amount of N retained in the soil, can control short-term ecosystem N retention. Aboveground biomass was positively related to belowground biomass, and the amount of ^{15}N retained in the soil was related to the ability of both the aboveground and belowground components to take up ^{15}N. Therefore, aboveground biomass and the amount of excess ^{15}N retained in the soil was used to construct the SEM and describe the whole plant–soil system ^{15}N retention. Thus, although the plant N retention by the ephemeral was significantly less than that of the annual, the plant–soil retention of the annual was significantly higher than that of the ephemeral due to the high retention of ^{15}N in the soil.

Plant–Soil ^{15}N Recovery

Consistent with our third hypothesis mentioned above, the average recovery rate of ^{15}N by the ephemeral and annual plant–soil systems were 70 and 50%, respectively. In previous research, the recovery of ^{15}N in a *Haloxylon ammodendron* dominant temperate desert ecosystem was approximately 52% on average, in which the soil and the plant accounted for about 40 and 12% of the total recovery, respectively (Cui et al., 2017). The higher recovery rate in the pot experiment compared to the field experiment could be due to the lack of drought stress and competition, and plant community differences, and of course the more effective exploitation of the soil by plant roots. Although the annual had a higher plant N recovery rate than the ephemeral, the whole plant–soil system N recovery of the annual was significantly less than that of the ephemeral. Deserts with coarse-textured soils usually have a lower water-holding capacity and labile C and N pools, and slower N mineralization and immobilization than other ecosystems (Austin et al., 2004). Increased inputs of N to coarse desert soils dominated by long growth period annuals is therefore likely to result in less N being retained in the soil and a higher risk of N loss to the environment (air or water or both) compared with the same system with shorter growth period ephemerals, especially in the artificial confines of a pot experiment maintained at 60–70% field capacity (**Supplementary Figure S1C**). This was confirmed by the negative relationship in the SEM between the atom% ^{15}N excess remaining in the soil and the growing period of the plants (**Figure 5**).

Increasing N inputs are likely to significantly decrease total ecosystem N recovery in both ephemeral and annual plant–soil systems. Consistent with this, a meta-analysis of natural terrestrial ecosystems showed that N recovery was negatively related to N addition when inputs exceeded 46 kg N ha^{-1} yr^{-1} (Templer et al., 2012). Similarly, Cui et al. (2017) concluded that N recovery significantly decreased when N deposition increased from 30 kg N ha^{-1} yr^{-1} to 60 kg N ha^{-1} yr^{-1} in a temperate desert ecosystem in Northwest China. Due to the poor nutrient content and dry conditions, plant coverage is sparse in desert ecosystems and microbial community sizes are small, so excessive N inputs could easily exceed the biotic demands and cause ecosystem nutrient imbalances and thus increased gaseous losses or leaching or both (McCalley and Sparks, 2008, 2009; Homyak et al., 2014). Zhou et al. (2018) pointed out that the responses to N of the community structure, richness, evenness, density and biomass of herbaceous plants were clearly N rate-dependent, with N addition increasingly selecting nitrophilic, fast-growing species rather than slower growing species. Therefore, under enhanced N deposition (Liu et al., 2013) and future climate scenarios, the N recovery of desert ecosystems may vary substantially and show its species dependence with change of community composition.

CONCLUSION

Our study has shown clear differences in plant growth, allocation and plant–soil system N recovery responses to increasing N addition for two typical temperate desert species, *M. Africana* (an ephemeral) and *S. affinis* (an annual). Low and moderate N additions significantly enhanced plant growth and biomass production of both the ephemeral and annual, whereas high N addition inhibited plant growth and biomass of the ephemeral but not the annual. The amount of N applied at which the maximum retention of N in the aboveground and belowground biomass of the ephemeral was significantly less than that of the annual. In addition, except at low N addition, the plant N retention of the ephemeral was significantly less than that of the annual, but the total plant–soil retention was significantly greater. The whole plant–soil ecosystem N recovery will therefore decrease with predicted increases in future N deposition. The results indicate that N recovery of this temperate desert ecosystem is likely to vary as species composition of the community also changes with future climate change and enhance N deposition.

AUTHOR CONTRIBUTIONS

XL designed the experiments. XC, PY, WW, YG, and KL conducted the experiments. XC, XL, KG, and TM wrote the manuscript. All authors reviewed and commented on the manuscript.

FUNDING

This work was supported by the National Natural Science Foundation of China (41425007), the National Program on Key Basic Research Project (2014CB954202 and 2017YFD0200101), the Newton Fund through the BBSRC project of China Virtual Joint Centre for Improved Nitrogen Agronomy (CINAG) (BB/N013468/1) and BBSRC project BBS/E/C/000I0320.

SUPPLEMENTARY MATERIAL

The Supplementary Material for this article can be found online at: https://www.frontiersin.org/articles/10.3389/fpls.2019.00356/full#supplementary-material

REFERENCES

Angert, A. L., Huxman, T. E., Barron-Gafford, G. A., Gerst, K. L., and Venable, D. L. (2007). Linking growth strategies to long-term population dynamics in a guild of desert annuals. *J. Ecol.* 95, 321–331. doi: 10.1111/j.1365-2745.2006.01203.x

Austin, A. T., Yahdjian, L., Stark, J. M., Belnap, J., Porporato, A., Norton, U., et al. (2004). Water pulses and biogeochemical cycles in arid and semiarid ecosystems. *Oecologia* 141, 221–235. doi: 10.1007/s00442-004-1519-1

Bardgett, R. D., Streeter, T. C., and Bol, R. (2003). Soil microbes compete effectively with plants for organic-nitrogen inputs to temperate grasslands. *Ecology* 84, 1277–1287. doi: 10.1890/0012-96582003084

Brooks, M. L. (2003). Effects of increased soil nitrogen on the dominance of alien annual plants in the mojave desert. *J. Appl. Ecol.* 40, 344–353.

Cabrera, M. L., and Kissel, D. E. (1989). Review and simplification of calculations in 15N tracer studies. *Fertil. Res.* 20, 11–15. doi: 10.1007/bf01055396

Cui, X., Yue, P., Gong, Y., Li, K., Tan, D., Goulding, K., et al. (2017). Impacts of water and nitrogen addition on nitrogen recovery in *Haloxylon ammodendron* dominated desert ecosystems. *Sci. Total Environ.* 601, 1280–1288. doi: 10.1016/j.scitotenv.2017.05.202

De Vries, F. T., and Bardgett, R. D. (2016). Plant community controls on short-term ecosystem nitrogen retention. *New Phytol.* 210, 861–874. doi: 10.1111/nph.13832

Fan, L. L., Li, Y., Tang, L. S., and Ma, J. (2013). Combined effects of snow depth and nitrogen addition on ephemeral growth at the southern edge of the gurbantunggut desert. *Chin. J. Arid Land* 5, 500–510. doi: 10.1007/s40333-013-0185-8

Fenn, M. E., Allen, E. B., Weiss, S. B., Jovan, S., Geiser, L. H., Tonnesen, G. S., et al. (2010). Nitrogen critical loads and management alternatives for N-impacted ecosystems in California. *J. Environ. Manage.* 91, 2404–2423. doi: 10.1016/j.jenvman.2010.07.034

Galloway, J. N., Townsend, A. R., Erisman, J. W., Bekunda, M., Cai, Z., Freney, J. R., et al. (2008). Transformation of the nitrogen cycle: recent trends, questions, and potential solutions. *Science* 320, 889–892. doi: 10.1126/science.1136674

Grassein, F., Lemauviel-Lavenant, S., Lavorel, S., Bahn, M., Bardgett, R. D., Desclos-Theveniau, M., et al. (2015). Relationships between functional traits and inorganic nitrogen acquisition among eight contrasting European grass species. *Ann. Bot. London* 115, 107–115. doi: 10.1093/aob/mcu233

Harrison, K. A., Bol, R., and Bardgett, R. D. (2007). Preferences for different nitrogen forms by coexisting plant species and soil microbes. *Ecology* 88, 989–999. doi: 10.1890/06-1018

Harrison, K. A., Bol, R., and Bardgett, R. D. (2008). Do plant species with different growth strategies vary in their ability to compete with soil microbes for chemical forms of nitrogen? *Soil Biol. Biochem.* 40, 228–237. doi: 10.1016/j.soilbio.2007.08.004

Homyak, P. M., Sickman, J. O., Miller, A. E., Melack, J. M., Meixner, T., and Schimel, J. P. (2014). Assessing nitrogen-saturation in a seasonally dry chaparral watershed: limitations of traditional indicators of N-saturation. *Ecosystems* 17, 1286–1305. doi: 10.1007/s10021-014-9792-2

Huang, G., Su, Y. G., Zhu, L., and Li, Y. (2016). The role of spring ephemerals and soil microbes in soil nutrient retention in a temperate desert. *Plant Soil* 406, 43–54. doi: 10.1007/s11104-016-2861-x

Ladwig, L. M., Collins, S. L., Swann, A. L., Xia, Y., Allen, M. F., and Allen, E. B. (2012). Above- and belowground responses to nitrogen addition in a chihuahuan desert grassland. *Oecologia* 169, 177–185. doi: 10.1007/s00442-011-2173-z

LeBauer, D. S., and Treseder, K. K. (2008). Nitrogen limitation of net primary productivity in terrestrial ecosystems is globally distributed. *Ecology* 89, 371–379. doi: 10.1890/06-2057

Li, K. H., Song, W., Liu, X. J., Shen, J. L., Luo, X. S., Sui, X. Q., et al. (2012). Atmospheric reactive nitrogen concentrations at ten sites with contrasting land use in an arid region of central Asia. *Biogeosciences* 9, 4013–4021. doi: 10.5194/bg-9-4013-2012

Liu, X. J., Zhang, Y., Han, W. X., Tang, A. H., Shen, J. L., Cui, Z. L., et al. (2013). Enhanced nitrogen deposition over China. *Nature* 494, 459–462. doi: 10.1038/nature11917

Mauritz, M., Cleland, E., Merkley, M., and Lipson, D. A. (2014). The influence of altered rainfall regimes on early season N partitioning among early phenology annual plants, a late phenology shrub, and microbes in a semi-arid ecosystem. *Ecosystems* 17, 1354–1370. doi: 10.1007/s10021-014-9800-6

McCalley, C. K., and Sparks, J. P. (2008). Controls over nitric oxide and ammonia emissions from mojave desert soils. *Oecologia* 156, 871–881. doi: 10.1007/s00442-008-1031-0

McCalley, C. K., and Sparks, J. P. (2009). Abiotic gas formation drives nitrogen loss from a desert ecosystem. *Science* 326, 837–840. doi: 10.1126/science.1178984

Miranda, J. D. D., Padilla, F. M., Lazaro, R., and Pugnaire, F. I. (2009). Do changes in rainfall patterns affect semiarid annual plant communities? *J. Veg. Sci.* 20, 269–276. doi: 10.1111/j.1654-1103.2009.05680.x

Muller, I., Schmid, B., and Weiner, J. (2000). The effect of nutrient availability on biomass allocation patterns in 27 species of herbaceous plants. *Perspect. Plant Ecol.* 3, 115–127. doi: 10.1078/1433-8319-00007

Nakaji, T., Fukami, M., Dokiya, Y., and Izuta, T. (2001). Effects of high nitrogen load on growth, photosynthesis and nutrient status of Cryptomeria japonica and *Pinus densiflora* seedlings. *Trees Struct. Funct.* 15, 453–461. doi: 10.1007/s00468-001-0130-x

Patterson, T. B., Guy, R. D., and Dang, Q. L. (1997). Whole-plant nitrogen- and water-relations traits, and their associated trade-offs, in adjacent muskeg and upland boreal spruce species. *Oecologia* 110, 160–168. doi: 10.1007/s004420050145

Poorter, H., and Nagel, O. (2000). The role of biomass allocation in the growth response of plants to different levels of light, CO2, nutrients and water: a quantitative review. *Aust. J. Plant Physiol.* 27, 595–607. doi: 10.1071/pp99173

Poorter, H., Niklas, K. J., Reich, P. B., Oleksyn, J., Poot, P., and Mommer, L. (2012). Biomass allocation to leaves, stems and roots: meta-analyses of interspecific variation and environmental control. *New Phytol.* 193, 30–50. doi: 10.1111/j.1469-8137.2011.03952.x

R Core Team (2016). *R: A Language and Environment for Statistical Computing*. Vienna: R Foundation for Statistical Computing.

Robertson, T. R., Bell, C. W., Zak, J. C., and Tissue, D. T. (2009). Precipitation timing and magnitude differentially affect aboveground annual net primary productivity in three perennial species in a chihuahuan desert grassland. *New Phytol.* 181, 230–242. doi: 10.1111/j.1469-8137.2008.02643.x

Salih, N., Agren, G. I., and Hallbacken, L. (2005). Modeling response of N addition on C and N allocation in scandinavian norway spruce stands. *Ecosystems* 8, 373–381. doi: 10.1007/s10021-003-0103-6

Song, W. (2015). *Characteristics of Chemical Composition and Deposition Fluxes of Atmospheric Particles and Reactive N in Typical Ecosystems of Xinjiang, China*. Ph.D. Thesis, Xinjiang Institute of Ecology and Geography, Urumqi.

Su, P., and Xie, T. (2011). 4 plant species and geographical distribution in relation to climate in the desert vegetation of China. *Sci. Cold Arid Regions* 3, 381–391.

Templer, P., Mack, M., Chapin, F. S. III., Christenson, L., Compton, J., Crook, H., et al. (2012). Sinks for nitrogen inputs in terrestrial ecosystems: a meta-analysis of 15N tracer field studies. *Ecology* 93, 1816–1829. doi: 10.1890/11-1146.1

Wang, X., Jiang, J., Wang, Y., Luo, W., Song, C., and Chen, J. (2006). Responses of ephemeral plant germination and growth to water and heat conditions in the southern part of gurbantunggut desert. *Chin. Sci. Bull.* 51, 110–116. doi: 10.1007/s11434-006-8214-z

Weigelt, A., Bol, R., and Bardgett, R. D. (2005). Preferential uptake of soil nitrogen forms by grassland plant species. *Oecologia* 142, 627–635. doi: 10.1007/s00442-004-1765-2

Wu, F. Z., Bao, W. K., Li, F. L., and Wu, N. (2008). Effects of drought stress and N supply on the growth, biomass partitioning and water-use efficiency of Sophora davidii seedlings. *Environ. Exp. Bot.* 63, 248–255. doi: 10.1016/j.envexpbot.2007.11.002

Xu, W., Luo, X. S., Pan, Y. P., Zhang, L., Tang, A. H., Shen, J. L., et al. (2015). Quantifying atmospheric nitrogen deposition through a nationwide monitoring network across China. *Atmos. Chem. Phys.* 15, 12345–12360. doi: 10.5194/acp-15-12345-2015

Yahdjian, L., Gherardi, L., and Sala, O. (2011). Nitrogen limitation in arid-subhumid ecosystems: a meta-analysis of fertilization studies. *J. Arid Environ.* 75, 675–680. doi: 10.1016/j.jaridenv.2011.03.003

Yahdjian, L., and Sala, O. E. (2006). Vegetation structure constrains primary production response to water availability in the Patagonian steppe. *Ecology* 87, 952–962. doi: 10.1890/0012-9658200687

Yuan, S., and Tang, H. (2009). Daily dynamics of gas exchange characteristics of three ephemeral plants in dzungaria desert. *Acta Ecol. Sin.* 29, 1962–1970.

Yuan, S., and Tang, H. (2010). Patterns of ephemeral plant communities and their adaptations to temperature and precipitation regimes in dzungaria desert, xinjiang. *Biodivers. Sci.* 18, 346–354.

Zhou, X., Bowker, M. A., Tao, Y., Wu, L., and Zhang, Y. (2018). Chronic nitrogen addition induces a cascade of plant community responses with both seasonal and progressive dynamics. *Sci. Total Environ.* 626, 99–108. doi: 10.1016/j.scitotenv.2018.01.025

Zhou, X., Zhang, Y., Ji, X., Downing, A., and Serpe, M. (2011). Combined effects of nitrogen deposition and water stress on growth and physiological responses of two annual desert plants in northwestern China. *Environ. Exp. Bot.* 74, 1–8. doi: 10.1016/j.envexpbot.2010.12.005

Zhou, X., Zhang, Y., and Niklas, K. J. (2014). Sensitivity of growth and biomass allocation patterns to increasing nitrogen: a comparison between ephemerals and annuals in the gurbantunggut desert, north-western China. *Ann. Bot. London* 113, 501–511. doi: 10.1093/aob/mct275

Conflict of Interest Statement: The authors declare that the research was conducted in the absence of any commercial or financial relationships that could be construed as a potential conflict of interest.

The reviewer XZ declared a shared affiliation, with no collaboration, with several of the authors, PY, WW, YG, and KL, to the handling Editor at the time of review.

frontiers in Plant Science

ORIGINAL RESEARCH
published: 16 April 2019
doi: 10.3389/fpls.2019.00231

Adaptation of Dominant Species to Drought in the Inner Mongolia Grassland – Species Level and Functional Type Level Analysis

Yongzhi Yan[1], Qingfu Liu[1,2], Qing Zhang[1], Yong Ding[3]* and Yuanheng Li[3]**

[1] Ministry of Education Key Laboratory of Ecology and Resource Use of the Mongolian Plateau, School of Ecology and Environment, Inner Mongolia University, Hohhot, China, [2] Center for Biodiversity Dynamics in a Changing World, BIOCHANGE, Aarhus University, Aarhus, Denmark, [3] Institute of Grassland Research, Chinese Academy of Agricultural Sciences, Hohhot, China

OPEN ACCESS

Edited by:
Zhiyou Yuan,
Northwest A&F University, China

Reviewed by:
Alexander Buyantuev,
University at Albany, United States
Jianyang Xia,
East China Normal University, China
Zhengwen Wang,
Institute of Applied Ecology (CAS), China

***Correspondence:**
Qing Zhang
qzhang82@163.com
Yong Ding
dingyong228@126.com
Yuanheng Li
nmglyh@hotmail.com

Specialty section:
This article was submitted to Plant Abiotic Stress, a section of the journal Frontiers in Plant Science

Received: *31 August 2018*
Accepted: *11 February 2019*
Published: *16 April 2019*

Citation:
Yan Y, Liu Q, Zhang Q, Ding Y and Li Y (2019) Adaptation of Dominant Species to Drought in the Inner Mongolia Grassland – Species Level and Functional Type Level Analysis. Front. Plant Sci. 10:231. doi: 10.3389/fpls.2019.00231

The adaptation of plants to drought through the adjustment of their leaf functional traits is a hot topic in plant ecology. However, while there is a good understanding of how individual species adapt to drought in this way, the way in which different functional types adapt to drought along a precipitation gradient remains poorly understood. In this study, we sampled 22 sites along a precipitation gradient in the Inner Mongolia grassland and measured eight leaf functional traits across 39 dominant species to determine the adaptive strategies of plant leaves to drought at the species and plant functional type levels. We found that leaf functional traits were mainly influenced by both aridity and phylogeny at the species level. There were four types of leaf adaptations to drought at the functional type level: adjusting the carbon-nitrogen ratio, the specific leaf area, the nitrogen content, and the specific leaf area and leaf nitrogen content simultaneously. These findings indicate that there is the trade-offs relationship between water and nitrogen acquisition as the level of drought increases, which is consistent with the worldwide leaf economics spectrum. In this study, we highlighted that the leaf economic spectrum can be adopted to reveal the adaptations of plants to drought in the Inner Mongolia grassland.

Keywords: drought, plant functional type, leaf economic spectrum, inner mongolia grassland, adaptation strategy

INTRODUCTION

Arid and semi-arid regions occupy approximately 45% of the Earth's land area and feed 38% of its population but also include some of the most vulnerable ecosystems and water resource systems (Narisma et al., 2007). In these regions, plant diversity maintains the ecosystem processes and functions and also affects ecosystem services (Balvanera et al., 2006). Water as the main limiting factor in these regions is one of the most important abiotic stresses influencing the survival, growth and distribution of plants. Therefore, the adaptation of plants to drought has always been a hot topic in ecological research (Chaves et al., 2002; Shavrukov et al., 2017). The characteristics of leaves are essential for the adaptation of plants to environmental change as leaves not only exhibit strong sensitivity and plasticity to spatial and temporal changes in the environment but can also improve the adaptability of plants through self-regulation (Picotte et al., 2009; Zhang et al., 2018). Therefore,

the adaptation of plants to drought through the adjustment of leaf morphology has received much attention (Stropp et al., 2017).

Plant leaf exhibit both morphological and anatomical adaptations to drought. For example, plants that have grown under water-deficient conditions for a long period of time produce thickened, smaller leaves with a cracked appearance and a small specific leaf area, among other characteristics. Indeed, the leaves of some xerophytes become fleshy or even degenerate into rods. Such characteristics are conducive to reducing transpiration and promoting more effective heat dissipation (Bosabalidis and Kofidis, 2002; Stropp et al., 2017). In addition, plant leaves exhibit physiological and stoichiometric changes under drought conditions. For example, the photosynthetic rate may decrease as the level of drought increases (Tanaka and Shiraiwa, 2009). Furthermore, changes in the photosynthetic rate will further affect the uptake and recycling of nutrient elements and eventually lead to changes in the ecological stoichiometric characteristics of the leaves (Yuan et al., 2006; Zhang et al., 2018). He and Dijkstra (2014) experimentally showed that drought has a significant negative effect on plant nitrogen and phosphorus contents and a positive effect on the plant nitrogen-phosphorus ratio, while other experiments have shown that moderate drought stress may increase the uptake of nitrogen and decrease the growth rate of plants, resulting in a decrease in the carbon-nitrogen ratio (Lu et al., 2009).

Wright et al. (2004) proposed the concept of "leaf economics spectrum" (LES), which is a universal spectrum consisting of key leaf chemical, structural and physiological traits. At one end of the LES are species that have a "rapid investment-return" strategy, i.e., species with high leaf nitrogen contents, photosynthetic rates and respiration rates, short life spans and low specific leaf weights, while at the other end are species that have a "slow investment-return" strategy, i.e., species with long life span, large specific leaf weight, low nitrogen content, photosynthetic rate and respiration rate (Osnas et al., 2013). The resource trade-offs strategy is an important mechanism for LES, whereby plants that invest more resources in a particular functional trait will inevitably reduce the input of resources into other traits due to the total amount of resources that are available to the plants being limited, and such a trade-offs strategy has provided a mechanism by which plants can adapt to the environment in different geographical regions and ecosystems (Wright et al., 2005; Shipley et al., 2006; Ocheltree et al., 2016). Zhang et al. (2017) found that the trade-offs strategy of hydrophytes functional traits coincided with the worldwide LES. Abrahamson (2007) found that both *Serenoa repens* and *Sabal etonia* used a trade-offs strategy for functional traits under drought conditions, such as miniature plant morphology, a relative decrease in leaf size, number and photosynthetic yield, and prolonged leaf longevity, observing significant correlations among these traits and the formation of a continuously changing trade-offs strategy zone with the same plant species and homologous plants growing in shady or humid areas. Lohbeck et al. (2013) found that the trade-offs strategy is important for functional composition changes with succession in the dry and wet forest.

Studies that focus on characteristics of leaves of individual single species under different environmental conditions are important for revealing specific adaptive strategies at the species level (Zhu et al., 2012; Ramirez-Valiente et al., 2015; Liu et al., 2018). However, to generalized the plant adaptive strategies and the effects of global climate change on ecosystems, it is essential to group vegetation that is ecologically similar. The plant functional type is an assemblage of plants that share a set of key functional traits, respond to the environment in equal ways and play similar roles in the main ecosystem processes, (Chapin et al., 1996; Semenova and van der Maarel, 2000) and it has been shown that adaptive mechanisms often vary at the species and plant functional type levels (Domínguez et al., 2012). Although the environment is considered a key factor affecting leaf functional traits at the species level (Albert et al., 2010; Bu et al., 2017), the phylogenetic relationship among different species should also be considered because species with similar phylogenetic relationship may have similar functional traits (Kaplan and Pigliucci, 2001; Webb et al., 2002; Grether, 2005; Losos, 2008). In contrast, some studies have shown that plant functional types are the consequence of the adaptive processes of plants rather than branching processes in plant lineage (Pie and Weitz, 2005; Silva and Batalha, 2011). Thus, plant functional types can represent different adaptive strategies and may thus represent an efficient tool for revealing patterns of adaptation to environmental change (Ian and Wolgang, 2010). Moreover, understanding what adaptive strategies allow plants to successfully pass through the filter along an environmental gradient is of major importance in ecology. Moreover, understanding what adaptation strategies allow plant to pass through filter along the environment gradient successfully is a major issue in ecology.

The Inner Mongolia Plateau is a typical arid and semi-arid region with a large spatial precipitation gradient, making it an ideal place to study the adaptive mechanisms of plants to drought (Wu et al., 2015). In this study, we sampled 22 sites along the precipitation gradient of the Inner Mongolia grassland and measured eight leaf functional traits in 39 dominant species to address the following questions: (1) How are plants adapted to drought by modifying their leaf functional traits at the species and plant functional type levels? (2) Is the LES existing and applied to the adaptation of plants to drought in the Inner Mongolia grassland?

MATERIALS AND METHODS

Study Sites

This study was conducted across the entire area of the Inner Mongolia grassland in northern China, which stretches from 41.31°N to 50.78°N and 108.16°E to 120.39°E and has an elevation ranging from 532 to 1725 m above sea level (**Figure 1**). The typical landforms in this region include gently rolling plains, tablelands, and hills. The mean annual temperature ranges from −3.0 to 6.7°C and the mean annual precipitation varies from approximately 150 to 450 mm, decreasing from the southeast to

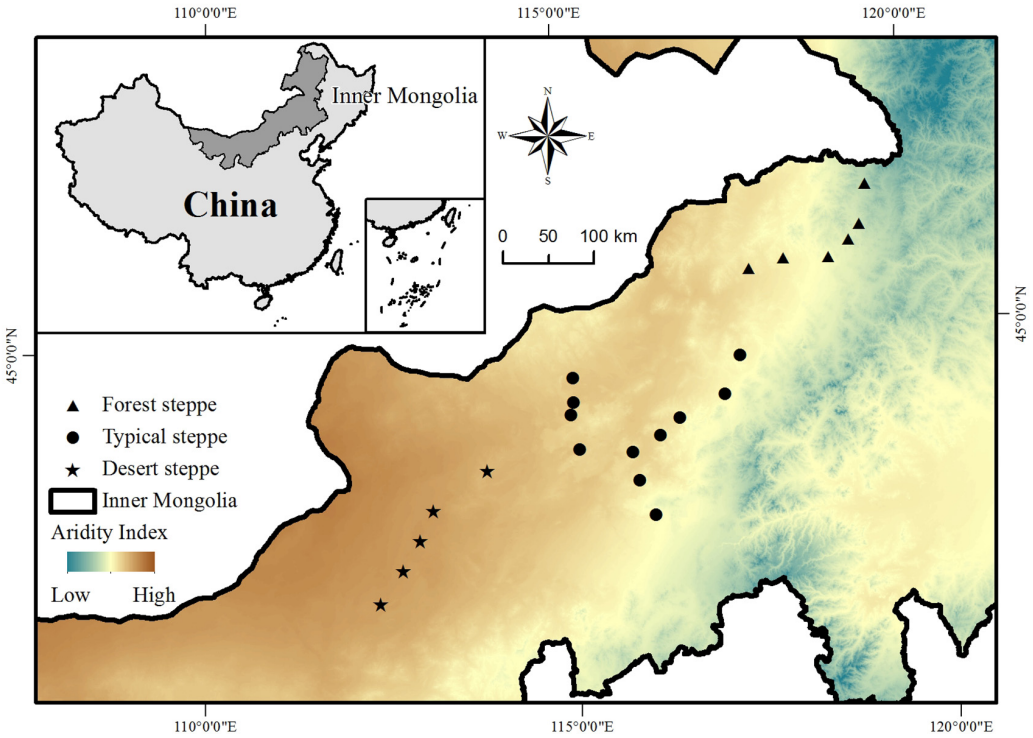

FIGURE 1 | Study area and sites.

the northwest (Inner Mongolia-Ningxia Joint Inspection Group of Chinese Sciences of Academy, 1985). The aridity at each study site (see below) was calculated as [1 - precipitation/potential evapotranspiration] (Delgado-Baquerizo et al., 2013). Along the climate gradient from the relatively humid southeast to the relatively dry northwest, there is a succession of soil types from chernozems to chestnut and calcic brown soils, and a succession of habitat types from forest steppe through to typical steppe and desert steppe grassland (**Figure 1**).

Data Collection

We surveyed 22 sites across the Inner Mongolia grassland in August 2017 during the peak period of aboveground biomass for the three main vegetation types: forest steppe, typical steppe, and desert steppe. The study sites had been banned grazing for over 3 years to minimize the potential effects of grazers and other disturbances. Five 1 × 1 m^2 quadrats were randomly set at each site and species within each quadrat were recorded. The functional traits were then recorded for all healthy and pest-free plants of each of the species found at each site following the standard measurement methods for plant functional traits (Cornelissen et al., 2003). Five individuals of each species with good vigor and no pests or diseases were selected in each quadrat and eight functional traits that are sensitive to environmental change were measured on three intact leaves per plant. The leaf area (LA) was measured using a leaf area meter (LI-3100 Area Meter; LI-COR, Lincoln, United States). The leaves were then oven-dried at 60°C to obtain the leaf dry weight (LDM). The specific leaf area (SLA) was calculated based on the leaf area and leaf dry weight. The leaf nitrogen and carbon contents (LNC, LCC) were measured with an elemental analyzer (Euro Vector EA3000; Milan), and the carbon-nitrogen (LC:N) and nitrogen-phosphorus ratios (LN:P) calculated. Finally, the total leaf phosphorus content (LPC) was determined using the ammonium molybdate spectrophotometric method (Bowman, 1988). The average values of the functional traits of each species at their respective sites were used in this study.

Statistical Analyses

We selected 39 species that had more than three occurrences across the entire sites for analysis. At the species level, we used the generalized linear model (Poisson distribution) to analyze the variation of eight plant functional traits that explained by climate (aridity) and phylogeny (genus). To analyze the respective and common interpretations of climate and phylogeny for each functional trait, we constructed three generalized linear models that included the trait as the response variable and aridity, genus, both aridity and genus as the explanatory variables, respectively. Thus, the R^2 values of the first and second models represented the amount of variation in a particular functional trait that explained by aridity and phylogeny, respectively, while the difference in the R^2 values between the sum of the first and second models and the third model indicated the combined effect of aridity and phylogeny on the each functional trait.

To analysis the adaptation of these species to drought at the plant functional type level, we first defined the plant functional

types using cluster analysis (Semenova and van der Maarel, 2000). We constructed the clustering tree based on the Euclidean distance calculated using the eight functional traits of each species, each of which was first standard (Chapin et al., 1996; Montes-Pulido et al., 2017). Once the 39 species had been divided into functional groups, one-way ANOVA and multiple comparisons were performed to examine the differences in the eight functional traits between the functional types. To evaluate how each of the plant functional types adapted to drought, the direct relationship between aridity and the proportion of each functional type at a site was assessed by Pearson correlation analysis and ordinary least squares regression analysis, in which the proportion of plant functional types was represented by the ratio of the number of species which belongs to a given functional type to the total number of species at the site. Finally, to reveal how the different plant functional types successfully passed through the drought filter along the precipitation gradient and adapted to drought in the Inner Mongolia grassland, we used structural equation model to assess the causal relationships between aridity, the mean functional traits of the plant functional types and the proportion of plant functional types at a site using standardized path coefficients.

The generalized linear model, Pearson correlation analysis, one-way ANOVA, ordinary least squares regression and cluster analysis were conducted in R version 3.5.1. The structural equation model was conducted using the AMOS software. Shapiro–Wilk test was used to test the normality of the data before analysis and a log-normal transformation was used to normalize any variables that did not conform to the normal distribution.

RESULTS

Effects of Aridity and Phylogeny on Variation in Plant Functional Traits at the Species Level

Both aridity and phylogeny had significant effects on plant leaf functional traits, with variation in the leaf area, specific leaf area and leaf carbon-nitrogen ratio being explained by both factors together, and variation in the leaf carbon content being explained only by aridity (**Table 1**).

TABLE 1 | Amount of variation in the leaf functional traits explained by phylogeny and aridity at the species level.

Plant functional trait	Phylogeny (%)	Aridity (%)	Phylogeny and aridity (%)
Single leaf area	22.88*	12.51*	2.26
Dry weight of single leaf	24.76	7.20	2.05
Specific leaf area	0.40*	22.32*	0.39
Leaf carbon	0.23	1.99*	0
Leaf nitrogen	1.70	5.00	0.98
Leaf phosphorus	0.14	0.99	0.11
Leaf carbon-nitrogen ratio	2.57*	9.78*	1.44
Leaf nitrogen-phosphorus ratio	0.04	1.55	0.04

*$p < 0.05$.

Classification of Plant Functional Types

The 39 plant species analyzed could be divided into five functional types based on the eight functional traits measured (**Figure 2**). The differences in the eight functional traits among the five functional types are shown in **Figure 3**. Functional type III had a significantly higher single leaf area (**Figure 3A**) and leaf dry weight (**Figure 3B**) than the other four types, while functional type V had a significantly higher specific leaf area (**Figure 3C**). In terms of the leaf carbon content, functional type IV had significantly higher levels than functional type I but there was no significant difference among the other three functional types (**Figure 3D**), while for leaf nitrogen content, functional types I and II had remarkably higher levels than the other three functional types (**Figure 3E**). For the leaf phosphorus content, functional type II had much higher levels than the other four functional types and functional type IV had the lowest level (**Figure 3F**). With respect to the leaf carbon-nitrogen ratio, functional types III, IV, and V had higher values than functional types I and II (**Figure 3G**), while for the leaf nitrogen-phosphorus ratio, functional types I and IV had much higher values than functional types II and V, with no significant difference being observed between functional type III and any other functional type (**Figure 3H**).

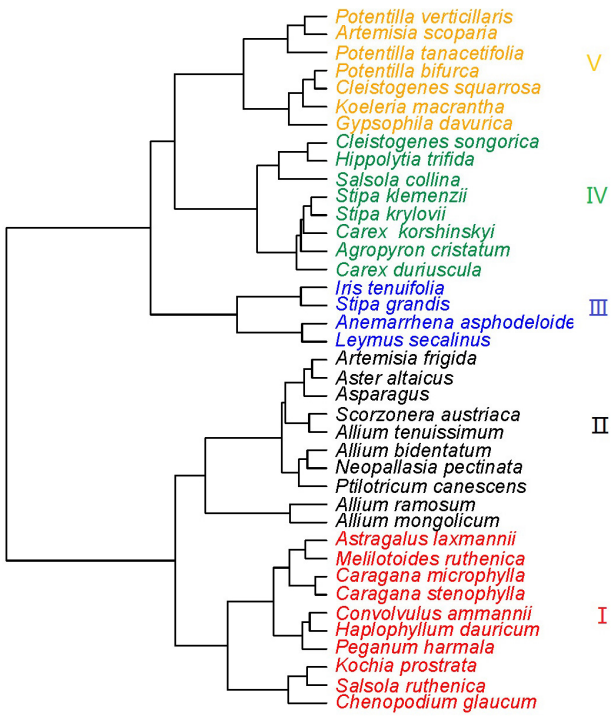

FIGURE 2 | Cluster diagram of the eight species functional traits (Red, functional type I; black, functional type II; blue, functional type III; green, functional type IV; orange, functional type V).

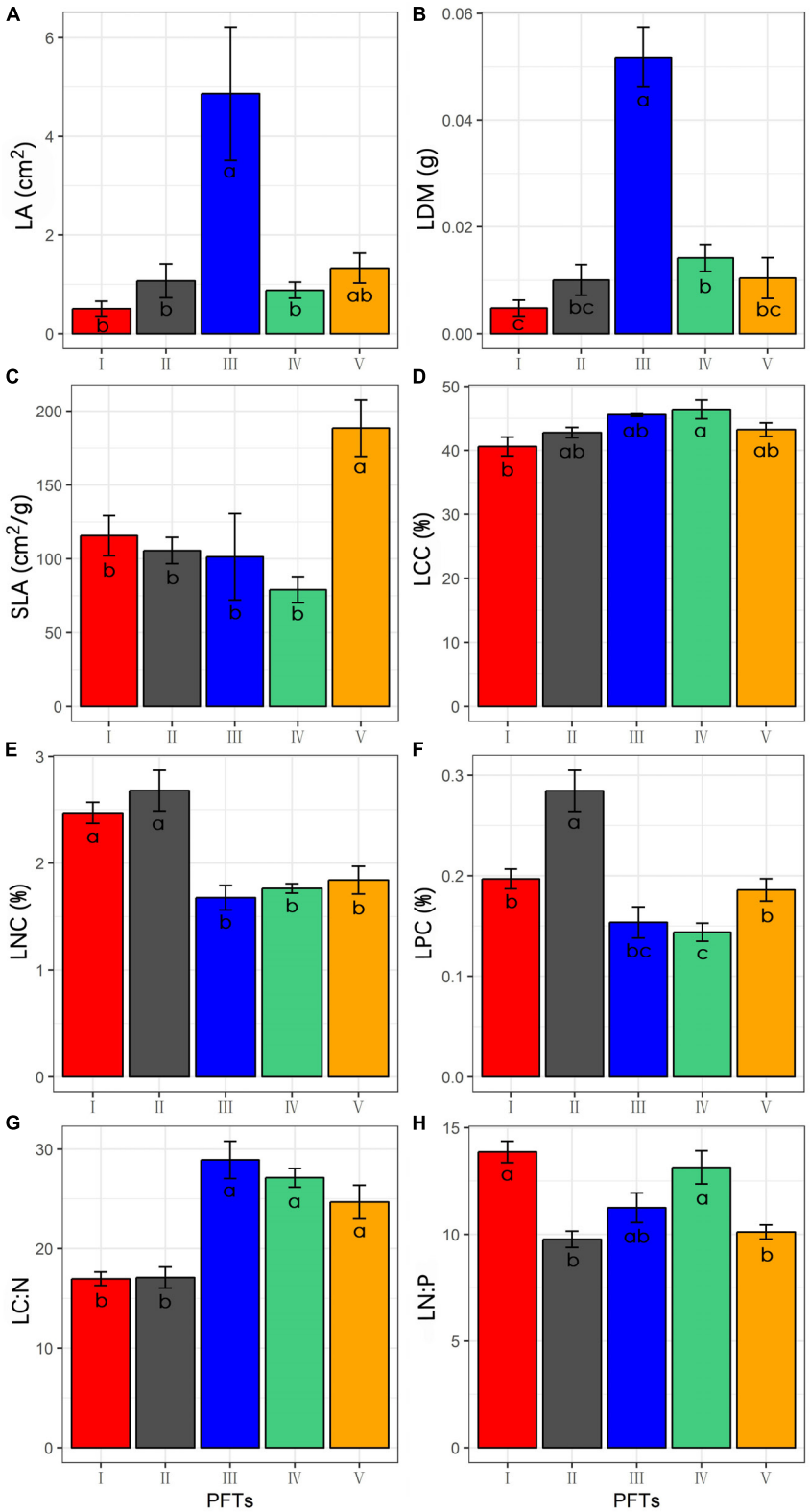

FIGURE 3 | Differences of functional traits among the five functional types (Data are the means and SE of eight functional traits in each of the five functional types). **(A)** Difference of the leaf area; **(B)** difference of the leaf dry weight; **(C)** difference of the specific leaf area; **(D)** difference of the leaf carbon content; **(E)** difference of the leaf nitrogen content; **(F)** difference of the leaf phosphorus content; **(G)** difference of the leaf carbon-nitrogen ratio; **(H)** difference of the leaf nitrogen-phosphorus ratio.

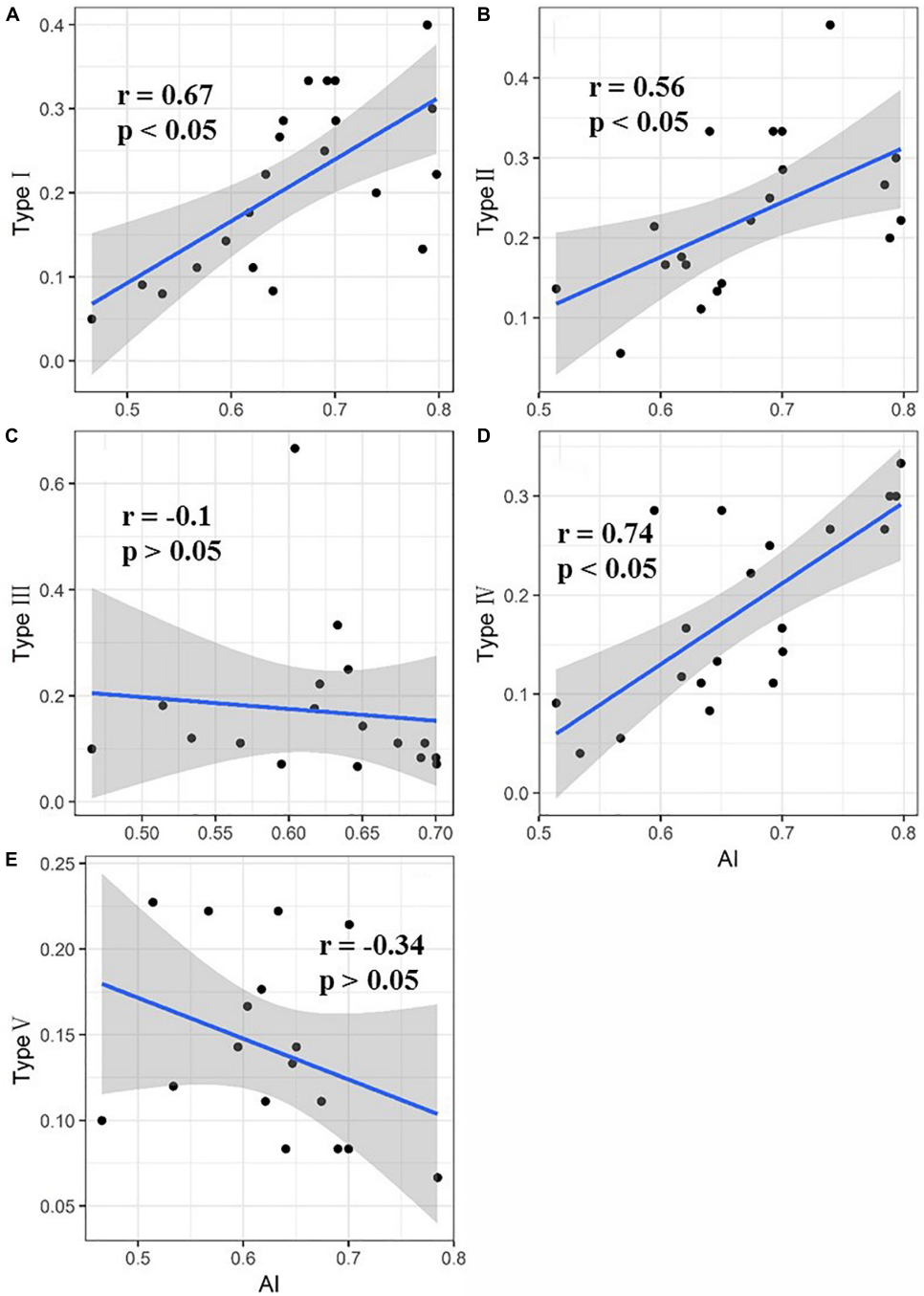

FIGURE 4 | Direct response of each of the five plant functional types to drought (Values for types I, II, III, IV, and V represent the proportion of each functional type in the sample plots. The shaded areas indicate the 95% confidence intervals). **(A)** Direct response of plant functional type I to drought; **(B)** direct response of plant functional type II to drought; **(C)** direct response of plant functional type III to drought; **(D)** direct response of plant functional type IV to drought; **(E)** direct response of plant functional type V to drought.

Adaptation of Plants to Drought at the Functional Level

The relationship between the proportion of each functional type at each site and the aridity is shown in **Figure 4**. The proportion of functional types I, II, and IV in the sample plots significantly increased as the aridity increased, while the proportion of functional types III and V tended to decrease but not significantly. Functional type I plants exhibited a simultaneous reduction in leaf area and leaf nitrogen content with the increase of

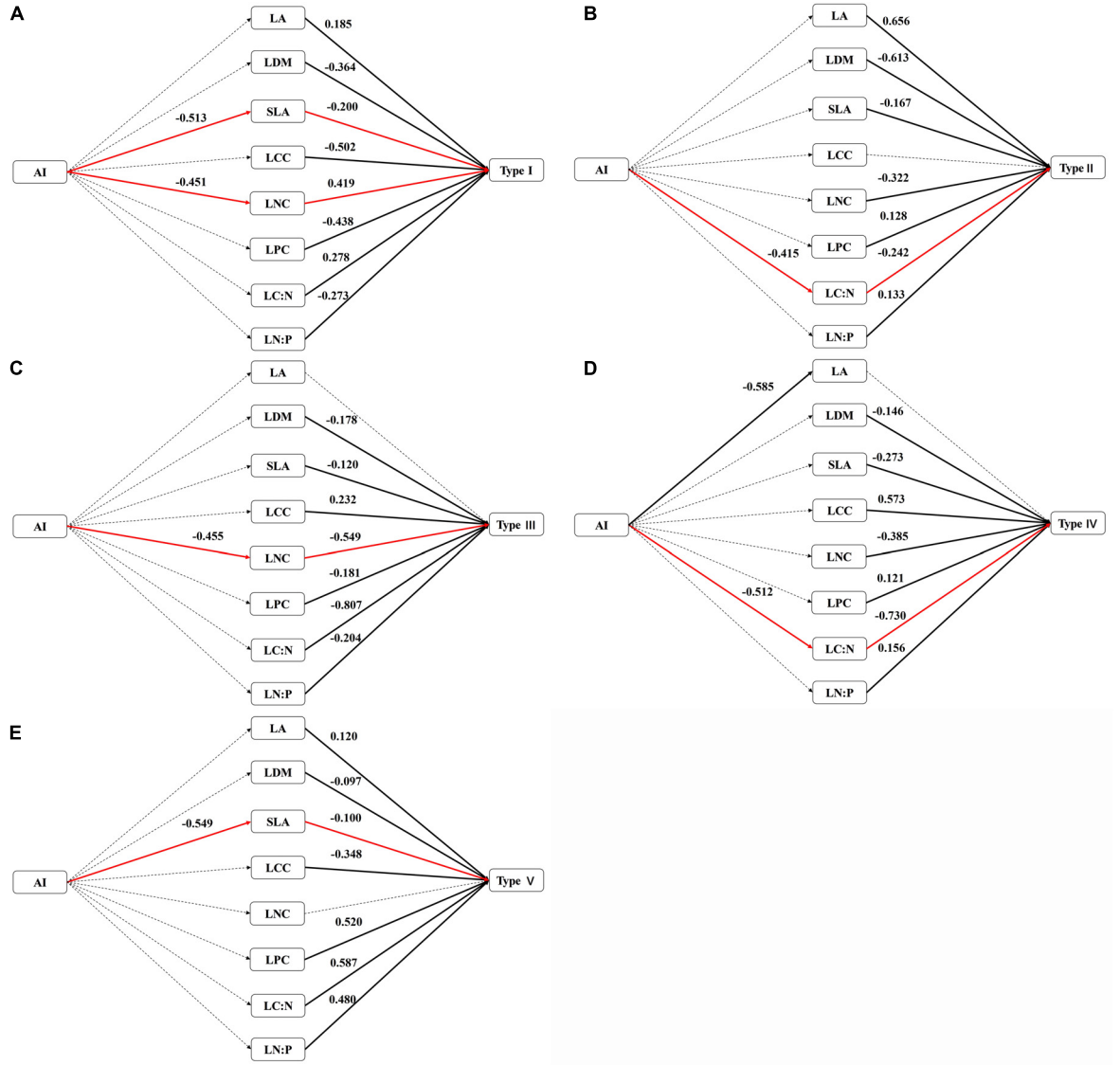

FIGURE 5 | Response paths of different functional types to drought (Dotted lines represent non-significant paths ($p > 0.05$), black lines represent significant paths ($p < 0.05$) and red lines represent significant paths across AI-Functional traits: the proportion of functional types; values for types I, II, III, IV, and V represent the proportion of each functional type in each site). **(A)** Response path of type I to drought; **(B)** response path of type II to drought; **(C)** response path of type III to drought; **(D)** response path of type IV to drought; **(E)** response path of type IV to drought.

aridity (**Figure 5A**), while functional type II plants reduced the carbon-nitrogen ratio in their leaves (**Figure 5B**), functional type III plants increased their leaf nitrogen content (**Figure 5C**), functional type IV plants reduced the leaf carbon-nitrogen ratio in their leaves (**Figure 5D**) and functional type V plants reduced the leaf nitrogen content (**Figure 5E**) in response to drought.

DISCUSSION

In the present study, we demonstrated that aridity significantly affected the plant specific leaf area, leaf carbon content and leaf carbon-nitrogen ratio at the species level in the Inner Mongolia grassland, which is consistent with the findings of previous studies which found that plants can adapt to drought by regulating their leaf functional traits (Wright et al., 2004; Jung et al., 2014; Valencia et al., 2015). Some studies have also demonstrated that phylogeny would impact the functional traits, i.e., species with close phylogenetic relationships have similar functional traits (Ackerly, 2009; Burns and Strauss, 2012). Similarly, we found that the single leaf area, specific leaf area and leaf carbon-nitrogen ratio were significantly affected by phylogeny at the species level, suggesting that these three functional traits may be "conserved traits" that have a have strong phylogenetic signal (Blomberg et al., 2003). Our finding that these three functional traits were significantly

affected by both phylogeny and drought suggests that species with adaptive functional traits are selected for and retained under long-term, strong environmental filtering, supporting the findings of previous studies (Grether, 2005; Liu et al., 2013). Further analysis showed that the variation in leaf area could be better explained by phylogeny than by climatic factors, while the specific leaf area and leaf carbon-nitrogen ratio were mainly affected by climatic factors, demonstrating that the importance of phylogeny and climatic factors differs between different functional traits.

Many studies have reported that plants adapt to drought conditions by adjusting leaf functional traits in various ways, such as the leaf dry matter content, specific leaf area, leaf carbon, nitrogen and phosphorus contents, and leaf stoichiometric ratio (Hameed et al., 2012; Stropp et al., 2017). In the present study, we found that plants in the Inner Mongolia grassland adapted to drought mainly by adjusting their leaf carbon-nitrogen ratios, specific leaf area and leaf nitrogen contents (**Figure 5**). Plant functional types II and IV showed the same adaptive strategy to drought, by decreasing the carbon-nitrogen ratio and then increasing in proportion in the sample plot (**Figures 4**, **5**). The carbon-nitrogen ratio of plant leaves reflects the growth rate of plants to a certain extent, as a large amount of proteins, chlorophyll and rRNA are required for plant growth which, in turn, require large amounts of nitrogen and phosphorus, reducing the carbon-nitrogen ratio in the leaves (Agren, 2004). The leaves of functional type II species contained higher nitrogen and phosphorus contents than those of the other functional types (**Figure 2**), indicating that these plants can increase their growth rate by increasing their photosynthetic capacity, allowing them to eventually adapt to drought conditions. By contrast, the leaves of functional type IV plants had relatively low nitrogen and phosphorus contents but relatively high carbon contents (**Figure 2**), indicating that they could accumulate dry matter quite efficiently to adapt to drought conditions. Functional type V plants experienced a decrease in specific leaf area in response to drought (**Figures 4E**, **5E**), which is speculated to increase water retention and thereby reduce transpiration and facilitate heat dissipation (Ackerly et al., 2002; Hameed et al., 2012). Finally, functional type III plants adapted to drought by increasing their leaf nitrogen content (**Figure 5C**), which is commonly associated with a high resource-acquisition capacity (Weih et al., 2011; Jung et al., 2014). This functional type mainly included species such as *Leymus chinensis* and *Stipa grandis*, which tend to predominate in areas with relatively abundant water (Inner Mongolia-Ningxia Joint Inspection Group of Chinese Sciences of Academy, 1985). However, the grassland in Inner Mongolia generally lacks nitrogen (Yuan et al., 2006), so the ability of these plants to obtain more nitrogen will be crucial for their adaptation to arid environments.

Numerous studies have documented that plants adapt to the environment by balancing resource utilization and allocation when resources are scarce (Gong et al., 2011; Ocheltree et al., 2016). In the present study, we found that functional type I plants exhibited a significant decrease in specific leaf area and leaf nitrogen content with an increase in aridity. A decrease in specific leaf area indicates an increased water use efficiency of plants (Ackerly et al., 2002), while a decrease in leaf nitrogen content indicates a lower nitrogen use efficiency (Yuan et al., 2006). Thus, this finding suggests that functional type I plants adapted to drought by trade-offs water use efficiency against nitrogen use efficiency. This result is consistent with the findings of Gong et al. (2011), who reported trade-offs between water use efficiency and nitrogen use efficiency in a semi-arid grassland. In areas with a high water supply, plants can improve their nitrogen use efficiency at the expense of water use efficiency. However, when water is restricted, it is a better strategy to improve water use efficiency to allow plants to increase dry matter accumulation, prolong their leaf life and complete their life cycle. Leaf thickness also tends to increase with a decrease in specific leaf area (Niinemets, 2001), further limiting the light intensity that reaches the chloroplasts inside the leaves, increasing the conduction resistance of CO_2 in the mesophyll tissues and reducing the proportion of nitrogen that is distributed to the photosynthetic organs (Poorter and Evans, 1998), thereby decreasing the nitrogen content in the leaves.

In summary, our study demonstrated that plants in the Inner Mongolia grassland adapt to drought in four different ways including adjusting the leaf carbon-nitrogen ratio, the specific leaf area, the leaf nitrogen content, as well as the specific leaf area and leaf nitrogen content simultaneously. This finding is consistent with the LES which runs from species with conservative resource-use strategy to predominant resource-acquisition strategy (Wright et al., 2004). Functional type II, III, and IV plants adjusted their leaf nitrogen contents and carbon-nitrogen ratios and thus correspond to conservative resource-use strategy plants, while functional type V plants adjusted their specific leaf area, corresponding with predominantly resource-acquisition strategy plants, and functional type I plants adjusted their specific leaf area and nitrogen content simultaneously indicate that the trade-offs in the LES. Thus, it is clear that the LES exists in the Inner Mongolia grassland and can be applied to reveal the adaptation of plants to drought.

AUTHOR CONTRIBUTIONS

QZ and YD conceived the ideas. YY and YL complied the experiments and ran further data analysis. YY, YL, QL, QZ, and YD led the writing.

FUNDING

This research is supported by National Basic Research program of China (Grant Nos. 31560180 and 31760150), Inner Mongolia Science and Technology Plan (Grant No. 201601061) and Postdoctoral Science Foundation (Grant No. 156409).

ACKNOWLEDGMENTS

Thanks to Ling Zhu and Yayuan Yan for the help of field work.

REFERENCES

Abrahamson, W. G. (2007). Leaf traits and leaf life spans of two xeric-adapted palmettos. *Am. J. Bot.* 94, 1297–1308. doi: 10.3732/ajb.94.8.1297

Ackerly, D. (2009). Conservatism and diversification of plant functional traits: evolutionary rates versus phylogenetic signal. *Proc. Natl. Acad. Sci. U.S.A.* 106, 19699–19706. doi: 10.1073/pnas.0901635106

Ackerly, D. D., Knight, C. A., Weiss, S. B., Barton, K., and Starmer, K. P. (2002). Leaf size, specific leaf area and microhabitat distribution of chaparral woody plants: contrasting patterns in species level and community level analyses. *Oecologia* 130, 449–457. doi: 10.1007/s004420100805

Agren, G. I. (2004). The C : N : P stoichiometry of autotrophs - theory and observations. *Ecol. Lett.* 7, 185–191. doi: 10.1111/j.1461-0248.2004.00567.x

Albert, C. H., Thuiller, W., Yoccoz, N. G., Soudant, A., Boucher, F., Saccone, P., et al. (2010). Intraspecific functional variability: extent, structure and sources of variation. *J. Ecol.* 98, 604–613. doi: 10.1111/j.1365-2745.2010.01651.x

Balvanera, P., Pfisterer, A. B., Buchmann, N., He, J.-S., Nakashizuka, T., Raffaelli, D., et al. (2006). Quantifying the evidence for biodiversity effects on ecosystem functioning and services. *Ecol. Lett.* 9, 1146–1156. doi: 10.1111/j.1461-0248.2006.00963.x

Blomberg, S. P., Garland, T., and Ives, A. R. (2003). Testing for phylogenetic signal in comparative data: behavioral traits are more labile. *Evolution* 57, 717–745. doi: 10.1111/j.0014-3820.2003.tb00285.x

Bosabalidis, A. M., and Kofidis, G. (2002). Comparative effects of drought stress on leaf anatomy of two olive cultivars. *Plant Sci.* 163, 375–379. doi: 10.1016/s0168-9452(02)00135-8

Bowman, R. A. (1988). A rapid method to determine total phosphorus in soils. *Soil Sci. Soc. Am. J.* 52, 1301–1304. doi: 10.2136/sssaj1988.03615995005200050016x

Bu, W., Schmid, B., Liu, X., Li, Y., Härdtle, W., Oheimb, G. V., et al. (2017). Interspecific and intraspecific variation in specific root length drives aboveground biodiversity effects in young experimental forest stands. *J. Plant Ecol.* 10, 158–169. doi: 10.1093/jpe/rtw096

Burns, J. H., and Strauss, S. Y. (2012). Effects of competition on phylogenetic signal and phenotypic plasticity in plant functional traits. *Ecology* 93, S126–S137. doi: 10.1890/11-0401.1

Chapin, F. S. III, Bret-Harte, M. S., Hobbie, S. E., and Zhong, H. (1996). Plant functional types as predictors of transient responses of arctic vegetation to global change. *J. Veg. Sci.* 7, 347–358. doi: 10.2307/3236278

Chaves, M. M., Pereira, J. S., Maroco, J., Rodrigues, M. L., Ricardo, C. P. P., Osorio, M. L., et al. (2002). How plants cope with water stress in the field. Photosynthesis and growth. *Ann. Bot.* 89, 907–916. doi: 10.1093/aob/mcf105

Cornelissen, J., Lavorel, S., Garnier, E., Diaz, S., Buchmann, N., Gurvich, D., et al. (2003). A handbook of protocols for standardised and easy measurement of plant functional traits worldwide. *Aust. J. Bot.* 51, 335–380. doi: 10.1071/BT02124

Delgado-Baquerizo, M., Maestre, F. T., Gallardol, A., Bowker, M. A., Wallenstein, M. D., Luis Quero, J., et al. (2013). Decoupling of soil nutrient cycles as a function of aridity in global drylands. *Nature* 502, 672–676. doi: 10.1038/nature12670

Domínguez, M. T., Aponte, C., Pérez-Ramos, I. M., García, L. V., Villar, R., and Marañón, T. (2012). Relationships between leaf morphological traits, nutrient concentrations and isotopic signatures for mediterranean woody plant species and communities. *Plant Soil* 357, 407–424. doi: 10.1007/s11104-012-1214-7

Gong, X. Y., Chen, Q., Dittert, K., Taube, F., and Lin, S. (2011). Nitrogen, phosphorus and potassium nutritional status of semiarid steppe grassland in Inner Mongolia. *Plant Soil* 340, 265–278. doi: 10.1007/s11104-010-0577-x

Grether, G. F. (2005). Environmental change, phenotypic plasticity, and genetic compensation. *Am. Nat.* 166:E115. doi: 10.1086/432023

Hameed, M., Batool, S., Naz, N., Nawaz, T., and Ashraf, M. (2012). Leaf structural modifications for drought tolerance in some differentially adapted ecotypes of blue panic (Panicum antidotale Retz.). *Acta Physiol. Plant.* 34, 1479–1491. doi: 10.1007/s11738-012-0946-6

He, M., and Dijkstra, F. A. (2014). Drought effect on plant nitrogen and phosphorus: a metaanalysis. *New Phytol.* 204, 924–931. doi: 10.1111/nph.12952

Ian, W. F., and Wolgang, C. (2010). Plant functional types and climatic changes: introduction. *J. Veg. Sci.* 7, 306–308.

Inner Mongolia-Ningxia Joint Inspection Group of Chinese Sciences of Academy (1985). *Vegetation of Inner Mongolia*. Beijing: Science Publishing House.

Jung, V., Albert, C. H., Violle, C., Kunstler, G., Loucougaray, G., and Spiegelberger, T. (2014). Intraspecific trait variability mediates the response of subalpine grassland communities to extreme drought events. *J. Ecol.* 102, 45–53. doi: 10.1111/1365-2745.12177

Kaplan, J. M., and Pigliucci, M. (2001). Genes for phenotypes: a modern history view. *Biol. Philos.* 16, 189–213. doi: 10.1023/A:1006773112047

Liu, B. B., Li, M., Li, Q. M., Cui, Q. Q., Zhang, W. D., Ai, X. Z., et al. (2018). Combined effects of elevated CO2 concentration and drought stress on photosynthetic performance and leaf structure of cucumber (*Cucumis sativus L.*) seedlings. *Photosynthetica* 56, 942–952. doi: 10.1007/s11099-017-0753-9

Liu, X., Swenson, N. G., Zhang, J., and Ma, K. (2013). The environment and space, not phylogeny, determine trait dispersion in a subtropical forest. *Funct. Ecol.* 27, 264–272. doi: 10.1111/1365-2435.12018

Lohbeck, M., Poorter, L., Lebrija-Trejos, E., Martinez-Ramos, M., Meave, J. A., Paz, H., et al. (2013). Successional changes in functional composition contrast for dry and wet tropical forest. *Ecology* 94, 1211–1216. doi: 10.1890/12-1850.1

Losos, J. B. (2008). Phylogenetic niche conservatism, phylogenetic signal and the relationship between phylogenetic relatedness and ecological similarity among species. *Ecol. Lett.* 11, 995–1003. doi: 10.1111/j.1461-0248.2008.01229.x

Lu, Y., Duan, B., Zhang, X., Korpelainen, H., and Li, C. (2009). Differences in growth and physiological traits of Populus cathayana populations as affected by enhanced UV-B radiation and exogenous ABA. *Environ. Exp. Bot.* 66, 100–109. doi: 10.1016/j.envexpbot.2008.12.006

Montes-Pulido, C. R., Parrado-Rosselli, A., and Alvarez-Davila, E. (2017). Palnt functional types as estimator of carbon in dry forest of the Colombian Caribbean. *Rev. Mex. Biodivers.* 88, 241–249. doi: 10.1016/j.rmb.2017.01.006

Narisma, G. T., Foley, J. A., Licker, R., and Ramankutty, N. (2007). Abrupt changes in rainfall during the twentieth century. *Geophys. Res. Lett.* 34:L06710. doi: 10.1029/2006gl028628

Niinemets, U. (2001). Global-scale climatic controls of leaf dry mass per area, density, and thickness in trees and shrubs. *Ecology* 82, 453–469. doi: 10.2307/2679872

Ocheltree, T. W., Nippert, J. B., and Prasad, P. V. V. (2016). A safety vs efficiency trade-off identified in the hydraulic pathway of grass leaves is decoupled from photosynthesis, stomatal conductance and precipitation. *New Phytol.* 210, 97–107. doi: 10.1111/nph.13781

Osnas, J. L. D., Lichstein, J. W., Reich, P. B., and Pacala, S. W. (2013). Global leaf trait relationships: mass, area, and the leaf economics spectrum. *Science* 340, 741–744. doi: 10.1126/science.1231574

Picotte, J. J., Rhode, J. M., and Cruzan, M. B. (2009). Leaf morphological responses to variation in water availability for plants in the Piriqueta caroliniana complex. *Plant Ecol.* 200, 267–275. doi: 10.1007/s11258-008-9451-9

Pie, M. R., and Weitz, J. S. (2005). A null model of morphospace occupation. *Am. Nat.* 166, E1–E13. doi: 10.1086/430727

Poorter, H., and Evans, J. R. (1998). Photosynthetic nitrogen-use efficiency of species that differ inherently in specific leaf area. *Oecologia* 116, 26–37. doi: 10.1007/s004420050560

Ramirez-Valiente, J. A., Koehler, K., and Cavender-Bares, J. (2015). Climatic origins predict variation in photoprotective leaf pigments in response to drought and low temperatures in live oaks (Quercus series Virentes). *Tree Physiol.* 35, 521–534. doi: 10.1093/treephys/tpv032

Semenova, G. V., and van der Maarel, E. (2000). Plant functional types - a strategic perspective. *J. Veg. Sci.* 11, 917–922. doi: 10.2307/3236562

Shavrukov, Y., Kurishbayev, A., Jatayev, S., Shvidchenko, V., Zotova, L., Koekemoer, F., et al. (2017). Early flowering as a drought escape mechanism in plants: how can it aid wheat production? *Front. Plant Sci.* 8:1950. doi: 10.3389/fpls.2017.01950

Shipley, B., Lechowicz, M. J., Wright, I., and Reich, P. B. (2006). Fundamental trade-offs generating the worldwide leaf economics spectrum. *Ecology* 87, 535–541. doi: 10.1890/05-1051

Silva, I. A., and Batalha, M. A. (2011). Plant functional types in Brazilian savannas: the niche partitioning between herbaceous and woody species. *Perspect. Plant Ecol. Evol. Syst.* 13, 201–206. doi: 10.1016/j.ppees.2011.05.006

Stropp, J., dos Santos, I. M., Correia, R. A., dos Santos, J. G., Silva, T. L. P., dos Santos, J. W., et al. (2017). Drier climate shifts leaf morphology in Amazonian trees. *Oecologia* 185, 525–531. doi: 10.1007/s00442-017-3964-7

Tanaka, Y., and Shiraiwa, T. (2009). Stem growth habit affects leaf morphology and gas exchange traits in soybean. *Ann. Bot.* 104, 1293–1299. doi: 10.1093/aob/mcp240

Valencia, E., Maestre, F. T., Le Bagousse-Pinguet, Y., Quero, J. L., Tamme, R., Borger, L., et al. (2015). Functional diversity enhances the resistance of ecosystem multifunctionality to aridity in Mediterranean drylands. *New Phytol.* 206, 660–671. doi: 10.1111/nph.13268

Webb, C. O., Ackerly, D. D., McPeek, M. A., and Donoghue, M. J. (2002). Phylogenies and community ecology. *Annu. Rev. Ecol. Syst.* 33, 475–505. doi: 10.1146/annurev.ecolysis.33.010802.150448

Weih, M., Bonosi, L., Ghelardini, L., and Ronnberg-Wastljung, A. C. (2011). Optimizing nitrogen economy under drought: increased leaf nitrogen is an acclimation to water stress in willow (Salix spp.). *Ann. Bot.* 108, 1347–1353. doi: 10.1093/aob/mcr227

Wright, I. J., Reich, P. B., Cornelissen, J. H. C., Falster, D. S., Garnier, E., Hikosaka, K., et al. (2005). Assessing the generality of global leaf trait relationships. *New Phytol.* 166, 485–496. doi: 10.1111/j.1469-8137.2005.01349.x

Wright, I. J., Reich, P. B., Westoby, M., Ackerly, D. D., Baruch, Z., Bongers, F., et al. (2004). The worldwide leaf economics spectrum. *Nature* 428, 821–827. doi: 10.1038/nature02403

Wu, J., Zhang, Q., Li, A., and Liang, C. (2015). Historical landscape dynamics of Inner Mongolia: patterns, drivers, and impacts. *Landsc. Ecol.* 30, 1579–1598. doi: 10.1007/s10980-015-0209-1

Yuan, Z. Y., Li, L. H., Han, X. G., Chen, S. P., Wang, Z. W., Chen, Q. S., et al. (2006). Nitrogen response efficiency increased monotonically with decreasing soil resource availability: a case study from a semiarid grassland in northern China. *Oecologia* 148, 564–572. doi: 10.1007/s00442-006-0409-0

Zhang, H., Li, W., Adams, H. D., Wang, A., Wu, J., Jin, C., et al. (2018). Responses of woody plant functional traits to nitrogen addition: a meta-analysis of leaf economics, gas exchange, and hydraulic traits. *Front. Plant Sci.* 9:683. doi: 10.3389/fpls.2018.00683

Zhang, L. X., Ma, D., Xu, J. S., Quan, J. X., Dang, H., Chai, Y. F., et al. (2017). Economic trade-offs of hydrophytes and neighbouring terrestrial herbaceous plants based on plant functional traits. *Basic Appl. Ecol.* 22, 11–19. doi: 10.1016/j.baae.2017.06.004

Zhu, Y., Kang, H., Xie, Q., Wang, Z., Yin, S., and Liu, C. (2012). Pattern of leaf vein density and climate relationship of Quercus variabilis populations remains unchanged with environmental changes. *Trees* 26, 597–607. doi: 10.1007/s00468-011-0624-0

Conflict of Interest Statement: The authors declare that the research was conducted in the absence of any commercial or financial relationships that could be construed as a potential conflict of interest.

frontiers in Plant Science

ORIGINAL RESEARCH
published: 11 July 2019
doi: 10.3389/fpls.2019.00903

Effects of Dark Septate Endophytes on the Performance of *Hedysarum scoparium* Under Water Deficit Stress

Xia Li[1], Xue-Li He[1], Yong Zhou[2], Yi-Ting Hou[1] and Yi-Ling Zuo[1]*

[1] College of Life Science, Hebei University, Baoding, China, [2] College of Landscape Architecture and Tourism, Hebei Agricultural University, Baoding, China

Hedysarum scoparium, a species characterized by rapid growth and high drought resistance, has been used widely for vegetative restoration of arid regions in Northwest China that are prone to desertification. Desert soil is typically deficient in available water and the alleviation of drought stress to host plants by endophytes could be an efficient strategy to increase the success of desert restoration. With the objective to seek more beneficial symbionts that can be used in the revegetation strategies, we addressed the question whether *H. scoparium* can benefit from inoculation by dark septate endophytes (DSEs) isolated from other desert plants. We investigated the influences of four non-host DSE strains (*Phialophora* sp., *Knufia* sp., *Leptosphaeria* sp., and *Embellisia chlamydospora*) isolated from other desert plants on the performance of *H. scoparium* under different soil water conditions. Differences in plant performance, such as plant growth, antioxidant enzyme activities, carbon, nitrogen, and phosphorous concentration under all the treatments, were examined. Four DSE strains could colonize the roots of *H. scoparium* successfully, and they established a positive symbiosis with the host plants depending on DSE species and water availability. The greatest benefits of DSE inoculation occurred in water stress treatment. Specifically, *Phialophora* sp. and *Leptosphaeria* sp. improved the root biomass, total biomass, nutrient concentration, and antioxidant enzyme activities of host plants under water deficit conditions. These data contribute to the understanding of the ecological function of DSE fungi in drylands.

Keywords: *Hedysarum scoparium*, dark septate endophytes, water deficit stress, non-host endophytes, inoculation

OPEN ACCESS

Edited by:
Zhiyou Yuan,
Northwest A&F University, China

Reviewed by:
Juliana S. Medeiros,
Holden Arboretum, United States
Raffaella Balestrini,
Institute for Sustainable Plant Protection (IPSP-CNR), Italy

****Correspondence:***
Xue-Li He
xlh3615@126.com

Specialty section:
This article was submitted to Plant Abiotic Stress, a section of the journal Frontiers in Plant Science

Received: *30 October 2018*
Accepted: *26 June 2019*
Published: *11 July 2019*

Citation:
Li X, He X-L, Zhou Y, Hou Y-T and Zuo Y-L (2019) Effects of Dark Septate Endophytes on the Performance of Hedysarum scoparium Under Water Deficit Stress. Front. Plant Sci. 10:903. doi: 10.3389/fpls.2019.00903

INTRODUCTION

Approximately 27% of the land area in China is exposed to desertification, causing critical ecological and environmental problems, especially in Northwest China (Tang et al., 2016). The Chinese government has implemented a variety of solutions, including afforestation projects, to reduce the effect of desertification (Su et al., 2007; Fan et al., 2016). Over the past few decades,

restoration of deserts using xerophyte shrubs is viewed as a common and effective method in many arid regions (Zhu and Chen, 1994; Wang et al., 2012; Deng et al., 2015). These plants have evolved various mechanisms, including altered morphological and physiological properties, to cope with drought stress (Deng et al., 2015; Li et al., 2017). Plants in natural habitats often harbor ubiquitous fungal endophytes, some of which are drought-tolerant and can stimulate plant growth in arid ecosystems (Ren et al., 2011; González-Teuber et al., 2018; Xie et al., 2018). Mitigating drought stress in host plants by endophytes may be an efficient strategy to improve the restoration rate of desert soils, which are typically deficient in available water (Gong et al., 2015; Shi et al., 2015; González-Teuber et al., 2018).

Most desert plants associate with a wide diversity of root endophytic fungi, including dark septate endophytes (DSEs) (Barrow, 2003; Porras-Alfaro et al., 2008; González-Teuber et al., 2017). These endophytes are characterized by melanized septate hyphae and microsclerotia and are found in the roots of more than 600 plant species (Jumpponen and Trappe, 1998). DSE are abundant root colonists especially in plants growing under extreme conditions such as arid environments (Jumpponen and Trappe, 1998; Barrow and Osuna, 2002). Many researchers have investigated and isolated a variety of DSE from grasses, shrubs, and trees in arid areas (Lugo et al., 2009, 2015; Knapp et al., 2012, 2015; Li et al., 2015, 2018; Xie et al., 2017). For instance, Lugo et al. (2015) investigated DSE in 42 plants from an arid region in Argentina and showed that DSE were frequently present in the roots. In Northwest China, DSE were also observed and identified in the roots of multiple desert shrubs, such as *Ammopiptanthus mongolicus*, *Hedysarum scoparium*, and *Gymnocarpos przewalskii* (Li et al., 2015, 2018; Xie et al., 2017). For example, in our previous survey conducted in seven arid and semi-arid locations in Northwest China, we showed that *H. scoparium* was highly colonized by DSE and we isolated nine DSE species from their roots (Xie et al., 2017). However, our understanding of DSE functions in relation to plants is still limited (Barrow, 2003).

Although not all DSE–plant relationships are beneficial, there is a strong evidence to suggest that DSE may positively influence plant resistance to drought by increasing plant growth, water and nutrient absorption, and/or facilitating plant resistance to oxidation stress (Perez-Naranjo, 2009; Santos et al., 2017). In field experiments, Barrow (2003) investigated the DSE of native grasses in arid southwestern United States rangelands. The author proposed that DSE may form a continuous integrated network that enhances nutrient and water transport in roots. DSE are readily isolated and cultured *in vitro*, which has facilitated the studies on the effects of DSE on host plants under water stress in controlled culture conditions. In pot experiments, desert plants *Agropyron cristatum* and *Psathyrostachys juncea* inoculated with DSE developed a higher shoot biomass and carbon content compared with non-inoculated plants under drought conditions (Perez-Naranjo, 2009). Similarly, Santos et al. (2017) conducted an inoculation experiment to study the influence of DSE isolates on rice under water deficit induced with polyethylene glycol 6000. Their results showed that DSE increase the growth and decrease the oxidative stress in rice plants. However, this positive effect occurred only in specific water stress conditions.

Hedysarum scoparium, a species characterized with rapid growth and high drought resistance, is a pioneer desert shrub that has been widely used for prevention of desertification and vegetative restoration in arid and semiarid regions of China (Hu et al., 2009). In a pot experiment conducted in our study, DSE isolated from healthy roots of *H. scoparium*, colonized the host roots and increased the shoot and root biomass of *H. scoparium* plants (**Supplementary Figure 1**). With the objective to seek more beneficial symbionts that can be used in revegetation strategies, we investigated whether *H. scoparium* can benefit from DSE isolated from other desert plants. Four DSE isolated from the roots of *G. przewalskii*, a species with similar growth habit and ecological distribution to that of *H. scoparium*, were selected for the inoculation experiment. These fungi colonized the roots of other desert plants with no apparent disease symptoms and enhanced plant growth under drought conditions (Li et al., 2018). In this study, we aimed to evaluate the effects of non-host DSE inoculation on *H. scoparium* plants growing in drought sandy soil under greenhouse conditions. We focused on plant growth, nutrient content, and activity of antioxidant enzymes to address the following questions: (1) Do DSE from other plants colonize the roots of *H. scoparium* under well-watered and water deficit conditions? (2) If yes, can these non-host DSE improve the growth and physiological performance of *H. scoparium* plants? (3) Does water availability affect the symbiosis-dependent benefits? (4) How non-host DSE help *H. scoparium* plants to overcome water deficit stress?

MATERIALS AND METHODS

Fungal Isolates and Plant Materials

Four DSE fungi isolated from the roots of *G. przewalskii*, which grows naturally in extreme arid deserts of Northwest China, were used in this experiment. Their species identification was confirmed previously through internal transcribed spacer (ITS) phylogeny (Li et al., 2018). All the fungal isolates belonged to different species and they included: *Phialophora* sp., *Knufia* sp., *Leptosphaeria* sp., and *Embellisia chlamydospora*. These fungi are deposited in the culture collection of the Laboratory of Plant Ecology, Hebei University, China, and their ITS sequences are available from GenBank under accession numbers MF036001 for *Phialophora* sp., MF036003 for *Knufia* sp., MF036004 for *Leptosphaeria* sp., and MF036005 for *E. chlamydospora*.

Hedysarum scoparium was chosen as a host plant in this study mostly for its important role in vegetation restoration and known high DSE colonization frequency (Xie et al., 2017). The seeds of *H. scoparium* were collected from natural populations in Gansu Province, Northwest China, and stored at 4°C.

Experimental Design

The experiment was conducted in a growth chamber in a completely randomized factorial design (5 inoculation treatments × 2 water treatments) with five replicates. The inoculation treatments included inoculation with *Phialophora*

sp., *Knufia* sp., *Leptosphaeria* sp., and *E. chlamydospora* and a non-inoculated control. The water treatments were well-watered and water deficit stress. A total of 50 pots were prepared.

The seeds of *H. scoparium* were surface-sterilized by dipping in 70% ethanol for 3 min and then in 2.5% sodium hypochlorite for 10 min with agitation. The sterilized seeds were gently washed by sterile water several times and then aseptically planted onto water agar medium (containing 10 g/L agar) in Petri dishes for germination at 27°C. Following pregermination, each seedling was transferred into sterile pot (8 cm diameter, 24 cm height) containing 500 g sand collected from the natural habitats of *H. scoparium* and autoclaved for 120 min at 121°C. The basic physicochemical characteristics of the sand were as follows: organic matter 23.17 mg/g, available nitrogen 21.63 mg/kg, and available phosphorus 1.53 mg/kg. One month later, half of the seedlings were maintained under well-watered conditions throughout the entire experiment (70% field water capacity), and the other half were exposed to water deficit stress (30% field water capacity). Water loss was daily supplemented with sterile distilled water to keep the desired field capacity by regular weighing. The water content for water deficit treatment was chosen according to the median value in the natural habitat of *H. scoparium* in Northwest China (Xie, 2017).

Fungal inocula were prepared by aseptically growing DSE isolates in Petri dishes with potato dextrose agar culture medium. For DSE inoculation, two 5 mm plugs excised from an edge of an actively growing colony on culture medium were inoculated at a 1 cm range close to the roots of *H. scoparium* seedlings. The non-inoculated controls were inoculated with plugs excised from the sterile medium without fungus. All the inoculation processes were carried out on a clean bench, and all the pots were kept in a growth chamber with a 14 h/10 h photoperiod, temperature of 27°C/22°C (day/night), and 60% mean air relative humidity. The duration of the stress experiment was 4 months.

Harvest of *Hedysarum scoparium* Seedlings

At the end of the experiment, the shoots and roots from each plant were separately harvested, and the roots were gently washed with tap water to remove the sand. Subsamples of fresh roots and shoots were set aside for assessing DSE colonization status and antioxidant enzyme activity, respectively, as described below. The remaining part of shoots and roots were weighed before drying in an oven at 70°C for 48 h and the water content was measured. The biomass production of plants was the sum of the dry weights of these two parts. After that the dried shoot and root materials were ground into a powder to measure the concentrations of carbon (C), nitrogen (N), and phosphorus (P).

Microscopic Observation of Root Colonization

Root colonization by DSE isolates was evaluated using the method described by Phillips and Hayman (1970). The sampled roots were cleared with 10% KOH in a water bath at 100°C for 60 min and then stained with 0.5% (w/v) acid fuchsin at 90°C for 20 min. Overall, 20 randomly selected 0.5 cm long root segments per sample were placed on slides and observed under an optical microscope.

Determination of Antioxidant Enzyme Activity

To determine the activity of different antioxidant enzymes, fresh leaf samples from each plant were homogenized in 5 mL of 50 mM potassium phosphate buffer (pH 7.8), which contained chilled 0.2 mM EDTA and 2% (w/v) polyvinylpyrrolidone kept in ice bath. Prechilled mortar and pestle were used for grinding. The homogenate was centrifuged at 15,294 × *g* and 4°C for 30 min. The supernatant was decanted and used for analysis of enzymes.

The superoxide dismutase (SOD) activity was determined using the photochemical method described by Elavarthi and Martin (2010) by recording the decrease in the absorbance of nitro blue tetrazolium complex due to its reduction by the enzyme. One unit of SOD was equivalent to the quantity of enzyme needed to inhibit the reduction rate of NBT by 50% at a wavelength of 560 nm. The catalase (CAT) activity was determined by measuring the consumption of H_2O_2 at 240 nm wavelength for 1 min. The reaction mixture consisted of 25 mM potassium phosphate buffer (pH 7.0), 10 mM H_2O_2, and enzyme extract (Cakmak and Marschner, 1992).

Carbon, Nitrogen, and Phosphorus Concentrations

The C and N concentrations in the shoots and roots were directly determined using the dry combustion method with an elemental analyzer (Vario EL/micro cube; Elementar, Hanau, Germany). For determination of P concentrations, dried ground shoot and root samples were digested in HNO_3, followed by a microwave-accelerated reaction in a Microwave-Accelerated Digestion System (MARS; CEM, Corp., Matthews, NC, United States). The P concentrations were measured by the molybdenum-antimony colorimetric method (Bao, 2000).

Statistical Analysis

All statistical analyses were performed with SPSS software (Version 21; SPSS, Chicago, IL, United States). A two-way analysis of variance was used to analyze the effects of DSE inoculation, water treatment, and their interaction on plant biomass, leaf antioxidant enzyme activity, and element concentrations in the roots and shoots. All data were tested for normality and homogeneity of variance before statistical analyses. The differences between the means among different treatments were compared using Duncan's multiple-range tests at $P < 0.05$.

RESULTS

DSE Root Colonization

After harvesting, no DSE structures were detected in the roots of control plants regardless of water treatment, while the presence of DSE hyphae and microsclerotia was confirmed in stained root segments of inoculated plants (**Supplementary Figure 2**).

TABLE 1 | Analysis of variance for the effects of DSE inoculation and water stress treatment on biomass production of *Hedysarum scoparium*.

	Shoot biomass (g)		Root biomass (g)		Total biomass (g)	
	F	***P***	***F***	***P***	***F***	***P***
DSE	11.6	**<0.001**	18.0	**<0.001**	17.2	**<0.001**
Water stress	406.7	**<0.001**	300.6	**<0.001**	420.7	**<0.001**
DSE × Water stress	1.8	0.156	3.8	**0.011**	3.2	**0.023**

Significant P-values are in bold.

Plant Biomass Production

The shoot biomass of *H. scoparium* was affected significantly by the DSE inoculation regardless of the water regime (**Table 1**). Specifically, the inoculation of *Phialophora* sp. and *Leptosphaeria* sp. resulted in significant increases in shoot biomass (by 9.0 and 17.9%, respectively) compared to control plants (**Figure 1**).

The interactions of DSE inoculation and water treatment were significant for both the root and total biomass of *H. scoparium* seedlings (**Table 1**). Under well-watered conditions, inoculation with *Leptosphaeria* sp. led to a significantly greater root and total biomass (40.0 and 35.1%, respectively) compared with those of the control plants, whereas the inoculation with *E. chlamydospora* resulted in a 14.8 and 11.7% decrease in both parameters, respectively (**Figure 1**). Under water stress conditions, *Phialophora* sp. and *Leptosphaeria* sp. inoculations caused a significantly greater root (27.5 and 40.0%) and total biomass (25.1 and 35.1%) compared with those observed in control plants, respectively. There was no significant difference in the root and total biomass production among plants inoculated with *Knufia* sp. and *E. chlamydospora* and the control (**Figure 1**).

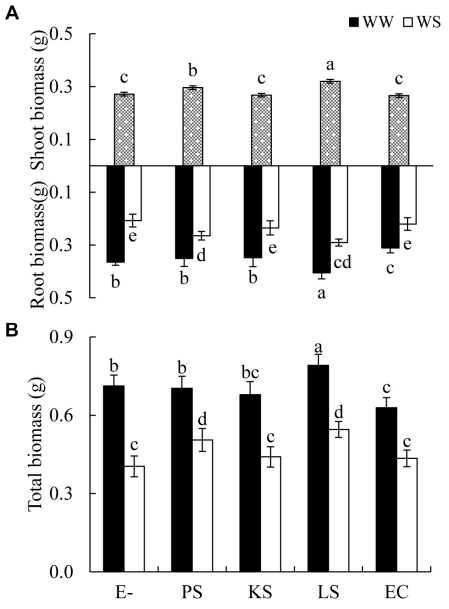

FIGURE 1 | Effects of dark septate endophyte (DSE) inoculation and water treatment on the biomass production of *Hedysarum scoparium*. **(A)** Shoot and root biomass of *Hedysarum scoparium*. **(B)** Total biomass of *Hedysarum scoparium*. The error bars represent the standard error (SE). Different letters above the error bars indicate significant difference at $P < 0.05$ by Duncan's multiple-range tests. Since DSE × water treatment interactions were not significant for shoot biomass, means for the main factor (DSE) were presented. E– indicates non-inoculated plants. PS, KS, LS, and EC indicate plants inoculated with *Phialophora* sp., *Knufia* sp., *Leptosphaeria* sp., and *Embellisia chlamydospora*, respectively. WW and WS indicate well-watered and water stress treatment.

Antioxidant Enzyme Activities in Leaves of *Hedysarum scoparium*

The interaction between DSE inoculation and water treatment showed significant effects on the antioxidant enzyme activities in leaves of *H. scoparium* (**Table 2**). In general, all the tested DSE caused remarkable increases in the activities of SOD and CAT under water stress conditions, which was closely related to the drought tolerance of *H. scoparium* (**Figure 2**). Plants inoculated with *Phialophora* sp., *Knufia* sp. and *Leptosphaeria* sp. showed significantly higher values of SOD (19.1, 26.4, and 36.4%) and CAT (43.2, 27.2, and 31.1%, respectively) activities compared with control plants under water stress conditions. However, under well-watered conditions, there were no significant differences in either SOD or CAT activity between DSE inoculated plants and control plants. *E. chlamydospora* inoculation had no significant effects on host plants compared with control plants under both water regimes (**Figure 2**).

Element Concentration in Plant Tissues

There was a significant interaction between the DSE inoculation and water treatment on the shoot C concentration of *H. scoparium* (**Table 2**). The shoot C concentration was significantly lower (2.5%) in *E. chlamydospora*-inoculated *H. scoparium* plants than in the control plants under well-watered conditions, but there was no significant effect of DSE inoculation on the shoot C content in host plants in all the other treatments (**Figure 3A**). The N concentration in the shoots of *H. scoparium* was affected significantly by the DSE inoculation, water treatment, and their interaction (**Table 2**). Under water stress conditions, inoculation with *Phialophora* sp. and *Leptosphaeria* sp. resulted in a significant increase in the N concentration in the shoots of *H. scoparium* by 22.9 and 20.2%, respectively, when compared with control plants. Under well-watered conditions, *Leptosphaeria* sp. induced a significant increase in the shoot N concentration (12.3%), while *E. chlamydospora* showed an opposite effect, with about 87.7% of control plants (**Figure 3B**). DSE inoculation did not affect the root C, N, and P concentrations and shoot P concentration of *H. scoparium* seedlings under all the treatments (**Figure 3** and **Table 2**).

DISCUSSION

As important root endophytes, DSE have been reported to have positive ecological roles in plant growth and nutrient uptake (Wu et al., 2010; Newsham, 2011; Surono and Narisawa, 2017; Vergara et al., 2018). They also provide increased plant resistance

TABLE 2 | Analysis of variance for the effects of dark septate endophyte (DSE) inoculation and water stress treatment on the antioxidant enzyme activities and element concentration of *Hedysarum scoparium*.

	SOD (U/g·FW·h)		CAT (U/g·FW·min)		Shoot C (mg/g)		Root C (mg/g)		Shoot N (mg/g)		Root N (mg/g)		Shoot P (mg/g)		Root P (mg/g)	
	F	*P*	*F*	*P*	*F*	*P*	*F*	*P*	*F*	*P*	*F*	*P*	*F*	*P*	*F*	*P*
DSE	2.4	0.064	2.9	**0.033**	2.3	0.071	0.4	0.775	6.4	**<0.001**	1.7	0.167	2.6	0.052	2.4	0.070
Water stress	137.6	**<0.001**	101.2	**<0.001**	127.8	**<0.001**	14.4	**<0.001**	152.6	**<0.001**	29.7	**<0.001**	10.2	**0.003**	11.9	**0.001**
DSE × Water stress	4.6	**0.004**	2.7	**0.046**	3.1	**0.026**	0.4	0.798	3.4	**0.018**	2.2	0.091	0.3	0.856	0.3	0.905

C, carbon; N, nitrogen; P, phosphorus; SOD, superoxide dismutase; CAT, catalase; FW, fresh weight. Significant P-values are in bold.

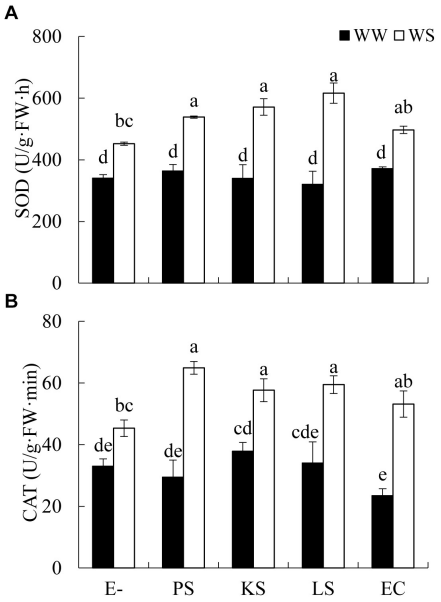

FIGURE 2 | Effects of DSE inoculation and water treatment on the antioxidant enzyme activities in leaves of *Hedysarum scoparium*. **(A)** Superoxide dismutase (SOD) in leaves of *Hedysarum scoparium*. **(B)** Catalase (CAT) in leaves of *Hedysarum scoparium*. The error bars represent the SE. Different letters above the error bars indicate significant difference at $P < 0.05$ by Duncan's multiple-range tests. E– indicates non-inoculated plants. PS, KS, LS, and EC indicate plants inoculated with *Phialophora* sp., *Knufia* sp., *Leptosphaeria* sp., and *Embellisia chlamydospora*, respectively. WW and WS indicate well-watered and water stress treatment.

to a wide range of environmental stressors (Andrade-Linares et al., 2011; Likar and Regvar, 2013; Su et al., 2013; Berthelot et al., 2017; Santos et al., 2017; Zhang et al., 2017; Jin et al., 2018). However, little is known about the relationship of non-host DSE and host plants, especially when water availability is considered (Zhang et al., 2017). In the studies using crops and plants growing in heavy metal-contaminated soils, DSE fungi, which have been considered non-host colonizers, showed the potential to improve plant growth (Li et al., 2011; Khastini et al., 2012; Berthelot et al., 2016, 2017; Wang et al., 2016). For example, *Gaeumannomyces cylindrosporus* isolated from plants naturally growing in an ancient Pb-Zn slag heap were reported to enhance the growth of maize under Cd stress (Ban et al., 2017). Similarly, the four DSE in this study isolated from *G. przewalskii* were able to colonize the roots of *H. scoparium* plants under both well-watered and water deficit conditions. Similarly, Zhang et al. (2017) reported that *Exophiala pisciphila* isolated from maize could colonize the roots of *Sorghum bicolor*. Our results indicated that DSE isolated from desert plants may be used in other plants. Moreover, they exhibited positive effects on shoot C and N content and biomass production of *H. scoparium* plants; however, these effects were strain-dependent. This observation corroborates previous reports that state that DSE fungal species may be one of the factors that influence the symbiotic relationship (Wilcox and Wang, 1987; Mandyam and Jumpponen, 2005; Newsham, 2011). In addition,

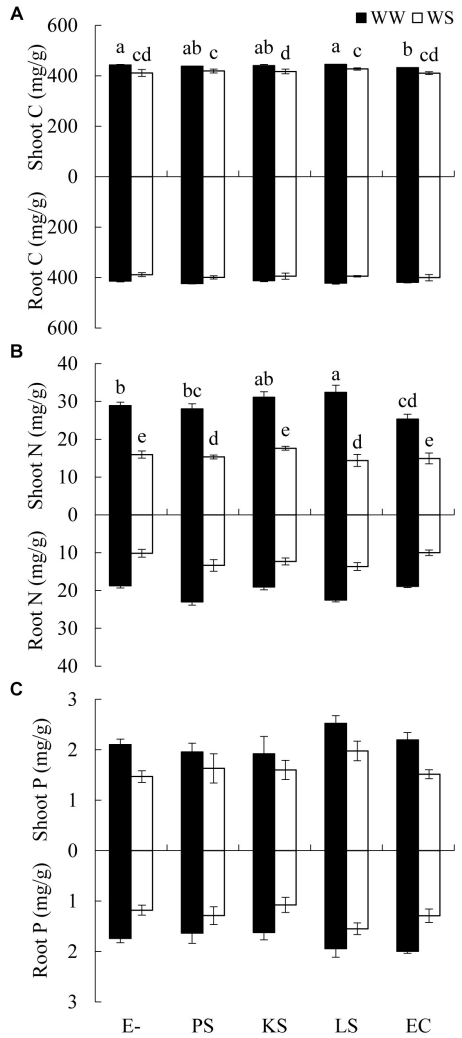

FIGURE 3 | Effects of DSE inoculation and water treatment on the elemental concentration of *Hedysarum scoparium*. **(A)** Shoot and root carbon concentration (C) of *Hedysarum scoparium*. **(B)** Shoot and root nitrogen concentration (N) of *Hedysarum scoparium*. **(C)** Shoot and root phosphorus concentration (P) of *Hedysarum scoparium*. The error bars represent the SE. Different letters above the error bars indicate significant difference at $P < 0.05$ by Duncan's multiple-range tests. The estimated means were presented when interactions were not significant. E– indicates non-inoculated plants. PS, KS, LS, and EC indicate plants inoculated with *Phialophora* sp., *Knufia* sp., *Leptosphaeria* sp., and *Embellisia chlamydospora*, respectively. WW and WS indicate well-watered and water stress treatment.

both DSE strains isolated from *H. scoparium* promoted the shoot and root growth of *H. scoparium* plants under well-watered condition in our previous study (**Supplementary Figure 1**). This indicates that the outcome of DSE – *H. scoparium* interactions may also depend on the host origin of the DSE involved. Therefore, choosing DSE strains that are most beneficial to the plants during the restoration of desert vegetation is vital.

The present study further demonstrated that the interaction between DSE and *H. scoparium* depended on water availability. Under water deficit conditions, no adverse effects were found in all the plants inoculated with DSE. The biomass production and shoot C and N content of plants inoculated with *Phialophora* sp. and *Leptosphaeria* sp. was increased compared with that of the control, whereas the inoculation of *H. scoparium* plants with *E. chlamydospora* negatively affected plant growth under well-watered conditions, but caused no significant decline in plant growth when exposed to water stress. This indicates that the interaction between DSE and *H. scoparium* becomes positive under water stress. Our results agree with previous studies in other crops, which have shown that the benefits of plant–endophyte associations seem to be stronger under soil water stress conditions (Zhang et al., 2017). For *H. scoparium* plants, benefits of symbiosis under water stress may be advantageous to the plant growth in their natural drought habitats.

The ability of DSE fungi to promote plant growth under water stress conditions may be related to the increased C and N absorption, as well as to the enhanced activities of antioxidant enzymes. Vergara et al. (2018) have reported that increased N absorption by tomato plants was in response to inoculation with DSE isolates—inoculated plants exhibited higher dry weight than non-inoculated plants when supplied with organic N. Similarly, in our study, *Phialophora* sp. and *Leptosphaeria* sp. may have facilitated the absorption of C and N in the shoots of *H. scoparium*. This might be due to the ability of DSE fungi to mineralize organic compounds containing C, N, and P, thereby making them available to plants (Della Monica et al., 2015; Surono and Narisawa, 2017). For example, *Phialocephala fortinii*, a plant growth promoter in many studies, was reported to have the ability to degrade polymeric forms of C, N, and P such as cellulose, starch and protein (Caldwell et al., 2000; Surono and Narisawa, 2017). The increased SOD and CAT activity is another possible mechanism of increased plant growth. Water stress usually exerts negative effects on organisms and causes cellular oxidative damage (Bartels and Sunkar, 2005). SOD and CAT are the primary enzymes involved in the antioxidant system of plants (Khan et al., 2018; Saleem et al., 2018). In the present study, plants inoculated with *Phialophora* sp., *Knufia* sp., and *Leptosphaeria* sp. contained significantly higher concentrations of SOD and CAT compared with control plants under water deficit conditions. These findings can be related with the work by Santos et al. (2017), who found that DSE increased the tolerance of rice plants to water stress through altered antioxidant enzyme activity. However, the mechanisms leading to an increase in the growth of plants inoculated with DSE fungi warrants further research.

CONCLUSION

We found that non-host DSE could colonize the roots of *H. scoparium* and benefit the plant growth, through combined mechanisms of increased nutrient absorption and enhanced antioxidant systems, under water deficit conditions. Our results complement previous insight that endophytes can promote drought resistance in plants and highlight the importance of using DSE in desert plants in water-stressed conditions (Kivlin et al., 2013; Shi et al., 2015; Zhang et al., 2017;

González-Teuber et al., 2018; Xie et al., 2018). As *H. scoparium* plays important roles in vegetative restoration, the DSE–*H. scoparium* association has the potential for further testing in the field to determine its ability to suppress desertification in arid regions of Northwest China.

AUTHOR CONTRIBUTIONS

XL and X-LH conceived and designed the experiments and wrote the manuscript. XL, YZ, Y-TH, and Y-LZ performed the experiments. XL and YZ analyzed the data.

FUNDING

This study was financially supported by the National Natural Science Foundation of China (Project Nos. 31470533, 31770561, and 31800345).

SUPPLEMENTARY MATERIAL

The Supplementary Material for this article can be found online at: https://www.frontiersin.org/articles/10.3389/fpls.2019.00903/full#supplementary-material

REFERENCES

Andrade-Linares, D. R., Grosch, R., Restrepo, S., Krumbein, A., and Franken, P. (2011). Effects of dark septate endophytes on tomato plant performance. *Mycorrhiza* 21, 413–422. doi: 10.1007/s00572-010-0351-1

Ban, Y., Xu, Z., Yang, Y., Zhang, H., Chen, H., and Tang, M. (2017). Effect of dark septate endophytic fungus *Gaeumannomyces cylindrosporus* on plant growth, photosynthesis and Pb tolerance of maize (*Zea mays* L.). *Pedosphere* 27, 283–292. doi: 10.1016/s1002-0160(17)60316-3

Bao, S. D. (2000). *Agrochemical Analysis of Soil*. Beijing: Chinese Agricultural Press.

Barrow, J. R. (2003). Atypical morphology of dark septate fungal root endophytes of *Bouteloua* in arid southwestern USA rangelands. *Mycorrhiza* 13, 239–247. doi: 10.1007/s00572-003-0222-0

Barrow, J. R., and Osuna, P. (2002). Phosphorus solubilization and uptake by dark septate fungi in fourwing saltbush, *Atriplex canescens* (Pursh) Nutt. *J. Arid. Environ.* 51, 449–459. doi: 10.1006/jare.2001.0925

Bartels, D., and Sunkar, R. (2005). Drought and salt tolerance in plants. *Crit. Rev. Plant Sci.* 24, 23–58. doi: 10.1080/07352680590910410

Berthelot, C., Blaudez, D., and Leyval, C. (2017). Differential growth promotion of poplar and birch inoculated with three dark septate endophytes in two trace element-contaminated soils. *Int. J. Phytoremediat.* 19, 1118–1125. doi: 10.1080/15226514.2017.1328392

Berthelot, C., Leyval, C., Foulon, J., Chalot, M., and Blaudez, D. (2016). Plant growth promotion, metabolite production and metal tolerance of dark septate endophytes isolated from metal-polluted poplar phytomanagement sites. *FEMS Microbiol. Ecol.* 92:fiw144. doi: 10.1093/femsec/fiw144

Cakmak, I., and Marschner, H. (1992). Magnesium deficiency and high light Intensity enhance activities of superoxide dismutase, ascorbate peroxidase, and glutathione reductase in bean leaves. *Plant Physiol.* 98, 1222–1227. doi: 10.1104/pp.98.4.1222

Caldwell, B. A., Jumpponen, A., and Trappe, J. M. (2000). Utilization of major detrital substrates by dark-septate, root endophytes. *Mycologia* 92, 230–232. doi: 10.2307/3761555

Della Monica, I. F., Saparrat, M. C. N., Godeas, A. M., and Scervino, J. M. (2015). The co-existence between DSE and AMF symbionts affects plant P pools through P mineralization and solubilization processes. *Fungal Ecol.* 17, 10–17. doi: 10.1016/j.funeco.2015.04.004

Deng, J., Ding, G., Gao, G., Wu, B., Zhang, Y., Qin, S., et al. (2015). The sap flow dynamics and response of *Hedysarum scoparium* to environmental factors in semiarid northwestern China. *PLoS One* 10:e0131683. doi: 10.1371/journal.pone.0131683

Elavarthi, S., and Martin, B. (2010). "Spectrophotometric assays for antioxidant enzymes in plants," in *Plant Stress Tolerance: Methods and Protocols*, ed. R. Sunkar (Totowa, NJ: Humana Press), 273–280.

Fan, B., Zhang, A., Yang, Y., Ma, Q., Li, X., and Zhao, C. (2016). Long-term effects of xerophytic shrub *Haloxylon ammodendron* plantations on soil properties and vegetation dynamics in Northwest China. *PLoS One* 11:e0168000. doi: 10.1371/journal.pone.0168000

Gong, C., Wang, J., Hu, C., Wang, J., Ning, P., and Bai, J. (2015). Interactive response of photosynthetic characteristics in *Haloxylon ammodendron* and *Hedysarum scoparium* exposed to soil water and air vapor pressure deficits. *J. Environ. Sci.* 34, 184–196. doi: 10.1016/j.jes.2015.03.012

González-Teuber, M., Urzúa, A., Plaza, P., and Bascuñán-Godoy, L. (2018). Effects of root endophytic fungi on response of *Chenopodium quinoa* to drought stress. *Plant Ecol.* 219, 231–240. doi: 10.1007/s11258-017-0791-1

González-Teuber, M., Vilo, C., and Bascuñángodoy, L. (2017). Molecular characterization of endophytic fungi associated with the roots of *Chenopodium quinoa* inhabiting the Atacama Desert. Chile. *Genomics Data* 11, 109–112. doi: 10.1016/j.gdata.2016.12.015

Hu, X. W., Wang, Y. R., and Wu, Y. P. (2009). Effects of the pericarp on imbibition, seed germination, and seedling establishment in seeds of *Hedysarum scoparium* Fisch. et Mey. *Ecol. Res.* 24, 559–564. doi: 10.1007/s11284-008-0524-y

Jin, H. Q., Liu, H. B., Xie, Y. Y., Zhang, Y. G., Xu, Q. Q., Mao, L. J., et al. (2018). Effect of the dark septate endophytic fungus *Acrocalymma vagum* on heavy metal content in tobacco leaves. *Symbiosis* 74, 89–95. doi: 10.1007/s13199-017-0485-4

Jumpponen, A., and Trappe, J. M. (1998). Dark septate endophytes: a review of facultative biotrophic root-colonizing fungi. *New Phytol.* 140, 295–310. doi: 10.1046/j.1469-8137.1998.00265.x

Khan, M. M., Islam, E., Irem, S., Akhtar, K., Ashraf, M. Y., Iqbal, J., et al. (2018). Pb-induced phytotoxicity in para grass (*Brachiaria mutica*) and castorbean (*Ricinus communis* L.) antioxidant and ultrastructural studies. *Chemosphere* 200, 257–265. doi: 10.1016/j.chemosphere.2018.02.101

Khastini, R. O., Ohta, H., and Narisawa, K. (2012). The role of a dark septate endophytic fungus, Veronaeopsis simplex Y34, in Fusarium disease suppression in Chinese cabbage. *J. Microbiol.* 50, 618–624. doi: 10.1007/s12275-012-2105-6

Kivlin, S. N., Emery, S. M., and Rudgers, J. A. (2013). Fungal symbionts alter plant responses to global change. *Am. J. Bot.* 100, 1445–1457. doi: 10.3732/ajb.1200558

Knapp, D. G., Kovács, G. M., Zajta, E., Groenewald, J. Z., and Crous, P. W. (2015). Dark septate endophytic pleosporalean genera from semiarid areas. *Persoonia* 35, 87–100. doi: 10.3767/003158515X687669

Knapp, D. G., Pintye, A., and Kovács, G. M. (2012). The dark side is not fastidious–dark septate endophytic fungi of native and invasive plants of semiarid sandy areas. *PLoS One* 7:e32570. doi: 10.1371/journal.pone.0032570

Li, B., He, X., He, C., Chen, Y., and Wang, X. (2015). Spatial dynamics of dark septate endophytes and soil factors in the rhizosphere of *Ammopiptanthus mongolicus* in inner mongolia. China. *Symbiosis* 65, 75–84. doi: 10.1007/s13199-015-0322-6

Li, L., Chen, X., Shi, L., Wang, C., Fu, B., Qiu, T., et al. (2017). A proteome translocation response to complex desert stress environments in perennial *Phragmites* sympatric ecotypes with contrasting water availability. *Front. Plant Sci.* 8:511. doi: 10.3389/fpls.2017.00511

Li, T., Liu, M. J., Zhang, X. T., Zhang, H. B., Sha, T., and Zhao, Z. W. (2011). Improved tolerance of maize (*Zea mays* L.) to heavy metals by colonization of a dark septate endophyte (DSE) Exophiala pisciphila. *Sci. Total Environ.* 409, 1069–1074. doi: 10.1016/j.scitotenv.2010.12.012

Li, X., He, X., Hou, L., Ren, Y., Wang, S., and Su, F. (2018). Dark septate endophytes isolated from a xerophyte plant promote the growth of *Ammopiptanthus mongolicus* under drought condition. *Sci. Rep.* 8:7896. doi: 10.1038/s41598-018-26183-0

Likar, M., and Regvar, M. (2013). Isolates of dark septate endophytes reduce metal uptake and improve physiology of *Salix caprea* L. *Plant Soil* 370, 593–604. doi: 10.1007/s11104-013-1656-6

Lugo, M. A., Molina, M. G., and Crespo, E. M. (2009). Arbuscular mycorrhizas and dark septate endophytes in bromeliads from South American arid environment. *Symbiosis* 47, 17–21. doi: 10.1007/s11104-013-1656-6

Lugo, M. A., Reinhart, K. O., Menoyo, E., Crespo, E. M., and Urcelay, C. (2015). Plant functional traits and phylogenetic relatedness explain variation in associations with root fungal endophytes in an extreme arid environment. *Mycorrhiza* 25, 85–95. doi: 10.1007/s00572-014-0592-5

Mandyam, K., and Jumpponen, A. (2005). Seeking the elusive function of the root-colonising dark septate endophytic fungi. *Stud. Mycol.* 53, 173–189. doi: 10.3114/sim.53.1.173

Newsham, K. K. (2011). A meta-analysis of plant responses to dark septate root endophytes. *New Phytol.* 190, 783–793. doi: 10.1111/j.1469-8137.2010.03611.x

Perez-Naranjo, J. C. (2009). *Dark Septate and Arbuscular Mycorrhizal Fungal Endophytes in Roots of Prairie Grasses*. Ph.D. Dissertation, Saskatoon: University of Saskatchewan.

Phillips, J. M., and Hayman, D. S. (1970). Improved procedures for clearing roots and staining parasitic and vesicular-arbuscular mycorrhizal fungi for rapid assessment of infection. *Trans. Br. Mycol. Soc.* 55, 158–163. doi: 10.1016/S0007-1536(70)80110-3

Porras-Alfaro, A., Herrera, J., Sinsabaugh, R. L., Odenbach, K. J., Lowrey, T., and Natvig, D. O. (2008). Novel root fungal consortium associated with a dominant desert grass. *Appl. Environ. Microb.* 74, 2805–2813. doi: 10.1128/aem.02769-07

Ren, A. Z., Li, X., Han, R., Yin, L. J., Wei, M. Y., and Gao, Y. B. (2011). Benefits of a symbiotic association with endophytic fungi are subject to water and nutrient availability in *Achnatherum sibiricum*. *Plant Soil* 346:363. doi: 10.1007/s11104-011-0824-9

Saleem, M., Asghar, H. N., Zahir, Z. A., and Shahid, M. (2018). Impact of lead tolerant plant growth promoting rhizobacteria on growth, physiology, antioxidant activities, yield and lead content in sunflower in lead contaminated soil. *Chemosphere* 195, 606–614. doi: 606-614. 10.1016/j.chemosphere.2017.12.117

Santos, S. G. D., Silva, P. R. A. D., Garcia, A. C., Zilli, J. É, and Berbara, R. L. L. (2017). Dark septate endophyte decreases stress on rice plants. *Brazilian. J. Microbiol.* 48, 333–341. doi: 10.1016/j.bjm.2016.09.018

Shi, Z., Mickan, B., Feng, G., and Chen, Y. (2015). Arbuscular mycorrhizal fungi improved plant growth and nutrient acquisition of desert ephemeral *Plantago minuta* under variable soil water conditions. *J. Arid. Land.* 7, 414–420. doi: 10.1007/s40333-014-0046-0

Su, Y. Z., Zhao, W. Z., Su, P. X., Zhang, Z. H., Wang, T., and Ram, R. (2007). Ecological effects of desertification control and desertified land reclamation in an oasis–desert ecotone in an arid region: a case study in hexi corridor, northwest China. *Ecol. Eng.* 29, 117–124. doi: 10.1016/j.ecoleng.2005.10.015

Su, Z. Z., Mao, L. J., Li, N., Feng, X. X., Yuan, Z. L., Wang, L. W., et al. (2013). Evidence for biotrophic lifestyle and biocontrol potential of dark septate endophyte *Harpophora oryzae* to rice blast disease. *PLoS One* 8:e61332. doi: 10.1371/journal.pone.0061332

Surono, and Narisawa, K. (2017). The dark septate endophytic fungus *Phialocephala fortinii* is a potential decomposer of soil organic compounds and a promoter of *Asparagus officinalis* growth. *Fungal Ecol.* 28, 1–10. doi: 10.1016/j.funeco.2017.04.001

Tang, Z., An, H., Deng, L., Wang, Y., Zhu, G., and Shangguan, Z. (2016). Effect of desertification on productivity in a desert steppe. *Sci. Rep.* 6:27839. doi: 10.1038/srep27839

Vergara, C., Araujo, K. E. C., Urquiaga, S., Santa-Catarina, C., Schultz, N., Araujo, E. D. S., et al. (2018). Dark septate endophytic fungi increase green manure-N-15 recovery efficiency, N contents, and micronutrients in rice grains. *Front. Plant Sci.* 9:613. doi: 10.3389/fpls.2018.00613

Wang, J. L., Li, T., Liu, G. Y., Smith, J. M., and Zhao, Z. W. (2016). Unraveling the role of dark septate endophyte (DSE) colonizing maize (*Zea mays*) under cadmium stress: physiological, cytological and genic aspects. *Sci. Rep.* 6:22028. doi: 10.1038/srep22028

Wang, X. P., Zhang, Y. F., Hu, R., Pan, Y. X., and Berndtsson, R. (2012). Canopy storage capacity of xerophytic shrubs in Northwestern China. *J. Hydrol.* 45, 152–159. doi: 10.1016/j.jhydrol.2012.06.003

Wilcox, H. E., and Wang, C. J. K. (1987). Ectomycorrhizal and ectendomycorrhizal associations of Phialophorafinlandia with *Pinus resinosa*, *Picear ubens*, and *Betula alleghaniensis*. *Can. J. Res.* 17, 976–990. doi: 10.1139/x87-152

Wu, L. Q., Lv, Y. L., Meng, Z. X., Chen, J., and Guo, S. X. (2010). The promoting role of an isolate of dark-septate fungus on its host plant *Saussurea involucrata* Kar. et Kir. *Mycorrhiza* 20, 127–135. doi: 10.1007/s00572-009-0268-8

Xie, L. (2017). *Species Diversity and Salt Tolerance of DSE in The Roots of Hedysarum Scoparium Fisch. et Mey. in Northwest China*. Ph.D. Dissertation, Baoding: Hebei University.

Xie, L., He, X., Wang, K., Hou, L., and Sun, Q. (2017). Spatial dynamics of dark septate endophytes in the roots and rhizospheres of *Hedysarum scoparium* in northwest China and the influence of edaphic variables. *Fungal Ecol.* 26, 135–143. doi: 10.1016/j.funeco.2017.01.007

Xie, W., Hao, Z., Zhou, X., Jiang, X., Xu, L., Wu, S., et al. (2018). Arbuscular mycorrhiza facilitates the accumulation of glycyrrhizin and liquiritin in *Glycyrrhiza uralensis* under drought stress. *Mycorrhiza* 28, 285–300. doi: 10.1007/s00572-018-0827-y

Zhang, Q. M., Gong, M. G., Yuan, J. F., Hou, Y., Zhang, H. M., Wang, Y., et al. (2017). Dark septate endophyte improves drought tolerance in *Sorghum*. *Int. J. Agric. Biol.* 19, 53–60. doi: 10.17957/ijab/15.0241

Zhu, Z. D., and Chen, G. T. (1994). *Land Sandy Desertification in China*. Beijing: Science Press.

Conflict of Interest Statement: The authors declare that the research was conducted in the absence of any commercial or financial relationships that could be construed as a potential conflict of interest.

Advantages of publishing in Frontiers

OPEN ACCESS
Articles are free to read for greatest visibility and readership

FAST PUBLICATION
Around 90 days from submission to decision

HIGH QUALITY PEER-REVIEW
Rigorous, collaborative, and constructive peer-review

TRANSPARENT PEER-REVIEW
Editors and reviewers acknowledged by name on published articles

Frontiers
Avenue du Tribunal-Fédéral 34
1005 Lausanne | Switzerland

Visit us: www.frontiersin.org
Contact us: info@frontiersin.org | +41 21 510 17 00

REPRODUCIBILITY OF RESEARCH
Support open data and methods to enhance research reproducibility

DIGITAL PUBLISHING
Articles designed for optimal readership across devices

FOLLOW US
@frontiersin

IMPACT METRICS
Advanced article metrics track visibility across digital media

EXTENSIVE PROMOTION
Marketing and promotion of impactful research

LOOP RESEARCH NETWORK
Our network increases your article's readership